Isotopic signatures in hydrothermal vent fluids and the oceanic crust

—

tracing of sub-seafloor magmatic and hydrothermal processes

Dissertation

zur Erlangung des
Doktorgrades der Naturwissenschaften
(Dr. rer. nat.)

im Fachbereich Geowissenschaften
der Universität Bremen

vorgelegt von

Frederike Kristina Wilckens

Bremen, Mai 2017

Erstgutachter: Prof. Dr. Simone Kasemann
Universität Bremen

Zweitgutachter: Prof. Dr. Wolfgang Bach
Universität Bremen

Die müdliche Prüfung fand am 30.08.2017 statt.

Erklärung

Erklärung zu meiner Dissertation mit dem Titel: „Isotopic signatures in hydrothermal vent fluids and the oceanic crust – tracing of sub-seafloor magmatic and hydrothermal processes“

Sehr geehrte Damen und Herren,

hiermit versichere ich, Frederike Kristina Wilckens, dass ich

1. die vorliegende Arbeit ohne unerlaubte fremde Hilfe angefertigt habe,

2. keine anderen als die von mir angegeben Quellen und Hilfsmittel benutzt habe und

3. die den benutzten Werken wörtlich oder inhaltlich entnommenen Stellen als solche kenntlich gemacht habe.

_____

Bremen, den 30.05.2017

Preface

This thesis was submitted for the degree of Doctor of Natural Sciences (Dr. rer. Nat.) at the Department of Geosciences, University of Bremen. The PhD project is part of the MARUM research area "From element and energy fluxes to vent ecosystems", which overall aim is to study the relationship between energy fluxes at vent systems and primary producers at vent sites. The thesis is written in the cumulative format and thus includes a collection of three manuscripts, which deal with the sources and processes affecting hydrothermal vent fluids and volcanic rocks in arc- and back-arc settings. In total, this dissertation has six chapters:

Chapter 1: The first chapter gives a broad overview over the processes during hydrothermal circulation in different tectonic settings and introduces the isotope systems, which were used in this PhD project. Further, it outlines the motivation and aims of the PhD project.

Chapter 2: The second chapter summarizes the methods, which were used during the PhD project: the sample collection, preparation, chemical procedures, concentration and isotope measurements and end-member calculations.

Chapter 3: The third chapter contains the first manuscript "The influence of magmatic fluids and phase separation on B systematics in submarine hydrothermal vent fluids – A case study from the Manus Basin and Nifonea volcano" which was submitted to *Geochimica et Cosmochimica Acta*. The manuscript discusses B systematics in vent fluids with respect to water-rock interaction, phase separation and magmatic influx.

Chapter 4: The fourth chapter includes the second manuscript "Lithium isotope ratios in submarine hydrothermal vent fluids from Manus Basin and Nifonea volcano reveal evidence for negligible Li isotope fractionation during water-rock interaction", which in in preparation for *Chemical Geology*. This chapter addresses the Li systematics in vent fluids. Special focus of the manuscript is on Li isotope fractionation during water-rock interaction.

Chapter 5: The fifth chapter includes the third manuscript "Assessing water-rock interaction and basement alteration from B, Mg, Li and Sr isotopes in acid-sulfate fluids", which is in preparation for *Journal of Volcanology and Geothermal Research.* The manuscript discusses whether the progressive basement alteration during interaction with acid-sulfate fluids can be identified from the fluid composition.

Chapter 6: This chapter summarizes the results of the subchapters and formulates the main conclusions, which could be achieved in this PhD project.

TABLE OF CONTENTS

Abbreviations

BABB	Back-arc basin basalt
EMVZ	Eastern Manus Volcanic Zone
IAB	Island arc basalt
IGT	Isobaric gas-tight
MORB	Mid ocean ridge basalt
MOR	Mid ocean ridge
MSC	Manus Spreading Centre
ROV	Remotely operated vehicle
SER	South East Ridges
SR	Southern Rifts
VHMS	Volcanic-hosted massive sulphide deposits
VMS	Volcanic-associated massive sulphide deposits

Abstract

The circulation of seawater through the oceanic crust plays an essential role for the heat and element budgets on our planet. A huge variety of processes such as interaction with the oceanic crust and marine sediments at low and high temperatures, phase separation and segregation, and magmatic fluid influx influence submarine hydrothermal vent fluids on their pathway through the oceanic crust. Since the discovery of first hydrothermal vent fields about 50 years ago, much effort in their exploration has been invested. Because it has long been stated that vent fluids from mid-ocean ridge systems control ocean's chemistry, most of the research was conducted on mid-ocean ridge vent systems. Since several years, vent fluids from arc- and back-arc basins have been the subject of increasing investigation. Several studies revealed that vent fluids from these subduction-related settings also have a huge impact on the ocean's chemistry and that their compositions differ from fluids venting along mid-ocean ridges. Although some of these differences have been identified, their individual impact on vent fluids' composition remains still poorly understood.

The thesis aims to unravel and understand the individual processes on the composition of hydrothermal vent fluids from back-arc basins. For this purpose vent fluids and volcanic rocks from the Manus Basin, Papua New Guinea, and Nifonea volcano, Vanuatu were analysed for their Li, B, Sr and Mg isotopic composition. Vent fluids from these settings have a high variability due to different host rock compositions, different proportions of altered oceanic crust in the hydrothermal circulation cell and variable influx of magmatic fluids. Further, some of the fluids from the Manus Basin and Nifonea indicate phase separation at different pressure and temperature conditions.

In accordance with studies on mid-ocean ridge fluids, B in black-smoker fluids from the Manus Basin displays mainly the interaction of seawater with the oceanic crust. B concentrations appear to be slightly affected by phase separation close to the two-phase curve of seawater. In contrast, B concentrations in the boiling fluids from Nifonea volcano are highly enriched suggesting that B preferentially partitions into the low-salinity, high-vapour phase. However, as the low B isotope ratios from Nifonea volcano cannot be explained by phase separation, we rather propose that B is enriched due to a preferential mobilisation from the oceanic crust during water-rock interaction with vapour-rich fluids. This is in accordance with the findings from the gas-rich acid-sulfate fluids from the Manus Basin. Nevertheless, it remains unclear whether B is added by magmatic fluids to the vent fluids or not. Further, the results also show that B in vent fluids might be used to assess the proportion of altered crust in the hydrothermal circulation cell.

Because δ^7Li values in vent fluids from back-arc basins have lower values compared to mid-ocean ridges although their host rocks have a similar isotopic composition, Li behaviour during water-rock interaction at back-arc basins appears to be distinct from mid-ocean ridges. Furthermore, the results demonstrate that the Li isotope ratios in the vent fluids characterized by the lowest water/rock ratios during water-rock interaction from the Manus Basin match the isotopic composition of their host rocks. This implies that the proposed isotope effect during water-rock interaction is not applicable to the vent fluids from the Manus Basin. It is rather suggested that Li in these vent fluids reflect simple leaching of Li from the oceanic crust with no or negligible isotope effect. This might be valid also for vent fluids from other arc- and back-arc environments.

The third part of the dissertation shows that the high Mg concentrations in acid-sulfate fluids have their source in unmodified seawater rather than in the oceanic crust. This supports the theory that they reflect submarine analogues of fumaroles. Nevertheless, the combination of Li, B and Sr isotopes in all acid-sulfate fluids shows a considerable amount of water-rock interaction. The data implies that multi-proxy isotope studies in these fluids offer the potential to trace the progressive alteration of the oceanic crust.

The results of this dissertation extended the existing databases on Li, B, Sr and Mg isotope ratios of vent fluids from back-arc basins. Furthermore, the findings of this project yield valuable insights into subduction-related hydrothermal processes and showed that water-rock interactions are distinct from those at mid-ocean ridges.

Kurzfassung

Die Zirkulation von Meerwasser durch die ozeanische Kruste spielt eine bedeutende Rolle für den Wärme- und Stoffhaushalt der Erde. Auf ihrem Weg durch die ozeanische Kruste werden hydrothermale Fluide durch eine Vielzahl von Prozessen, wie Wasser-Gesteins-Wechselwirkungen mit der ozeanischen Kruste und marinen Sedimenten bei niedrigen und hohen Temperaturen, Phasentrennung sowie durch den Zufluß magmatischer Fluide, beeinflusst. Seit der Entdeckung der ersten hydrothermalen Quellen vor etwa 50 Jahren wurde viel Aufwand in ihre Erforschung investiert. Da jedoch lange Zeit angenommen wurde, dass die hydrothermalen Fluide, die an den Mittelozeanischen Rücken austreten, die chemische Zusammensetzung des Meerwassers kontrollieren, wurde ein Großteil der Forschung an diesen Fluiden durchgeführt. Seit einigen Jahren werden zunehmend auch Studien an hydrothermalen Fluiden von Inselbögen und Backarc-Becken durchgeführt. Diese Studien konnten zeigen, dass hydrothermale Fluide aus diesen tektonischen Milieus auch einen großen Einfluss auf die chemische Zusammensetzung des Ozeans haben und dass sich ihre Zusammensetzung von den Fluiden, die an den mittelozeanischen Rücken entgasen, unterscheidet. Obwohl einige Ursachen dieser Unterschiede identifiziert wurden, ist ihre individuelle Auswirkung auf die Zusammensetzung der hydrothermalen Fluide noch immer schlecht verstanden.

Das Ziel der vorliegenden Dissertation ist, die einzelnen Prozesse, die die Zusammensetzung der hydrothermalen Fluide in Backarc-Becken beeinflussen, zu entschlüsseln und zu verstehen. Zu diesem Zweck wurden hydrothermale Fluide und vulkanische Gesteine aus dem Manus-Becken, Papua-Neuguinea und dem Nifonea Vulkan, Vanuatu auf ihre Lithium- (Li), Bor- (B), Strontium- (Sr) und Magnesium- (Mg) Isotopenzusammensetzung untersucht. Aufgrund unterschiedlicher Zusammensetzungen der Wirtsgesteine, unterschiedlichen Anteilen an alterierter ozeanischer Kruste in der hydrothermalen Zirkulationszelle und variablem Zustrom von magmatischen Fluiden, haben die Fluide aus diesen Gebieten eine starke chemische Variabilität. Zudem zeigen einige der Fluide Indikatoren für Phasentrennung unter verschiedenen Druck- und Temperatur-Bedingungen.

In Übereinstimmung mit verschiedenen Studien an Mittelozeanischen Spreizungszonen, reflektiert B in den schwarzen Rauchern vom Manus-Becken vor allem die Wechselwirkung zwischen Meerwasser und ozeanischer Kruste. Die B-Konzentrationen scheinen durch Phasentrennung nahe der Zweiphasen-Kurve von Meerwasser nur geringfügig beeinflusst. Im Gegensatz dazu ist B in den gasreichen, siedenden Fluiden des Nifonea Vulkans stark angereichert, was darauf hindeutet, dass B vorzugsweise in die salzarme und gasreiche Phase fraktioniert. Da die niedrigen B-Isotopenverhältnisse in den Fluiden vom Nifonea-Vulkan jedoch nicht durch Phasentrennung erklärt werden können, kann stattdessen angenommen werden, dass

B während Wasser-Gesteins-Wechselwirkungen mit gasreichen Fluiden bevorzugt aus der ozeanischen Kruste gelaugt wird. Diese Hypothese wird durch die Ergebnisse von gasreichen Säure-Sulfat-Fluide aus dem Manus-Becken bestätigt. Es bleibt jedoch unklar, ob B auch durch magmatische Fluide beeinflusst wird. Weiterhin zeigen die Ergebnisse, dass B in hydrothermal Fluiden das Potential bietet, die Alteration der Ozeankruste in der hydrothermischen Zirkulationszelle zu erforschen.

Die δ^7Li-Werte in den Fluiden aus Backarc-Becken sind generell niedriger im Vergleich zu denen an Mittelozeanischen Rücken. Obwohl die Isotopenzusammensetzung der ozeanischen Kruste an beiden Lokalitäten ähnlich ist, scheint sich daher das Verhalten von Li während Wasser-Gesteins-Wechselwirkungen in Backarc-Becken von dem an Mittelozeanischen Spreizungszonen zu unterscheiden. Darüber hinaus zeigen die Ergebnisse, dass die Hydrothermalfluide, die die geringsten Wasser/Gesteins-Verhältnissen haben, in ihrer Isotopenzusammensetzung mit den δ^7Li-Werten der Wirtsgesteine übereinstimmen. Das impliziert, dass der von anderen Studien vorausgesagte Isotopeneffekt während Wasser-Gesteins-Wechselwirkungen nicht auf die hydrothermalen Fluide aus dem Manus-Becken anwendbar ist. Stattdessen weisen die Ergebnisse darauf hin, dass Li in den hydrothermalen Fluiden aus dem Manus-Becken eine einfache Laugung von Li aus der ozeanischen Kruste mit keinem oder einem vernachlässigbaren Isotopeneffekt reflektiert, was auch für andere Fluide in Backarc-Becken gelten könnte.

Der dritte Teil der Dissertation zeigt, dass die hohen Mg-Konzentrationen in den Säure-Sulfat-Fluiden die Mg-Isotopensignatur von unmodifiziertem Meerwasser haben. Dies unterstützt die Theorie, dass diese Fluide die submarinen Gegenstücke von Fumarolen darstellen. Zudem zeigt die Kombination von Li-, B- und Sr-Isotopenverhältnissen in den Säure-Sulfat-Fluiden, dass alle Fluide durch Wasser-Gesteins-Wechselwirkungen überprägt wurden. Die Daten implizieren, dass Studien, die diese Isotopensysteme in Säure-Sulfate-Fluiden miteinander kombinieren, das Potential haben, die fortschreitende Alteration der ozeanischen Kruste während der Interaktion mit diesen sehr sauren und gasreichen Fluiden zu verstehen und zu quantifizieren.

Die Ergebnisse dieser Dissertation erweitern die vorhandenen Datenbanken der Li-, B-, Sr- und Mg-Isotopenverhältnisse von submarinen hydrothermalen Fluiden aus Backarc-Becken. Darüber hinaus liefern die Ergebnisse dieses Projekts wertvolle Einblicke in die hydrothermalen Prozesse in von Subduktion beeinflussten Umgebungen und zeigen, dass sich die Wasser-Gesteins-Wechselwirkungen von denen an Mittelozeanischen Rücken unterscheiden.

Chapter 1: Introduction

1.1 Submarine hydrothermal circulation

Understanding the processes related to submarine hydrothermal circulation is of major scientific interest for a variety of reasons. Hydrothermal vent systems are thought to represent the modern analogue for some of the submarine volcanic-associated (VMS) and volcanic-hosted massive sulphide (VHMS) deposits, which can be found on the continents. The formation of such ore deposits is associated with a leaching of metals from the oceanic crust during hydrothermal circulation, leading to an alteration of the oceanic crust. Thus, the investigation of hydrothermal circulation and the composition of vent fluids may help to better constrain the mechanisms behind the formation of submarine sulphide deposits and associated alteration of oceanic crust (Alt, 1995). Furthermore, vent fluids can give valuable insights into processes, which occur in the young oceanic crust. Because young crust is still too fragile for scientific drilling, the study of vent fluids provides the only possibility to disentangle these processes. In addition, serving as a major source and sink for elements in the ocean, submarine hydrothermal circulation also bears a huge influence on the chemical composition of seawater (Edmond et al., 1979; 1982).

An intense exploration at mid ocean ridge (MOR) systems, arc and back-arc basins led to the discovery of more than 100 submarine high-temperature venting sites within the last 50 years (Hannington et al., 2005). First geochemical evidences for submarine hydrothermal systems were found in 1966 in the Red Sea, where hot brines (40-60°C) and layers of metal-rich sediments were discovered (Bischoff, 1969). Subsequently it was hypothesized that similar fluids might also occur along other young mid-ocean ridges, which are comparable to the rift system in the Red Sea, and indeed, Bostrom et al. (1969) found high concentrations of metalliferous sediments along MORs. In 1977, low-temperature venting (up to 17°C) was discovered at the Galapagos rift (Corliss et al., 1979, Edmond et al., 1979) and only two years later the first high-temperature hydrothermal vent fields were detected at the East Pacific Rise (MacDonald et al., 1980). In 1986, the first hydrothermal system associated with back-arc spreading was spotted in the Western Pacific in the Manus Basin (Both et al., 1986).

Because hydrothermal circulation requires seawater entrainment into a fractured, permeable crust and a heat source in the subseafloor, submarine hydrothermal systems are concentrated along MORs, island arcs and back-arc basins; some are also related to intra-plate volcanoes (Fig. 1).

The chemical composition of hydrothermal vent fluids is manifold and almost every discovered vent has a unique chemical fingerprint, which itself may vary within minutes (Von Damm, 1995). This renders it challenging to identify and understand the sources and processes that modify the chemical and physical characteristics of hydrothermal vent fluids. Nevertheless, many processes, which affect vent fluids during hydrothermal circulation, have been identified. The vent fluids

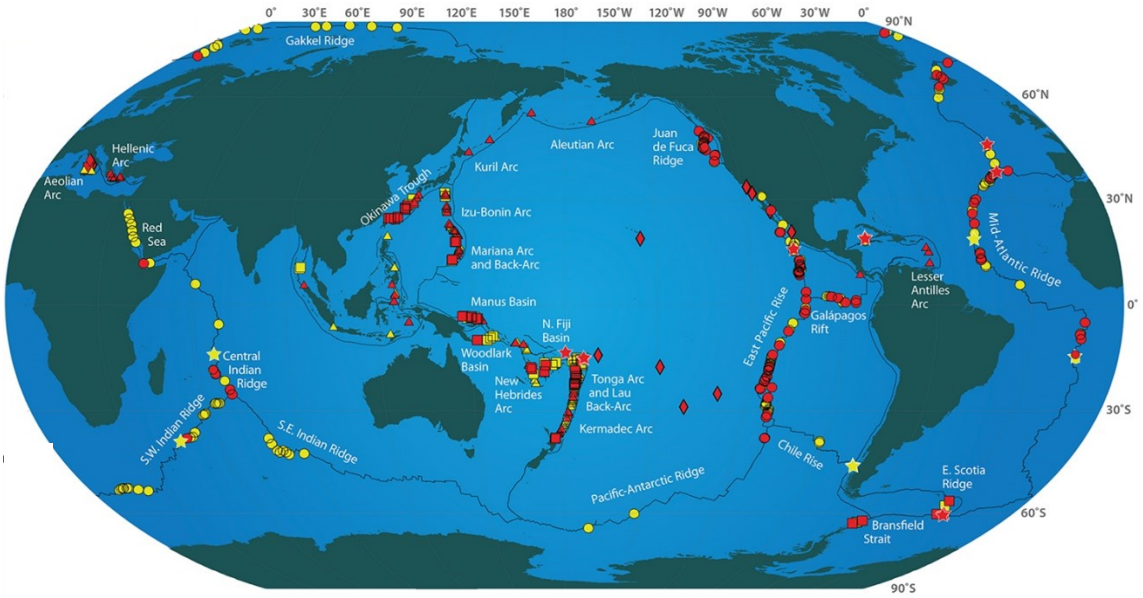

Figure 1: Map showing the active vent systems, which have been discovered directly (red symbols) or are known to exist (e.g. through the detection of hydrothermal plumes in the water column) (yellow symbols). The different symbols refer to their tectonic setting: circles= mid-ocean ridges, triangle= arc volcano, square = back- arc basins, diamond = intra-plate volcanos and other, and stars = vent sites discovered in 2010 and 2011. Solid lines indicate the major tectonic plates. This map was made available by InterRidge program (http://vents-data.interridge.org/maps, accessed on 25.05.2017).

composition appears to be mainly controlled by the host rock composition as well as size and depth of the heat source (Hannington et al., 2005; Tivey, 2007).

1.1.1 Hydrothermal circulation at MORs

At MORs a hydrothermal circulation cell is comprised of three major zones: (I) the "recharge zone", (II) the "root zone" or "reaction zone" and (III) the "discharge zone" (Alt, 1995) (Fig. 2a). In the "recharge zone" seawater interacts with the oceanic crust at low-temperatures. During this reaction, elements can be precipitated and incorporated into secondary minerals, most notably, sulphate (SO_4) and magnesium (Mg). Mg is lost due to the formation of Mg-OH silicates. This reaction leads to an H^+ excess in the fluid, which directly decreases the fluid pH (Seyfried and Shanks, 2004) (Fig. 2b). In the so-called "root zone" or "reaction zone", fluids have the highest temperatures due to their proximity to the heat source. Temperatures in this zone can even exceed 400°C. At these high temperatures alkali elements, metals as well as sulphur are leached from the oceanic crust (Hannington et al., 2005). Furthermore, phase separation and magmatic degassing can influence the fluid composition (Lilley et al., 2003, Mottl et al., 2011). During magmatic degassing, magmatic volatiles (CO_2, HF, CH_4, SO_2, He or H_2) rise from the magma chamber and mix with the hydrothermal fluid leading to higher gas concentrations and a lower pH value. In the third zone, the "discharge zone", hot fluid rises towards the seafloor and interacts on its way with the surrounding rocks. In addition, it can mix in the subseafloor with entrained seawater, causing

precipitation of minerals due to rapid cooling. During venting hydrothermal fluids mix with the cold seawater, leading to a precipitation of metal-rich sulphides or sulphates.

In addition to water-rock interaction and addition of magmatic volatiles, the chemical composition of vent fluids can also be modified by phase separation and segregation (Von Damm, 1988), which is mainly displayed by Cl variations in the vent fluids. To understand the behaviour of seawater during phase separatiation, it is important to note that seawater is a two-component system consisting of H_2O/NaCl. Its phase boundaries, depending on the temperature and pressure of the fluid, are displayed in the two-phase curve for seawater (Bischoff and Rosenbauer, 1984; Bischoff and Pitzer, 1985) with the critical point of seawater at 407°C at 298 bar (Bischoff and Rosenbauer, 1985). If the fluid has a temperature and pressure lower than the critical point of seawater "boiling" occurs, leading to a separation of a low-salinity, high-vapour phase (subcritical phase separation). The amount of salt in these fluids depends on the distance to the critical point of seawater. At temperatures and pressures above the critical point of seawater, supercritical phase separation occurs. In contrast to subcritical phase separation, a high-salinity brine condensates from the fluid. Vent fluids can also be influenced by microbial communities, which influence mainly the H_2, H_2S and CH_4 contents of vent fluids (Von Damm and Lilley, 2004). However, since the limit of life lies at about 120°C (Kashefi and Lovley, 2003), this process is negligible for understanding high-temperature vent fluids.

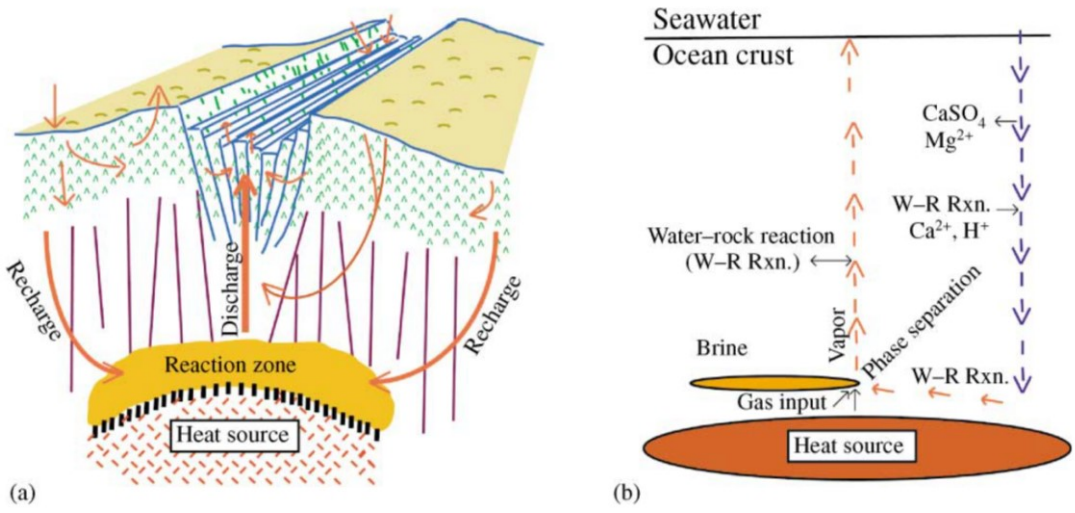

Figure 2: Illustrations by German and Von Damm (2004). (a) illustrates the three major zones during submarine hydrothermal circulation after Alt (1995). In the "recharge" zone seawater entrains into the crust and reacts under low temperatures with the oceanic crust. In the "reaction" zone the fluid fluids interacts at high temperatures and pressures. The "discharge" zone describes the area, where the fluid rises towards the seafloor. (b) shows an schematic illustration of the processes occurring during hydrothermal circulation. After entrainment into the oceanic crust, anhydrite precipitates, Mg is lost from the fluid due to the formation of Mg-OH silicate and Ca-ions as well as protons can be added to the fluid. Water-rock interaction occurs also in the reaction zone and discharge zone. In addition the fluid can be affected by inputs from magmatic degassing as well as phase separation (with the potential of brine segregation) before it rises to the surface.

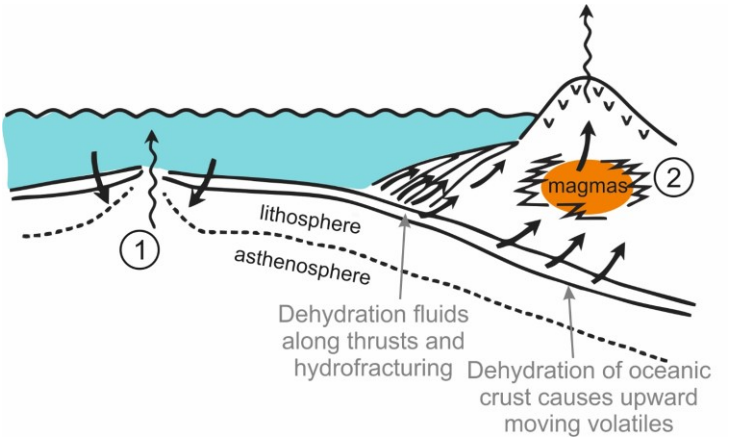

Figure 3: Schematic illustration modified from Piranjo (2008). The graphic shows the additional influences of vent fluids during hydrothermal circulation at volcanic arc systems (2) relative to mid ocean ridges (1). At MOR settings vent fluids are mostly influenced by mid ocean ridge basalts, which represent a mantle source. At arc- and back-arc basins vent fluids are additionally influenced by magmatic fluids and volatiles, which form during dehydration of the subducting slab. Furthermore there are more influenced by magmatic volatiles degassing from the underlying magma source.

Thus, depending on whether hydrothermal circulation represents a source or sink for a specific element, it influences the elemental distribution in seawater. Most of the observed chemical variability in hydrothermal vent fluids can be related to changing water/rock ratios (W/R) during water-rock interaction and phase separation as described above. However, there are also major differences between vent fluids from different tectonic settings (Hannington et al., 2005).

More than 80% of the active volcanoes on the Earth surface are located on the ocean seafloor and the majority of hydrothermal activity is concentrated along MORs and island arcs (Hannington et al., 2005). About 33% of the known hydrothermal vent fields are associated with back-arc basins and volcanic arcs (Baker and German, 2004; Hannington et al., 2005, Mottl et al., 2011, Reeves et al., 2011). However, although hydrothermal systems from island arcs and back-arcs also contribute in a large amount to the hydrothermal heat and chemical fluxes into the ocean, vent systems from these settings are still understated and most of the hydrothermal element fluxes into the ocean were estimated using the chemical compositions from MOR settings.

1.1.2 Hydrothermal circulation at arc- and back-arc settings

In contrast to MOR settings, the variation of hydrothermal vent fluids from island arcs and back-arc basins is remarkably diverse. This is mainly due to the high variability of rock types in back-arc and arc settings. The composition of the oceanic crust in arc and back-arc basins ranges from mid-ocean ridge-like basalts at spreading centres to high-K calc-alkaline andesites to rhyolites. This compositional range can be explained by contributions from different melt sources, which depend on the proximity to the subducting slab (Binns and Scott, 1993; Sinton et al., 2003; Hannington et al., 2005; Pearce and Stern, 2006) (Fig. 3).

Mainly all vent fluids from back-arc spreading centres match in their chemical composition with MOR fluids, mainly due to a similar composition of the oceanic crust (Mottl et al., 2011; Reeves et al., 2011). However, most of the other fluids are characterized by lower pH values and higher gas contents compared to MOR fluids and have a higher variability in their main and trace elements as well as their isotopic compositions. The higher gas contents (especially higher CO_2 concentrations) are related to higher inputs of magmatic volatiles in back-arc systems, which can degas from the underlying magma (Ishibashi and Urabe, 1995; Mottl et al., 2011; Reeves et al., 2011). In several arc and back-arc settings, so called acid-sulfate fluids were discovered. They are thought to be the submarine analogues to subaerial fumaroles. Hence, they are thought to show evidence for a direct injection of magmatic fluids or volatile phases into unmodified seawater (Sakai et al., 1990; Gamo et al., 1997; Seewald et al., 2015). During their rise, these acidic hot fluids are associated with preferential leaching of metalloids and metals from the oceanic crust, which makes them in particular interesting to study the formation of VMS and VHMS deposits (Hedenquist and Lowenstern, 1994; Hannington et al., 2005).

1.2 Isotopic tracers in hydrothermal vent fluids

The chemical composition of vent fluids displays an integrated record of all processes, which occur during hydrothermal circulation at certain pressure and temperature conditions in the hydrothermal circulation cell. Since many of these processes mask each other, their individual effect on the vent fluid's chemistry is still poorly understood. Possible and promising tools, which may help to understand, quantify and unravel the processes and sources during hydrothermal circulation are isotopic systems. Because each isotopic system has different properties and sources, they can reflect different processes in the vent fluids. In the following, the state of research for the isotope systems of strontium (Sr), lithium (Li), boron (B) and magnesium (Mg) isotopes in hydrothermal vent fluids or during water-rock interaction will be introduced.

1.2.1. Strontium

Since the residence time of Sr in the ocean is much higher than its mixing time, Sr in seawater has a uniform $^{87}Sr/^{86}Sr$ ratio of 0.70916 (Hodell et al., 1990). In contrast, $^{87}Sr/^{86}Sr$ in the oceanic crust is less radiogenic with ratios from 0.7025 to 0.703. The isotopic composition of the hydrothermal fluids displays the mixture of Sr in seawater and Sr derived from the oceanic crust. During water-rock interaction, Sr is leached from the oceanic crust leading to less radiogenic $^{87}Sr/^{86}Sr$ ratios in the hydrothermal fluid. The mean estimated hydrothermal flux into the ocean has a $^{87}Sr/^{86}Sr$ ratio of 0.7037, which is close to the composition of the oceanic crust (Bach and Humphris, 1999; Davis et al., 2003). Because $^{87}Sr/^{86}Sr$ is apparently not affected by phase separation or magmatic volatiles, it appears to be a promising proxy to estimate water/rock (W/R) ratios during water-rock interaction in the hydrothermal circulation cell. However, leaching of Sr from the oceanic

crust is a temperature-dependent process and is most effective at temperatures ≥350°C. Furthermore, Sr can be affected by anhydrite dissolution and precipitation (Reeves et al., 2011), which modifies Sr concentrations and more importantly also its isotope ratios. Although it is possible to correct for the latter effect, it still may influence the calculated W/R ratios.

1.2.2 Lithium

Li behaves as a conservative element in the ocean and has (similar to Sr) a higher residence (about one million years) than mixing time in the ocean. Due to its fluid mobility, the large relative mass difference between its two stable isotopes, and the huge difference between the isotopic composition of seawater (δ^7Li = +31‰, Millot et al., 2004) and the oceanic crust (δ^7Li_{MORB} = +3.7±1.0‰, (1σ, n = 53) Tomascak et al., 2008), Li appears to be a good proxy to investigate water-rock interactions during hydrothermal circulation.

Studies on Li isotopes in hydrothermal vent fluids show a range of +1.6 to +11.0‰ (average value of 8.0±1.9‰, (1σ, n = 33), Foustoukos et al., 2004). Analysed vent fluids within arc and back-arc sites in the Western Pacific revealed lower Li isotope ratios between +1.6 and +7.2‰ (Araoka et al., 2016) than the average composition in vent fluids from MOR environments. Hence, they match closer to the composition of the oceanic crust as compared to the Li signature of MOR fluids. Nevertheless, most of the submarine hydrothermal vent fluids from both MOR and arc/back-arc settings appear to be isotopically fractionated relative to the oceanic crust. The absence of any correlation between Li and Sr isotope ratios in these vent fluids also supports this hypothesis (Araoka et al., 2016). However, the processes explaining the fractionation as well as the quite small range in Li isotope ratios of hydrothermal vent fluids are highly debated and not well known. An idea to explain the isotopic offset between vent fluids and oceanic crust is Li isotopic fractionation during the incorporation of Li into alteration phases (Chan et al., 1993). Altered oceanic crust has generally lower Li isotope ratios compared to fresh volcanic rocks implying that ^6Li is preferentially incorporated into secondary minerals (Seyfried et al., 1998; James et al., 2003). Furthermore, there is no evidence that ^7Li is preferentially released from fresh basalts (Wimpenny et al., 2010; Verney-Carron et al. (2011). This is in accordance with mass balance calculations, which show that most of the vent fluids can be explained by leaching of Li from the oceanic crust without isotopic fractionation and preferential incorporation of ^6Li into alteration phases dependent on the temperature (Magenheim et al., 1995; Verney-Carron et al., 2015, Araoka et al., 2016). In addition to that, some vent fluids are also influenced by the interaction with oceanic sediments (Araoka et al., 2016). In contrast, phase separation appears to have no or only a negligible effect on the Li isotope ratios although it can influence the concentration of Li in the fluid (Foustoukos et al., 2004). Another process, which can affect Li systematics in vent fluids, is enrichment of ^6Li in the fluid by diffusion. Diffusion can have a significant effect on the Li vent fluids composition at high temperatures (Verney-Carron et al.

2011). However, high leaching rates of Li from the oceanic crust at high temperatures most probably mask the diffusion effects.

It appears that Li concentrations and isotope ratios are also a powerful tool to understand water-rock interactions during hydrothermal circulation and in particular hydrothermal alteration of the basement. Nevertheless, the whole range of variations in Li isotope ratios of submarine vent fluids or the reason for the differences in the Li isotopic composition of vent fluids from MOR settings and arc/back-arc settings are still poorly understood. This could be explained for example through poorly constrained distribution coefficients and isotope fractionation factors between solid and fluid or through the unknown effect of Li due to diffusion (e.g. Araoka et al., 2016).

1.2.3 Boron

B is also a fluid mobile element, has two stable isotopes (^{10}B and ^{11}B) and a volatile character. Similar to Li and Sr, B has the potential to trace W/R ratios during water-rock interaction as it has significant differences in both concentration and isotopic composition between the oceanic crust and seawater (Spivack et al. 1990; You et al., 1994). Seawater has a B concentration of 0.41 mmol/kg and a $\delta^{11}B$ of +39.6 ‰ (Foster et al., 2010). B compositions in MORB (~1 mg/kg and $\delta^{11}B$ = -4‰), back-arc basin basalts (BABB) (~12 mg/kg and $\delta^{11}B$ = -4‰) and Island-Arc Basalts (IAB) (2 to 30 mg/kg and $\delta^{11}B$ = +7‰) are distinct from each other (Ryan and Langmuir, 1993; Chaussidon and Jambon, 1994; Chaussidon and Marty, 1995, Bebouth et al., 1999, Leeman et al., 2017). This variability offers the possibility to study the composition of oceanic crust in vent fluids and trace crustal heterogeneities, which is especially beneficial in arc and back-arc settings due to their complex tectonic settings.

Studies on B isotope ratios in hydrothermal vent fluids from mid-ocean ridges (Butterfield et al., 1990; Palmer, 1991; You et al., 1994; James et al., 1995), island arcs and back-arc basins (Palmer, 1991; You et al., 1994; Yamaoka et al., 2015) showed that B isotopes in vent fluids display mainly the water-rock interaction between hydrothermal fluid and oceanic crust (Yamaoka et al., 2015) or marine sediments (Yamaoka et al., 2015; Wu et al., 2016; Baumberger et al., 2016). During water-rock interaction B isotopes fractionate in a temperature depending reaction, where ^{11}B is preferentially leached from the oceanic crust, which is why the vent fluids are isotopically heavier in comparison to their host rocks (Wunder et al., 2005; Yamaoka et al., 2015). Due to its volatile behaviour, B can also be affected by phase separation and segregation or by magmatic degassing in the reaction zone of the hydrothermal circulation cell. B systematics of magmatic gases and fluids, which can rise from the magma reservoir are largely unknown, but can be estimated from studies of subaerial fumaroles. B isotope ratios in fumaroles show similar values compared with the surrounding rocks (Leeman et al., 2005), implying that there is no significant B isotope fractionation during magma degassing. Another process, which can affect B

concentrations and its isotope ratios in hydrothermal fluids is phase separation. Although B isotope ratios are mostly unaffected by phase separation, B concentrations can vary significantly (Spivack et al., 1990; You et al., 1994; Liebscher et al., 2005, Foustoukos and Seyfried, 2007; Yamaoka et al., 2015). The strong volatile behaviour of B is mainly related to the formation of $B(OH)_3$ (aq) species in the low-salinity, vapour-rich fluid. This effect is indeed obvious, when halite stability in the coexisting brine is reached (Foustoukos and Seyfried, 2007). In contrast, if the coexisting brine has a low Cl content, B may preferentially partition into the brine phase (Liebscher et al., 2005; Foustoukos and Seyfried, 2007, Yamaoka et al., 2015). This shows that B in hydrothermal fluids is not only influenced by water/rock interactions, but offers also the potential to track crustal heterogeneities and to better understand the addition of magmatic fluids and phase separation.

1.2.4 Magnesium

Because Mg is quantitatively removed during hydrothermal circulation (Seyfried and Bischof, 1981; Von Damm et al., 1985; Mottl and Holland, 1978), analysing Mg isotope ratios in hydrothermal vent fluids appears to be pointless. However, the isotopic composition of Mg in seawater is, similar to B, Li and Sr, significantly distinct from those of the oceanic crust. Mg in seawater has a δ^{26}Mg value of -0.82‰, (Tipper et al., 2006), whereas fresh and altered MORB has an isotopic composition of -0.25±0.11‰ (Huang et al., 2015). Island arc basalts can have slightly higher values between -0.25 and -0.10‰ (Teng et al., 2016). Since some hydrothermal vent fluids, especially the so called “acid-sulfate” fluids have high Mg concentrations, they might be contaminated with Mg leached from the oceanic crust in the reaction or discharge zone. Hence, Mg isotope ratios offer the opportunity to test whether Mg in these high-Mg fluids is either seawater derived or Mg, which was leached from the oceanic crust. Furthermore, it is also an interesting element to study because the Mg budget in the ocean is still poorly understood. One of the main reasons for this is that it is unclear, whether Mg isotopes fractionate during their incorporation into the oceanic crust or not (e.g. Tipper et al., 2006).

1.3 Study Areas

1.3.1 Manus Basin

The Manus Basin is a relatively young back-arc basin in the northeastern Bismarck Sea. It is bordered to the northeast by the nowadays inactive Manus Trench and to the South by the New Britain Trench and Willaumez Rise (Fig. 4) (Taylor et al., 1994; Lee and Ruellan, 2006). The formation of the Manus Basin started during the Cenozoic due to the rapid subduction of the Pacific underneath the Australian plate along the Manus Trench (Lee and Ruellan, 2006). In the late Miocene the Ontong Java Plateau collided with the subduction zone causing a subduction reversal (Kroenke and Rodda, 1984, Martinez and Taylor, 1996), where the Solomon Plate

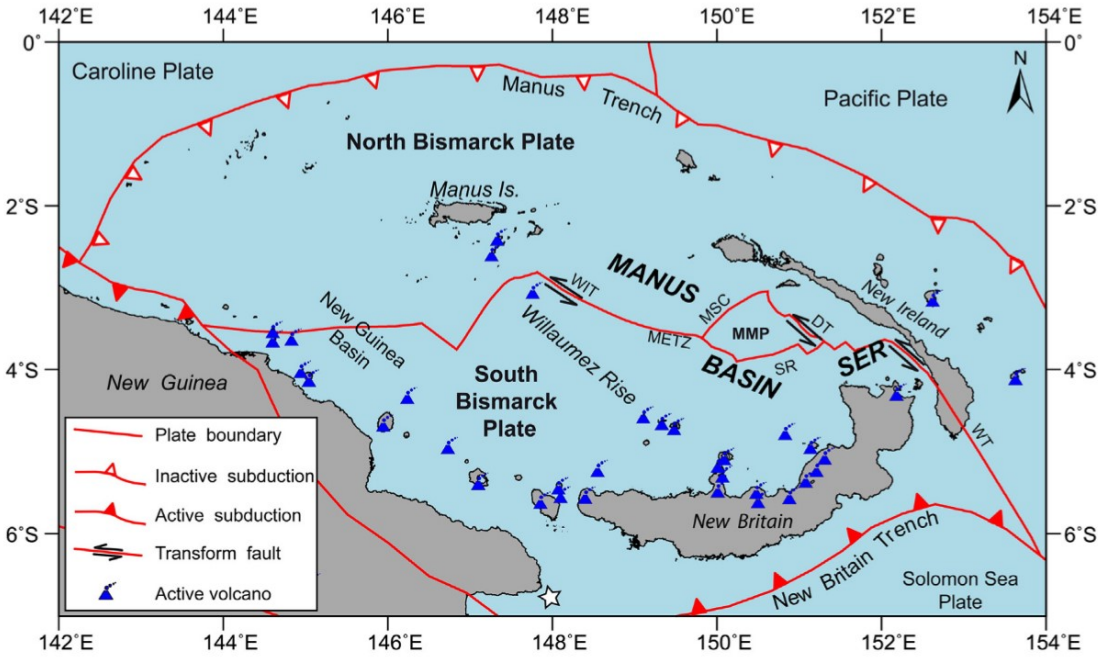

Figure 4: Tectonic map from the Manus Basin (from Thal et al., 2014). Abbreviations used in this figure: DT = Djaul Transform, METZ = Manus Extensional Transform Zone, MMP = Manus Microplate, MSC = Manus Spreading Centre, MMP = Manus Microplate; SER = Southeastern Ridges; SR = Southern

subducted northwards underneath the Pacific Plate along the New Britain Trench. The opening of the Bismarck Sea is related to the collision of New Guinea and parts of the island arc, which formed during the former southward subduction at the Manus Trench (Taylor, 1979; Lee and Ruellan, 2006). Today, crustal extension occurs along the Manus Spreading Centre (MSC), the Manus Extensional Transform Zone (METZ), the Southern Rifts (SR) and the Eastern Manus Volcanic Zone or Southeastern rifts (EMVZ/SER) with fully developed spreading along the MSC and METZ. Volcanic rocks along the MSC and METZ have MORB-like composition, which is related to the relatively small amount of subduction supply (Sinton et al., 2003). In contrast, the basement in the eastern Manus Basin consists of Eocene to Oligocene island arc crust, which formed during the subduction at the Manus Trench. The area between the Weitin and Djaul transform faults features neovolcanic ridges and solitary volcanoes that represent initial rifting in a pull-apart basin (Martinez and Taylor, 1996). The neovolcanic rocks have andesitic to dacitic composition and reveal a strong geochemical and isotopic island arc affinity, which can be either related to the subduction of the Solomon plate or are a relic from the former subduction at the Manus trench (Kamenetsky et al., 2001).

1.3.1.1 Hydrothermal vent sites

Hydrothermal activity in the Manus Basin is concentrated along the MSC and EMVZ. Vienna Woods was the first vent field that was discovered within Manus Basin and is located at the MSC (Both et al., 1986). These days, several hydrothermal vent areas in the SER are known:

PACMANUS, Northeast Pual, DESMOS and SuSu Knolls (Fig. 5). Due to their proximity to the New Britain Trench, the variability in the oceanic crust composition, input of magmatic volatiles, mixing with unmodified seawater in the subsurface and phase separation, vent fluids within Manus Basin have a broad chemical and isotopic compositional range (Gamo et al., 1997; Craddock et al., 2010; Reeves et al., 2011; Seewald et al., 2015).

Hydrothermal activity at Vienna Woods occurs in a water depth of 2470m within the rift zone of the MSC (Fig. 5). Temperatures of almost clear vent fluids range from 270°C to 290°C with moderate pH values around 4.4 (Tivey et al., 2006, Craddock et al., 2010, Reeves et al., 2011). The chemical and isotopic composition of vent fluids from Vienna Woods is similar to those found at mid-ocean ridges (Reeves et al., 2011) reflecting the composition of the oceanic crust.

The PACMANUS (Papua New Guinea – Australia – Canada – MANUS) hydrothermally active area (Binns and Scott, 1993) expands over a roughly 1.5 km long section across Pual Ridge (Fig. 5) in a water depth from 1639 to 1774 m. A total of ten discrete vent fields with variable hydrothermal activity were mapped during two cruises in 2006 and 2011 (Fenway, Mimosa, Roman Ruins, Roger's Ruins, Satanic Mills, Snowcap, Solwara 6, Solwara 7, Solwara 8, and Tsukushi) (Thal et al., 2014). Hydrothermal activity ranges from predominantly high temperature black smoker fluids with temperatures up to 358°C to low temperature diffuse flows of 55°C (Tivey et al., 2006; Craddock et al., 2010; Reeves et al., 2011). Northeast Pual is an area of patchy diffuse venting (temperatures around 35°C) on the crest of Pual Ridge 8 km northeast of PACMANUS (Reeves et al., 2011). The compositions of the vent fluids from PACMANUS and Northeast Pual reveal variable influence of phase separation, magmatic degassing and subseafloor entrainment of seawater (Craddock et al., 2010; Reeves et al., 2011).

DESMOS caldera is located between SuSu Knolls and Pual Ridge. Hydrothermal activity at DESMOS is limited to the hedge of the northern caldera wall and is less in comparison with the other hydrothermal vent fields within the EMVZ. Hydrothermal vents at DESMOS (Onsen Site)

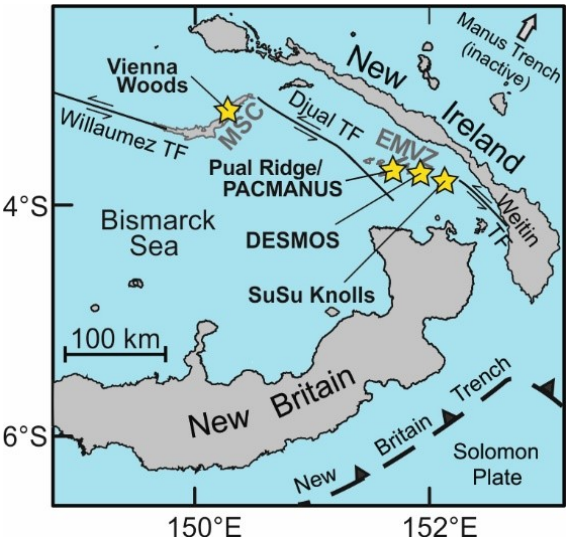

Figure 5: Tectonic map of the Manus Basin showing the active hydrothermal vent fields: Vienna Woods, PACMANUS, DESMOS and SuSu Knolls and Nifonea volcano (stars), major tectonic plates and the plate motions (gray and black arrows).MSC = Manus Spreading Centre, EMVZ = Eastern Manus Volcanic Zone (modified after Seewald et al., 2015)

occur in 1810 m depth from poorly focussed exit sites over an area 30 m in diameter (Gamo et al., 1997). The milky-white acid-sulfate fluids from DESMOS are characterized by moderate venting temperatures of 69°C to 117°C and low pH from 1.0 to 1.4 (Seewald et al., 2015).

The SuSu Knolls area is located 45km east of PACMANUS (Fig. 5) and includes three isolated volcanic centres: Suzette, North Su and South Su with active vent systems in water depths between 1153 to 1504 m. Hydrothermal activity at Suzette is characterized by high-temperature (226°C to 303°C) venting from sulphide-rich chimneys. At North Su the highest diversity in the vent fluid's chemistry was found (Craddock et al., 2010). In this area, venting of white, acid-sulfate fluids as well as black smoker fluid takes place, especially in the summit area of North Su (Craddock et al., 2010; Seewald et al., 2015; Thal et al., 2016). In the summit area of North Su and west of it (in water depths between 1150 and 1200 m), black smoker fluids vent at temperatures up to 332°C (temperature of boiling of seawater at 120 bar). South of the main summit expansive fields of white smokers can be observed. Acid-sulfate fluids are venting at North Su with exit temperatures between 48 and 241°C and pH lower than 2. Prior to the cruise in 2011, the white smoker site with most vigorous venting in 2006 was buried by the products of volcanic cryptodome eruption (Thal et al., 2016). During the sampling campaign in 2011, the Sulfur Candle field, an area with meter-thick flows of liquid sulfur as well as hundreds of white smokers and bubbling of liquid CO_2 was located (Thal et al. 2016). At South Su hydrothermal activity is more limited in comparison with North Su ranging from diffuse fluids (not sampled during the cruises) to high-temperature fluids in the south and southeast (up to 290°C) (Craddock et al., 2010).

1.3.2. New Hebrides Ridge

During the Oligocene to Early Miocene the New Hebrides arc formed due to the subduction of the Pacific Plate underneath the Indo-Australian Plate along the Vitiaz Trench (Hall, 2002; Schellart et al., 2002). Due to the collision with the Melanesian Border Plateau in the Middle to Late Miocene the subduction was accompanied by slab rollback, the opening of the North Fiji Basin (Auzende et al., 1995), and a clockwise rotation of the island arc. Due to this rotation, the D'Entrecasteaux Ridge (a fossil island arc or fracture zone) is subducted since 7.5 Ma as well. Since 3 Ma the Coriolis Troughs in the south and Jean Charcot Troughs in the north (Fig. 6) formed due to drifting of the New Hebrides Ridge. The Coriolis Troughs are located in the eastern back-arc of the southern New Hebrides island arc, located east of the New Hebrides Trench and describe three narrow (up to 40km) graben structures: Vate, Erromango and Futuna from north to south (McConachy et al., 2005; Anderson et al., 2016). Hydrothermal activity was discovered at the Vate Trough. Back-arc rifting at Vate Trough started about 3 Ma ago and is in its incipient stage of spreading (Monjaret et al., 1991, McConachy et al., 2005). The oceanic crust at Vate is comprised of old arc crust at the basin walls and caldera lavas and volcanic cones at the summit

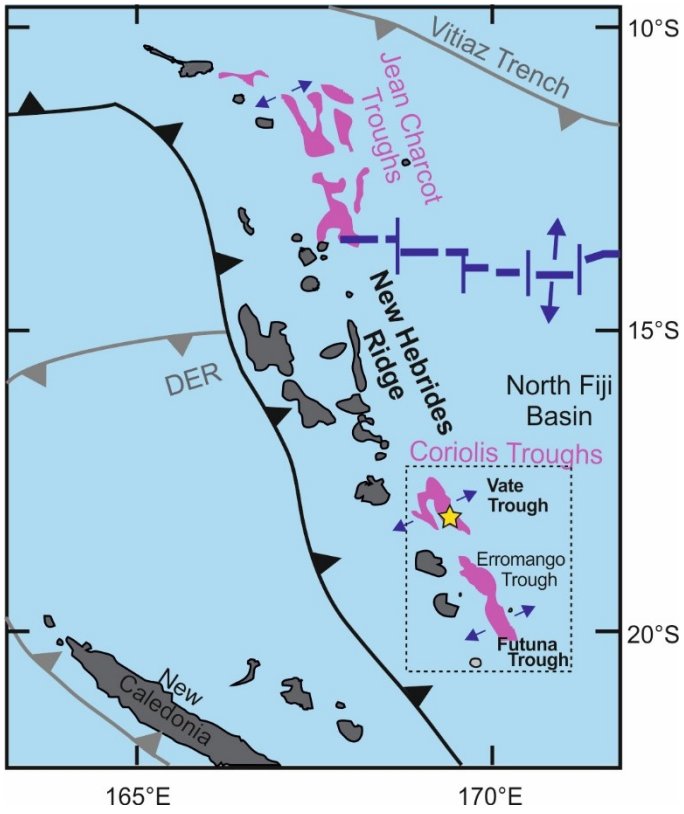

Figure 6: Tectonic map of the New Hebrides back-arc. The back-arc rifts are indicated in purple and spreading centers in blue. The active hydrothermal vent field at Nifonea volcano is indicated by the yellow star. Modified from Anderson et al. (2016). DER = d'Entrecasteaux Ridge

plateau (Anderson et al., 2016). Dominant rock types are subalkalic to alkali basalts, trachybasalts and basaltic trachyandesites (Lima et al., in press).

1.3.2.1 Hydrothermal activity

Hydrothermal activity in the Coriolis Troughs was discovered in the southern part of the Vate trough at Nifonea volcano (Fig. 6). Nifonea volcano is located in a water depth of 1860 to 1875m. Hydrothermal activity occurs within the central part of the caldera in three clusters of several small chimneys. Black smoker and clear vent fluids in this area have temperatures up to 368°C (Table 1; Schmidt et al, 2017). Vent fluids from Nifonea volcano are characterized by limited water-rock interaction and show in their low-Cl contents the effects of extreme boiling.

1.4 Scientific objectives and overview of own research

1.4.1 Motivation and Research aims

One major aim of geochemistry is the evaluation of inputs and sinks that control ocean's chemistry today and through time. Main sources and sinks for most of the elements relate to the riverine and hydrothermal fluxes into seawater, carbonate precipitation, and the alteration of the oceanic crust. Serving as a crucial part for the geochemical cycles for many elements it is thus important to understand and quantify hydrothermal circulation (Edmond et al., 1979; Von Damm, 1985; Palmer and Edmond, 1989). However, the impact of hydrothermal circulation on the composition of seawater is hard to estimate because of large uncertainties in the heat and water

fluxes. Vent systems transfer approximately 11 TW of heat to the ocean, which is about 25 to 30% of the total heat loss of the earth (Stein and Stein, 1994; Jaupart and Mareschal, 2003). The estimates on the global discharge of hydrothermal vent fluids are in the order of $3.5 * 10^{12}$ kg/year for high temperature vent fluids (Elderfield and Schultz, 1996). To estimate the hydrothermal element fluxes into the ocean, the broad chemical range of hydrothermal vent fluids needs to be investigated and the processes and variables controlling the fluid chemistry need to be understood.

The fact that it is often speculated about the processes, which affect the vent fluid's chemistry, manifests that the current knowledge on how to quantify and unravel the processes which occur during hydrothermal circulation and particularly their effect on single components in vent fluids and on the alteration of the oceanic crust is still rather incomplete. Individual factors have been studied intensively in experimental studies (e.g. Foustoukos and Seyfried, 2007) and natural systems (e.g. Edmond et al., 1982, James et al., 1995; Von Damm, 1995). Many processes during hydrothermal circulation have already been quantified. However, experimental setups cannot simulate the complexity of natural hydrothermal vent sites, which makes it challenging to apply experimental data on natural systems.

It has long been stated that vent fluids from MOR settings control the ocean chemistry and hence, most studies on natural submarine hydrothermal systems were conducted along the global MOR systems. However, vent fluids from arc and back-arc settings have a higher variability and some of their components (e.g. Al, B, and CO_2) are considerably enriched relative to MOR fluids (Craddock et al., 2010, Mottl et al., 2011, de Ronde and Stucker, 2015). Still there is only limited data for vent fluids from the subduction-influenced settings. Equally important in this context is not only the limited dataset of vent fluids from arc and back-arc basins, but as well the question, which processes might lead to the high variability in these fluids. Case studies help to expand the datasets, which can be used to understand vent fluid compositions and to estimate hydrothermal fluxes in the ocean.

Vent fluids, which were chosen for the PhD project, are from two different back-arc basins in the Western Pacific (Manus Basin, New Hebrides back-arc). Vent fluids in these settings cover a wide compositional range (Craddock et al., 2010; Reeves et al., 2011, Seewald et al., 2015; Schmidt et al., 2017). To understand and unravel the different processes (magmatic input, phase separation, water-rock interaction) and their influence on the vent fluid's composition, the focus of this dissertation will be on radiogenic strontium (Sr) isotope ratios and "non-traditional" stable metal isotopes (lithium (Li), boron (B) and magnesium (Mg) isotope ratios). These isotopes were analysed in hydrothermal vent fluids and samples from fresh and altered volcanic crust.

The high variability of vent fluids from Manus Basin and the New Hebrides back-arc allow a detailed study on fluids, which are influenced by different sources (different host rock

compositions, altered versus fresh oceanic crust, magmatic gases) and processes (water-rock interaction at different temperatures and different fluid acidities, phase separation and segregation). Due to their different properties (e.g. fluid mobility, volatility, ionic radii) (Chapter 1.2), the examined isotope systems are affected differently during hydrothermal circulation. Consequently, the main objective of this thesis is to identify and understand the individual influences on Sr, Li, B and Mg isotopes during hydrothermal circulation in back-arc basins. This may help to broaden the knowledge on the individual processes during hydrothermal circulation in general and in arc and back-arc settings in specific.

1.4.2 Overview of own research

The research goals of this PhD project, which were outlined in chapter 1.4.1, were addressed within three individual manuscripts (Chapter 3-5). All manuscripts and figures within were written and designed by myself. Furthermore, all Li, B and Mg isotope ratios and most of the Sr isotope ratios in the hydrothermal fluids and volcanic rocks, which are presented in these manuscripts, were prepared and analysed by myself. Eoghan Reeves and Wolfgang Bach provided additional datasets (main and trace elements, Sr isotope ratios) for rocks and fluids from the Manus Basin. All co-authors contributed to the manuscripts through productive discussions, suggestions and comments on the interpretation of the data. The following section briefly summarizes the outcomes of each manuscript with respect to the before mentioned research goals.

Chapter 3: *The influence of magmatic fluids and phase separation on B systematics in submarine hydrothermal vent fluids – case studies from the Manus Basin and Nifonea volcano*

F. Wilckens, E. P. Reeves, W. Bach, A. Meixner, J. S. Seewald, A. Koschinsky, S. A. Kasemann

This manuscript aims to unravel the influences of B concentrations and isotope ratios in a broad range of vent fluids. The study reveals that B in most fluids is influenced by water-rock interaction with fresh and altered oceanic crust and hence might be a good proxy for accessing water-rock interaction during hydrothermal circulation and the basement alteration in the hydrothermal circulation cell. However, the vapour-rich fluids from the Manus Basin and Nifonea volcano deviate from this trend. We found that phase separation at PT-condition well above the two-phase curve may lead to an enrichment of B in the vapour-rich fluids. Because the low B isotope ratios in these fluids apparently do not relate to phase separation, we suggest that they rather reveal evidence for a preferential mobilisation of B from the oceanic crust during interaction with vapour-rich fluids with long residence times in the subsurface. In contrast, fluids with shorter residence times in the subsurface define a trend towards lower B concentrations and might reflect a mixing between hydrothermal fluids and a magmatic fluid rising from the subsurface.

Chapter 4: *Lithium isotope ratios in submarine hydrothermal vent fluids from Manus Basin and Nifonea volcano reveal evidence for negligible Li isotope fractionation during water-rock interaction*

F. K. Wilckens, W. Bach, A. Mexiner, E.P. Reeves, J. S. Seewald, A. Koschinsky, S. A. Kasemann

This manuscript reports on Li isotope systematics in the vent fluids and discusses Li isotope fractionation during water-rock interaction at hydrothermal conditions. The data shows that Li isotope ratios in vent fluids from back-arc basins differ from vent fluids at MOR settings. δ^7Li values are on average about 4‰ lower at back-arc basins, although the composition of the oceanic crust is similar. The manuscript discusses potential reasons for the isotopic offset. Further, the data shows that Li in fluids, which are affected by extreme boiling, is depleted in the vapour-rich phase. In general, the data opens the questions whether leaching of Li from the oceanic crust differs from MOR settings and whether the estimated Li isotopic composition of the global hydrothermal Li flux is valid.

Chapter 5: *Assessing water-rock interaction and basement alteration from B, Mg, Li and Sr isotopes in acid-sulfate fluids*

F. Wilckens, W. Bach, A. Meixner, J. S. Seewald, S.A. Kasemann

The last manuscript presents data of Li, B, Mg and Sr isotope ratios in acid-sulfate fluids. Mg isotope ratios show that Mg in these fluids has not an isotopic signature of the oceanic crust, but is mostly seawater derived. Nevertheless, the combination of Sr, Li and B isotopes show that acid-sulfate fluids are influenced to a significant amount by water-rock interaction. Especially Li and B deviate in their leaching behaviour during argillic alteration. Li appears to be depleted fast in the oceanic crust, whereas B appears to be leached more slowly. The combination of Li and B isotope ratios might thus help to assess the alteration of the oceanic crust in these extreme acidic environments in order to estimate the alteration period during which the fluids have reacted with the host rocks.

1.5 References

Alt, J. (1995) Subseafloor processes in mid-ocean ridge hydrothermal systems, in: Humphris, S.E., Zierenberg, R.A., Mullineaux, L.S., Thomson, R.E. (Eds.), Seafloor Hydrothermal Systems: Physical, Chemical, Biological, and Geological Interactions. American Geophysical Union, Washington, D. C., pp. 85–114.

Anderson, M. O., Hannington, M. D., Haase, K. E., Schwarz-Schampera, U., Augustin, N., McConachy, T.F., Allen, K. (2016) Tectonic focusing of voluminous basaltic eruptions in magma-deficient backarc rifts. *Earth Planet Sci. Lett.* **440**, 43-55.

Araoka, D., Nishio, Y., Gamo, T., Yamaoka, K., Kawahata, H. (2016) Lithium isotopic systematics of submarine vent fluids from arc and back-arc hydrothermal systems in the western Pacific. *Geochim. Geophys. Geosys.* **17**, 3835-3853.

Auzende, J.-M., Pelletier, B., Eissen, J.-P. (1995) The North Fiji basin: geology structure, and geodynamic evolution. In: Taylor, B. (Ed.), *Back-arc Basins: Tectonics and Magmatism*. Plenum, New York, pp. 139-175.

Bach, W., Humphris, S. E. (1999) Relationship between the Sr and O isotope compositions of hydrothermal fluids and the spreading and magma-supply rates at oceanic spreading centres. *Geology* **27**, 1067-1070.

Baker, E.T., German, C.R. (2004) On the global distribution of mid-ocean ridge hydrothermal vent-fields, in: German, C.R., Lin, J., Parson, L.M. (Eds.), Mid-Ocean Ridges: Hydrothermal Interactions between the Lithosphere and Oceans. American Geophysical Union, Washington, D. C., pp. 245–266.

Baumberger, T., Früh-Green, G. L., Dini, A., Boschi, C., van Zuilen, K., Thorseth, I. H., Pedersen, R. B. (2016) Constraints on the sedimentary input into the Loki's Castle hydrothermal system (AMOR) from B isotope data. *Chem. Geol.* **443**, 111-120.

Bebout, G. E., Ryan, J. G., Leeman, W. P., Bebout, A. E. (1999) Fractionation of trace elements by subduction-zone metamorphism – effect of convergent-margin thermal evolution. *Earth Plant. Sci. Lett.* **171**, 63-81.

Binns R. A. and Scott S. D. (1993) Actively forming polymetallic sulfide deposits associated with felsic volcanic-rocks in the Eastern Manus Back-Arc Basin, Papua New Guinea. *Econ. Geol.* **88**(8), 2226–2236.

Bischoff, J. L. (1969) Red Sea geothermal brine deposits: Their mineralogy, chemistry, and genesis. In: Degens ET and Ross DA (eds.) *Hot Brines and Recent Heavy Metal Deposits in the Red Sea*, 368-401. New York: Springer Verlag.

Bischoff, J. L., Rosenbauer, R. J. (1984) The critical point and two-phase boundary of seawater, 200-500°C. *Earth Planet. Sci. Lett.* **68**, 172-180.

Bischoff, J. L., Rosenbauer, R. J. (1985) An empirical equation of state for hydrothermal seawater (3.2 percent NaCl). *Am. J. Sci.* **285**, 725–763.

Bischoff, J. L., Pitzer, K. S. (1985) Phase relations and adiabats in boiling seafloor geothermal systems. *Earth Planet. Sci. Lett*. **75**(4), 327-338.

Bostrom, K., Peterson, M. N. A., Joensuu, O., Fisher, D. E. (1969) Aluminium-poor ferromanganoan sediments on active ocean ridges. *Journal of Geophys. Res.* **74**, 3261-3270.

Both, R., Crook, K., Tylor, B., Brogan, S., Chappell, B., Frankel, E., Liu, L., Sinton, J., Tiffin, D. (1986) Hydrothermal chimneys and associated fauna in the Manus Back-Arc Basin, Papua New Guinea. *EOS* **67**, 489-490.

Butterfield, D.A., Massoth, G.J., McDuff, R.E., Lupton, J.E., Lilley, M.D. (1990) Geochemistry of hydrothermal fluids from Axial Seamount Hydrothermal Emissions Study vent field, Juan de Fuca Ridge: subseafloor boiling and subsequent fluid-rock interaction. *J. Geophys. Res.* **95**, 12895–12921.

Chan, L. H., Edmond, J. M., Thompson, G. (1993) A lithium isotope study of hot springs and metabasalts from mid ocean ridge hydrothermal systems. *J. Geophys. Res.* **98**, 9653–9659.

Chan, L. H., Gieskes, J. M., You, C. F., Edmond, J. M. (1994) Lithium isotope geochemistry of sediments and hydrothermal fluids of the Guaymas Basin, Gulf of California. *Geochim. Cosmochim. Acta* **58**, 4443–4454.

Chaussidon, M., Jambon, A. (1994) Boron content and isotopic composition of oceanic basalts: Geochemical and cosmochemical implications. *Earth and Planet. Sci. Lett.* **21**(3-4), 277-291.

Chaussidon, M., Marty, B. (1995) Primitive boron isotope composition of the mantle. *Science* **269**, 383–386.

Corliss, J.B., Dymond, J., Gordon, L.I., Edmond, J.M., von Herzen, R.P., Ballard, R.D., Green, K., Williams, D., Bainbridge, A., Crane, K., van Andel, T.H. (1979) Submarine thermal springs on the Galapagos rift. *Science* **203**(4385), 1073–83.

Craddock, P. R., Bach, W., Seewald, J. S., Rouxel, O. J., Reeves ,E. and Tivey, M. K. (2010) Rare earth element abundances in hydrothermal fluids from the Manus Basin, Papua New Guinea: indicators of sub-seafloor hydrothermal processes in back-arc basins. *Geochim. Cosmochim. Acta* **74**, 5494–5513.

Davis, A. C., Bickle, M. J., Teagle, D. A. H. (2001) Imbalance in the oceanic strontium budget. *Earth Planet. Sci. Lett.* **211**, 173-187.

Edmond, J. M., Measures, C., McDuff, R. E., Chan, L. H., Grant, C. B. (1979) Ridge crest hydrothermal activity and the balances of the major and minor elements in the ocean: The Galapagos data. *Earth Planet. Sci. Lett*. **46**, 1-18.

Edmond, J. M., Von Damm, K. L., McDuff, R. E., Measures, C. I. (1982) Chemistry of hot springs on the East Pacific Rise and their effluent dispersal. *Nature* **297**, 187-191.

Elderfield, H. and Schultz, A. (1996) Mid-Ocean Ridge Hydrothermal Fluxes and the Chemical Composition of the Ocean. *Annual Rev. of Earth and Plan. Sciences* **24**, 191-224.

Foster, G.L., Pogge von Strandmann, P. A. E., Rae, J. W. B. (2010) Boron and magnesium isotopic composition of seawater. *Geochem. Geophys. Geosyst.* **11**(8), Q08015, doi:10.1029/2010GC003201.

Foustoukos, D.I., James, R.H., Berndt, M.E., Seyfried Jr., W.E. (2004) Lithium isotopic systematic of hydrothermal vent fluids at the Main Endeavour Field, Northern Juan de Fuca Ridge. *Chem. Geol.* **212**, 17–26.

Foustoukos, D. I., Seyfried Jr., W. E. (2007) Trace element partitioning between vapour, brine and halite under extreme phase separation conditions. *Geochim. Cosmochim. Acta* **71**, 2056-2071.

Gamo T., Okamura K., Charlou J. L., Urabe T., Auzende J. M., Ishibashi J., Shitashima K. and Chiba H. (1997) Acidic and sulfate-rich hydrothermal fluids from the Manus back-arc basin, Papua New Guinea. *Geology* **25**(2), 139–142.

German, C. R., Von Damm, K. L. (2005) Hydrothermal Processes. In Treatise on Geochemistry Vol 6 (Eds: H. D. Holland and K. K. Turekian), 182 – 216.

Hall, R. (2002) Cenozoic geological and plate tectonic evolution of SE Asia and the SW Pacific: computer-based reconstructions, model and animations. *Journal of Asian Earth Sciences* **20**, 353-431.

Hannington, M.D., de Ronde, C.E.J., Petersen, S., (2005) Sea-Floor Tectonics and Submarine Hydrothermal Systems. *Econ. Geol.* 100th Anniv., 111–141.

Hedenquist, J. W., Lowenstern, J. B. (1994) The role of magmas in the formation of hydrothermal ore deposits. *Nature* **370**, 519-527.

Hodell, D. A., Mead, G. A., Mueller, P. A. (1990) Variation in the strontium isotopic composition of seawater (8 Ma to present) implications for chemical weathering rates and dissolved fluxes to the oceans. *Chem. Geol.* (Isotope Geosci. Sect.) **80**, 291-307.

Huang, J., Li, S.-G., Xiao, Y., Ke, S., Li, W.-Y., Tian, Y. (2015) Origin of low δ^{26}Mg Cenozoic basalts from South China Block and their geodynamic implications. *Geochim. Cosmochim. Acta* **164**, 298-317.

Huh, Y., Chan, L.H., Zhang, L., Edmond, J.M. (1998) Lithium and its isotopes in major world rivers: implication for weathering and the oceanic budget. *Geochim. Cosmochim. Acta* **62**, 2039-2051.

Ishibashi, J.-I., Urabe, T. (1995) Hydrothermal activity related to arc-backarc magmatism in the western Pacific, in: Taylor, B. (Ed.), *Backarc Basins: Tectonics and Magmatism*. Plenum Press, New York, pp. 451–495.

James, R. H., Elderfield, H., Palmer, M. R. (1995) The chemistry of hydrothermal fluids from the Broken Spur site, 29°N Mid-Atlantic Ridge. *Geochim. Cosmochim. Acta* **59**, 651–659.

James, R. H., D. E. Allen, and W. E. Seyfried Jr. (2003), An experimental study of alteration of oceanic crust and terrigenous sediments at moderate temperatures (51 to 350°C): Insights as to chemical processes in near-shore ridge-flank hydrothermal systems, *Geochim. Cosmochim. Acta* **67**, 681–691.

Jaupart, C and Mareschal, J.C. (2005) Constraints on Crustal Heat Production from Heat Flow Data. In: *Treatise on Geochemistry* Vol **2** (Eds: H. D. Holland and K. K. Turekian), Elsevier Pergamon, 65-84.

Kamenetsky, V. S., Binns, R. A., Gemmell, J. B., Crawford, A. J., Mernagh, T. P., Maas, R., Steele, D. (2001) Parental basaltic melts and fluids in eastern Manus backarc Basin: implications for hydrothermal mineralisation. *Earth Planet. Sci. Lett.* **184** (3-4), 685-702.

Kashefi, K., Lovley, D. R. (2003) Extending the upper temperature limit of life. *Science* **301**, 934.

Kroenke, L. W., Rodda, P- U. (1984) Cenozoic tectonic development of the Southwest Pacific. No. 6. Technical Secretariat of CCOP/SOPAC c/o Mineral Resources Department.

Lee, S. M. and Ruellan, E. (2006) Tectonic and magmatic evolution of the Bismarck Sea, Papua New Guinea: review and new synthesis. In *Back-Arc Spreading Systems: Geological, Biological, Chemical, and Physical Interactions*, vol. **166** (eds. D. M. Christie, C. R. Fisher, S.-M. Lee and S. Givens). AGU Monograph. American Geophysical Union, 263–286.

Leeman, W. P., Tonarini, S., Pennisi, M., Ferrara, G. (2005) Boron isotopic variations in fumarolic condensates and thermal waters from Vulcano Island: Implications for evolution of volcanic fluids. *Geochim. Cosmoch. Acta* **69**, 143-163.

Leeman, W. P., Tonarini, S., Turner, S. (2017) Boron isotope variations in Tonga-Kermadec-New Zealand arc lavas: Implications for origin of subduction components and mantle influences, *Geochemistry, Geophysics, Geosystems*, doi: 10.1002/2016GC006523.

Liebscher, A., Meixner, A., Romer, R. L., Heinrich, W. (2005) Liquid-vapor fractionation of boron and boron isotopes: experimental calibration at 400°C/23 MPa to 450°C/42 MPa. *Geochim. Cosmochim. Acta* **69** (24), 5693-5704.

Lilley, M. D., Lupton, J. E., Butterfield, D. A., Olson, E. (2003) Magmatic events produce rapid changes in hydrothermal vent chemistry. *Nature* **422**, 878-881.

Lima, S.M., Haase. K.M., Beier, C., Regelous, M., Brandl, P.A., Hauff, F., Krumm, S. (accepted for publication) Magmatic evolution and source variation at the Nifonea Ridge (New Hebrides Island Arc). *J. Petrol.* (2017).

Macdonald, K. C., Becker, K., Spiess, F. N., Ballard, R. D. (1980) Hydrothermal heat flux of the "black smoker" vents on the East Pacific Rise. *Earth Planet. Sci. Lett*. **48**(1), 1-7.

Magenheim, A.J., Spivack, A.J., Alt, J.C., Bayhurst, G., Chan, L.H., Zuleger, E., Gieskes, J.M. (1995) Borehole fluid chemistry in hole 504B, leg 137: Formation water or in-situ reaction?, *Proc. Ocean Drill. Program Sci. Results* **137/140**, 141–152.

Martinez F. and Taylor B. (1996) Backarc spreading, rifting, and microplate rotation, between transform faults in the Manus basin. *Mar. Geophys. Res.* **18**(2–4), 203–224.

McConachy, T. F., Arculus, R. J., Yeats, C. J., Binns, R. A., Barriga, F.J.A.S., McInnes, B.I.A., Sestak, S., Sharpe, R., Rakau, B., Tevi, T (2005): New hydrothermal activity and alkali volcanism in the backarc Coriolis Troughs, Vanuatu. *Geology* **33**, 61-64.

Millot, R., Guerrot, C., Vigier, N. (2004) Accurate and high-precision measurement of lithium isotopes in two reference materials by MC-ICP-MS. *Geostand. Geoanal. Res.* **28**, 153–159.

Misra, S., Froelich, P.N. (2012) Lithium isotope history of Cenozoic seawater: changes in silicate weathering and reverse weathering. *Science* **335**, 818–823.

Monjaret, M. C., Bellon, H., Maillet, P. (1991) Magmatism of the troughs behind the New Hebrides island arc (RV Jean Charcot SEAPSO 2 cruise): K-Ar geochronology and petrology. *J. Volcanol. and Geotherm. Res.* **46**, 265-280.

Mottl, M. J. and Holland, H. D. (1978) Chemical exchange during hydrothermal alteration of basalt by seawater: I. Experimental results for major and minor components of seawater. *Geochim.Cosmochim. Acta* **42**(8), 1103–1115.

Mottl, M. J., Seewald, J. S., Wheat, C. G., Tivey, M. K., Michael, P. J., Proskurowski, G., McCollom, T. M., Reeves, E., Sharkey, J., You, C.-F., Chan, L.-H., Pichler, T. (2011) Chemistry of hot springs along the Eastern Lau Spreading Center. *Geochim. Cosmochim. Acta* **75**, 1013–1038.

Palmer, M.R., Edmond, J.M. (1989) The strontium isotope budget of the modern ocean. *Earth. Planet. Sci. Lett.* **92**, 11-26.

Palmer, M. R. (1991) Boron-isotope systematics of Halmahera arc (Indonesia) lavas: evidence for involvement of the subducted slab. *Geology* **19**, 215–217.

Palmer, M. R., Edmond, J. M. (1992) Controls over the strontium isotope composition of river water. *Geochim. Cosmochim. Acta* **56**(5), 2099-2111.

Pearce, J. A., Stern, R. J. (2006) Origin of Back-Arc Basin Magmas: Trace Element and Isotope Perspectives, in: Christie, D.M., Fisher, C.R., Lee, S.-M., Givens, S. (Eds.), *Back-Arc*

Spreading Systems: Geological, Biological, Chemical, and Physical Interactions. American Geophysical Union, Washington, D. C., pp. 63–86.

Piranjo, F. (2008) Water and Hydrothermal Fluids on Earth. In: *Hydrothermal Processes and Mineral Systems*, Springer.

Reeves, E. P., Seewald, J. S., Saccocia, P., Bach, W., Craddock, P. R., Shanks, W. C., Sylva, S. P., Walsh, E., Pichler, T. and Rosner, M. (2011) Geochemistry of hydrothermal fluids from the PACMANUS, Northeast Pual and Vienna Woods hydrothermal fields, Manus Basin, Papua New Guinea. *Geochim. Cosmochim. Acta* **75**, 1088–1123.

Ryan, J.G., Langmuir, C. H. (1993) The systematics of boron abundances in young volcanic rocks. *Geochim. Cosmochim. Acta* **57**, 1489-1498.

Sakai, H., T. Gamo, E. S. Kim, M. Tsutsumi, T. Tanaka, J. Ishibashi, H. Wakita, M. Yamano, and T. Oomori (1990b), Venting of carbon dioxide-rich fluid and hydrate formation in Mid-Okinawa Trough backarc basin, *Science* **248**, 1093–1096.

Schellart, W. P., Lister, G. S., Jessel, M. W. (2002) Analogue modelling of arc and backarc deformation in the New Hebrides arc and North Fiji Basin. *Geology* **30**, 311-314.

Schmidt, K., Garbe-Schönberg, D., Hannington. M. D., Anderson, M. O., Bühring, B., Haase, K., Haruel, C., Lupton, J. E., Koschinsky, A. (2017) Boiling vapour-type fluids from the Nifonea vent field (New Hebrides Back-Arc, Vanuatu, SW Pacific): Geochemistry of an early-stage, post-eruptive hydrothermal system. *Geochim. Cosmochim. Acta* **207**, 185-209.

Seewald, J. S., Reeves, E. P., Bach, W., Saccocia, P. J., Craddock, P. R., Shanks III, W. C., Sylva, S. P., Pichler, T., Rosner, M., Walsh, E. (2015) Submarine Venting of magmatic volatiles in the Eastern Manus Basin, Papua New Guinea. *Geochim. Cosmochim. Acta* **163**, 179-199.

Seyfried, W. E. and Bischoff, J. L. (1981) Experimental seawater–basalt interaction at 300 C, 500 bars, chemical exchange, secondary mineral formation and implications for the transport of heavy metals. *Geochim. Cosmochim. Acta* **45**(2), 135–147.

Seyfried, W. E. Jr., Chen, X., Chan, L.-H. (1998) Trace Element Mobility and Lithium Isotope Exchange During Hydrothermal Alteration of Seafloor Weathered Basalt: An Experimental Study at 350°C, 500 bars. *Geochim. Cosmochim. Acta* **62**, 949-960.

Seyfried, W. E. Jr., Shanks, W. C. III (2004) Alteration and mass transport in hydrothermal systems at mid-ocean ridges: Controls on the chemical and isotopic composition of axial vent fluid. In: Davis E and Elderfield H (eds.) *The Hydrology of the Ocean Crust*, pp. 451-495. Cambridge, UK: Cambridge University Press.

Sinton, J. M., Ford, L. L., Chappell, B. and McCulloch, M. T. (2003) Magma genesis and mantle heterogeneity in the Manus back-arc basin, Papua New Guinea. *J. Petrol.* **44**(1), 159–195.

Spivack, A. J., Berndt, M. E., Seyfried Jr, W. E. (1990) Boron isotope fractionation during supercritical phase separation. *Geochim. Cosmochim. Acta* **54**, 2337-2339.

Stein, C. A., Stein, S. (1994) Constraints on hydrothermal heat flux through the oceanic lithosphere from global heat flow. *Journal of Geophysical Research* **99**, 3081-3095.

Taylor, B. (1979) Bismarck Sea: Evolution of a back-arc basin. *Geology* **7**, 171–174.

Taylor, B., Crook, K. and Sinton, J. (1994) Extensional transform zones and oblique spreading centers. *J. Geophys. Res.: Solid Earth* **99**(B10), 19707–19718.

Teng, F.-Z., Hu, Y., Chauvel, C. (2016) Magnesium isotope geochemistry in arc volcanism. *Proc. Natl. Acad. Sci.* **113**(26), 7082-7087.

Thal, J., Tivey, M. A., Yoerger, D, Jöns, N., Bach, W. (2014) Geologic setting of PACManus hydrothermal vents – High-resolution mapping and in situ observations. *Marine Geology* **355**, 98-114.

Thal, J., Tivey, M., Yoerger, D. R., Bach, W. (2016) Subaqueous cryptodome eruption, hydrothermal activity and related seafloor morphologies on the andesitic North Su volcano. *J.of Volcanol. Geotherm. Res*. **323**, 80-96.

Tipper, E. T., Galy, A., Gaillardet, J., Bickle, M.J., Elderfield, H., Carder, E.A. (2006) The magnesium isotope budget of the modern ocean: Constraints from riverine magnesium isotope ratios. *Earth Planet. Sci. Lett.* **250**(1-2), 241-253.

Tivey M., Bach W., Seewald J., Tivey M. K., Vanko D. A. and the Shipboard Science (2006) Cruise Report for R/V Melville cruise MGLN06MV – Hydrothermal systems in the Eastern Manus Basin: Fluid Chemistry and Magnetic Structure as Guides to Subseafloor Processes. Woods Hole Oceanographic Institution (available upon request to authors).

Tivey, M.K. (2007) Generation of seafloor hydrothermal vent fluids and associated mineral deposits. *Oceanography* **20**, 50–65.

Tomascak, P.B., Langmuir, C.H., Roux, P.J., Shirey, S.B. (2008) Lithium isotopes in global mid-ocean ridge basalts. *Geochim. Cosmochim. Acta* **72**, 1626-1637.

Verney-Carron, A., N. Vigier, and R. Millot (2011), Experimental determination of the role of diffusion on Li isotope fractionation during basaltic glass weathering, *Geochim. Cosmochim. Acta* **75**, 3452–3468.

Verney-Carron, A., Vigier, N., Millot, R., Hardarson, B.S. (2015) Lithium isotopes in hydrothermally altered basalts from Hengill (SW Iceland). *Earth Planet. Sci. Lett.* **41**, 62-71.

Von Damm K. L., Edmond J. M., Measures C. I. and Grant B. (1985) Chemistry of submarine hydrothermal solutions at Guaymas Basin, Gulf of California. *Geochim. Cosmochim. Acta* **49**, 2221-2237.

Von Damm, K. L. (1988) Systematics of and postulated controls on submarine hydrothermal solution chemistry. *Journal of Geophys. Res. Solid Earth* **93**, 4551-4561.

Von Damm, K.L. (1995) Controls on the chemistry and temporal variability of seafloor hydrothermal fluids, in: Humphris, S.E., Zierenberg, R.A., Mullineaux, L.S., Thomson, R.E. (Eds.), *Seafloor Hydrothermal Systems: Physical, Chemical, Biological, and Geological Interactions*. American Geophysical Union, Washington, D. C., pp. 222–247.

Von Damm, K. L., Lilley, M. D. (2004) Diffuse flow hydrothermal fluids from 9°50′N East Pacific Rise: Origin, evolution and biogeochemical controls. In: Wilcock WS, Delong EF, Kelley, DS, Baross, JA, Cary, SC (eds.) *The Subseafloor Biosphere at Mid-Ocean Ridges*, Geophysical Monograph Series, vol. 144, pp. 245-268. Washington, DC: American Geophysical Union.

Wimpenny, J., S. R. Gislason, R. H. James, A. Gannoun, P. A. E. Pogge von Strandmann, and K. W. Burton (2010), The behavior of Li and Mg isotopes during primary phase dissolution and secondary mineral formation in basalt, *Geochim. Cosmochim. Acta* **74**, 5259–5279.

Wu, S.-F., You, D.-F., Lin, Y.-P., Valsami-Jones, E., Baltatzis, E. (2016) New boron isotopic evidence for sedimentary and magmatic fluid influence in the shallow hydrothermal vent system of Milos Island (Aedean Sea, Greece). J. of Volcanol. Geotherm. Res. **310**, 58-71.

Wunder, B., Meixner, A., Romer, R. L., Wirth, R., Heinrich, W., (2005) The geochemical cycle of boron: constraints from boron isotope partitioning experiments between mica and fluid. *Lithos* **84**, 206–216.

Yamaoka, K., Hong, E., Ishikawa, T., Gamo, T., Kawahata, H. (2015) Boron isotope geochemistry of vent fluids from arc/back-arc seafloor hydrothermal systems in the western Pacific. *Chem. Geol.* **392**, 9-18.

You, C.-F., Butterfield, D. A., Spivack, A. J., Gieskes, J. M., Gamo, T., Campbell, A. J. (1994) Boron and halide systematics in submarine hydrothermal systems: effects of phase separation and sedimentary conditions. *Earth Planet. Sci. Lett.* **123**, 227–238.

Chapter 2: Methodology

2.1 Sample collection

This study is based on vent fluids and rock samples from Manus Basin and Nifonea volcano, which were sampled during three different expeditions:

- the MAGELLAN-06 cruise aboard R/V Melville in 2006 (July to August) (cruise report: Tivey et al., 2006)
- the BAMBUS cruise (SO-216) aboard R/V Sonne in 2011 (June to July) (cruise report: Bach et al., 2011)
- the VANUATU cruise (SO-229) aboard R/V Sonne in 2013 (July) (cruise report: Koschinsky et al., 2013)

During the MAGELLAN-06 cruise (Tivey et al., 2006), samples were taken from the Manus MSC and the EMVZ (SER). Sampling of both vent fluids and volcanic rocks was conducted with ROV (Remotely Operated Vehicle) Jason II (Tivey et al., 2006). Vent fluids were collected with titanium isobaric gas-tight (IGT) fluid samplers (Seewald et al., 2002) and titanium syringe-style "major" samplers (Edmond et al., 1992). For most orifices, two gas-tight and one "major" sample were collected, always accompanied by fluid temperature measurements. Coevally to the sample collection with IGT samplers, temperature was measured with attached thermocouples. At those sample sites restricted to "major" samplers only, temperature was measured prior to sampling with the Jason II temperature probe. In total, 70 gas-tight fluid samples and 34 "major" fluid samples were collected. Fluid samples were homogenized and subsamples for isotope measurements were extracted within ten hours of vehicle recovery to ensure comparability of fluid analyses and prevent sample modifications. Volcanic rock samples were collected using the ROV Jason II. Upon recovery, the samples were weighed, measured for size and described in terms of colour, texture, mineral composition, grain size, vesicularity, phenocryst size and alteration. Then they were dissected and split for the different institutes.

The BAMBUS cruise was a follow-up cruise of the MAGELLAN-06 expedition. Samples during this expedition were taken from PACMANUS and SuSu Knolls, both located in the EMVZ (Fig. 5). Samples were collected using titanium IGT samplers (Seewald et al., 2002) and the Kiel Pumping System (KIPS) (Garbe-Schönberg et al., 2006) installed on ROV MARUM QUEST (Bach et al., 2011). As for the 2006 samples, temperature was measured simultaneously during sampling with IGT-samplers. In total, 21 successful IGT fluid samples were taken. Subsequent to sampling, samples were homogenized and subsamples for isotope measurements were taken.

Samples from Nifonea volcano and Futuna Trough (Fig. 6) were collected during the VANUATU cruise in 2013. Fluids and rocks were sampled with ROV Kiel 6000. For fluid sampling KIPS was installed on the ROV with an integrated high-temperature probe mounted on the slurpgun nozzle.

In total, eight fluids from five individual vent sites were taken at Nifonea volcano, using the KIPS system.

For this study a subset of 91 fluid samples and 22 rock samples were chosen for boron (B) isotope analysis, 82 fluid samples and 25 rock samples for lithium (Li) isotope analysis, 62 fluid samples and 24 rock samples for strontium (Sr) isotope analysis and 18 fluid samples for magnesium (Mg) isotope analysis. Selection of fluid and rock samples was based on their major and trace elemental compositions with the idea to analyse a representative amount of samples, which cover the entire chemical variation in both rocks and fluids from each of the different study areas.

2.2 Sample preparation

Sample preparation for the methods used in this PhD project were conducted in the clean and sample preparation labs from the "Isotope Geochemistry Group" at MARUM – Centre for Marine and Environmental Sciences and in the sample preparation lab of the working group "Petrology of the ocean crust" located in the "Geo-building" at the University of Bremen.

2.2.1 Vent fluids

To prepare the vent fluid samples for Li, Mg and Sr column procedures, between 0.05 to 2.1 ml of the fluid samples (depending on the individual concentrations of Li, Mg and Sr) were dried at 90°C in Savillex beaker in the clean lab. Fluid samples for the chemical separation of B were not prepared.

2.2.2 Volcanic rocks

Prior to the chemical purification volcanic rock samples were cleaned and milled. In a first step, samples were checked for alteration rinds on the rock surface. If significant alteration rinds (change in mineralogy, texture, wider than 0.5 cm) were observable, they were separated from the bulk rock using a diamond saw, which is installed in the "Sägeraum-Labor" (room 0030, Geo-building). These rinds were also processed and analysed, since they serve as an alteration counterpart to the fresh rock. Afterwards, the rock samples and their alteration rims were crushed into smaller pieces using a simple hammer and sonicated with ultrapure water (to get rid of entrained seawater and pore water), dried at 110°C and pulverized using a planetary mill with agate grinding bowls and balls (Pulverisette 5 from Fritsch). All of these steps were conducted in the preparation lab of the working group "Petrology of the ocean crust".

The digestion of the rock powders for the preparation of Li, Mg and Sr isotope ratios was done in the clean laboratory (Isotope Geochemistry, MARUM). About 50 mg of the samples was dissolved in 2 ml of a mixture of concentrated, ultrapure HF and HNO_3 (4:1). This mixture reacted for at least 24 hours in closed 15 ml Savillex beakers at 120°C. After cooling, the samples

were vaporized at 90°C. Subsequently, to get rid of potential organic matter, concentrated H_2O_2 was added to the sample and vaporized at 90°C. To remove the residual fluorides, which formed during the reaction with HF, 1 ml of concentrated HCl was added and vaporized at 90°C. This step was repeated at least for two times.

Because lithium can form insoluble fluorides, it can be lost in the residue. Furthermore, we had analytical problems during the purification procedure of lithium (lithium loss during column chemistry) in the sulphide and metal rich rock samples. Thus the samples for Li separation were additionally treated with 1 ml of concentrated HCl and HNO_3 (1:1) and vaporized at 110°C and afterwards two times with 0.5 ml of 6M HCl, which was vaporized at 90°C. After this additional treatment lithium loss during column separation did not occur.

Rock samples for the preparation and measurement of B isotope ratios were treated differently. Boron was extracted from the rock powders using an alkaline fusion technique modified after Tonarini et al. (1997). 250 to 500 mg of sample powder was mixed with the quadruple amount of K_2CO_3 in platinum-crucibles and fused for about 20 minutes at temperatures above 900°C (melting point of K_2CO_3 = 891°C) with a gas burner. After cooling down to room temperature, the sample was moistened with about 3 to 5 ml ultrapure water (up to one quarter of the platinum-crucible) and stored overnight in the drying oven at 50°C. The samples were then transferred into 30 ml Savillex beaker and reacted for 3 additional hours at 70°C in the drying oven. Subsequently, the suspension was centrifuged and transferred into 30 ml Savillex beaker. To transfer the solution quantitatively, the solid residue was flushed three times with ultrapure water. In a next step about 300 µl of the resin Amberlit IRA743 (20 – 50 mesh) was added to the solution and reacted for two days either at 60°C on the hot plate or on the magnetic stirrer.

2.3 Sample purification for concentration and isotope measurements

Since isotope ratio measurements can be altered through matrix elements, Li, B, Mg and Sr were separated from the sample matrix with different chemical separation methods. Chemical separations of the sample matrixes and the measurements of all isotope systems were performed in the Isotope Geochemistry Laboratory at MARUM – Centre for Marine Environmental Sciences, University of Bremen, Germany.

2.3.1 Strontium

Sr was separated from the sample matrix using an ion exchange chromatography technique. Solid and liquid samples were separated with the same separation procedure. For Sr isotope analysis sample amounts containing about 300 ng Sr were dried and redissolved in 0.5 ml 2M HNO_3. The chromatographic separation was done with Sr spec resin using a method modified after Pin and Bassin (1992), which is described in detail in the separation instruction (Appendix 1). About 70 µl of Sr spec was filled with a pasteur pipette into homemade columns (cropped tips from pasteur

pipettes) out of polyethylene. For each separation series 20 columns were available. Prior to sample loading the resin was cleaned with ultrapure water (4x column volume) and 2M HNO_3 (2x column volume). The sample was loaded onto the column in 100 µl steps. Afterwards the columns were rinsed with 12 times 100 µl 2M HNO_3, two times 500 µl 7M HNO_3 and three times 2M HNO_3 to remove the sample matrix. The strontium fraction was eluted using five times 200 µl 0.05M HNO_3. The resin was discarded. 20 µl of 0.1M H_3PO_4 was added to the Sr fraction and the Sr fraction was dried at 120°C on the hot plate. Subsequently, to remove residual resin material 40 µl of conc. HNO_3 was added to the sample and dried at 120°C and afterwards 40 µl of H_2O_2 was added into the warm beaker and dried at 110°C. The separated Sr fraction was dissolved in 3 µl 0.1M H_3PO_4 and loaded together with a tantalum emitter (Birck HB) prior and subsequent to the sample ("sandwich" technique) onto degassed rhenium filaments (Birck, 1986). Strontium isotope ratios were measured using a Triton thermal ionization mass spectrometer (TIMS) by ThermoFischer Scientific. Measurements were done in the dynamic mode. Instrumental mass fractionation was corrected using $^{88}Sr/^{86}Sr=8.375$. The instrumental precision for $^{87}Sr/^{86}Sr$ was obtained by repeated analysis of the international reference NIST 987, which has a value of 0.710248±15 (2SD, n=12). To validate and verify the chemical separation and digestion techniques used in this study, several international reference materials were separated and measured as well (BHVO-2, IAEA-B5, BM). The results for BHVO-2 ($^{87}Sr/^{86}Sr$ = 0.70347±2 (2SD, n=2)) are within analytical uncertainty in agreement with literature values ($^{87}Sr/^{86}Sr$ = 0.70348±6 (2SD, n=80).

2.3.2 Lithium

Li was separated from the sample matrix by ion exchange chromatography as well. Both liquid and solid samples were separated in the same procedure. For Li isotope analysis at least 100 ng Li was loaded onto the column. Li was separated from its sample matrix using a two-step column separation modified after Moriguti and Nakamura (1998). Due to its small resin volumes, this separation technique has its advantage in the low procedural blanks. The first separation was done with PP-BIORAD columns using 1.4 ml BIORAD resin AG 50WX8 (200-400 mesh) (resin volume in 6M HCl). The second separation was done in PE BIORAD Bio-spin® columns using 1.0 ml BIORAD resin AG 50WX8 (200-400 mesh) (resin volume in 6M HCl). The detailed separation instruction is given in Appendix 2. In each separation series 12 columns were available. At least one column was always blocked for a procedure blank and one for a reference material (L-SVEC, seawater, BHVO-2, IAEA-B5). After the second separation step, samples were evaporated at 90°C and afterwards redissolved in 1 ml of 2% HNO_3 to check Li concentrations on a ThermoFischer Scientific Neptune Plus Multicollector-inducitvely coupled plasma-mass spectrometer (MC-ICP-MS). For this, 50 µl of each sample and 200 µl of 2% HNO_3 were pipetted into clean tubes used for MC-ICP-MS measurements. Since Li isotopes fractionate

during ion exchange chromatography, the fractions before and after the Li fraction were sampled during the separation steps as well, and were redissolved after evaporation in 0.5 ml of 2% HNO_3 to check for Li loss. Because the elution curve of sodium (Na) during the column chemistry is close to the elution curve of Li, the separated Li fractions were also checked for Na contamination, since it can influence the Li isotope ratio measurements. Li isotope ratios were measured on the MC-ICP-MS using the standard-sample-bracketing method with the international reference material L-SVEC as bracketing standard. 2% HNO_3 was used for baseline corrections and was measured before and after each standard and sample. ^{6}Li and ^{7}Li were measured simultaneously on the Faraday cups L4 and H4. Typical intensities for ^{7}Li in samples and bracketing standards during the isotope measurements were around 1.4 V; the baseline had typical intensities around 10 mV. Isotope data for Li is reported in delta notation relative to the bracketing standard and expressed in per mill (‰).

$$\delta^{7}Li\ [‰] = \left[\frac{\left(\frac{^{6}Li}{^{7}Li}\right)_{sample}}{\left(\frac{^{6}Li}{^{7}Li}\right)_{L-SVEC}} - 1\right] \cdot 1000 \qquad (1)$$

To control the preparation procedure and examine the effects of contamination and parameter change, solutions of continuously measured standard materials were included in each sample batch and handled in the same way as the actual samples. Procedural blanks were lower than 0.01%. Hence, they were not affecting the sample composition. The accuracy and precision of the method was obtained by repeated preparation and analysis of an internal seawater standard (bottom seawater from SuSu Knolls), and the international reference materials L-SVEC and BHVO-2. Long-time reproducibility of L-SVEC was δLi of 0.0±0.1‰ (2SD, n=17). Li isotope ratios and concentrations of an internal laboratory seawater standard (bottom seawater from SuSu Knolls) ($\delta^{7}Li$ of 31.1±0.2‰ (2SD, n=5)) are in agreement with literature values (+31.1±0.3‰ (2SD), Huang et al., 2010; Wimpenny et al., 2010; Pogge von Strandmann et al., 2010). The basalt reference material BHVO-2 has a $\delta^{7}Li$ value of 4.3±0.3‰ (2SD, n=2), which is within the range of the published isotope values (4.5±0.3‰, 2SD; Gao et al., 2012; Genske et al., 2014; Magna et al., 2015).

2.3.3 Boron

B in liquid and solid samples was separated from the sample matrix by two different methods. B in fluids was purified using a sublimation method modified after Wang et al. (2010). For each sublimation, sample amounts containing a minimum of 300 ng boron were used and placed on the lid of a conical Savillex beaker. Maximum sample amounts were 45 µl due to the limitations of this method. If sample volumes were smaller than 45 µl, the sample was mixed with ultrapure water to acquire a total volume of 45 µl. Afterwards 5 µl of 7M HNO_3 was added to the 45 µl mixture of ultrapure water and sample. After closing the beaker carefully, it was covered with

aluminium foil and placed liddown for 18 hours at 98°C on the hot plate. After cooling, the condensate was diluted in 1 ml 2% HNO_3. 50 µl of this sample solution was mixed with 200 µl 2% HNO_3 to check the concentrations in the sample solutions. In each sublimation series typically 12 samples and two reference materials were processed.

B in the solid samples was purified by ion exchange chromatography. The solid samples were prepared for the purification as described in chapter 2.2. For the preparation of solid samples 6 platinum crucibles were available, so that the sample preparation was repeated once to separate ten samples and two solid reference materials at the same time. Care must be taken here, since B should not be stored for a long time due to B loss from the fluid. After preparation the samples were passed through a two-step column separation as described in Romer et al. (2014). During the first column separation, B in the samples is separated from the anions. Empty PP BIORAD columns are cleaned and conditioned with 6.6M HCl, ultrapure H_2O, 2M NH_4OH and ultrapure H_2O as described in the separation instruction (Appendix 3) (Fig. 1a). Afterwards resin is filled into the columns. The resin (Amberlite IRA 743, 20 – 50 mesh) already reacted with the sample (as described in Chapter 2.2) to absorb B from the solution. The resin was rinsed in the columns two times with 1 ml H_2O, two times with 1 ml NH_4OH and four times with 1 ml H_2O. Afterwards, the B fraction was eluted in weighed 30 ml Savillex beaker in 24 times 0.5 ml of 0.5M HCl. In addition, 2 ml after the B fraction ("tail") were also rinsed with 0.5 ml 0.5M HCl to check for B loss. This is important, since B isotopes fractionate similar to Li during ion exchange chromatography, which makes it necessary to obtain a high recovery yield during the separation procedure. 30 ml Savillex beaker containing the B fraction were weighed again and the solution was homogenized by shaking. 50 µl of the B fraction was pipetted into sample tubes and diluted with 450 µl of 0.5M HCl. B concentrations of these samples were measured using the MC-ICP-MS. Additionally, B concentration in the 2 ml, which were rinsed after the B fraction, were measured to check for B loss. Afterwards, B contents of the samples were calculated and 0.2%

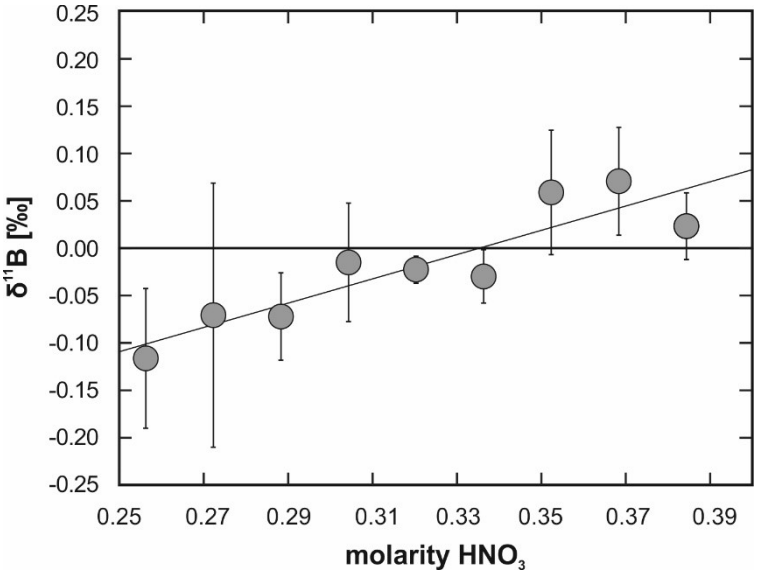

Figure 7: Shown are the effects of a molarity missmatch between sample and bracketing standart. In this figure all measured samples should have a $\delta^{11}B$ value of 0.0‰. However, isotope ratios of the samples, which are dissolved in HNO_3 with a deviating molarity relative to the HNO_3 used for the bracketing standart, have lower and higher ratios. Furthermore, the measurements are less stable, which results in higher errors.

mannitol solution was added in a ratio of 1:40 (boron : mannitol). Subsequently, the samples were dried at temperatures lower than 65°C. In a second separation step, B was separated from cations in PP BIORAD Bio-Spin® columns with 1 ml of the BIORAD resin AG 50WX8 (200-400 mesh). Prior to sample loading, the resin was stirred up and cleaned in 6.2N HCl. Conditioning of the resins was done with 0.02N HCl. The separation procedure is described in the separation instructions (Appendix 3). Similar to the first separation step, the "tail" fraction rinsed in the 2 ml after the B fraction was also sampled. Evaporation of the sample and tail solutions was done at temperatures lower than 65°C. Caution is advised here, since it is important that the samples do not dry completely to prevent B loss. Afterwards the B fractions of the samples were dissolved in variable amounts of 2% HNO_3 depending on the B content to approximately 150 ng/g solutions. Tails were dissolved in 0.5 ml 2% HNO_3. Concentrations in the sample solutions and tails were measured on the MC-ICP-MS. During each series of samples, 14 columns were available. Two columns were blocked for the international reference material IAEA-B5, one for a procedure blank and one for the international reference material NIST SRM 951.

B isotope ratios measurements for both liquid and solid samples were also measured on the MC-ICP-MS. Isotope measurements were performed using a stable introduction system (SIS) and a high-efficiency x-cone. All sample solutions were diluted to a concentration of 100 ng/g B in 2% HNO_3. The isotope ratio measurements were done using the standard-sample-bracketing method in 100 ppb B solutions with the boric acid NIST SRM 951 as bracketing standard. It is essential to dissolve the sample and bracketing standard in the same acid to avoid systematic errors during the measurement (Fig.7). 2% HNO_3 was used for baseline corrections and was measured before and after each standard and sample. ^{10}B and ^{11}B were measured simultaneously on the Faraday cups L3 and H3. Typical intensities for ^{10}B in samples and bracketing standard during the isotope measurements were around 1.5V, the baseline had typical intensities around 20mV. Isotope data is reported in delta notation relative to the certified reference material NIST SRM 951 and expressed in per mill (‰):

$$\delta^{11}B\ [‰] = \left[\frac{\left(\frac{^{11}B}{^{10}B}\right)_{sample}}{\left(\frac{^{11}B}{^{10}B}\right)_{NBS-951}} - 1\right] \cdot 1000 \qquad (2)$$

To validate and verify the chemical separation and digestion techniques used in this study, each separation step during the B purification in the silicate phases was checked for B loss. B loss was always smaller than 0.1% for solid samples and procedural blanks were lower than 0.5% of total B for solid samples and less than 1% of total B for liquid samples and hence had no influence on the B composition of the samples. The external precision based on repeately prepared and analysed reference materials is better than 5% (2SD) for B concentrations and 0.3‰ (2SD) for $\delta^{11}B$. Long-time reproducibility of NIST SRM 951 was $\delta^{11}B$ of 0.0±0.3‰ (2SD, n=12). B isotope

ratios and concentrations of the international seawater standard IAEA-B-1 ($\delta^{11}B$ of 39.8±0.3‰ (2SD, n=4)) and an internal laboratory seawater standard (bottom seawater from SuSu Knolls) ($\delta^{11}B$ of 39.8±0.3‰ (2SD, n=6), 445±26 µmol/kg (2SD, n=6)) are in agreement with literature values (+39.61±0.2‰ (2SD), Foster et al., 2010). The basalt reference material IAEA-B5 has a B concentration of 9.3±0.5 mg/kg (2SD, n=4) and a $\delta^{11}B$ value of -4.2±0.1‰ (2SD, n=4), which is within the range of the published concentration values (8.9 to 11.3 mg/kg B) and in agreement with reccommended (-3.8±2.0‰, 2SD) and published isotope values (-4.3±.2‰, 2SD; 3.71±0.73‰, 2 SD),(Gonfiantini et al., 2003; Romer et al., 2014, Berryman et al. 2017).

2.3.4 Magnesium

Similar to Li and B, Mg was separated from the sample matrix using a two-step column separation. The calibration of the column separation was part of the PhD project. Based on published methods and K_D values a separation scheme was developed, which is suitable for various materials (high- and low-salinity fluids, carbonates, silicates). The selection of the eluent was done based on published distribution coefficients for different molarities of HNO_3 and HCl (Strelow, 1960; Strelow et al., 1965). For the calibration total amounts of 5 µg Mg of a seawater sample, a carbonate sample and a pure Mg solution were used. Therefore, a maximum of 5 µg, but usually only 2 µg Mg, of the sample was loaded onto the columns. The elution curves for the two separation steps are displayed in Fig. 8. The first separation step was performed with 1 ml of the BIORAD cation exchange resin AG 50W X8 (volume in 6M HCl), 200-400 mesh in BIORAD BIO-spin® columns in 1M HCl as described in the separation instruction (Appendix 4). The second separation step was performed in the same columns with 1M HNO_3 (separation instruction in the Appendix 4). During each series of samples, 14 columns were available. The reliability and accuracy of the developed method and of each chemical series was verified by blocking one column for a procedure blank and at least one column for an international reference material.

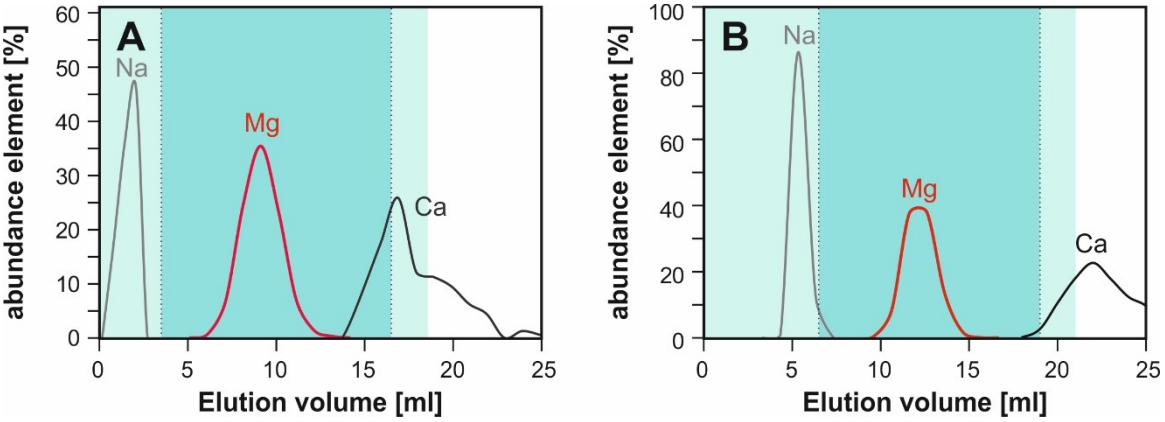

Figure 8: Elution curves for a carbonate (JCP-I) in the two separation step during Mg purification. (A) shows the elution of sodium (Na), magnesium (Mg) and calcium (Ca) in the first separation step and (B) in the second step (as decribed in the separation instruction in the Appendix). The blue shaded areas mark the area, where the Mg fraction was collected. The light blue areas are the fractions before and after the Mg fraction, which were checked for Mg loss.

Used international reference materials are pure Mg standards (DSM-3, Cambridge-I) and an internal seawater standard (bottom seawater from SuSu Knolls). Similar to Li and B, the elution fractions, which were rinsed directly before and after the Mg fractions, were also sampled and checked for Mg loss. These fractions were dried at 90°C and re-dissolved in 0.5 ml of 2% HNO_3. The Mg fractions were also evaporated at 90°C and redissolved in 1 ml 2% HNO_3. For the Mg concentration check 50 µl of sample solution was mixed with 400 µl 2% HNO_3 in ICP tubes. These fractions were also checked for impurities with Na or Ca on the Neptune MC-ICP-MS. For Mg isotope ratio measurements, pure Mg solutions were adjusted to a Mg concentration of 200 ng/g. Samples were measured using the standard-sample bracketing technique to correct for instrumental mass bias with 10 cycles of 4.194s per sample, blank and standard. A Mg ICP standard (Alfa Aesar Magnesium plasma standard solution, Specpure) is used as bracketing standard. Each sample was analysed at least three times in blocks. The three Mg isotopes were detected simultaneously using three Faraday collectors. ^{24}Mg is measured on L3, ^{25}Mg on the centre cup and ^{26}Mg on H3. Measurements had typical intensities of ^{24}Mg in samples and standards of 10 V and for the baseline (2% HNO_3) of 12 mV. For the evaluation of data the sample solutions were corrected for the intensities of 2% HNO_3. Isotope data for Mg is reported in the delta notation relative to the Mg ICP standard and expressed in per mill (‰).

$$\delta^{26}Mg_{MgICP}\,[‰] = \left[\frac{\left(\frac{^{26}Mg}{^{24}Mg}\right)_{sample}}{\left(\frac{^{26}Mg}{^{24}Mg}\right)_{Mg\ ICP}} - 1\right] \cdot 1000 \qquad (3)$$

To evaluate single measurement sequences and to convert Mg isotope ratios into the DSM-3 scale (for a better international comparison) the international reference materials DSM-3 and Cambridge-1 (Cam-I) were analysed in every sequence. The conversion of Mg isotope ratios into the DSM-3 scale was done using the following expression by Young and Galy (2004):

$$\delta^{26}Mg_{DSM-3}^{sample} = \delta^{26}Mg_{MgICP}^{sample} + \delta^{26}Mg_{DSM-3}^{MgICP} + 0.001\delta^{26}Mg_{MgICP}^{sample}\ \delta^{26}Mg_{DSM-3}^{MgICP} \qquad (4)$$

To validate and verify the chemical separation and digestion techniques used in this study, in each series of samples international reference materials were separated and measured as well. Results for these reference materials are within analytical uncertainty in agreement with literature values.

The instrumental precision for $\delta^{26}Mg$ is ±0.09‰ (2 SD, n=8), that was obtained by the repeated analysis of the international reference material Cambridge-I (Cam-I) and DSM-3. Procedural blanks were lower than 80 pg and thus did not affect isotope ratios of the samples (<0.1% of sample). The external precision is based on a repeatedly prepared and analysed internal seawater standard (bottom water SuSu Knolls) and is better than 0.02‰ (2SD) for $\delta^{26}Mg$. $\delta^{26}Mg$ values for

seawater (δ^{26}Mg = -0.87±0.02‰, n = 3) and Cam-I (δ^{26}Mg = -2.56±0.09‰, n = 8) are within analytical uncertainty in agreement with literature values (-0.82±0.06, n = 26, Foster et al., 2010 and -2.62±0.04, Tipper et al., 2006, 2010; Pogge von Strandmann et al., 2011).

2.4 End-member calculation

During sample collection as well as prior to venting in the vent structures or in the subseafloor, vent fluids can mix with unmodified seawater. Thus, the collected samples represent two-component mixtures of an "end-member" hydrothermal fluid and unmodified seawater. However, it is assumed that end-member hydrothermal fluids contain no Mg due to a removal of Mg from seawater during the interaction with the oceanic crust. This hypothesis is approved by experimental studies, which show an almost quantitative removal of Mg from seawater during hydrothermal interaction with andesite, basalt and rhyolite (Mottl and Holland, 1987; Seyfried and Bischof, 1981; Ogawa et al., 2005). All samples analysed in this study contained considerable amounts of Mg. Furthermore, it was discussed that back-arc basin fluids may dissolve Mg-bearing minerals in the reaction or discharge zone, because of their high acidity (Gamo et al., 1997; Douville et al., 1999; Butterfield et al., 2003). However, since all samples, which were investigated in this study, show a linear relationship between Mg and those elements, which behave conservative during mixing with seawater, we assume that the hydrothermal end-member contains no Mg. Therefore, the calculation of elemental concentrations in the hydrothermal end-member was done, as in the usual practise, by a weighted least-square linear regression to Mg=0, forced to pass through seawater (Von Damm et al., 1985). Mg concentrations were taken from Craddock et al. (2010), Reeves et al. (2011), Seewald et al. (2015) and Schmidt et al. (2017). Mg concentration of the vent fluids collected in 2011 from Manus Basin is described here for the first time. Calculation of isotope ratios for the hydrothermal end-member is based on the same assumptions and was done with a weighted linear regression forced to pass through seawater between the inverse concentration of B, Li or Sr and δ^{11}B, δ^{7}Li and ^{87}Sr/^{86}Sr, respectively, by using the end-member elemental contents. Calculating end-member fluid compositions is essential for the comparison of different fluids with each other and with fluids from other areas. Additionally, it is essential to know the pure end-member composition in order to understand and quantify the processes in the subseafloor during hydrothermal circulation.

2.5 References

Bach W., Dubilier N., Borowski C., Breuer C., Brunner B., Franke P., Herschelmann O., Hourdez S., Jonda L., Jöns N., Klar S., Koloa K., Mai A., Meyerdierks A., Müller I., Petersen S., Pjevac P., Ratmeyer V., Reeves E., Rehage R., Reuter C., Schaen A., Shu L., Thal J., Zarrouk M. (2011) Cruise Report for SONNE cruise SO 216 – BAMBUS, Back-Arc Manus Basin Underwater Solfataras. Universität Bremen (https://elib.suub.uni-bremen.de/edocs/00102250-1.pdf).

Berryman E.J., Kutzschbach M., Trumbull R.B., Meixner A., van Hinsberg V., Kasemann S.A., Franz G. (2017). Tourmaline as a petrogenetic indicator in the Pfitsch Formation, Western

Tauern Window, Eastern Alps. *Lithos,* doi.org/10.1016/j.lithos.2017.04.008.
Birck J.L. (1986) Precision K-Rb-Sr isotopic analysis: Application to Rb-Sr chronology. *Chem. Geol.* **56** (1-9), 73-83.
Butterfield, D., Seyfried, W. E. and Lilley, M. (2003) Composition and evolution of hydrothermal fluids. In Dahlem Workshop Report: *Energy and Mass Transfer in Marine Hydrothermal Systems*, vol. 89 (eds. P. E. Halbach, V. Tunnicliffe and J. R. Hein). Dahlem University Press, 123–161.
Craddock, P. R., Bach, W., Seewald, J. S., Rouxel, O. J., Reeves ,E. and Tivey, M. K. (2010) Rare earth element abundances in hydrothermal fluids from the Manus Basin, Papua New Guinea: indicators of sub-seafloor hydrothermal processes in back-arc basins. *Geochim. Cosmochim. Acta* **74**, 5494–5513.
Douville, E., Bienvenu, P., Charlou, J. L., Donval, J. P., Fouquet, Y., Appriou, P., & Gamo, T. (1999). Yttrium and rare earth elements in fluids from various deep-sea hydrothermal systems. *Geochim. Cosmochim. Acta* **63**(5), 627-643.
Foster G.L., Pogge von Strandmann P. A. E., Rae J. W. B. (2010) Boron and magnesium isotopic composition of seawater. *Geochem. Geophys. Geosyst.* **11**(8), Q08015, doi:10.1029/2010GC003201.
Gamo T., Okamura K., Charlou J. L., Urabe T., Auzende J. M., Ishibashi J., Shitashima K. and Chiba H. (1997) Acidic and sulfate-rich hydrothermal fluids from the Manus back-arc basin, Papua New Guinea. *Geology* **25**(2), 139–142
Gao Y, Vils F., Cooper K.M., Banerjee N., Harris M., Hoefs J., Teagle D.A.H., Casey J.F., Elliott T., Altzitzoglou T., Alt J.C., Muehlenbachs K. (2012) Downhole variation of lithium and oxygen isotopic compositions of oceanic crust at East Pacific Rise, ODP Site 1256. *Geochem. Geophys. Geosys*. **13** (10), doi: 10.1029/2012GC004207.
Garbe-Schönberg D., Koschinsky A., Ratmeyer V., Jähmlich H., Westernströer U. (2006) KIPS – A new multiport valve-based all-Teflon fluid sampling system for ROVs. In *Geophys. Res. Abstr.* **8** p. 07032.
Genske F.S., Turner S.P., Beier C., Chu M.-F., Tonarini S., Pearson N.J., Haase K.M. (2014) Lithium and boron isotope systematics in lavas from the Azores islands reveal crustal assimilation. *Chem. Geol*. **373**, 27-36.
Gonfiantini R., Tonarini S., Groening, M., et al. (2003) Intercomparison of boron isotope and concentration measurements; part II, evaluation of results. *Geostandard Newslett.* **27**, 41-57.
Huang K.-F., You C.-F., Liu Y.-H., Wang R.-M., Lin P.-Y., Chung C.-H. (2010) Low memory, small sample size, accurate and high-precision determinations of lithium isotopic ratios in natural materials by MC-ICP-MS. *J. Anal. At. Spectrom*. **25**, 1019-1024.
Magna T., Day J.M.D., Mezger L., Fehr M.A., Dohmen R., Aoudjehane H.C.A., Agee C.B. (2015) Lithium isotope constraints on crust–mantle interactions and surface processes on Mars. *Geochim. Cosmochim. Acta* **162**, 46-65.
Moriguti, T., & Nakamura, E. (1998). High-yield lithium separation and the precise isotopic analysis for natural rock and aqueous samples. *Chemical Geology* **145**(1-2), 91-104.
Mottl, M. J. and Holland, H. D. (1978) Chemical exchange during hydrothermal alteration of basalt by seawater: I. Experimental results for major and minor components of seawater. *Geochim.Cosmochim. Acta* **42**(8), 1103–1115.
Ogawa, Y., Shikazono, N., Ishiyama, D., Sato, H. and Mizuta, T. (2005) An experimental study on felsic rock–artificial seawater interaction: implications for hydrothermal alteration and sulfate formation in the Kuroko mining area of Japan. *Mineral. Deposita* **39**(8), 813–821.
Pin, C., & Bassin, C. (1992). Evaluation of a strontium-specific extraction chromatographic method for isotopic analysis in geological materials. *Analytica Chimica Acta* **269**(2), 249-255.
Pogge von Strandmann P.A.E., Burton K.W., James R.H., van Calsteren P., Gislason S.R. (2010) Assessing the role of climate on uranium and lithium isotope behaviour in rivers draining a basaltic terrain. *Chem. Geol*. **270** (1-4), 227-239.

Pogge von Strandmann, P. A. E., Elliott, T., Marschall, H. R., Coath, C., Lai, Y. J., Jeffcoate, A. B., & Ionov, D. A. (2011). Variations of Li and Mg isotope ratios in bulk chondrites and mantle xenoliths. *Geochim. Cosmochim. Acta* **75**(18), 5247-5268.

Reeves, E. P., Seewald, J. S., Saccocia, P., Bach, W., Craddock, P. R., Shanks, W. C., Sylva, S. P., Walsh, E., Pichler, T. and Rosner, M. (2011) Geochemistry of hydrothermal fluids from the PACMANUS, Northeast Pual and Vienna Woods hydrothermal fields, Manus Basin, Papua New Guinea. *Geochim. Cosmochim. Acta* **75**, 1088–1123.

Romer R. L., Meixner A., Hahne K. (2014) Lithium and boron isotopic composition of sedimentary rocks – The role of source history and depositional environment: A 250 Ma record from the Cadomian orogeny to the Variscan orogeny. *Gondwana Research* **26**, 1093-1110.

Schmidt, K., Garbe-Schönberg, D., Hannington. M.D., Anderson, M.O., Bühring, B., Haase, K., Haruel, C., Lupton, J.E., Koschinsky, A. (2017) Boiling vapour-type fluids from the Nifonea vent field (New Hebrides Back-Arc, Vanuatu, SW Pacific): Geochemistry of an early-stage, post-eruptive hydrothermal system. *Geochim. Cosmochim. Acta* **207**, 185-209.

Seewald, J. S., Doherty, K. W., Hammar, T. R., & Liberatore, S. P. (2002). A new gas-tight isobaric sampler for hydrothermal fluids. *Deep Sea Research Part I: Oceanographic Research Papers* **49**(1), 189-196.

Seewald, J. S., Reeves, E. P., Bach, W., Saccocia, P. J., Craddock, P. R., Shanks III, W. C., Sylva, S. P., Pichler, T., Rosner, M., Walsh, E. (2015) Submarine Venting of magmatic volatiles in the Eastern Manus Basin, Papua New Guinea. *Geochim. Cosmochim. Acta* **163**, 179-199

Seyfried, W. E. and Bischoff, J. L. (1981) Experimental seawater–basalt interaction at 300 C, 500 bars, chemical exchange, secondary mineral formation and implications for the transport of heavy metals. *Geochim. Cosmochim. Acta* **45**(2), 135–147.

Strelow, F. W. E. (1960). An ion exchange selectivity scale of cations based on equilibrium distribution coefficients. *Analytical Chemistry* **32**(9), 1185-1188.

Strelow, F. W., Rethemeyer, R., & Bothma, C. J. C. (1965). Ion Exchange Selectivity Scales for Cations in Nitric Acid and Sulfuric Acid Media with a Sulfonated Polystyrene Resin. *Analytical Chemistry* **37**(1), 106-111.

Tivey M., Bach W., Seewald J., Tivey M. K., Vanko D. A. and the Shipboard Science (2006) Cruise Report for R/V Melville cruise MGLN06MV – Hydrothermal systems in the Eastern Manus Basin: Fluid Chemistry and Magnetic Structure as Guides to Subseafloor Processes. Woods Hole Oceanographic Institution (available upon request to authors).

Tipper, E. T., Galy, A., Gaillardet, J., Bickle, M. J., Elderfield, H., & Carder, E. A. (2006). The magnesium isotope budget of the modern ocean: constraints from riverine magnesium isotope ratios. *Earth Planet. Sci.Lett.* **250**(1), 241-253.

Tipper, E. T., Gaillardet, J., Louvat, P., Capmas, F., & White, A. F. (2010). Mg isotope constraints on soil pore-fluid chemistry: evidence from Santa Cruz, California. *Geochim. Cosmochim. Acta* **74**(14), 3883-3896.

Tonarini, S., Pennisi, M., & Leeman, W. P. (1997). Precise boron isotopic analysis of complex silicate (rock) samples using alkali carbonate fusion and ion-exchange separation. *Chem. Geol.***142**(1-2), 129-137.

Von Damm K. L., Edmond J. M., Measures C. I. and Grant B. (1985) Chemistry of submarine hydrothermal solutions at Guaymas Basin, Gulf of California. *Geochim. Cosmochim. Acta* **49**, 2221-2237.

Wang B. S., You C. F., Huang K. F., Wu S. F., Aggarwal S. K., Chung C. H., Lin P. Y. (2010) Direct separation of boron from Na-and Ca-rich matrices by sublimation for stable isotope measurement by MC-ICP-MS. *Talanta* **82**, 1378-1384.

Wimpenny J., James R.H., Burton K.W., Gannoun A., Mokadem F., Gislason S.R. (2010) Glacial effects on weathering processes: New insights from the elemental and lithium isotopic composition of West Greenland rivers. *Earth Planet. Sci. Lett.* **290**, 427-437.

Young, E. D., & Galy, A. (2004). The isotope geochemistry and cosmochemistry of magnesium. *Reviews in Mineralogy and Geochemistry* **55**(1), 197-230.

Chapter 3: The influence of magmatic fluids and phase separation on B systematics in submarine hydrothermal vent fluids – case studies from the Manus Basin and Nifonea volcano

Frederike K. Wilckens[1]*, Eoghan P. Reeves[1,2,3], Wolfgang Bach[1], Anette Meixner[1], Jeffrey S. Seewald[3], Andrea Koschinsky[4], Simone A. Kasemann[1]

[1] MARUM – Center for Marine Environmental Sciences and Faculty of Geosciences, University of Bremen, Germany (*corresponding author: fwilckens@marum.de, telephone: +49 (0) 421 218 65941)

[2] Department of Marine Chemistry and Geochemistry, Woods Hole Oceanographic Institution, USA

[3] Present address: Department of Earth Science & Centre for Geobiology, University of Bergen, Norway

[4] Department of Physics and Earth Sciences, Jacobs University, Bremen, Germany

Submitted on the 26th of May 2017 to *Geochimica et Cosmochimica Acta*

(submission #: GCA-S-17-00498)

3.1 Abstract

The composition of submarine hydrothermal vent fluids is affected by a variety of processes such as interaction of heated seawater with rocks and sediments, addition of magmatic fluids, as well as phase separation and segregation. How these processes specifically impact vent fluid composition is still poorly understood. In particular, the relative role of phase separation and magmatic degassing, which is common in arc/backarc hydrothermal systems, is not well known. To provide new insights into these processes, we analysed B contents and isotope ratios in hydrothermal vent fluids from the Manus Basin, Papua New Guinea, and Nifonea volcano, New Hebrides backarc. These fluids show a range of salinities, gas contents, acidities, and host rock compositions; many of them are influenced by phase separation and by addition of magmatic volatiles (both CO_2 and SO_2). Previous studies of hydrothermal vents in arc/backarc settings suggest that B contents and isotopic composition of vent fluids are controlled by interactions between seawater, basement and sediments, and propose that phase separation and magmatic fluids play only a subordinate role. In our study, we demonstrate that vent fluids with minor magmatic input indeed reflect the interaction between seawater and oceanic crust. However, the low-salinity Nifonea fluids as well as some of the acid-sulfate fluids from the Manus Basin have higher B contents as expected, whereas other volatile-rich fluids show B depletions. The lack of correlation between B contents and the intensity of magmatic fluid influx (CO_2 and SO_2) indicates that magma degassing is likely not responsible for the B enrichments or depletions in these vent fluids. Instead, B enrichments might relate to preferential partitioning of B into the vapour during phase separation under PT-conditions well above the two-phase curve and critical line. However, this cannot explain the low B isotope ratios in the Nifonea fluids, because of the small B isotope effects associated with phase separation. Hence, we propose that B excesses in the vapour-rich vent fluids are linked to extreme boiling and a preferential mobilization of B from the oceanic crust into vapour-rich fluids. This extreme mobility of B in systems affected by SO_2 degassing is also obvious in the high variability in B contents of both rocks and fluids from acid-sulfate vents. Our data show that the water-gas-rock interactions in vent systems affected by magma degassing result in B systematics that are distinct from simple water-rock interactions in mid-ocean ridge environments. Further, B in these systems may provide a tool for estimating the extent of B leaching and hence hydrothermal alteration in the subseafloor.

3.2 Introduction

Understanding submarine hydrothermal circulation is crucial to assess chemical fluxes in the ocean (Edmond et al., 1979, 1982; Von Damm, 1985, Elderfield and Schultz, 1996; Mottl, 2003), but also the formation of submarine metal sulfide deposits (Hedenquist and Lowenstern, 1994; de Ronde et al, 2005; Hannington et al., 2011). Hydrothermal venting along the 55000-km long mid-

ocean ridge system has long been recognized as a key player in regulating ocean chemistry. In recent years, hydrothermal research in submarine arcs (7000 km length) and back-arc spreading centres (11000 km) has demonstrated that vents are abundant and chemically diverse (de Ronde et al., 2003, Reeves et al., 2011; Mottl et al., 2011). In addition, vents in arc and back-arc settings are thought to account for ~10% of the global hydrothermal discharge (Baker et al., 2008). The chemical composition of hydrothermal vent fluids in arc and backarc settings differs from those at mid ocean ridge sites, indicating variations in physical and chemical processes during fluid-rock interaction in the oceanic lithosphere (Gamo et al., 1997; Craddock et al., 2010; Mottl et al., 2011; Reeves et al., 2011, de Ronde and Stucker, 2015).

The composition of submarine hydrothermal vent fluids in back-arc and arc settings is highly variable due to the range of sources of elements and processes during hydrothermal circulation. The main source of water in submarine hydrothermal vent fluids is seawater, which interacts with the surrounding host rocks in both low and high temperature processes. During low- and high-temperature interaction with the oceanic crust, elements can be either precipitated into secondary minerals or leached from the oceanic crust (Edmond et al. 1979; 1982, Seyfried and Bischoff, 1981, Von Damm et al., 1985, Mottl et al., 1978). Prior and subsequent to water-rock interaction, vent fluids can also be influenced by subcritical (boiling) or supercritical phase separation followed by phase segregation. Phase separation affects the distribution of elements in the vent fluids by preferential partitioning of volatile elements into the low-salinity "vapour" phase (Massoth et al., 1989, Butterfield et al., 1990, Douville et al., 2002; Foustoukos and Seyfried, 2007). In contrast, elements with a high affinity for chloro-complexing become enriched in the salt-rich and gas-poor phase (brine). The partitioning of elements between brine and vapour phases is dependent on pressure and temperature and hence on the distance to the two-phase boundary of the $NaCl/H_2O$ system (Foustoukos and Seyfried, 2007). In addition to water-rock interaction and phase separation, magmatic fluids may be released from the crystallizing magma reservoir and mix with hydrothermal fluids, modifying the chemical composition and physical parameters of vent fluids (Hedenquist and Lowenstein, 1994; Hannington et al., 2011, Seewald et al., 2015). In contrast to mid-ocean ridge vent systems, where the magmatic influx is strongly dominated by CO_2, arc and back-arc vent systems are additionally affected by degassing of H_2O, H_2S, SO_2, as well as HCl and HF. A promising tool to disentangle the complex interplay between these different sources and processes in vent systems and to understand which of them modifies the composition of vent fluids in different geological settings is the boron (B) concentration and isotope composition.

B is a fluid mobile element, which is incompatible in magmatic systems and has two stable isotopes (^{10}B and ^{11}B). Its potential as a tracer of water-rock interactions in submarine hydrothermal systems is related to the significant differences in both concentration and isotopic

composition between the oceanic crust and seawater (Spivack et al., 1990, Chaussidon and Jambon, 1994; You et al., 1994; Foster et al., 2010; Yamaoka et al., 2015). Seawater is characterized by a B concentration of 0.41 mmol/kg and a $\delta^{11}B$ value of +39.6 ‰ (Foster et al., 2010). Mid-Ocean-Ridge Basalts (MORB) (~1 mg/kg and $\delta^{11}B$ = -4‰) and Island-Arc Basalts (IAB) (2 to 30 mg/kg and $\delta^{11}B$ up to +7‰) are isotopically distinct from each other, owing to recycling of sediment- and seawater-derived B in subduction zones (Nakamura et al., 1992; Ryan and Langmuir, 1993; Chaussidon and Jambon. 1994; Chaussidon & Marty, 1995; Bebout et al., 1999; Leeman et al., 2017). Back-arc-Basin Basalts (BABB) are intermediate between MORB and IAB and show a range in B isotope composition, reflecting variable slab influx. B concentrations in BABB are between 0.5 to 12 mg/kg and $\delta^{11}B$ is around -4‰ (Ryan and Langmuir, 1993; Chaussidon and Jambon, 1994; Shaw et al., 2012).

B isotopes in hydrothermal vent fluids have already been analysed in many different geological settings at mid-ocean ridges (Butterfield et al., 1990; Palmer, 1991; You et al., 1994; James et al., 1995) and arc as well as back-arc settings (Palmer, 1991; You et al., 1994; Yamaoka et al., 2015). The studies showed that B isotopes in submarine hydrothermal vent fluids display mainly the water-rock interaction between hydrothermal fluid and oceanic crust (Yamaoka et al., 2015) and the interaction of hydrothermal fluids with marine sediments, if they are present in greater amounts (Yamaoka et al., 2015; Wu et al., 2016; Baumberger et al., 2016). However, B can also be affected by phase separation and segregation or by the influx of magmatic fluids. Due to its volatile character, B may get enriched in the fluid phase upon magmatic degassing. Because B in acidic hydrothermal fluids favours the formation of $B(OH)_3$ (aq) species, it is expected to partition into the low-salinity, gas-rich fluid (hereinafter loosely termed “vapour phase”). This effect is indeed obvious, when halite stability in the coexisting brine is reached (Foustoukos and Seyfried, 2007). Nevertheless, if the coexisting brine has a low Cl content, B may preferentially partition into the brine phase (Liebscher et al., 2005; Foustoukos and Seyfried, 2007). The results of different experimental studies indicate that B isotopes do not fractionate significantly during phase separation and segregation at high temperatures (>350°C) ($\Delta^{11}B$ between -0.4 and 0.9‰, Spivack et al., 1990; Liebscher et al., 2005) and thus do not necessarily influence B isotope systematics in vent fluids (Spivack et al., 1990; Liebscher et al., 2005; Wunder et al., 2005; Foustoukos and Seyfried, 2007). Investigations of natural phase-separated systems show small effects of phase separation on B systematics in hydrothermal fluids. In accordance with the experimental studies, these studies suggest that $\delta^{11}B$ values are generally not affected by phase separation at temperatures above 300°C, whereas B concentrations can show small changes tending either to higher or lower B concentrations in the vapour phase depending on the halite saturation in the brine phase and pressure and temperature conditions during phase separation (Butterfield et al., 1990, Leeman et al., 1992; You et al, 1994, Giggenbach, 1995, Yamaoka et al,

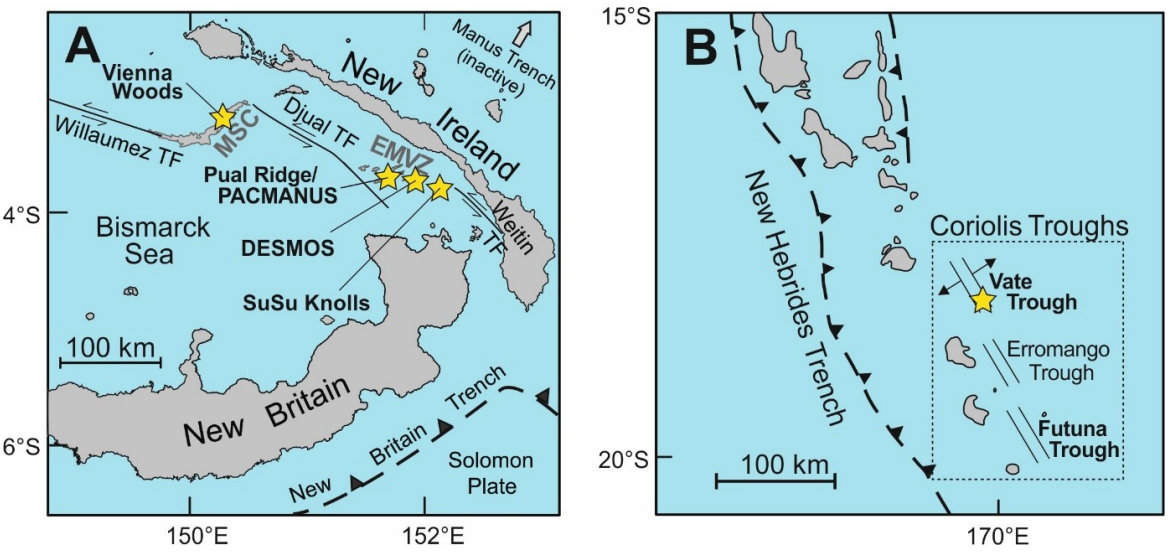

Figure 9: Tectonic setting of (A) Manus Basin and (B) showing the active hydrothermal vent fields , Vienna Woods, PACMANUS, DESMOS and SuSu Knolls and Nifonea volcano (stars), major tectonic plates and the plate motions (gray and black arrows).MSC = Manus Spreading Centre, EMVZ = Eastern Manus Volcanic Zone (modified after Seewald et al., 2015 and Schmidt et al., 2017)

2015, Wu et al, 2016). However, most of these investigated fluids have also a strong contribution of B from marine sediments, which may obscure B partitioning due to phase separation. The B systematics of magmatic fluids that rise from the magma reservoir are largely unknown, but can be estimated from studies of subaerial fumaroles. B isotope ratios in fumaroles show similar values to the surrounding rocks (Leeman et al., 2005), implying no significant B isotope fractionation during magma degassing. A magma degassing- related B contribution may thus be associated with correlations between gas and B contents paired with a rock-like B isotopic signature.

To get a more comprehensive understanding of the influence of the different sources and processes on the vent fluids composition, we analysed the B concentration and isotope composition in vent fluids from individual hydrothermal vent fields in the Manus Basin, Papua New Guinea, and from Nifonea volcano, Vanuatu. These active tectonic areas show a wide range of hydrothermal fluid compositions. The vent fluids from Manus Basin range from black smoker fluids with small amounts of magmatic volatiles (Reeves et al., 2011) to acid-sulfate fluids with significant influx of magmatic SO_2 (Seewald et al., 2015). In addition, fluids from Nifonea volcano show evidence for extreme boiling during venting (Schmidt et al., 2017). This variability makes the Eastern Manus Volcanic Zone (EMVZ) and Nifonea volcano perfect study areas to investigate the different factors affecting B systematics in vent fluids.

3.3. Study areas

3.3.1. Manus Basin

The Manus Basin is a relatively young back-arc basin in the northeastern Bismarck Sea (Fig. 9a). This rapidly opening back-arc basin formed during the northward subduction of the Solomon plate along the New Britain Trench. To the northeast it is bordered by the presently inactive Manus Trench and to the South by the New Britain Trench and Willaumez Rise (Taylor et al., 1994; Lee and Ruellan, 2006) (Fig. 9a). Our study focuses on the eastern part of the Manus Basin where basement consists of Eocene to Oligocene island arc crust formed during the subduction at the Manus Trench. The area between the Weitin and Djaul transform faults features neovolcanic ridges and solitary volcanoes that represent initial rifting in a pull-apart basin (Martinez and Taylor, 1996). The neovolcanic rocks reveal a strong geochemical and isotopic island arc affinity, which can be either related to the subduction of the Solomon plate or a relic from the former subduction at the Manus trench (Kamenetsky et al., 2001; Sinton et al., 2003; Pearce and Stern, 2006; Park et al., 2010; Beier et al., 2015).

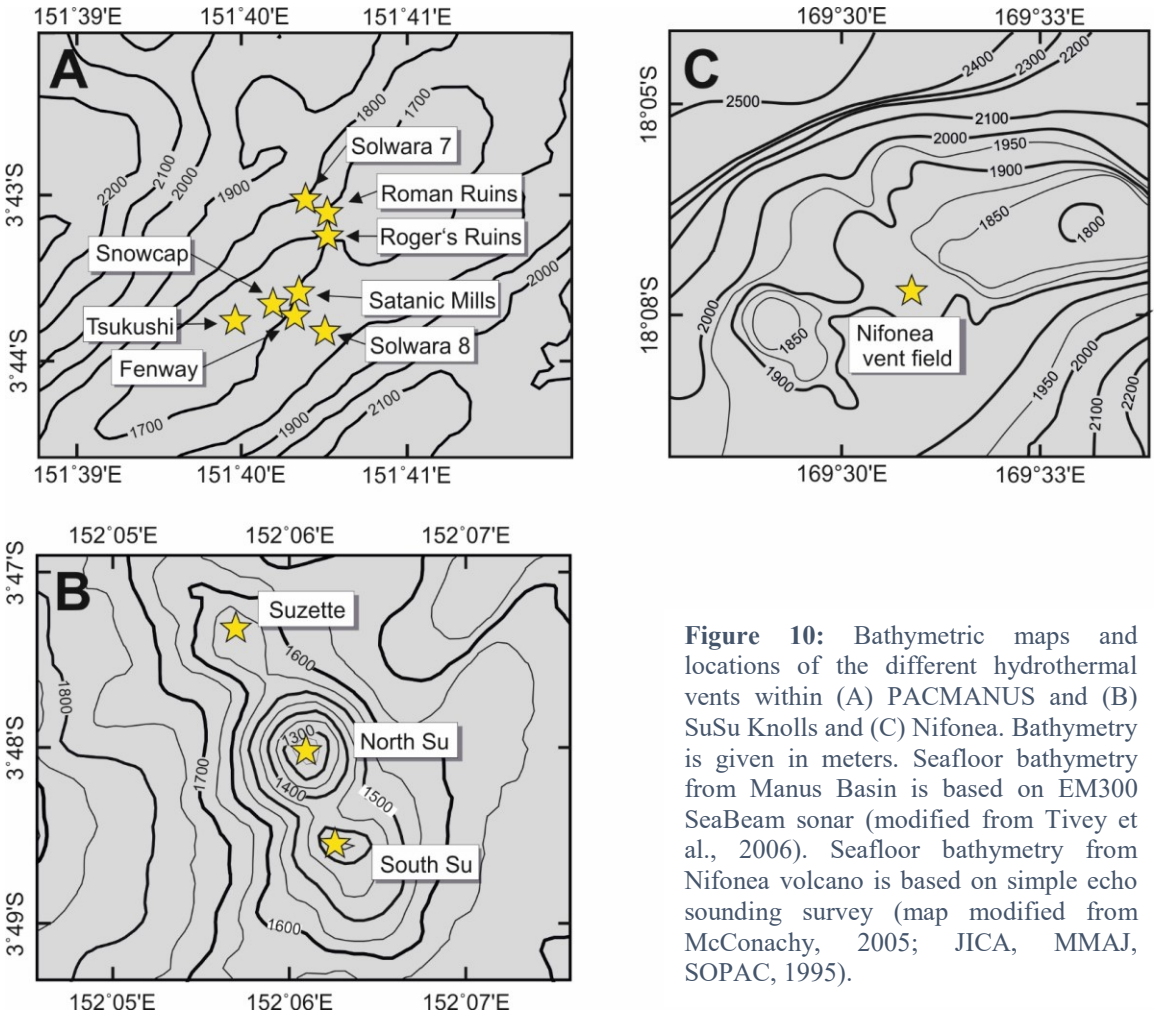

Figure 10: Bathymetric maps and locations of the different hydrothermal vents within (A) PACMANUS and (B) SuSu Knolls and (C) Nifonea. Bathymetry is given in meters. Seafloor bathymetry from Manus Basin is based on EM300 SeaBeam sonar (modified from Tivey et al., 2006). Seafloor bathymetry from Nifonea volcano is based on simple echo sounding survey (map modified from McConachy, 2005; JICA, MMAJ, SOPAC, 1995).

3.3.1.1 PACMANUS and Northeast Pual

The PACMANUS (Papua New Guinea – Australia – Canada – MANUS) hydrothermally active area (Binns and Scott, 1993) expands over a roughly 1.5 km long section across Pual Ridge (Fig. 9a) in a water depth of 1639 to 1774 m. A total of eight discrete vent fields with variable hydrothermal activity were mapped and sampled during two cruises in 2006 and 2011 (see section 3.1) (Fig. 10a). Each of the sampled hydrothermal vent fields at PACMANUS (Fenway, Roman Ruins, Roger's Ruins, Satanic Mills, Snowcap, Solwara 7, Solwara 8, and Tsukushi) expands over areas between 50 to 200 m in diameter. Thal et al. (2014) summarized the mapping results of both research cruises, provided a detailed account of the vent fields and discussed possible volcanic and tectonic controls of the vent distribution. Hydrothermal vent activity ranges from predominantly high temperature black smoker fluids with temperatures up to 358°C to few low temperature diffuse flows of 55°C (Craddock et al. (2010) and Reeves et al. (2011); summarized in Table 1). Northeast Pual is an area of patchy diffuse venting (temperatures around 35°C) on the crest of Pual Ridge 8 km northeast of PACMANUS (Reeves et al., 2011). The compositions of the vent fluids sampled in 2006 are reported in Craddock et al. (2010) and Reeves et al. (2011). They reveal variable influence of phase separation, magmatic degassing, and subseafloor entrainment of seawater.

3.3.1.2 SuSu Knolls

The SuSu Knolls area is located 45km east of PACMANUS (Fig. 9a) and includes three isolated volcanic centres: Suzette, North Su and South Su (Fig. 10b) with active vent systems in water depths between 1153 to 1504 m. Hydrothermal activity at Suzette is characterized by high-temperature (226°C to 303°C) venting from sulphide-rich chimneys (Craddock et al., 2006). At North Su, vent fluids are extremely diverse (Craddock et al., 2010). In this area, venting of white, acid-sulfate fluids as well as black smoker fluid takes place, especially in the summit area of North Su (Craddock et al., 2010; Seewald et al., 2015; Thal et al., 2016). In the summit area of North Su and west of it (in water depths between 1150 and 1200 m), black smoker fluids vent at temperatures up to 332°C (temperature of boiling of seawater at 120 bar). South of the main summit, expansive fields of white smokers can be observed. Acid-sulfate fluids are venting at North Su with exit temperatures between 48 and 241°C and pH lower than 2 (Seewald et al. 2015; Reeves et al. 2015). Prior to the cruise in 2011, the white smoker site with most vigorous venting in 2006, was buried by the products of volcanic cryptodome eruption (Thal et al., 2016). During the sampling campaign in 2011, the Sulfur Candle field was located, an area with meter-thick flows of liquid sulfur as well as widespread milky-white venting of acid-sulfate type compositions with bubbling liquid CO_2 (Reeves et al. 2015; Thal et al. 2016). At South Su hydrothermal activity is more limited in comparison with North Su ranging from diffuse fluids (not sampled

during the cruises) to high-temperature fluids in the south and southeast (up to 290°C) (Craddock et al., 2010).

3.3.1.3 DESMOS caldera

DESMOS caldera is located between SuSu Knolls and Pual Ridge (Fig. 9a); it has a depression of 150 to 250 m, a width of about 1.5 to 2 km and negligible sediment cover. Hydrothermal activity at DESMOS is limited to the hedge of the northern caldera wall and is less compared with the other hydrothermal vent fields within the EMVZ. Hydrothermal vents at DESMOS (Onsen Site) occur in 1810 m depth from poorly focussed exit sites over an area 30 m in diameter (Gamo et al., 1997). Similar to acid-sulfate fluids from North Su, the milky-white acid-sulfate fluids from DESMOS are characterized by moderate venting temperatures of 69°C to 117°C and low pH from 1.0 to 1.4 (Seewald et al., 2015).

3.3.1.4 Vienna Woods

In contrast to the hydrothermal vent fields in the EMVZ, basalts in this area are characterized by seafloor spreading and have a similar composition to MORB (Shaw et al., 2004; Shaw et al., 2012). Hydrothermal activity occurs in a water depth of 2470m within the rift zone of the Manus spreading centre (MSC) (Fig. 9a). Temperatures of almost clear vent fluids range from 270°C to 290°C with moderate pH values around 4.4 (Tivey et al., 2006, Craddock et al., 2010, Reeves et al., 2011). The composition of vent fluids from Vienna Woods is similar to those found at mid-ocean ridges (Reeves et al., 2011), reflecting the high influence of the source rock on the vent fluids.

3.3.2 Coriolis Troughs

The Coriolis Troughs are located in the eastern back-arc of the southern New Hebrides island arc (Fig. 9b), located east of the New Hebrides Trench. The Coriolis Troughs describe three narrow (up to 40km) graben structures: Vate, Erromango and Futuna from north to south (McConachy et al., 2005; Anderson et al., 2016). Volcanism in the Vate and Futuna troughs occurs as lava flows, volcanic ridges and larger volcanic structures. There are no indications for volcanic activity at Erromango Trough.

3.3.2.1 Futuna Trough

Futuna Trough is located west of Futuna Island (Fig. 9b) and the deepest graben structure within this tectonic setting is up to 3600 m below sea-level with a high sediment filling (Neef and McCulloch, 2001; McConachy et al., 2005). K-Ar ages indicate that the volcanic activity at Futuna Trough started about 6.5Ma ago. (Monjaret et al., 1991). The oceanic crust at Futuna is comprised of old island-arc crust and submarine volcanoes ranging from basalts to andesites.

Hydrothermal deposits at Futuna Trough show indications that they originated from hydrothermal sources, which are located further from the deposit (Iizasa et al., 1998).

3.3.2.2 Vate Trough and Nifonea volcano

Nifonea volcano is located in the southern part of Vate trough and shows the highest magmatic activity in this area. Back-arc rifting at Vate Trough started about 3 Ma ago and is in its incipient stage of spreading (Monjaret et al., 1991, McConachy et al., 2005). Nifonea volcano is located in a water depth of 1860 to 1875m. Dominant rock types of the oceanic crust are subalkalic to alkali basalts, trachybasalts and basaltic trachyandesites (Lima et al., 2017). Hydrothermal activity occurs within the central part of the caldera in three clusters of several small chimneys (Fig. 10c). Black smoker and clear vent fluids in this area have temperatures up to 368°C (Table 1; Schmidt et al, 2017).

3.4 Methods

3.4.1 Sampling of vent fluids and rocks

Vent fluids and rocks from Manus Basin were sampled from six vent sites within PACMANUS hydrothermal area, three vent sites within SuSu Knolls area, one vent site from Northeast Pual, one from DESMOS caldera and one vent site from the Manus Spreading centre in July-August of 2006 during the MAGELLAN-06 expedition aboard the R/V Melville with ROV (Remotely Operated Vehicle) Jason II (Tivey et al., 2006). A follow-up cruise SO-216 (BAMBUS) in June-July of 2011 with R/V Sonne and ROV MARUM Quest 4000 collected additional samples from the EMVZ (Bach et al., 2011; Reeves et al. 2015). During cruise SO-216 additional fluid samples were collected from seven vent sites within the PACMANUS hydrothermal area as well as from North Su (SuSu Knolls area).

During both cruises, vent fluids were collected with isobaric gas-tight (IGT) samplers (Seewald et al., 2002). The concentrations of dissolved gases were determined on board. In addition, syringe-style “major” samplers (in 2006) and (in 2011) the Kiel Pumping System (KIPS) (Garbe-Schönberg et al., 2006) were used to collect fluids. Volcanic rock samples were collected from PACMANUS, SuSu Knolls and DESMOS during MAGELLAN-06 expedition using the ROV Jason II. Sampling methods and locations from the cruise in 2006 are described in more detail by Craddock et al. (2010), Reeves et al. (2011) and Seewald et al. (2015) for the fluids, and by Beier et al. (2015) for fresh volcanic rocks. A subset of those fluid samples was selected for this study.

Nifonea volcano was investigated during R/V Sonne cruise SO-229 (VANUATU) in July of 2013. During the SO-229 cruise, fluids were sampled with ROV Kiel 6000. In total, eight fluids from five individual vent sites were taken at Nifonea volcano, using the KIPS fluid pump system. Volcanic rocks were sampled from Nifonea volcano and Futuna Trough during the same cruise

and were collected using ROV Kiel 6000 and a TV-grab. Schmidt et al. (2017) describe sampling methods and locations for fluids and Lima et al. (2017) fresh volcanic samples in more detail.

In all fluid sampling events, temperature was measured simultaneously, and the bottles were triggered, when temperatures were high and steady to minimize entrainment of seawater upon sampling.

3.4.2 Sample preparation and isotope ratio measurement

Measurements of B isotope ratios and concentrations as well as the chemical preparation of fluid and solid phases were performed in the Isotope Geochemistry Laboratory at MARUM - Centre for Marine Environmental Sciences, University of Bremen (Germany). Previous to concentration and isotopic analysis B was separated from the sample matrix. Boron in fluids was purified using a sublimation technique after Wang et al. (2010), described in detail in Hüpers et al. (2016). For every sublimation a minimum of 300 ng B was used. 5 µl of 7N HNO_3 was added to the 45 µl mixture of ultrapure water and sample in the lid of a 5 ml conical Savillex beaker. After closing the beaker, it was covered with aluminium foil and reacted for 18 hours at 98°C on the hot plate. Overall, 52 vent fluids from 36 individual vent sites at Manus Basin and 7 vent fluids from 6 vent sites at Nifonea volcanoe have been analyzed for their B concentration and isotopic composition (Table 1).

Boron in solid phases was dissolved and purified using the method described in Romer et al. (2014) and Kutzschbach et al. (2017). 250 to 500 mg of sample powder was fused with the quadruple amount of K_2CO_3 in platinum-crucibles and afterwards dissolved in ultrapure water. The sample solution was passed through a two-step column separation as described in Romer et al. (2014).

Concentrations and isotope ratios for B were measured using a ThermoFischer Scientific Neptune Plus Multicollector-inductively coupled plasma-mass spectrometer (MC-ICP-MS). Isotope measurements were performed using a stable introduction system (SIS) and a high-efficiency x-cone. The measurements were done using the standard-sample-bracketing method in 100 ppb B solutions with the boric acid NIST SRM 951 as bracketing standard. 2% HNO_3 was used for baseline corrections. Boron isotope valuesare reported in the conventional $\delta^{11}B$ (‰) notation relative to the certified standard reference material NIST SRM 951. To validate and verify the chemical separation and digestion techniques used in this study, each separation step during the B purification in solid phases was checked for B loss. Furthermore, contamination of B from acids and K_2CO_3 during the chemical procedures were checked with procedural blanks. B loss was always smaller than 0.1% for solid samples and procedural blanks were lower than 0.5% of total B for solid samples and less than 1% of total B for liquid samples and hence had no influence on the B composition of the samples. The external precision based on repeatedly prepared and

analysed reference materials is better than 5% (2SD) for B concentrations and 0.3‰ (2SD) for $\delta^{11}B$. Long-time reproducibility of NIST SRM 951 was $\delta^{11}B$ of 0.0±0.3‰ (2SD, n=12). B isotope ratios and concentrations of the international seawater standard IAEA-B-1 ($\delta^{11}B$ of 39.8±0.3‰ (2SD, n=4)) and an internal laboratory seawater standard (bottom seawater from SuSu Knolls) ($\delta^{11}B$ of 39.8±0.3‰ (2SD, n=6), 445±26 µmol/kg (2SD, n=6)) are in agreement with literature values (+39.61±0.2‰ (2SD), Foster et al., 2010). The basalt reference material IAEA-B5 has a B concentration of 9.3±0.5 mg/kg (2SD, n=4) and a $\delta^{11}B$ value of -4.2±0.1‰ (2SD, n=4), which is within the range of the published concentration values (8.9 to 11.3 mg/kg B) and in agreement with reccommended (-3.8±2.0‰, 2SD) and published isotope values (-4.3±.2‰, 2SD; 3.71±0.73‰, 2 SD),(Gonfiantini et al., 2003; Romer et al., 2014, Berryman et al. 2017).

3.4.3. End-member calculation for vent fluids

Major and IGT samplers were prefilled with small amounts of seawater. In addition, vent fluids can mix with unmodified seawater during sample collection as well as prior to venting. Hence, the analysed samples represent a two-component mixture of hydrothermal fluid and unmodified seawater. The calculation of elemental concentrations for the pure hydrothermal end-member with vent fluid samples from the same orifices was done, as in the usual practise, by a weighted linear regression to Mg=0, which was forced to pass through seawater (Von Damm et al., 1985). Magnesium (Mg) concentrations in the fluid samples are from Craddock et al. (2010), Reeves et al. (2011), Seewald et al. (2015) and Schmidt et al. (2017). Mg concentrations for the vent fluids collected in 2011 are reported here for the first time. Assumptions for the end-member calculation are a complete removal of Mg during seawater-rock interaction in the hydrothermal circulation (Mottl and Holland, 1978, Seyfried and Bischof, 1981, Ogawa et al., 2005), and conservative behaviour of B during mixing between seawater and hydrothermal fluid. Calculation of $\delta^{11}B$ values for the pure hydrothermal end-member is based on the same assumptions and was done with a weighted linear regression forced to pass through seawater between the inverse concentration of B and $\delta^{11}B$ of vent fluid samples. By using the end-member B contents, we calculated the end-member B isotope ratios. Calculation of end-member fluids was only done for vent sites, where at least one fluid from the same orifice contains less than 44 mmol/kg Mg (<84% of bottom seawater) to keep errors at a minimum. Therefore, end-member fluid compositions for F5 at Fenway, Tsukushi, and Northeast Pual are not estimated and hence will not be discussed further. Exceptions were made for acid-sulfate fluids, because of their generally higher Mg concentrations.

The formation of acid-sulfate fluids is thought to occur through a direct injection of magmatic fluids into seawater (Seewald et al., 2015). During this process, convective hydrothermal circulation is limited and hence, end-member compositions in acid-sulfate fluids are not determined because of Mg removal during water-rock interaction. Instead, as discussed by

Seewald et al. (2015), end-member calculations for acid-sulfate fluids from DESMOS and North Su can be done, assuming near-zero concentrations of Na, K and Mg in the end-member of the magmatic fluid. Thus an extrapolation to Mg=0 will give the composition of the magmatic fluid.

3.5 Results

3.5.1 Boron concentrations and isotope ratios

B concentrations and isotope ratios for all individual vent fluid samples are reported in table 1 and zero-Mg end-member values for specific vent orifices are reported in table 2.

3.5.1.1 "Smoker-type" fluids

B concentrations in the vent fluids at all sites exceed that of seawater (419 µmol/kg), whereas $\delta^{11}B$ values are systematically lower than seawater (39.6‰) in the vent fluids. In general, vent fluids have the highest variability in end-member B concentrations in the PACMANUS and SuSu Knolls areas (Fig. 11a). End-member B concentrations are highest in the high temperature fluids from PACMANUS (up to 2664 µmol/kg) (Fig. 11a). Those vent fluids from PACMANUS that are characterized by Cl concentrations below seawater (<540 mmol/kg), have end-member B concentrations between 1111 and of 1882 µmol/kg, which is similar to the end-member B concentrations in most of the vent fluids from the SuSu Knolls area (1253 to 1886 µmol/kg). At Vienna Woods, vent fluids have uniform but low end-member B concentrations between 556 and 584 µmol/kg. End-member B concentration in vent fluids from Nifonea volcano (999 – 1588 µmol/kg) are similar to "low Cl"-fluids from PACMANUS.

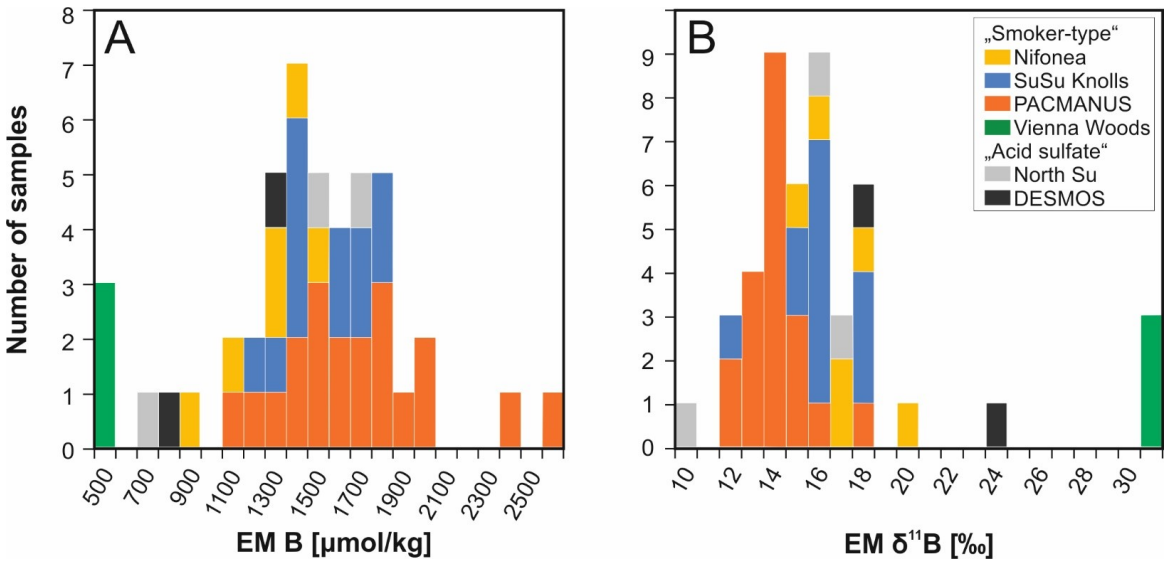

Figure 11: Frequency of (A) end-member B concentrations and (B) $\delta^{11}B$ values in the "smoker-type" vent fluids from Nifonea, SuSu Knolls, PACMANUS and Vienna Woods and acid-sulfate fluids from North Su (SuSu Knolls) and DESMOS. "Smoker-type" fluids from PACMANUS and SuSu Knolls and acid-sulfate fluids have the highest variability in both B concentrations and isotope ratios, whereas the vent fluids from Vienna Woods are homogenous.

Table 1: B concentrations and isotope ratios together with previously reported chemical and physical parameter in hydrothermal fluids and acid sulfate fluids from vent fields located in the Eastern Manus Volcanic Zone, the Manus Spreading Center and from Nifonea volcano

Vent field	Area: Vent	Sample	Year of sampling	Water depth[a] [m]	IGT T[a] [°C]	pH[a] 25°C	Mg[a] (mmol/kg)	B (µmol/kg)	Cl[a] (mmol/kg)	ΣCO_2[a] (mmol/kg)	$\delta^{11}B$ ± (‰)	2sd
"Smoker-type" fluids												
Eastern Manus Volcanic Zone (EMVZ)												
PACMANUS												
Fenway	F1	J2-210-IGT1	2006	1710	296	2.5	6.0	1581	463[a]	61	15.0 ±	0.1
		J2-210-M4	2006	1710		2.6	5.8	1592	465		14.8 ±	0.1
	F3	J2-212-M2	2006	1706	330	2.8	8.9	1408	573		15.3 ±	0.1
		J2-212-IGT2	2006	1706	358	2.7	4.5	2062	586	24	16.2 ±	0.1
	F4	J2-216-M2	2006	1710		2.4	10.2	1538	527	55	15.2 ±	0.1
		J2-216-IGT6	2006	1710	284	2.5	8.7	1581	524	52	15.0 ±	0.1
	F5	J2-216-M4	2006	1709		5.8	48.8	485	535		35.1 ±	0.1
		J2-216-IGT3	2006	1709	80	4.9	44.0	621	517	16	29.4 ±	0.1
	F7	029-ROV-01	2011	1715	304	2.5	12.4	1685	625	39	15.6 ±	0.1
		029-ROV-02	2011	1715	304	2.4	9.4	1783	625	48	15.0 ±	0.1
	F8	041-ROV-03	2011	1714	314	2.7	11.8	1554	531	54	16.3 ±	0.1
Roger's Ruins	RGR1	J2-213-IGT3	2006	1709	320	2.7	5.1	1558	635	7	16.2 ±	0.1
Roman Ruins	RMR1	J2-208-IGT8	2006	1677	312	2.3	7.3	2200	617	15	13.6 ±	0.0
	RMR3	J2-213-IGT7	2006	1660	278	3.2	22.7	1692	648	7	15.9 ±	0.1
	RMR4	J2-222-IGT1	2006	1680	341	2.7	3.6	1966	650	10	14.5 ±	0.1
	RMR5	039-ROV-02	2011	1679	333	3.3	20.3	1298	656	12	18.5 ±	0.0
		039-ROV-03	2011	1679	324	2.6	5.3	1585	716	18	15.5 ±	0.1
Snowcap	SC1	J2-210-IGT8	2006	1643	120	4.6	30.8	704	499	112	21.8 ±	0.0
	SC2 2006	J2-211-M4	2006	1639		3.4	24.5	1046	530	102	18.6 ±	0.0
	SC2 2011	027-ROV-02	2011	1644	102	4.8	41.0	630	557	19	29.9 ±	0.1
		027-ROV-03	2011	1644	224	4.0	26.7	839	562	39	23.6 ±	0.1
Solwara 7	SL7	037-ROV-01	2011	1774	348	2.9	3.9	1375	661	3	17.2 ±	0.1
Solwara 8	SL8	049-ROV-01	2011	1740	305	3.0	7.1	1493	566	11	16.4 ±	0.0
		049-ROV-02	2011	1740	305	2.9	4.0	1524	567	12	16.1 ±	0.2
Satanic Mills	SM1	J2-209-M4	2006	1685		2.6	8.2	1426	519		15.6 ±	0.1
		J2-209-IGT6	2006	1685	295	2.7	9.8	1255	523	168	15.8 ±	0.1
	SM2	J2-209-M2	2006	1688		2.4	16.9	1278	455		16.9 ±	0.1
		J2-209-IGT4	2006	1688	241	2.7	26.6	884	478	80	19.6 ±	0.1
	SM3	J2-214-IGT8	2006	1682	281	2.5	9.7	1307	510	216	15.9 ±	0.1
		J2-214-IGT5	2006	1682	288	2.5	9.8	1236	510	230	16.2 ±	0.0
	SM4	031-ROV-12	2011	1689	345	3.0	4.2	1294	371	271	14.8 ±	0.1
	SM5	043-ROV-01	2011	1688	291	2.8	7.6	1667	596	135	15.1 ±	0.1
		043-ROV-02	2011	1688	339	2.8	4.8	1737	598	152	14.7 ±	0.1
Tsukushi	TK1	J2-214-IGT2	2006	1660	55	5.8	45.2	671	570	6	28.9 ±	0.1

Table 1 (continued)

Vent field	Area: Vent	Sample	Year of sampling	Water depth[a] [m]	IGT T[a] [°C]	pH[a] 25°C	Mg[a] (mmol/kg)	B (µmol/kg)	Cl[a] (mmol/kg)	ΣCO_2[a] (mmol/kg)	$\delta^{11}B$ ± (‰)	2sd
NE Pual	NP1	J2-218-IGT3	2006	1879	33	6.9	50.6	475	536	3	37.7 ±	0.1
		J2-218-IGT4	2006	1879	35	6.9	49.9	487	535	3	37.0 ±	0.2
SuSu Knolls												
South Su	SS1	J2-224-IGT4	2006	1307	265	2.6	5.3	1646	612	127	16.6 ±	0.1
		J2-224-M2	2006	1307		4.5	36.9	694	564		24.8 ±	0.0
	SS2	J2-224-IGT2	2006	1327	287	2.7	8.4	1249	598	128	17.4 ±	0.1
Suzette	SZ1	J2-217-IGT5	2006	1504	303	3.8	5.4	1300	617	15	18.8 ±	0.1
	SZ5	J2-226-IGT5	2006	1500	249	2.3	6.0	1250		16	18.8 ±	0.0
North Su	NS3	J2-223-IGT7	2006	1157	300	3.5	3.4	1416	665	11	16.0 ±	0.1
	NS4	J2-223-IGT5	2006	1204	241	1.5	23.5	1047			20.7 ±	0.1
		J2-223-IGT6	2006	1204	203	1.5	24.2	1057	562		20.7 ±	0.0
	NS5	J2-227-IGT2	2006	1153	299	3.4	7.4	1073	550	19	17.7 ±	0.1
		J2-227-M2	2006	1533		4.8	27.4	934	544		22.1 ±	0.1
	NS6	J2-227-IGT3	2006	1183	325	2.8	1.6	1740		7	17.0 ±	0.1
		J2-227-M4	2006	1183		2.9	5.1	1555	668		17.5 ±	0.1
	NS7	019-ROV-01	2011	1192	332	3.2	15.3	1298	662	4	18.3 ±	0.1
	NS8	021-ROV-01	2011	1228	169	2.4	43.5	626	555	2	30.0 ±	0.2
	NS10	045-ROV-02	2011	1154	312	4.8	18.9	1356	662	6	18.7 ±	0.1
	NS11	047-ROV-03	2011	1218	149	2.0	44.2	570	553	26	30.2 ±	0.1
		047-ROV-04	2011	1218	129	1.9	40.8	662	553	37	28.1 ±	0.1
Manus Spreading Centre												
Vienna Woods												
	VW1	J2-207-IGT3	2006	2470	282	4.4	1.5	552	683	4	31.2 ±	0.0
	VW2	J2-207-IGT4	2006	2474	273	4.2	1.0	558	660	4	31.2 ±	0.3
	VW3	J2-207-IGT8	2006	2475	285	4.7	1.1	580		4	31.2 ±	0.1
	VW3	J2-207-IGT6	2006	2475	240	5.4	14.9		611	4		
Vate Trough												
Nifonea volcano												
	NIF-1	27 ROV 14 KIPS C	2013	1862	>>250		15.1	880	193		20.8 ±	0.1
	NIF-1	66 ROV 1 KIPS B	2013	1862	107	4.4	27.6	622	311		28.1 ±	0.1
	NIF-2	60 ROV 1 KIPS B	2013	1873	345	4.7	25.4		296			
	NIF-2	60 ROV 1 KIPS C	2013	1873			42.5	616	462		29.7 ±	0.1
	NIF-3	66 ROV 6 KIPS D	2013	1862	165		43.3	544	458		31.6 ±	0.0
	NIF-4	77 ROV 6 KIPS A	2013	1862	368	2.9	14.9	1109	340		19.8 ±	0.1
	NIF-5	77 ROV 10 KIPS B	2013	1862	368	3.4	3.9	1502	63		17.7 ±	0.0
	NIF-7	66 ROV 3	2013	1862	132		43.2	588	484		30.9 ±	0.0
	NIF-7	66 ROV 5 NISKIN	2013	1862			51.7	441	545		37.9 ±	0.1

table 1 (continued)

Vent field	Area: Vent	Sample	Year of sampling	Water depth[a] [m]	IGT T[a] [°C]	pH[a] 25°C	Mg[a] (mmol/kg)	B (µmol/kg)	Cl[a] (mmol/kg)	ΣCO_2[a] (mmol/kg)	$\delta^{11}B$ ± (‰)	2sd
Acid-sulfate fluids												
Eastern Manus Volcanic Zone (EMVZ)												
SuSu Knolls												
North Su	NS1	J2-221-IGT7	2006	1253	48	1.8	49.6	505	520	20	35.0 ±	0.1
		J2-221-IGT8	2006	1253	47	1.9	50.4	484	527	16	36.0 ±	0.1
		J2-221-M4	2006	1253		1.9	49.8	464	524		36.0 ±	0.1
North Su	NS2	J2-221-IGT6	2006	1257	206	0.9	39.2	797	443	82	23.3 ±	0.1
		J2-221-IGT5	2006	1257	215	0.9	41.1	718	456	74	24.8 ±	0.2
		J2-221-M2	2006	1257		0.9	41.1	704	457		24.9 ±	0.1
	NS9	023-ROV-01	2011	1220	95	1.4	44.7	465	477	689	33.0 ±	0.2
		023-ROV-02	2011	1220	103	1.2	42.7	472	456	1073	31.4 ±	0.1
DESMOS caldera												
Onsen field	D1	J2-220-IGT1	2006	1908	113	1.0	44.9	474	492	23	35.3 ±	0.1
		J2-220-IGT2	2006	1908	117	1.0	45.1	471	495	21	35.0 ±	0.1
		J2-220-M4	2006	1908		1.3	50.0	446			38.6 ±	0.1
	D2	J2-220-IGT3	2006	1908	69	1.4	49.2	471	502	11	36.0 ±	0.1
		J2-220-M2	2006	1908		1.4	49.4	473	501		35.8 ±	0.1
		J2-220-IGT4	2006	1908	70	1.4	49.3	487		11	35.8 ±	0.1
bottom seawater			2006		3	7.9	52.4	419	540	2.3	39.6 ±	0.0

[a] Previously reported by: Tivey et al., 2006; Craddock et al., 2010; Reeves et al., 2011 ; Seewald et al (2015) for fluids from Manus Basin collected in 2006; Bach et al., 2011 andunpublished data for fluids from the EMVZ collected in 2011 and Schmidt et al. (2017) for vent fluids from Nifonea volcano.

The variability in end-member B isotope ratios is highest at PACMANUS (Fig. 11b). End-member $\delta^{11}B$ values at this location vary between 12.2 and 18.6 ‰ with both the lowest (SC1) and highest (SC2 2011) values at the Snowcap vent site. Vent fluids with low Cl concentrations from Snowcap have end-member $\delta^{11}B$ between 12.2 and 14.8 ‰. Most of the other vent fluids from PACMANUS fall in a range between 13.0 and 15.6 ‰. End-member $\delta^{11}B$ values from SuSu Knolls have higher values in comparison with PACMANUS and range between 15.5 and 18.1 ‰, whereas values from Vienna Woods are even higher around 31 ‰. End-member $\delta^{11}B$ values from Nifonea volcano range between 15.2 to 20.1‰.

Some of the vent sites that were sampled for fluids in both 2006 and 2011 show variations in their B signature. At Snowcap, the vent fluid from the same orifice (SC2 2011) has a lower B concentration and a significantly higher $\delta^{11}B$ value than in 2006 (SC2 2006). At Roman Ruins, B concentrations are also lower and $\delta^{11}B$ values higher in the vent fluid end-member from 2011 (RMR5) when compared with the samples from 2006. In contrast, at Fenway and Satanic Mills, B concentrations and $\delta^{11}B$ values apparently have not changed between 2006 and 2011. However, B concentrations in the vent fluids from Satanic Mills sampled in 2011 appear to be more variable than in 2006.

3.5.1.2 Acid-sulfate fluids

B concentrations and isotope ratios in the acid-sulfate fluids are summarized in table 1. All fluids are enriched in B and have lower B isotope ratios relative to seawater. B concentrations in acid-sulfate fluids from North Su and DESMOS range from 464 to 1057 µmol/kg and from 446 to 487 µmol/kg, respectively. These concentrations match B concentrations in smoker fluids with similar Mg concentrations. $\delta^{11}B$ values in acid-sulfate fluids from North Su range from 20.7 to 36‰ and from DESMOS from 35 to 38.6‰. B concentrations in end-member fluids range from 715 to 1792 µmol/kg at North Su and between 800 and 1390 µmol/kg at DESMOS. $\delta^{11}B$ values range from 10.7 to 17.2 ‰ at North Su and from 18.6 to 24.0 ‰ at DESMOS (Table 2).

3.5.1.3 Volcanic rocks

Twelve volcanic rocks from different sites at PACMANUS (Fenway and Satanic Mills), SuSu Knolls (North Su and South Su) and DESMOS, four volcanic lavas around Nifonea volcano, and three rocks NW of Futuna Trough were analysed for their B concentration and $\delta^{11}B$ values. Results are summarized in table 3.

We separated the rocks analysed from the EMVZ into two different groups depending on their degree of alteration. One group represents fresh basaltic rocks and the other group hydrothermally altered rocks. The altered volcanic rocks, which also had initially andesitic to dacitic compositions, were affected by interaction with vent fluids and minor low-temperature oxidative alteration with seawater. Five samples, classified as fresh or only slightly altered rocks, have an

Table 2: End-member compositions for "smoker-type" and acid-sulfate fluids from the vent fields within the EMVZ, Vienna Woods and Nifonea volcano

Edifice	Area (T_{max}[a])	Year of sampling	B (µmol/kg)	Cl[a] (mmol/kg)	B/Cl [*10^3]	ΣCO_2 [a] (mmol/kg)	ΣCO_2/Cl	$\delta^{11}B$ (‰)
"Smoker-type" fluids								
Eastern Manus Volcanic Zone								
PACMANUS								
Fenway	F1 (329°C)	2006	1735	454	3.8	69	0.15	14.1
	F3 (358°C)	2006	1943	586	3.3	56	0.10	14.7
	F4 (284°C)	2006	1811	522	3.5	64	0.12	13.8
	F7 (304°C)	2011	2080	647	3.2	54	0.08	14.0
	F8 (314°C)	2011	1882	529	3.6	69	0.13	14.8
Roger's Ruins	RGR1 (320°C)	2006	1680	645	2.6	7	0.01	15.6
Romain Ruins	RMR1 (314°C)	2006	2486	629	4.0	18	0.03	12.9
	RMR3 (278°C)	2006	2664	730	3.6	10	0.01	13.0
	RMR4 (341°C)	2006	2081	658	3.2	10	0.02	14.1
	RMR5 (324°C)	2011	1759	733	2.4	19	0.03	15.2
Snowcap	SC1 (152°C)	2006	1111	440	2.5	268	0.61	12.2
	SC2 2006 (180°C)	2006	1596	521	3.1	187	0.36	13.7
	SC2 2011	2011	1291	589	2.2	76	0.13	18.6
Solwara 7	SL7 (348°C)	2011	1453	671	2.2	3	0.00	16.7
Solwara 8	SL8 (305°C)	2011	1636	569	2.9	12	0.02	15.5
Satanic Mills	SM1 (295°C)	2006	1533	517	3.0	212	0.41	14.3
	SM2 (241°C)	2006	1578	414	3.8	160	0.39	13.6
	SM3 (288°C)	2006	1467	503	2.9	274	0.54	14.5
	SM4 (345°C)	2011	1370	356	3.8	294	0.83	14.1
	SM5 (339°C)	2011	1874	605	3.1	163	0.27	14.2
SUSU Knolls								
North Su	NS3 (290°C)	2006	1485	674	2.2	12	0.02	15.5
	NS4 (241°C)	2006	1575	581	2.7		0.00	16.4
	NS5 (299°C)	2006	1253	551	2.3	22	0.04	16.6
	NS6 (325°C)	2006	1733	682	2.5	7	0.01	16.8
	NS7 (332°C)	2011	1660	713	2.3	4	0.01	16.1
	NS8 (169°C)	2011	1631	629	2.6		0.00	18.0
	NS10 (312°C)	2011	1886	731	2.6	8	0.01	16.0
	NS11 (149°C)	2011	1477	606	2.4	148	0.24	16.1
South Su	SS1 (271°C)	2006	1746	620	2.8	142	0.23	15.1
	SS2 (288°C)	2006	1408	609	2.3	153	0.25	16.1
Suzette	SZ1 (303°C)	2006	1401	625	2.2	16	0.03	18.1
	SZ5 (249°C)	2006	1357			18		18.0
Manus Spreading Centre (MSC)								
Vienna Woods								
Vienna Woods	VW1 (282°C)	2006	556	687	0.8	4	0.01	31.0
	VW2 (273°C)	2006	561	663	0.8	4	0.01	31.0
	VW3 (285°C)	2006	584	639	0.9	4	0.01	31.1
Vate Trough								
Nifonea volcano								
Nifonea	Nif-1 (>>250°C)	2013	999	53	18.9			20.1
	Nif-2 (345°C)	2013	1431	71	20.2			15.2
	Nif-3 (165°C)	2013	1115	61	18.1			18.6
	Nif 4 (368°C)	2013	1380	259	5.3			17.8
	Nif 5 (368°C)	2013	1588	24	65.5			17.1
	Nif 7	2013	1351	209	6.5			16.0
Acid-sulfate fluids								
Eastern Manus Volcanic Zone (EMVZ)								
SuSu Knolls								
North Su	NS1 (48°C)	2006	1617	188	8.6	341	1.81	14.5
	NS2 (215°C)	2006	1750	153	11.4	326	2.13	11.6
	NS9 (103°C)*	2011	715	95	7.5			10.7
DESMOS caldera								
Onsen field	D1 (117°C)	2006	707	213	3.3	142	0.67	24.4
	D2 (70°C)	2006	911	-100	-9.1	142	-1.42	21.8
bottom seawater (3°C)			419	540	0.8	2	0.00	39.6

[a] Previously reported by: Tivey et al., 2006; Craddock et al., 2010; Reeves et al., 2011, Seewald et al., 2015 for fluids from Manus Basin collected in 2006; Bach et al., 2011 and unpublished values for fluids from the EMVZ collected in 2011 and Schmidt et al., 2017 for vent fluids from Nifonea volcano

*fluid was bubbling CO2, since it is saturated an endmember composition is not meaningful to calculate (Reeves et al., 2015)

Table 3: SiO_2, TiO_2 and B concentrations and isotope ratios of fresh and altered rocks from Nifonea volanco and the Eastern Manus Volcanic Zone

Sample	Location	alteration degree	SiO_2[a] [%]	TiO_2[a] [%]	B [mg/kg]	$\delta^{11}B$ ± 2sd [‰]
New Hebrides Back-Arc						
62-TVG-03 WR	Nifonea	fresh	50.6	2.1	5.3	2.3 ± 0.1
73-TVG-01 WR	Nifonea	fresh	48.5	1.3	3.6	7.2 ± 0.1
73-TVG-01 A	Nifonea	alteration rind			6.0	9.1 ± 0.1
73-TVG-02 WR	Nifonea	fresh	48.6	1.3	4.5	5.9 ± 0.0
73-TVG-02 A	Nifonea	alteration rind			6.0	10.4 ± 0.1
72-ROV-10 WR	Vate Trough	fresh	50.2	1.1	5.2	0.4 ± 0.0
39-ROV-01 II WR	Futuna	fresh	48.8	1.1	1.2	-0.5 ± 0.0
44-ROV-16 WR	Futuna	fresh	53.0	1.0	28.9	9.0 ± 0.0
50-TVG-15 WR	Futuna	fresh	48.1	0.8	4.5	8.6 ± 0.1
Eastern Manus Volcanic Zone						
J2-209-9-R1	Satanic Mills	fresh	66.3	0.7	20.3	6.5 ± 0.1
J2-224-10-R1	South Su	fresh	62.8	0.7	23.7	8.0 ± 0.1
J2-221-16-R2	North Su	fresh	60.1	0.5	11.8	8.3 ± 0.1
J2-220-13 R1	DESMOS	slightly altered	58.0	0.6	12.1	8.8 ± 0.1
J2-221-4-R1	North Su	slightly altered	64.1	0.6	9.4	9.0 ± 0.1
J2-216-11-R2	Fenway	altered	26.2	0.9	7.3	10.5 ± 0.2
J2-209-8-R1	Satanic Mills	altered	27.9	1.1	7.0	18.5 ± 0.1
J2-224-2-R1	South Su	altered	79.7	1.1	1.8	20.0 ± 0.1
J2-221-6-R1	North Su	altered	59.2	0.5	11.6	7.0 ± 0.3
J2-220-8-R1	DESMOS	altered	67.4	0.7	18.9	5.3 ± 0.1
J2-220-9-R1 crust	DESMOS	altered	68.2	0.7	1.8	9.6 ± 0.2
J2-220-9-R1 interior	DESMOS	altered	50.2	0.5	7.2	5.6 ± 0.1

[a] Unpublished values and data previously reported by Beier et al. (2015) for volcanic rocks from Manus Basin and Lima et al. (2017) for volcanic rocks samples from Nifonea volcano, errors for B are smaller than 5% (2SD)

andesitic to dacitic composition. B concentrations in those samples range from 9.4 to 23.7 mg/kg, and $\delta^{11}B$ values range between 6.5 and 9.0 ‰. Samples with higher degrees of alteration have B concentrations ranging from 1.8 to 18.9 mg/kg and $\delta^{11}B$ values between 5.3 and 20.0 ‰.

Fresh volcanic samples from Nifonea and Vate Trough have a basaltic composition and B concentrations ranging from 3.6 to 5.3 mg/kg and isotopic compositions from 0.4 to 7.2‰, respectively. Alteration rinds (73-TVG-01 A, 73-TVG-02 A) are enriched in B (6 mg/kg) and show higher $\delta^{11}B$ values (9.1 to 10.4‰) compared to their fresh counterparts (73-TVG-01 WR, 73-TVG-02 WR). Fresh samples from Futuna have a higher variability ranging from basaltic to basaltic andesitic composition and B concentrations from 1.2 to 28.9 mg/kg. B isotope ratios are similar to those at Nifonea volcano (-0.5 to 9.0‰).

3.6 Discussion

3.6.1 Arc signature in volcanic rocks

To understand the variability of B concentrations and $\delta^{11}B$ values in the vent fluids, volcanic rock samples from the EMVZ as well as Nifonea volcano are discussed first. Volcanic rocks from the EMVZ were previously characterized as having similarities to island arc basalts with respect to their major, trace and Sr-Nd-Pb isotope ratios (Sinton et al., 2003; Park et al., 2010; Beier et al.,

2015), whereas volcanic rocks from the MSC are similar to MORB, although enriched in fluid mobile elements (Sinton et al., 2003). Mid ocean ridge basalts (MORB) have B concentrations less than 1 mg/kg and $\delta^{11}B$ values between -10.8 to -1‰ (Ryan and Langmuir, 1993; Chaussidon and Jambon, 1994; Chaussidon and Marty, 1995; Shaw et al., 2012). In contrast, island arc and back-arc crust has a characteristic boron signature that is distinct from MORB. Back-arc basin basalts (BABB) and island arc basalts (IAB) are more enriched in B and have higher $\delta^{11}B$ values compared to fresh MORB (Ryan and Langmuir, 1993; Ishikawa and Nakamura, 1994; Ishikawa and Tera, 1997, 1999; Smith et al., 1997; Ishikawa et al., 2001, Shaw et al., 2012). BABB can have variations in B from 0.5 to 12 mg/kg and in $\delta^{11}B$ from -6.7 to +5.8‰ (Ryan and Langmuir, 1993; Chaussidon and Jambon, 1994; Shaw et al., 2012). IABs vary in their B composition from 2 to 30 mg/kg and +1 to +7‰ (Palmer, 1991; Nakamura et al., 1992; Ryan and Langmuir, 1993; Ishikawa and Nakamura, 1994; Shaw et al., 2012). The fresh rocks from the EMVZ fall within the B range of IAB, which is in accordance with previous studies on volcanic rocks from the EMVZ (Kamenetsky et al., 2001; Sinton et al., 2003; Pearce and Stern, 2006; Park et al., 2010; Beier et al., 2015). $\delta^{11}B$ values of the fresh rocks between 6.5 and 8.3‰ are exceptionally high for rocks from a back-arc basin. Likewise, B concentrations are high. These values provide further evidence of the exceptional high slab flux and a large extent of melt depletion in the mantle wedge of the EMVZ.

The two slightly altered samples have marginally higher $\delta^{11}B$ values, indicative of minor ^{11}B enrichment due to seawater interaction. B isotope ratios in four of the hydrothermally altered volcanic rocks fall within the same range as the fresh samples. B concentrations are similar or significantly lower than in the fresh samples. This implies leaching of B during alteration without isotope fractionation. Three of the altered samples have significantly higher $\delta^{11}B$ values and lower B concentration in comparison to the fresh samples from the EMVZ. These signatures can be explained by a preferential leaching of ^{10}B during hydrothermal alteration.

B concentrations and isotopic ratios in the volcanic lava from the area around Nifonea volcano have a broader range in comparison with fresh volcanic samples from the EMVZ. All fresh samples, which have a basaltic composition, are in the range of BABB and IAB, whereas the basaltic andesite (44-ROV-16 WR) is in the range of IAB. Since this sample represents a volcanic rock from the old island arc crust, the enrichment of B can be explained by the addition of a slab-derived subduction component. High B concentrations and isotope ratios in the alteration rinds of 73-TVG-01 and -02 can be explained by a low-temperature alteration of these rocks.

3.6.2 B signatures in hydrothermal vent fluids – water-rock interaction and phase separation

All vent fluids from the Manus Basin and Nifonea volcano are enriched in B relative to seawater, whereas B isotope ratios of the vent fluids are significantly lower relative to seawater. Depending on their chlorine and sulfate concentrations, we divided the vent fluids in three groups: (I) Black smoker fluids that are characterized by moderate to high Cl concentrations (517 to 733 mmol/kg). These are interpreted as vent fluids that are slightly enriched in a brine component formed during supercritical phase separation (Reeves et al., 2011). (II) Fluids that have Cl concentrations lower than seawater (F1 from Fenway, SC1 from Snowcap, SM2, SM3 and SM4 from Satanic Mills and all vent fluids from Nifonea). These low Cl concentrations are a good indicator for phase separation and the presence of the low-salinity vapour phase (Foustoukos and Seyfried, 2007; Reeves et al., 2011). The extremely low chlorinities of the Nifonea fluids suggest that they may be dominated by condensed vapours generated by boiling (Schmidt et al., 2017). (III) Acid-sulfate fluids, which are characterized by high-sulfate concentrations, low pH (<2, measured at 25°C) and limited interaction with unaltered rocks during hydrothermal circulation. These fluids are

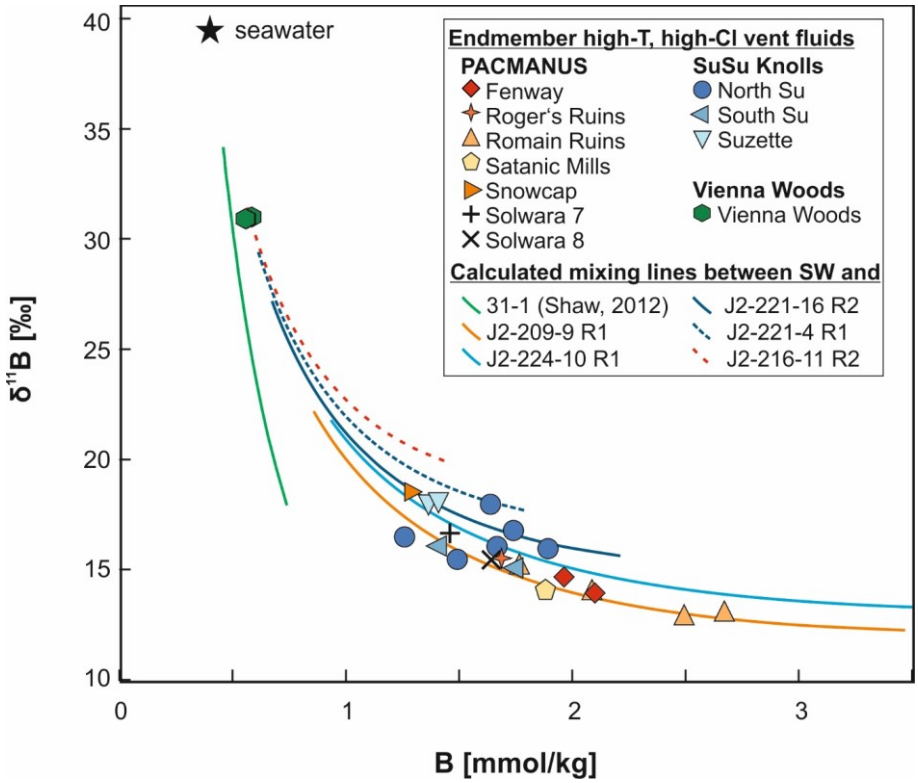

Figure 12: End-member B concentration versus B isotope ratios of high temperature, high Cl vent fluids from Vienna Woods, PACMANUS and SuSu Knolls. The different lines represent the calculated mixing lines between seawater (SW) and MORB from the MSC (green line, composition from Shaw et al., 2012), fresh volcanic rocks from the EMVZ (blue and orange solid lines) and altered volcanic rocks from the EMVZ (blue and red dashed lines) modified after Yamaoka et al. (2015). It shows that almost all vent fluids reflect different W/R ratios during water-rock interaction with fresh volcanic rocks from the EMVZ. The B composition of most vent fluids reflects a basement composition of $\delta^{11}B$ = +6.5‰ (orange line). However, the oceanic crust appears to be more heterogeneous at SuSu Knolls and some vent fluids from SuSu Knolls were probably modified by the reaction with altered oceanic crust.

strongly influenced by magmatic fluids and represent a submarine analogue to subaerial fumaroles (Seewald et al., 2015).

Fluids from group (I) and (II) have in common that water-rock reactions are inevitably involved. The effect of reactions between seawater and back-arc basin crust on B systematics of the interacting fluids can be approximated by computing a seawater-rock mixing line, while accounting for partitioning and isotopic fractionation between altered rock and fluid. The model developed by Yamaoka et al. (2015) uses a temperature-dependent partition coefficient and isotope fractionation factor between fluid and solid phases. We modified this model using B concentrations and isotope data for both fresh and altered volcanic rocks from rock samples measured in this study. In addition, we used data for MORB from the Manus Spreading Centre analysed by Shaw et al. (2012) to conduct mixing calculations relevant for the Vienna Woods system at the MSC. These computations are conducted for each of the three groups of fluids. Water-rock mass ratios (W/R) were varied between 4 and 0.5 in these calculations. Processes affecting B systematics in addition to water-rock interactions (phase separation, magma degassing) are identified by deviations from these predicted water-rock trends. To unravel the potential influences of these processes on the B composition of vent fluids, the individual groups of fluids will be discussed separately.

3.6.2.1 Group (I): high-Cl vent fluids in the Manus Basin

Fig.12 shows that end-member compositions of group I fluids are strongly controlled by interaction of seawater with the basement. Most noticeable, all PACMANUS fluids, except for one sample from Snowcap (SC2 2011), plot in the range of the calculated mixing line between seawater and the fresh volcanic rock from Satanic Mills with a B concentration of 20.3 mg/kg and a $\delta^{11}B$ value of +6.5‰ (Fig. 12, orange line). Vent fluids from South Su and two from North Su (NS3 and NS11) plot on the same trend. The other vent fluids from North Su, those from Suzette and SC2 2011 from Snowcap, plot on a model trend resulting from a basement composition of 11.8 mg/kg B and +8.3‰ (light blue line, Fig. 12). Vent fluids from North Su appear to show more scatter and are not matched by a single calculated mixing line. The dashed lines in Fig. 12 show that the interaction of seawater with altered volcanic rocks from the EMVZ can explain shifts to higher $\delta^{11}B$ (and lower B concentration) data. Having a variably altered basement can lead to a broader range for the calculated fluid composition assuming isotopic equilibrium between seawater and oceanic crust.

The fluid samples from Vienna Woods plot close to the mixing line (green solid line) between seawater and MORB (31-1, Shaw et al., 2012). This is perhaps the clearest identification of the very strong effect that basement composition has on B systematics in back-arc vent fluids. Small offsets in B concentrations to higher values in the vent fluids may be due to an underestimation of

the B content of the basement. For instance, the mixing lines at Vienna Woods would be a closer match if higher B concentrations in the volcanic basement were assumed. Another source of uncertainty is the fluid-rock distribution coefficient and isotope fractionation factors for B between solid and fluid. In this study, we used the bulk distribution coefficient K_d = 0.1 (Yamaoka et al., 2012) and a B isotope fractionation factor of $\alpha_{solid\text{-}fluid}$ = 0.985 (Wunder et al., 2005), which were calculated for a uniform temperature of 300°C. Since the B isotope fractionation factor was calibrated using a synthetic boromuscovite, which might be not applicable to the basaltic host rocks from the MSC and most of the B leaching in hydrothermal systems is taking place in the reaction zone at higher temperatures, K_d and α might differ. However, assuming a B isotope fractionation factor of $\alpha_{solid\text{-}fluid}$ = 0.988 (400°C) and a bulk distribution coefficient (K_d) of 0, would also not explain the higher B concentrations in the Vienna Woods vent fluids. Cl concentrations in the vent fluids from Vienna Woods are about 122%. Hence, supercritical phase separation could also drive B enrichment in the residual brine phase (Foustoukos and Seyfried, 2007; Liebscher et al. 2005).

In summary, the group I fluids are clearly dominated by the B content of the basement. Both the PACMANUS and the Vienna Wood hydrothermal areas are hosted by magmatically robust volcanic centres and the B signatures of the vent fluids indicates interaction of seawater with fresh rocks. The offset in the Vienna Woods fluids relative to the calculated mixing line might relate to phase separation with partitioning of B into the brine phase or to higher B concentrations in the host rocks. In contrast, the greater variability in B systematics in fluids from SuSu Knolls can be explained by interaction with a higher proportion of altered oceanic crust. This may indicate that the volcanic basement in the hydrothermal root zone is more altered at SuSu Knolls than in the PACMANUS area and at Vienna Woods.

3.6.2.2 Group (II): low-Cl vent fluids in the EMVZ and Nifonea volcano

Vent fluids with low Cl concentrations from the EMVZ have B concentrations and isotopic signatures that plot outside the range of the model trends for interaction between seawater and fresh as well as altered volcanic rocks from the EMVZ (Fig. 13a). These fluids have lower B concentrations compared to the high-Cl fluids (group I) from the same vent sites. The vast majority of vent fluids from Nifonea volcano, which all have extremely low Cl concentrations (24 to 259 mmol/kg), fall close to the calculated mixing lines between seawater and fresh and altered volcanic rocks with basaltic composition (solid lines, Fig. 13b). However, Li contents in the Nifonea fluids reveal high W/R ratios (25 – 50) during water-rock interaction (Schmidt et al., 2017), whereas B isotope ratios point to extreme low W/R ratios (even lower than 0.5). Only if we use the B content of the basaltic andesite sample (green dashed line, Fig. 13b) from Futuna

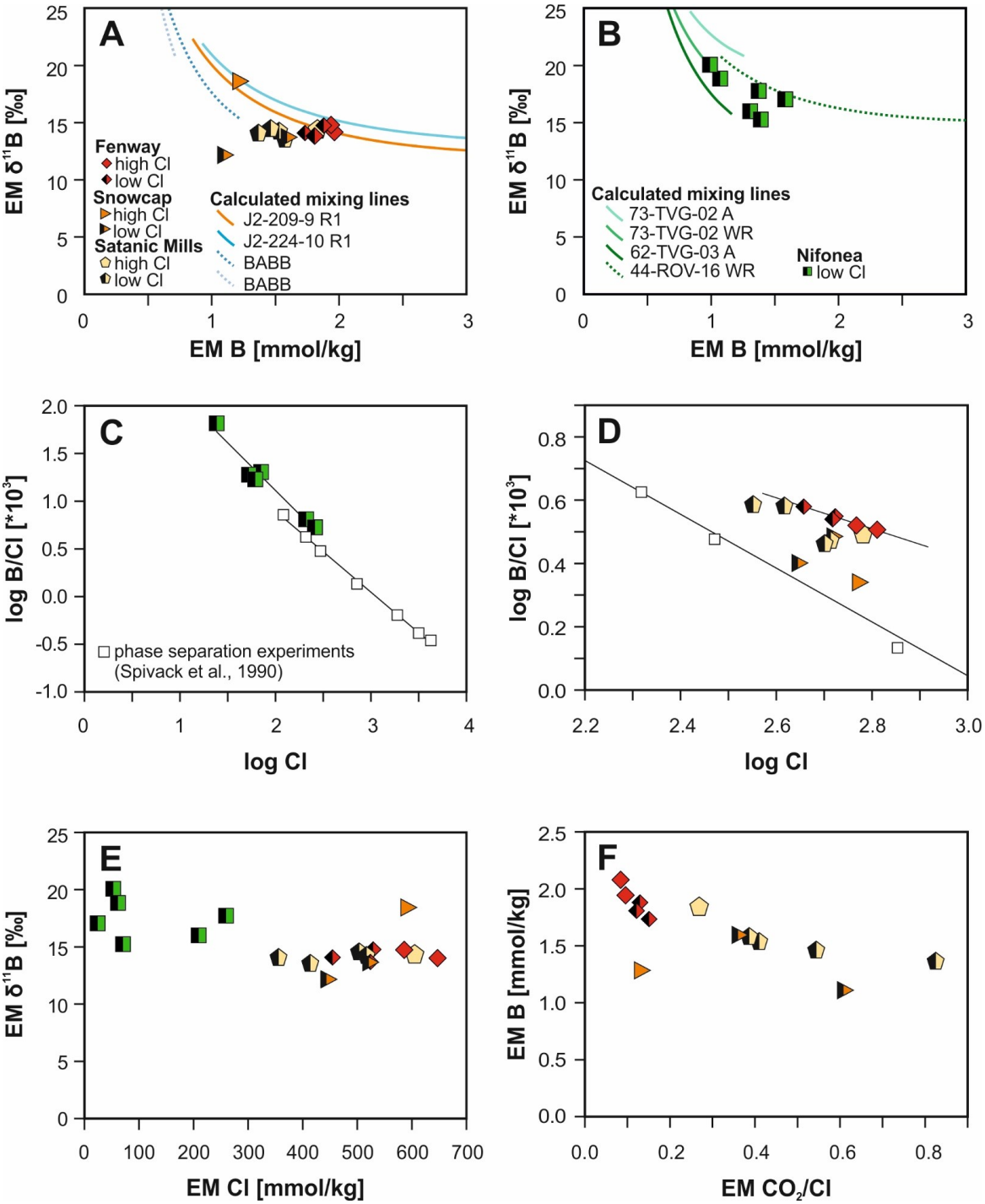

Figure 13: End-member (EM) B versus B isotope ratios in high and low Cl fluids from (A) Fenway, Snowcap and Satanic Mills within PACMANUS and (B) Nifonea volcano show that B in the phase separated fluids from PACMANUS do plot close to the calculated mixing lines. However, the B composition in vent fluids from Nifonea display much lower W/R ratios compared to those calculated with Li and Cs concentrations. (C) and (D) show that B in the fluids from Nifonea and Snowcap is most probably influenced by phase separation as the Cl to B/Cl ratio displays a constant fractionation during phase separation similar to phase separation experiments from Spivack et al. (1990), however (E) shows, that the isotopic composition is not influenced. (F) suggests that B in the fluids from the EMVZ is probably also influenced by the alteration effects of magmatic gases, which somehow lead to lower B concentrations in the vent fluids (see text).

Trough in the mixing calculation, four of the vent fluids could be explained by slightly higher W/R ratios. However, B compositions point to W/R ratios that are still lower than 4 and the high B concentrations found in the basaltic andesite (44-ROV-16 WR) from Futuna Trough (150 km away) might be not representative for Nifonea volcano. In fact, none of the analysed basaltic rocks from Nifonea volcano has high B concentrations. To understand B signatures in the low-Cl vent fluids from the EMVZ and Nifonea, we have to consider additional processes that can modify the B signature in vent fluids during hydrothermal circulation. Schmidt et al. (2017) suggested (i) B enrichment during boiling of the fluids, (ii) B addition via magmatic fluids and (iii) preferential mobilisation of B from B enriched rocks.

Chlorine contents in vent fluids that deviate from seawater chlorinity are most plausibly explained by phase separation during hydrothermal circulation (Berndt and Seyfried, 1997; Von Damm et al., 1997; Von Damm, 2000, Seyfried et al., 2003; Seyfried and Foustoukos, 2007). The significant depletion of Cl in the vent fluids from Fenway, Satanic Mills, and Snowcap as well as Nifonea volcano compared to seawater has thus been interpreted as evidence for phase separation (Reeves et al., 2011, Schmidt et al., 2017). Experimental studies have shown that B is slightly enriched in the saline phase if a fluid with seawater chlorinity undergoes phase separation (Berndt and Seyfried, 1990; Liebscher et al., 2005). Subsequently, Foustoukos and Seyfried (2007) addressed how the liquid-vapour partitioning of B varies as a function of pressure and temperature and found that B becomes enriched in the vapour phase when phase separation takes place under PT-conditions far from the two-phase curve of the NaCl-H_2O system. Accordingly, phase separation can influence B concentrations subsequently to water-rock interaction and B-enrichment through boiling may be responsible for the high B contents of the Nifonea fluids.

Yamaoka et al. (2015) analysed fluids from the North Fiji Basin (NFB), which have also been interpreted as condensed vapours, owing to their low chlorinities. Because of the small variations in B concentrations and isotope ratios in the NFB fluids, these authors argue that water-rock interaction controls B systematics and that the effect of phase separation is small. In contrast to the NFB fluids, chlorinities in the Nifonea fluids are even smaller pointing to extreme conditions of phase separation, which would lead to B enrichment in the vapour phase (Foustoukos and Seyfried, 2007). Indeed, end-member vent fluids from Nifonea show a significant linear correlation between LogCl and LogB/Cl (Fig. 13c). This is in accordance with previous studies of phase-separated vent fluids and results of experimental investigations, indicating a constant fractionation of B and Cl during phase separation (You et al., 1994; Spivack et al., 1990; Foustoukos and Seyfried, 2007). Vent fluids from Fenway, which were undergoing active phase separation (boiling) when sampled in 2006 (Reeves et al., 2011) also show this linear correlation (Fig. 13d). For the vent fluids from Nifonea and Fenway, these results indicate that B concentrations are indeed influenced by phase separation. However, the vent fluids from Satanic

Mills and Snowcap (Fig. 13d) display compositions in the LogB/Cl vs LogCl plane that are shifted to higher B/Cl, suggesting that earlier phase separation under more extreme PT conditions may have led to preferential partitioning of B into the vapour phase. The lack of correlation between Cl and B isotope ratios (Fig. 13e) suggests that phase separation has a negligible effect on the B isotope ratio in the vent fluids. It appears that the B-Cl relations may be affected by water-rock reactions (affecting B) and phase separation (affecting both B and Cl).

As mentioned earlier, Li contents in the Nifonea fluids point to high W/R ratios (25 – 50), whereas B isotope ratios point to extreme low W/R ratios (even lower than 0.5). However, since B and Li may show contrasting liquid-vapour partitioning behaviour (e.g., Foustoukos and Seyfried, 2007) these apparent difference in W/R ratios can be also a result of the different partitioning behaviour during phase separation. Nevertheless, phase separation does still not explain the low B isotope ratios in Nifonea's vent fluids, since B isotope fractionation during phase separation at high temperatures appears to be negligible, with a slight tendency of ^{11}B to partition into the vapour phase (Spivack et al., 1990, Leeman et al., 1992; Liebscher et al., 2005). Moreover, the missing correlations between LogCl and LogB/Cl at Satanic Mills or Snowcap imply that phase separation and water-rock interaction cannot be the only influence at least on the fluids from PACMANUS. Furthermore, B/Cl ratios do not necessarily reflect phase separation in hydrothermal fluids but can also be used as a proxy for the CO_2/Cl ratio and thus as proxy for magmatic fluid influx (Giggenbach et al., 1995). Thus, B from magmatic fluids may also affect B in the vent fluids.

3.6.3 Influence of magmatic fluids on B in vent fluids

Recent studies show evidence for inputs of magmatic fluids into vent fluids of the EMVZ (Bach et al., 2003; Kim et al., 2004; Craddock et al., 2010; Craddock and Bach, 2010; Reeves et al., 2011; Webber et al., 2011; Seewald et al., 2015). However, vent fluids in the EMVZ show variable amounts of magmatic volatiles. Reeves et al. (2011) for example found much higher proportions of magmatic volatiles in fluids at Snowcap compared with Roman Ruins. Vent fluids from Satanic Mills, Snowcap and Fenway within PACMANUS have extreme enrichments of carbon dioxide. A simple leaching of CO_2 from magmatic rocks cannot explain the CO_2 enrichments in some of the vent fluids from PACMANUS (Butterfield et al., 1994, 2003; Seewald et al., 2003, Reeves et al., 2011). Hence, CO_2 needs to be added by active degassing of a magma chamber, which is supported by negative $\delta^{34}S_{H2S}$ values in the vent fluids (Reeves et al., 2011). It was also discussed for vent fluids from Nifonea volcano, whether the high As and B concentrations in the vent fluids can be explained by an addition from magmatic fluids (Schmidt et al., 2017). Unfortunately, there are no carbon dioxide concentrations for the vent fluids from Nifonea volcano and we will concentrate in the following discussion on the vent fluids from PACMANUS.

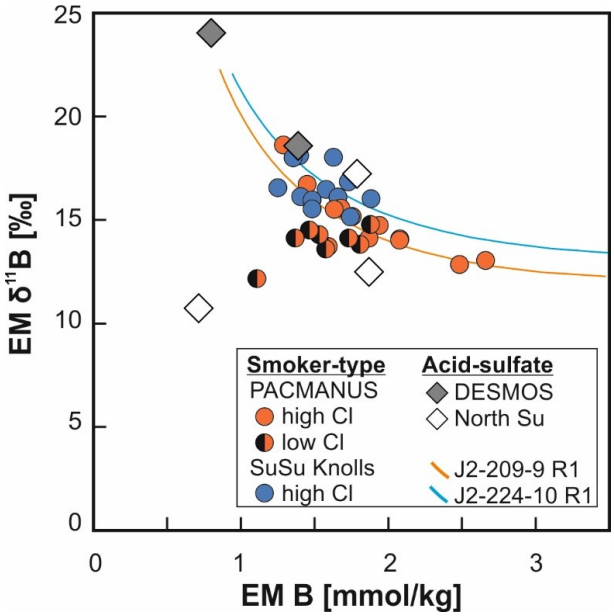

Figure 14: B concentration versus B isotope ratios in end-member acid-sulfate fluids from the Manus Basin in comparison with high- and low-Cl fluids from the same area. Most of the acid sulfate fluids overlap with the high Cl smoker fluids. Several have a high degree of variability with often low EM B values, however, likely attributable to variable alteration of the basement due to acid-sulfate fluid flow.

To test whether the influx of magmatic fluids influences B concentrations and isotopic signatures in the vent fluids, we compared ΣCO_2/Cl ratio in the vent fluids with B concentrations (Fig. 13f). Since ΣCO_2 contents and thus the proportions of magmatic input in the fluids can be overprinted by phase separation, we used the ΣCO_2/Cl ratio instead of ΣCO_2. Fig 13f shows, that B concentrations decrease with increasing gas contents. This trend could either indicate that B is not added to the fluid along with CO_2 from magma degassing or that CO_2 is preferentially partitioning into a low salinity vapour phase relative to B. The Snowcap fluids show lower B contents for given CO_2/Cl than other PACMANUS fluids in Fig. 13f. This could be related to a larger extent of B leached from a more extensively altered basement at Snowcap, which appears unlikely, taking into account that B isotope ratios would shift to higher values.

Another type of vent fluids affected by magmatic degassing (of dominantly SO_2) are acid-sulfate fluids, which can be considered as submarine analogue of subaerial fumaroles (Seewald et al., 2015). Studies of subaerial fumaroles gases show that their B contents and isotopic compositions are controlled by basement rocks (Leeman et al., 1992). However, different studies show that B isotopes have the potential to fractionate during magmatic degassing with ^{11}B preferentially partitioning into the vapour phase (Jiang and Palmer, 1998, Jiang et al., 2008). Indeed, sample NS9 from North Su is slightly enriched in ^{11}B relative to the basement rocks from North Su. In contrast, the other acid-sulfate fluids have B concentrations and isotope ratios following the mixing trend between seawater and oceanic crust (Fig. 14). Hence, they match the high-Cl fluids from the EMVZ. In general, the lack of correlations between CO_2 and B contents may indicate that the low-Cl, vapour-rich fluids from the EMVZ are not influenced by contributions from magmatic B influx. Much rather, B appears predominantly influenced by phase separation and water-rock interaction. For the acid-sulfate fluids, the trend implies that B might be added due to

preferential mobilisation from rocks in acidic, vapour-rich fluids as discussed for the Nifonea vent fluids. The high variability of B contents in the acid-sulfate fluids may be attributed to variable alteration in the basement, which is affected by interaction with acidic fluids and B leaching.

3.7 Summary and conclusion

Boron contents and isotopic data of the hydrothermal vent fluids from backarc basins show systematic variations that yield insights into complex interactions between seawater, basement rock and magmatic fluids. Fluids with moderate to high Cl contents (>540 mmol/kg) plot on the calculated mixing lines between seawater and fresh oceanic crust. This supports the idea that B in vent fluids reflects exchange between oceanic crust and interacting seawater. Interaction with altered basement results in shifts to higher $\delta^{11}B$ and lower B concentrations of the vent fluids. These shifts can be observed in some fluids from North Su, as well as in the fluids from Suzette and Snowcap (SC2 2011). The B contents, but not necessarily the isotope ratios, are also affected by phase separation. Results of this study also show that B in vent fluids with low Cl contents (<540 mmol/kg) from the EMVZ deviate from the calculated mixing lines and define a trend to lower B concentrations and isotope ratios. The fluids displaying these trends are also associated with phase separation and high magmatic fluid influx. End-member compositions of acid-sulfate fluids, which are affected by influx of SO_2 in addition to CO_2, are generally not too dissimilar from high Cl-vent fluids. Some of these fluids appear affected by a preferential mobilization of B from the surrounding rocks during their rise towards the seafloor, as indicated by their higher B concentrations and isotope ratios. Nevertheless, it remains unclear why some of the vapour-rich fluids from North Su (NS9), Satanic Mills and Snowcap (SC1) plot on a trend to lower B concentrations and isotope ratios. The interpretation is ambiguous, but might relate either to the addition of magmatic fluids or to a deviating leaching behaviour during the interaction between strongly altered oceanic crust and acidic, gas-rich fluids, which could influence the B partition coefficients and isotope fractionation factors between liquid and solid.

On the contrary, B in low Cl vent fluids from Nifonea volcano, which are characterized by extreme boiling, have higher B concentrations and lower $\delta^{11}B$ values than expected from Li or Cs concentrations in the fluids (Schmidt et al., 2017). Although the data suggest B enrichment in the vapour phase during phase separation, this process cannot explain the low B isotope ratios in the vent fluids. B concentrations and isotope ratios in the vent fluids from Nifonea might be best explained by a combination of phase separation and preferential leaching from fresh volcanic lava similar to the B systematics in most of the acid-sulfate fluids from the Manus Basin.

Our findings show that the complexity of sources and processes in back-arc settings leads to a higher variability in B concentrations and isotope ratios of vent fluids than observed at mid-ocean ridges. B signatures in the vent fluids are influenced by a broad compositional range of host rocks

and phase separation processes. Further, our data implies that B is preferentially leached from the host rocks during the reaction with gas-rich fluids, which leads to high B concentrations and isotope ratios even at high W/R ratios. In combination with other proxies for water-rock interaction, this offers the possibility to study hydrothermal alteration processes in the vent fluids.

3.8 Acknowledgments

The authors would like to thank the crew of the R/V Melville and R/V Sonne as well as the technical groups of ROV Jason II, ROV-MARUM-QUEST and ROV Kiel 6000. We thank Katja Schmidt and Selma Lima for discussion and data access. This study was part of MARUM project GB4 and was funded by the DFG-Research Centre/Cluster of Excellence "The Ocean in the Earth System" at MARUM – Centre for Environmental Sciences, University of Bremen and was supported from the German Research Foundation (DFG) Major Research Instrumentation Program (INST 144/308-1).

3.9 References

Anderson M. O., Hannington M. D., Haase K. E., Schwarz-Schampera U., Augustin N., McConachy T.F., Allen K. (2016) Tectonic focusing of voluminous basaltic eruptions in magma-deficient backarc rifts. *Earth Planet Sci. Lett.* **440**, 43-55.

Bach W., Roberts S., Vanko D. A., Binns R. A., Yeats C. J., Craddock P. R. and Humphris S. E. (2003) Controls of fluid chemistry and complexation on rare-earth element contents of anhydrite from the Pacmanus subseafloor hydrothermal system, Manus Basin, Papua New Guinea. *Miner. Deposita* **38**(8), 916–935.

Bach W., Dubilier N., Borowski C., Breuer C., Brunner B., Franke P., Herschelmann O., Hourdez S., Jonda L., Jöns N., Klar S., Koloa K., Mai A., Meyerdierks A., Müller I., Petersen S., Pjevac P., Ratmeyer V., Reeves E., Rehage R., Reuter C., Schaen A., Shu L., Thal J., Zarrouk M. (2011) Cruise Report for SONNE cruise SO 216 – BAMBUS, Back-Arc Manus Basin Underwater Solfataras. Universität Bremen (https://elib.suub.uni-bremen.de/edocs/00102250-1.pdf).

Baker E. T., Embley R. W., Walker S. L., Resing J. A., Lupton J. E., Nakamura K., de Ronde C. E. J., Massoth G. J. (2008) Hydrothermal activity and volcano distribution along the Mariana arc. *J. Geophys. Res.: Solid Earth* **113**, B08S09, doi:10.1029/2007JB005423.

Baumberger T., Früh-Green G. L., Dini A., Boschi C., van Zuilen K., Thorseth I. H., Pedersen R. B. (2016) Constraints on the sedimentary input into the Loki's Castle hydrothermal system (AMOR) from B isotope data. *Chem. Geol.* **443**, 111-120.

Bebout G. E., Ryan J. G., Leeman W. P., Bebout, A. E. (1999) Fractionation of trace elements by subduction-zone meatamorphism – effect of convergent-margin thermal evolution. *Earth Plant. Sci. Lett.* **171**, 63-81.

Beier C., Bach W., Turner S., Niedermeier D., Woodhead J., Erzinger J., Krumm S. (2015) Origin of Silicic Magmas at Spreading Centres – an Exampe from the South East Rift, Manus Basin. *J Petrol.* **56**, 255-277.

Berndt M. E., Seyfried Jr. W. E. (1997) Calibration of Br/Cl fractionation during subcritical phase separation of seawater; possible halite at 9 to 10°N East Pacific Rise. *Geochim. Cosmochim. Acta* **61**, 2849-2854.

Berryman E.J., Kutzschbach M., Trumbull R.B., Meixner A., van Hinsberg V., Kasemann S.A., Franz G. (2017). Tourmaline as a petrogenetic indicator in the fitsch Formation, Western Tauern Window, Eastern Alps. *Lithos,* doi.org/10.1016/j.lithos.2017.04.008

Binns R. A. and Scott S. D. (1993) Actively forming polymetallic sulfide deposits associated with felsic volcanic-rocks in the Eastern Manus Back-Arc Basin, Papua New Guinea. *Econ.*

Geol. **88**(8), 2226–2236.
Butterfield D.A., Massoth G.J., McDuff R.E., Lupton J.E., Lilley M.D. (1990) Geochemistry of hydrothermal fluids from Axial Seamount Hydrothermal Emissions Study vent field, Juan de Fuca Ridge: subseafloor boiling and subsequent fluid-rock interaction. *J. Geophys. Res.* **95**, 12895–12921.
Butterfield D. A. and Massoth G. J. (1994) Geochemistry of North Cleft Segment vent fluids—temporal changes in chlorinity and their possible relation to recent volcanism. *J. Geophys. Res.: Solid Earth* **99**(B3), 4951–4968.
Butterfield D., Seyfried W. E. and Lilley M. (2003) Composition and evolution of hydrothermal fluids. In Dahlem Workshop Report: *Energy and Mass Transfer in Marine Hydrothermal Systems*, vol. 89 (eds. P. E. Halbach, V. Tunnicliffe and J. R. Hein). Dahlem University Press, 123–161.
Chaussidon M., Jambon A. (1994) Boron content and isotopic composition of oceanic basalts: Geochemical and cosmochemical implications. *Earth and Planet. Sci. Lett.* **21**(3-4), 277-291.
Chaussidon M., Marty B. (1995) Primitive boron isotope composition of the mantle. *Science* **269**, 383–386.
Craddock P. R., Bach W., Seewald J. S., Rouxel O. J., Reeves E. and Tivey M. K. (2010) Rare earth element abundances in hydrothermal fluids from the Manus Basin, Papua New Guinea: indicators of sub-seafloor hydrothermal processes in back-arc basins. *Geochim. Cosmochim. Acta* **74**, 5494–5513.
Craddock P. R. and Bach W. (2010) Insights to magmatic-hydrothermal processes in the Manus back-arc basin as recorded by anhydrite. *Geochim. Cosmochim. Acta* **74**(19), 5514–5536.
de Ronde C.E.J., Massoth G.J., Baker E.T., Lupton J.E. (2003) Submarine hydrothermal venting related to volcanic arcs. In: Simmons, S.F., Graham, I.J. (Eds.), *Volcanic, geothermal, and ore-forming fluids: rulers and witnesses of processes within the earth*. Littleton, Colo: Society of Economic Geologists. Special publication / Society of Economic Geologists, **10**, pp. 91e109.
De Ronde C. E. J., Hannington M. D., Stoffers P., Wright I. C., Ditchburn R. G., Reyes A. G., Baker E. T., Massoth G. J., Lupton J. E., Walker S. L., et al. (2005) Evolution of a submarine magmatic-hydrothermal system: brothers volcano, southern Kermadec arc, New Zealand. *Econ. Geol*. **100**(6), 1097-1133.
De Ronde C. E. J., Stucker V. K. (2015) Seafloor Hydrothermal Venting at Volcanic Arcs and Backarcs. In *The Encyclopedia of Volcanoes (Second Edition* (eds. H. Sigurdsson, B. Houghton, S. McNutt, H. Rymer, J. Stix). Academic Press Elsevier, 823-849.
Douville E., Charlou J. L., Oelkers E. H., Bienvenu P., Jove Colon C. F., Donval J. P., Fouquet Y., Prieur D., Appriou P. (2002) The rainbow vent fluids (36°14′N, MAR): the influence of ultramafic rocks and phase separation on trace metal content in Mid-Atlantic Ridge hydrothermal fluids. *Chem. Geol.* **184**, 37-48.
Edmond J. M., Measures C., McDuff R. E., Chan L. H., Grant C. B. (1979) Ridge crest hydrothermal activity and the balances of the major and minor elements in the ocean: The Galapagos data. *Earth Planet. Sci. Lett*. **46**, 1-18.
Edmond J. M., Von Damm K. L., McDuff R. E., Measures C. I. (1982) Chemistry of hot springs on the East Pacific Rise and their effluent dispersal. *Nature* **297**, 187-191.
Elderfield H. and Schultz A. (1996) Mid-Ocean Ridge Hydrothermal Fluxes and the Chemical Composition of the Ocean. *Annual Rev. of Earth and Plan. Sciences* **24**, 191-224
Foster G.L., Pogge von Strandmann P. A. E., Rae J. W. B. (2010) Boron and magnesium isotopic composition of seawater. *Geochem. Geophys. Geosyst.* **11**(8), Q08015, doi:10.1029/2010GC003201.
Foustoukos D. I., Seyfried Jr. W. E. (2007) Trace element partitioning between vapour, brine and halite under extreme phase separation conditions. *Geochim. Cosmochim. Acta* **71**, 2056-2071.
Gamo T., Okamura K., Charlou J. L., Urabe T., Auzende J. M., Ishibashi J., Shitashima K. and Chiba H. (1997) Acidic and sulfate-rich hydrothermal fluids from the Manus back-arc basin, Papua New Guinea. *Geology* **25**(2), 139–142.

Garbe-Schönberg D., Koschinsky A., Ratmeyer V., Jähmlich H., Westernströer U. (2006) KIPS – A new multiport valve-based all-Teflon fluid sampling system for ROVs. In *Geophys. Res. Abstr.* **8** p. 07032.

Giggenbach W. F. (1995) Variations in the chemical and isotopic composition of fluids discharged over the Taupo Volcanic Zone. *J. Volcanol. Geotherm. Res*. **68**, 89-116.

Hannington M., Jamieson J., Monecke T., Petersen S., Beaulieu S. (2011) The abundance of seafloor massive sulfide deposits. *Geology* **39** (12), 1155-1158.

Hedenquist J. W., Lowenstern J. B. (1994) The role of magmas in the formation of hydrothermal ore deposits. *Nature* **370**, 519-527.

Gonfiantini R., Tonarini S., Groening, M., et al. (2003) Intercomparison of boron isotope and concentration measurements; part II, evaluation of results. *Geostandard Newslett.* **27**, 41-57.

Hüpers A., Kasemann S. A., Kopf A.J., Meixner A., Toki T., Shinjo R., Wheat C. G., You C. F. (2016) Pore flow and water-rock interaction across the active Nankai Trough subduction zone forearc revealed by boron isotope geochemistry. *Geochim. Cosmochim. Acta* **193**, 100-118.

Iizasa K., Kawasaki K., Maeda K., Matsumoto T., Saito N., Hirai K. (1998) Hydrothermal sulfide-bearing Fe-Si oxyhydroxide deposits from the Coriolis Troughs, Vanuatu backarc, southwestern Pacific. *Marine Geology* **145**, 1-21

Ishikawa T., Nakamura E. (1994) Origin of the slab component in arc lavas from across-arc variation of B and Pb isotopes. *Nature* **370**, 205–208.

Ishikawa T., Tera F. (1997) Source, composition and distribution of the fluid in the Kurile mantle wedge: constraints from across-arc variations of B/Nb and B isotopes. *Earth Planet. Sci. Lett.* **152**, 123–138.

Ishikawa T., Tera F. (1999) Two isotopically distinct fluid components involved in the Mariana arc: evidence from Nb/B ratios and B, Sr, Nd, and Pb isotope systematics. *Geology* **27**, 83–86.

Ishikawa T., Tera F., Nakazawa T. (2001) Boron isotope and trace element systematics of the three volcanic zones in the Kamchatka arc. *Geochim. Cosmochim. Acta* **65**, 4523–4537.

James R. H., Elderfield H., Palmer M. R. (1995) The chemistry of hydrothermal fluids from the Broken Spur site, 29°N Mid-Atlantic Ridge. *Geochim. Cosmochim. Acta* **59**, 651–659.

Jiang S.-Y., Palmer M. R. (1998) Boron isotope systematics of Tourmaline from granites and pegmatites: A synthesis. *Europoean Journal of Mineralogy* **10**, 1253-1265.

Jiang S.-Y., Radvanec M., Nakamura E., Palmer M., Kobayashi K., Zhao H.-X., Zhao K.-D. (2008) Chemical and boron isotopic variations of tourmaline in the Hnilec granite-related hydrothermal system, Slovakia: Constraints on magmatic and metamorphic fluid evolution. *Lithos* **106** (1-2), 1-11.

JICA (Japan International Cooperation Agency), MMAJ (Metal Mining Agency of Japan), and SOPAC (South Pacific Applied Geoscience Commission), 1995, South Pacific seafloor atlas. Japan-SOPAC cooperative study on deep sea mineral resources in the southwest Pacific 1985–1994: *JICA Report* no. 95-063, 24 p.

Kamenetsky V. S., Binns R. A., Gemmell J. B., Crawford A. J., Mernagh T. P., Maas R., Steele D. (2001) Parental basaltic melts and fluids in eastern Manus backarc Basin: implications for hydrothermal mineralisation. *Earth Planet. Sci. Lett.* **184** (3-4), 685-702

Kim J., Lee I., Lee K. Y. (2004) S, Sr, and Pb isotopic systematics of hydrothermal chimney precipitates from the eastern Manus Basin, western Pacific; evaluation of magmatic contribution to hydrothermal system. *J. Geophys. Res.* **109**, B12, 13.

Kutzschbach M., Wunder B., Meixner A., Wirth R., Heinrich W., Franz G. (2017) Jeremejevite as a precursor for olenitic tourmaline: consequences of non-classical crystallization pathways for composition, textures and B isotope patterns of tourmaline. *European Journal of Mineralogy* **29**, 239-255.

Lee S. M. and Ruellan E. (2006) Tectonic and magmatic evolution of the Bismarck Sea, Papua New Guinea: review and new synthesis. In *Back-Arc Spreading Systems: Geological, Biological, Chemical, and Physical Interactions*, vol. **166** (eds. D. M. Christie, C. R. Fisher, S.-M. Lee and S. Givens). AGU Monograph. American Geophysical Union, 263–286.

Leeman W. P., Vocke R. D., McKibben M. A. (1992) Boron isotopic fractionation between coexisting vapor and liquid in natural geothermal systems. *7th international Symposium on Water-Rock interaction WRI-7*, Park City, Utah, USA, 13-18 July 1992 2. AA Balkema, Rotterdam, 1007-1010.

Leeman W. P., Tonarini S., Pennisi M., Ferrara G. (2005) Boron isotopic variations in fumarolic condensates and thermal waters from Vulcano Island: Implications for evolution of volcanic fluids. *Geochim. Cosmoch. Acta* **69**, 143-163.

Leeman W. P., Tonarini S., Turner S. (2017) Boron isotope variations in Tonga-Kermadec-New Zealand arc lavas: Implications for origin of subduction components and mantle influences, *Geochemistry, Geophysics, Geosystems*, doi: 10.1002/2016GC006523.

Liebscher A., Meixner A., Romer R. L., Heinrich, W. (2005) Liquid-vapor fractionation of boron and boron isotopes: experimental calibration at 400°C/23 MPa to 450°C/42 MPa. *Geochim. Cosmochim. Acta* **69** (24), 5693-5704.

Lima S.M., Haase K.M., Beier C., Regelous M., Brandl P.A., Hauff F., Krumm S. (in press) Magmatic evolution and source variation at the Nifonea Ridge (New Hebrides Island Arc). *J. Petrol.* (2017).

Martinez F. and Taylor B. (1996) Backarc spreading, rifting, and microplate rotation, between transform faults in the Manus basin. *Mar. Geophys. Res.* **18**(2–4), 203–224.

Massoth G.J., Butterfield D.A., Lupton J.E., McDuff R.E., Lilley M.D., Jonasson I.R. (1989) Submarine venting of phase-separated hydrothermal fluids at Axial Volcano, Juan de Fuca Ridge. *Nature* **340**, 702-705.

McConachy T. F., Arculus R. J., Yeats C. J., Binns R. A., Barriga F.J.A.S., McInnes B.I.A., Sestak S., Sharpe R., Rakau B., Tevi T (2005): New hydrothermal activity and alkali volcanism in the backarc Coriolis Troughs, Vanuatu. *Geology* **33**, 61-64.

Monjaret M. C., Bellon H., Maillet P. (1991) Magmatism of the troughs behind the New Hebrides island arc (RV Jean Charcot SEAPSO 2 cruise): K-Ar geochronology and petrology. *J. Volcanol. and Geotherm. Res.* **46**, 265-280.

Mottl M. J. and Holland H. D. (1978) Chemical exchange during hydrothermal alteration of basalt by seawater: I. Experimental results for major and minor components of seawater. *Geochim. Cosmochim. Acta* **42**(8), 1103–1115.

Mottl M. J. (2003) Partitioning of energy and mass fluxes between mid-ocean ridge axes and flanks at high and low temperature. In: Halbach, P.E., Tunnicliffe, V., Hein, J.R. (eds.) *Energy and Mass Transfer in Marine Hydrothermal Systems*, Berlin: Dahlem University Press, 271-287.

Mottl M. J., Seewald J. S., Wheat C. G., Tivey M. K., Michael P. J., Proskurowski G., McCollom T. M., Reeves E., Sharkey J., You C.-F., Chan L.-H., Pichler T. (2011) Chemistry of hot springs along the Eastern Lau Spreading Center. *Geochim. Cosmochim. Acta* **75**, 1013–1038.

Nakamura E., Ishikawa T., Birck J.-L., Allegre C.-J. (1992) Precise boron isotopic analysis of natural rock samples using a boron-mannitol complex. *Chem. Geol.* **94**, 193-204.

Neef G., McCulloch M. T. (2001) Pliocene-Quaternary history of Futuna Island, south Vanuatu, southwest Pacific. *Australian Journal of Earth Sciences* **48**, 805-814.

Nielsen S. G., Rehkämper M., Teagle D. A. H., Butterfield D. A., Alt J. C., Halliday A. N. (2006) Hydrothermal fluid fluxes calculated from the isotopic mass balance of thallium in the ocean crust. *Earth Planet. Sci. Lett.* **251**, 120-133.

Ogawa Y., Shikazono N., Ishiyama D., Sato H. and Mizuta T. (2005) An experimental study on felsic rock–artificial seawater interaction: implications for hydrothermal alteration and sulfate formation in the Kuroko mining area of Japan. *Mineral. Deposita* **39**(8), 813–821.

Palmer M. R. (1991) Boron-isotope systematics of Halmahera arc (Indonesia) lavas: evidence for involvement of the subducted slab. *Geology* **19**, 215–217.

Park S. H., Lee S.-M., Kamenov G. D., Kwon S.-T. and Lee K.-Y. (2010) Tracing the origin of subduction components beneath the South East rift in the Manus Basin, Papua New Guinea. *Chem. Geol.* **269**, 339–349.

Pearce J. A. and Stern R. J. (2006) Origin of back-arc basin magmas: trace element and isotope perspectives. In *Back-Arc Spreading Systems: Geological, Biological, Chemical, and*

Physical Interactions, vol. **166** (eds. D. M. Christie, C. R. Fisher, S.-M. Lee and S. Givens). AGU Monograph. American Geophysical Union, 63–86.

Reeves E. P., Seewald J. S., Saccocia P., Bach W., Craddock P. R., Shanks W. C., Sylva S. P., Walsh E., Pichler T., Rosner M. (2011) Geochemistry of hydrothermal fluids from the PACMANUS, Northeast Pual and Vienna Woods hydrothermal fields, Manus Basin, Papua New Guinea. *Geochim. Cosmochim. Acta* **75**, 1088–1123.

Reeves E.P., Thal J., Schaen A., Ono S., Seewald J., Bach W. (2015) Temporal evolution of magmatic-hydrothermal systems in the Manus Basin, Papua New Guinea: Insights from vent fluid chemistry and bathymetric observations (Invited). AGU Fall Meeting, abstract OS42A-05, San Francisco

Romer R. L., Meixner A., Hahne K. (2014) Lithium and boron isotopic composition of sedimentary rocks – The role of source history and depositional environment: A 250 Ma record from the Cadomian orogeny to the Variscan orogeny. *Gondwana Research* **26**, 1093-1110.

Ryan J.G., Langmuir C.H. (1993) The systematics of boron abundances in young volcanic rocks. *Geochim. Cosmochim. Acta* **57**, 1489-1498.

Schmidt K., Garbe-Schönberg D., Hannington M. D., Aderson M. O., Bühring B., Haase K., Haruel C., Lupton J. E., Koschinsky A. (2017) Boiling vapour-type fluids from the Nifonea vent field (New Hebrides Back-Arc, Vanuatu, SW Pacific): Geochemistry of an early-stage, post-eruptive hydrothermal system. *Geochim. Cosmochim. Acta* **207**, 185-209.

Seewald J. S., Doherty K. W., Hammar T. R. and Liberatore S. P. (2002) A new gas-tight isobaric sampler for hydrothermal fluids. *Deep Sea Res*. Part I **49**(1), 189–196.

Seewald J., Cruse A., Saccocia P. (2003) Aqueous volatiles in hydrothermal fluids from the Main Endeavour Field, northern Juan de Fuca Ridge: temporal variability following earthquake activity. *Earth Planet. Sci. Lett.* **216**(4), 575–590.

Seewald J. S., Reeves E. P., Bach W., Saccocia P. J., Craddock P. R., Shanks III W. C., Sylva S. P., Pichler T., Rosner M., Walsh E. (2015) Submarine Venting of magmatic volatiles in the Eastern Manus Basin, Papua New Guinea. *Geochim. Cosmochim. Acta* **163**, 179-199

Seyfried W. E. and Bischoff J. L. (1981) Experimental seawater–basalt interaction at 300°C, 500 bars, chemical exchange, secondary mineral formation and implications for the transport of heavy metals. *Geochim. Cosmochim. Acta* **45**(2), 135–147.

Seyfried Jr W. E., Seewald J. S., Berndt M. E., Ding K., Foustoukos D. I. (2003) Chemistry of hydrothermal vent fluids from the Main Endeavour Field, Northern Juan de Fuca Ridge: Geochemical controls in the aftermath of June 1999 seismic events. *J. Geophys. Res.* **108**, 2429.

Shaw A. M., Hilton D. R., Macpherson C. G., Sinton J. M. (2004) The CO_2-He-Ar-H_2O systematics of the Manus back-arc basin: resolving source composition from degassing and contamination effects. *Geochim. Cosmochim. Acta* **68**(8), 1837-1856.

Shaw A. M., Hauri E. H., Behn M. D., Hilton D. R., Macpherson C. G., Sinton J. M. (2012) Long-term preservation of slab signatures in the mantle inferred from hydrogen isotopes. *Nature Geoscience* **5**, 224-228.

Sinton J. M., Ford L. L., Chappell B. and McCulloch M. T. (2003) Magma genesis and mantle heterogeneity in the Manus back-arc basin, Papua New Guinea. *J. Petrol.* **44**(1), 159–195.

Smith H. J., Leeman W. P., Davidson J., Spivack A. J. (1997) The B isotopic composition of arc lavas from Martinique, Lesser Antilles. *Earth Planet. Sci. Lett.* **146**, 303–314.

Spivack A. J., Berndt M. E., Seyfried Jr W. E. (1990) Boron isotope fractionation during supercritical phase separation. *Geochim. Cosmochim. Acta* **54**, 2337-2339.

Taylor B., Crook K., Sinton J. (1994) Extensional transform zones and oblique spreading centers. *J. Geophys. Res.: Solid Earth* **99**(B10), 19707–19718.

Thal J., Tivey M. A., Yoerger D, Jöns N., Bach W. (2014) Geologic setting of PACManus hydrothermal vents – High-resolution mapping and in situ observations. *Marine Geology* **355**, 98-114.

Thal J., Tivey M., Yoerger D. R., Bach W. (2016) Subaqueous cryptodome eruption, hydrothermal activity and related seafloor morphologies on the andesitic North Su volcano. *J.of Volcanol. Geotherm. Res*. **323**, 80-96.

Tivey M., Bach W., Seewald J., Tivey M. K., Vanko D. A. and the Shipboard Science (2006) Cruise Report for R/V Melville cruise MGLN06MV – Hydrothermal systems in the Eastern Manus Basin: Fluid Chemistry and Magnetic Structure as Guides to Subseafloor Processes. Woods Hole Oceanographic Institution (available upon request to authors).

Von Damm K. L., Edmond J. M., Measures C. I. and Grant B. (1985) Chemistry of submarine hydrothermal solutions at Guaymas Basin, Gulf of California. *Geochim. Cosmochim. Acta* **49**, 2221-2237.

Von Damm K. L., Buttermore L. G., Oosting S. E., Bray A. M., Fornari D. J., Lilley M. D., Shanks III W. C. (1997) Direct observation of the evolution of a seafloor 'black smoker' from vapor to brine. *Earth Planet. Sci. Lett*. **149**, 101-111.

Von Damm K. L. (2000) Chemistry of hydrothermal vent fluids from 9°N-10°N, East Pacific Rise; "time zero," the immediate posteruptive period. *J. Geophys. Res.* **105**, 11203-11222.

Wang B. S., You C. F., Huang K. F., Wu S. F., Aggarwal S. K., Chung C. H., Lin P. Y. (2010) Direct separation of boron from Na-and Ca-rich matrices by sublimation for stable isotope measurement by MC-ICP-MS. *Talanta* **82**, 1378-1384.

Webber A. P., Roberts S., Burgess R., Boyce A. J. (2011) Fluid mixing and thermal regimes beneath the PACMANUS hydrothermal field, Papua New Guinea: Helium and oxygen isotope data. *Earth Planet. Sci. Lett.* **304**, 93-102.

Wilckens, F.K., Reeves, E.P., Bach, W., Meixner, A., Seewald, J.S., Koschinsky, A., Kasemann, S.A. (submitted) The influence of magmatic fluids and phase separation on B systematics in submarine hydrothermal vent fluids – A case study from the Manus Basin and Nifonea volcano. Submitted to *Geochim. Cosmochim Acta.*

Wu S.-F., You C.-F., Lin Y.-P., Valsami-Jones E., Baltatzis E. (2016) New boron isotopic evidence for sedimentary and magmatic fluid influence in the shallow hydrothermal vent system of Milos Island (Aedean Sea, Greece). J. of Volcanol. Geotherm. Res. **310**, 58-71.

Wunder B., Meixner A., Romer R. L., Wirth R., Heinrich W., (2005) The geochemical cycle of boron: constraints from boron isotope partitioning experiments between mica and fluid. *Lithos* **84**, 206–216.

Wunder, B., Meixner, A., Romer, R. L., Heinrich, W. (2006) Temperature-dependent isotopic fractionation of lithium between clinopyroxene and high-pressure hydrous fluids. *Contributions to Mineralogy and Petrology* **151**(1), 112-120

Yamaoka K., Hong E., Ishikawa T., Gamo T., Kawahata H. (2015) Boron isotope geochemistry of vent fluids from arc/back-arc seafloor hydrothermal systems in the western Pacific. *Chem. Geol.* **392**, 9-18.

You C.-F., Butterfield D. A., Spivack A. J., Gieskes J. M., Gamo T., Campbell A. J. (1994) Boron and halide systematics in submarine hydrothermal systems: effects of phase separation and sedimentary conditions. *Earth Planet. Sci. Lett.* **123**, 227–238.

Chapter 4: Lithium isotope ratios in submarine hydrothermal vent fluids from Manus Basin and Nifonea volcano reveal evidence for negligible Li isotope fractionation during water-rock interaction

Frederike K. Wilckens[1]*, Wolfgang Bach[1], Anette Meixner[1], Eoghan P. Reeves[1,2,3], Jeffrey S. Seewald[3], Andrea Koschinsky[4], Simone A. Kasemann[1]

[1] MARUM – Center for Marine Environmental Sciences and Faculty of Geosciences, University of Bremen, Germany (*corresponding author: fwilckens@marum.de, telephone: +49 (0) 421 218 65941)

[2] Department of Marine Chemistry and Geochemistry, Woods Hole Oceanographic Institution, USA

[3] Present address: Department of Earth Science & Centre for Geobiology, University of Bergen, Norway

[4] Department of Physics and Earth Sciences, Jacobs University, Bremen, Germany

In preparation for submission to *Chemical Geology*

4.1 Abstract

Li is mainly added by the riverine and hydrothermal influxes and subduction reflux to seawater and removed by reverse weathering reactions. Hence, the balance between these sources and sink control the Li budget of the ocean. Since the hydrothermal flux is assumed to be higher than the riverine influx or subduction reflux, it has a huge influence on seawater Li. In general, the composition of Li in hydrothermal vent fluids is thought reflect water-rock interaction at high temperatures. During hydrothermal circulation, Li is leached from the host rocks without any isotopic effects. However, there is a significant Li isotope fractionation during the formation of alteration minerals, which leads to an isotopic offset between hydrothermal fluids and oceanic crust. Most of the previous studies were conducted on submarine vent fluids along mid-ocean ridges. To better constrain the global hydrothermal Li flux into the ocean and further to understand the behaviour of Li in hydrothermal vent fluids, we present data from hydrothermal vent fluids and volcanic rocks from two back-arc basins in the Western Pacific: the Manus Basin, Papua New Guinea, and Nifonea Volcano, Vanuatu. Li concentrations and isotope ratios in vent fluids from the Manus Basin match with other vent fluids form arc and back-arc settings, having lower Li isotope ratios relative to vent fluids from mid-ocean ridge sites. Because the Li isotope ratios of those vent fluids are in accordance with the composition of fresh oceanic crust, we propose that the assumed isotopic fractionation of Li isotopes is negligible in arc and back-arc settings. Vent fluids from Nifonea volcano have the highest observed Li isotope ratios found so far in submarine hydrothermal vents, indicating extremely limited water-rock interaction during hydrothermal circulation. Besides these finding, the study shows that the previous assumed isotopic composition of the global hydrothermal Li flux might be invalid due to the significant differences in the Li composition of vent fluids from MOR and subduction-related settings.

4.2. Introduction

The behaviour of lithium (Li) and its isotopes in earth-surface processes has been subject of intense research within the last decades (e.g. Chan et al., 1992; Elliott et al., 2004; Huh et al., 2001). Li is a fluids mobile element and has two stable isotopes (^{6}Li and ^{7}Li) with abundances of 7.52 and 92.48%, respectively. Because of the large relative mass difference between ^{6}Li and ^{7}Li of about 16%, there is a strong isotopic fractionation during the interaction of water and rocks resulting in a large variation of δ^{7}Li (> 40‰) in the different reservoirs on the earth surface. For example, seawater has a Li isotopic composition of +31‰ (Millot et al., 2004), whereas mid ocean ridge basalts (MORB) range from +1.6 to +5.6‰ (Elliott et al., 2006; Tomascak et al., 2008). Due to its fluid mobility and the wide range of its isotopic signatures in the different reservoirs, Li and its isotopes appear to be a useful tool to investigate water-rock interaction during hydrothermal circulation.

Different studies suggested that Li in hydrothermal vent fluids is mainly controlled by seawater-basalt interaction at high temperatures. Li isotopes appear to be unaffected by phase separation processes (Chan et al., 1993; Huh et al., 1998; Foustoukos et al., 2004; Millot et al., 2010). Indeed, δ^7Li in hydrothermal vent fluids from MORs have compositions close to fresh oceanic crust with values ranging from +2.6 to +11‰ (Chan and Edmond, 1988; Chan et al., 1993, 1994, Foustoukos et al., 2004). Using these results, the hydrothermal Li flux from high-temperature sediment starved MOR systems was estimated to have a range between 1.2 and 3.9 × 10^{10} mol/a with an average isotopic composition of 8.3‰ (Palmer and Edmond, 1992, Chan et al., 1994, Elderfield and Schultz, 1996, Huh et al., 1998, Elliott et al., 2004; Misra and Froehlich, 2012). Hence, the average isotopic composition of Li in vent fluids is about 4‰ higher than in fresh oceanic crust. As a possible reason for this isotopic offset, Chan et al. (1993) suggested that the Li isotope ratios in high-temperature vent fluids are not only influenced by leaching of Li from primary minerals, but also by a Li loss due to Li incorporation into alteration phases. Indeed, mass balance calculations show that most of the fluids can be explained by leaching of Li from the host rocks without isotope effects and incorporation of Li into alteration phases considering an isotopic fractionation (Magenheim et al., 1995; Verney-Carron et al., 2015, Araoka et al., 2016).

First studies on Li systematics in vent fluids from arc and back-arc sites in the Western Pacific show that Li isotope ratios in vent fluids of these tectonic settings range between +1.6 and +7.2‰ (Mottl et al., 2011; Araoka et al., 2016). Lithium concentrations in these vent fluids are mainly consistent with those vent fluids from MOR settings, while δ^7Li values were found to be lower than the average assumed hydrothermal δ^7Li signature. Araoka et al. (2016) explained some of these differences with fluid-sediment interaction leading to lower Li isotope ratios in some of the arc- and back-arc settings. However, vent fluids from Vienna Woods site (Manus Basin), that are not influenced by large amounts of sediments and that match in their temperature, pH, boron concentrations, δ^{11}B and ^{87}Sr/^{86}Sr with hydrothermal fluids from MOR sites (Reeves et al., 2011, Yamaoka et al., 2015, Araoka et al., 2016), have also significantly lower δ^7Li values relative to vent fluids from mid-ocean ridges. As a consequence Araoka et al. (2016) suggested poorly known distribution coefficients and Li isotopic fractionation factors as well as diffusive isotopic fractionation as possible explanations for this offset. However, since no study had been undertaken, which combines hydrothermal fluids and rock samples from the same study area, these hypotheses are onöy speculative.

We present new evidence from Li and Sr isotope data in hydrothermal vent fluids and their host rocks from well characterized vent fields in the Manus Basin and at Nifonea volcano. These locations host a broad range of hydrothermal fluids from high-temperature black smoker fluids, fluids with magmatic inputs, phase separated vent fluids to diffuse fluids in the Manus Basin and boiling fluids from an early stage hydrothermal system at Nifonea volcano. The aim is to

investigate the behaviour of Li during water-rock interaction in a hydrothermal system knowing both the composition of the oceanic crust and the vent fluid composition. Furthermore, we can test whether phase separation or magmatic inputs influence the composition of Li and its isotopes in the vent fluids. Understanding Li systematics in vent fluids may offer the chance to investigate and understand differences in water-rock interaction during hydrothermal circulation at MOR and arc- and backarc sites. Further, the hydrothermal Li flux is considered almost as high as the riverine Li flux in the ocean (Misra and Froehlich, 2012). Thus, it represents one of the main sources of Li into the ocean. However, since most of the studies on Li systematics in hydrothermal vents were conducted at MOR settings, there are still huge uncertainties in the hydrothermal Li flux and it isotopic composition. Our data thus extend the Li dataset in a broad range of vent fluids, which might help to better quantify the global hydrothermal Li flux into the ocean.

4.3 Study Areas

4.3.1. Manus Basin

The Manus Basin is a young, rapidly opening back-arc basin. It is located in the northeastern Bismarck Sea (Fig. 15a) bordered to the South by the Willaumez Rise and New Britain trench and to the northeast by the inactive Manus Trench (Taylor et al., 1994; Lee and Ruellan, 2006) (Fig. 15a). The formation of the Manus Basin is related to the northward subduction of the Solomon plate along the New Britain Trench. Our study focuses on the Manus Spreading Centre, with a MORB like composition and the eastern part of the Manus Basin where basement consists of

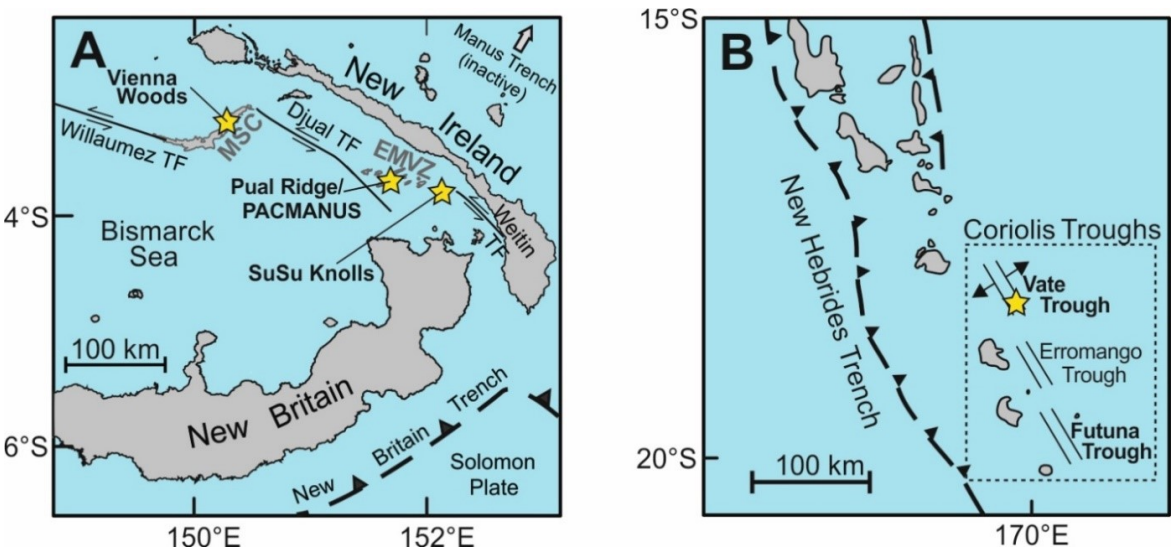

Figure 15: Tectonic setting of (A) the Manus Basin and (B) New Hebrides Trench. Yellow stars indicate the active hydrothermal vent fields PACMANUS, SuSu Knolls, Vienna Woods and Nifonea volcano within Vate Trough. Major tectonic plates and the plate motions are indicated with black and grey arrows. (A) was modified after Seewald et al., 2015 and (B) after Schmidt et al., 2017. MSC = Manus Spreading Centre, EMVZ = Eastern Manus Volcanic Zone, TF = Transform Fault

Eocene to Oligocene island arc crust formed during the subduction at the Manus Trench. The area between the Weitin and Djaul transform faults features neovolcanic ridges and solitary volcanoes that represent initial rifting in a pull-apart basin (Martinez and Taylor, 1996). The neovolcanic rocks reveal a strong geochemical and isotopic island arc affinity, which can be either related to the subduction of the Solomon plate or a relic from the former subduction at the Manus trench (Kamenetsky et al., 2001; Sinton et al., 2003; Pearce and Stern, 2006; Park et al., 2010; Beier et al., 2015).

Hydrothermal activity in the Manus Basin was discovered first in the late 1980s along the MSC (Vienna Woods vent site) (Both et al., 1986). Later three hydrothermal vent fields in the Eastern Manus Volcanic Zone were discovered: PACMANUS, SuSu Knolls and DESMOS (Fig. 15a) (e.g. Binns and Scott, 1993; Gamo et al., 1997).

4.3.1.1 PACMANUS and Northeast Pual

The PACMANUS (Papua New Guinea – Australia – Canada – MANUS) hydrothermally active area (Binns and Scott, 1993) expands over a roughly 1.5 km long section across Pual Ridge (Fig. 15a) in a water depth of 1639 to 1774 m. A total of eight discrete vent fields with variable

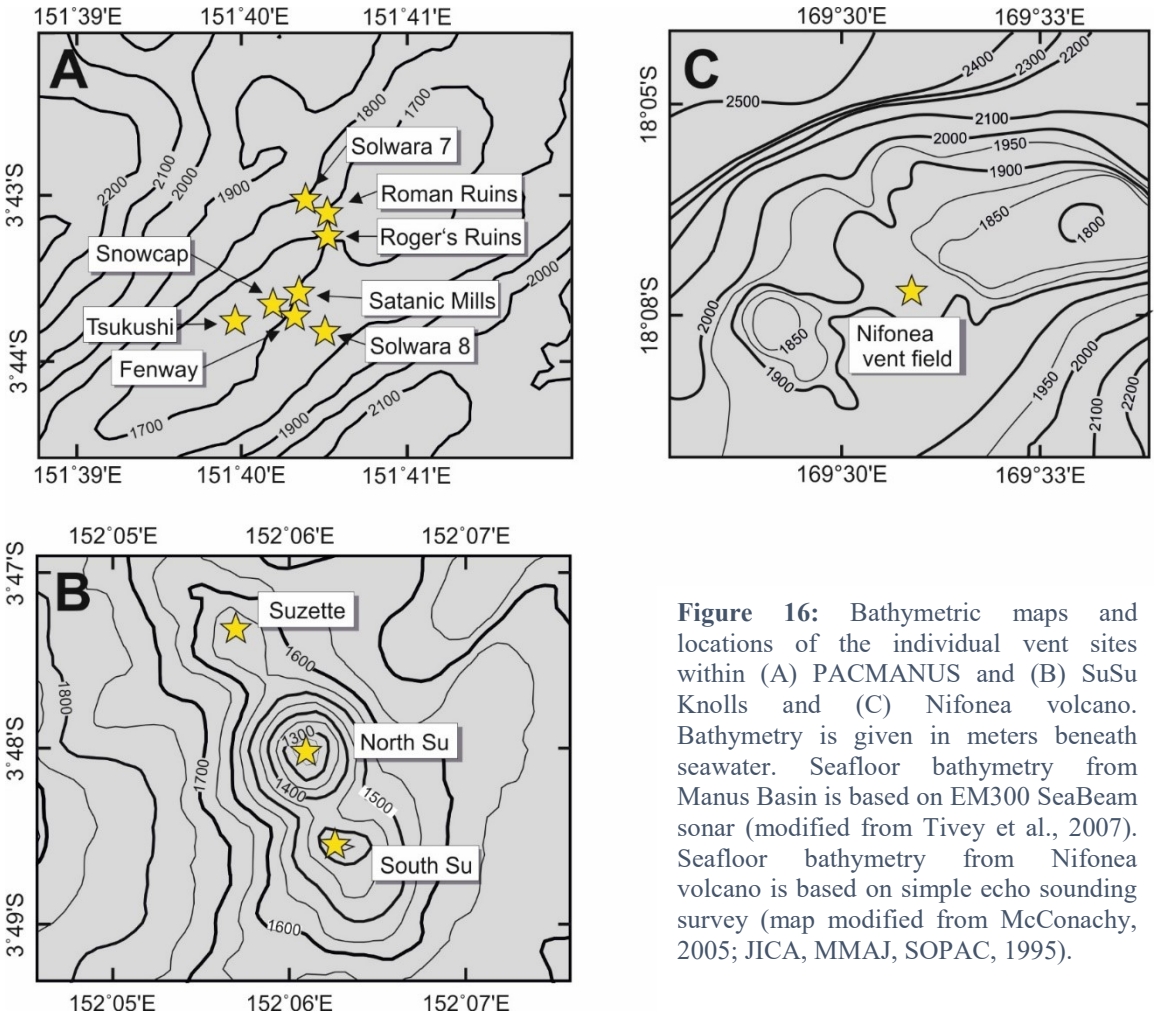

Figure 16: Bathymetric maps and locations of the individual vent sites within (A) PACMANUS and (B) SuSu Knolls and (C) Nifonea volcano. Bathymetry is given in meters beneath seawater. Seafloor bathymetry from Manus Basin is based on EM300 SeaBeam sonar (modified from Tivey et al., 2007). Seafloor bathymetry from Nifonea volcano is based on simple echo sounding survey (map modified from McConachy, 2005; JICA, MMAJ, SOPAC, 1995).

hydrothermal activity were mapped and sampled during two cruises in 2006 and 2011 (see section 3.1) (Fig. 16a). Each of the sampled hydrothermal vent fields at PACMANUS (Fenway, Roman Ruins, Roger's Ruins, Satanic Mills, Snowcap, Solwara 7, Solwara 8, and Tsukushi) expands over areas between 50 to 200 m in diameter. Thal et al. (2014) summarized the mapping results of both research cruises, provided a detailed account of the vent fields and discussed possible volcanic and tectonic controls of the vent distribution. Hydrothermal vent activity ranges from predominantly high temperature black smoker fluids with temperatures up to 358°C to few low temperature diffuse flows of 55°C (Craddock et al. (2010) and Reeves et al. (2011); summarized in Table 1). Northeast Pual is an area of patchy diffuse venting (temperatures around 35°C) on the crest of Pual Ridge 8 km northeast of PACMANUS (Reeves et al., 2011). The compositions of the vent fluids sampled in 2006 are reported in Craddock et al. (2010) and Reeves et al. (2011). They reveal variable influence of phase separation, magmatic degassing, and subseafloor entrainment of seawater.

4.3.1.2 SuSu Knolls

The SuSu Knolls area is located 45km east of PACMANUS (Fig. 15a) and includes three isolated volcanic centres: Suzette, North Su and South Su (Fig. 16b) with active vent systems in water depths between 1153 to 1504 m. Hydrothermal activity at Suzette is characterized by high-temperature (226°C to 303°C) venting from sulphide-rich chimneys. At North Su, vent fluids are extremely diverse (Craddock et al., 2010). In this area, venting of white, acid-sulfate fluids as well as black smoker fluid takes place, especially in the summit area of North Su (Craddock et al., 2010; Seewald et al., 2015; Thal et al., 2016). In the summit area of North Su and west of it (in water depths between 1150 and 1200 m), black smoker fluids vent at temperatures up to 332°C (temperature of boiling of seawater at 120 bar). South of the main summit, expansive fields of white smokers can be observed. At South Su hydrothermal activity is more limited in comparison with North Su ranging from diffuse fluids (not sampled during the cruises) to high-temperature fluids in the south and southeast (up to 290°C) (Craddock et al., 2010).

4.3.1.3 Vienna Woods

In contrast to the hydrothermal vent fields in the EMVZ, basalts in this area are characterized by seafloor spreading and have a similar composition to MORB (Shaw et al., 2004; Shaw et al., 2012). Hydrothermal activity occurs in a water depth of 2470m within the rift zone of the Manus spreading centre (MSC) (Fig. 15a). Temperatures of almost clear vent fluids range from 270°C to 290°C with moderate pH values around 4.4 (Tivey et al., 2006, Craddock et al., 2010, Reeves et al., 2011). The composition of vent fluids from Vienna Woods is similar to those found at mid-ocean ridges (Reeves et al., 2011), reflecting the high influence of the source rock on the vent fluids.

4.3.2 New Hebrides back-arc

The New Hebrides Ridge formed during the subduction of the Pacific Plate underneath the Australian Plate in the Late Oligocene to Middle Miocene (Schellart et al., 2006). In the Middle Miocene the Fiji Basin opened due to the collision of the New Hebrides Ridge with the Melanesian Border Plateau. Afterwards the rollback of the New Hebrides Trench led to a rotation of the island arc. Since 3 Ma years the Trench is rifting, which formed the Coriolis Troughs (Fig. 15b). The Coriolis Troughs describe three major depressions, Vate, Erromango and Futuna from north to south. Hydrothermal activity is occurring at the Vate Trough. Back-arc rifting at Vate Trough started about 3 Ma ago and is in its incipient stage of spreading (Monjaret et al., 1991, McConachy et al., 2005).

4.3.2.1 Vate Trough and Nifonea volcano

Nifonea volcano is located in the southern part of Vate trough and shows the highest magmatic activity in this area. Nifonea volcano is located in a water depth of 1860 to 1875m. Dominant rock types of the oceanic crust are subalkalic to alkali basalts, trachybasalts and basaltic trachyandesites (Lima et al., 2017). Hydrothermal activity occurs within the central part of the caldera in three clusters of several small chimneys (Fig. 16c). Black smoker and clear vent fluids in this area have temperatures up to 368°C (Table 1; Schmidt et al, 2017). The composition of the hydrothermal vent fluids indicates extreme boiling and limited water-rock interaction with high water/rock ratios (Schmidt et al., 2017).

4.4 Methods

Vent fluids and rocks from Manus Basin were sampled from six vent sites within PACMANUS hydrothermal area, three vent sites within SuSu Knolls area, one vent site from Northeast Pual, one from DESMOS caldera and one vent site from the Manus Spreading centre in July-August of 2006 during the MAGELLAN-06 expedition aboard the R/V Melville with ROV (Remotely Operated Vehicle) Jason II (Tivey et al., 2006). A follow-up cruise SO-216 (BAMBUS) in June-July of 2011 with R/V Sonne and ROV MARUM Quest 4000 collected additional samples from the EMVZ (Bach et al., 2011; Reeves et al. 2015). During cruise SO-216 additional fluid samples were collected from seven vent sites within the PACMANUS hydrothermal area as well as from North Su (SuSu Knolls area).

During both cruises, vent fluids were collected with isobaric gas-tight (IGT) samplers (Seewald et al., 2002). The concentrations of dissolved gases were determined on board. In addition, syringe-style “major” samplers (in 2006) and (in 2011) the Kiel Pumping System (KIPS) (Garbe-Schönberg et al., 2006) were used to collect fluids. Volcanic rock samples were collected from PACMANUS, SuSu Knolls and DESMOS during MAGELLAN-06 expedition using the ROV Jason II. Sampling methods and locations from the cruise in 2006 are described in more detail by

Craddock et al. (2010), Reeves et al. (2011) and Seewald et al. (2015) for the fluids, and by Beier et al. (2015) for fresh volcanic rocks. A subset of those fluid samples was selected for this study.

Nifonea volcano was investigated during R/V Sonne cruise SO-229 (VANUATU) in July of 2013. During the SO-229 cruise, fluids were sampled with ROV Kiel 6000. In total, eight fluids from five individual vent sites were taken at Nifonea volcano, using the KIPS fluid pump system. Volcanic rocks were sampled from Nifonea volcano and Futuna Trough during the same cruise and were collected using ROV Kiel 6000 and a TV-grab. Schmidt et al. (2017) describe sampling methods and locations for fluids and Lima et al. (2017) fresh volcanic samples in more detail.

In all fluid sampling events, temperature was measured simultaneously, and the bottles were triggered, when temperatures were high and steady to minimize entrainment of seawater upon sampling.

4.4.1 Sample preparation and isotope ratio measurement

Prior to isotopic analysis Li and Sr were separated from their sample matrix using different separation methods. For the preparation of rock samples, the rock chips were pulverized and digested using a mixture of HF, HNO_3 and H_2O_2. To prepare the vent fluids for Sr and Li column separations the fluids were dried.

For Sr isotope analysis about 300 ng Sr was loaded onto the columns. The chromatographic separation was done with Sr spec resin using a method modified by Pin and Bassin (1992). The separated Sr fraction was than loaded together with an tantalum emitter onto rhenium filaments and measured with TIMS (thermal ionization mass spectrometry). Strontium isotopic ratios are given in $^{87}Sr/^{86}Sr$ notation and were normalizuzed to $^{86}Sr/^{88}Sr$ of 0.1194. The instrumental precision for $^{87}Sr/^{86}Sr$ was obtained by repeated analysis of the international reference NIST 987, which has a value of 0.710248±15 (2SD, n=12). To validate and verify the chemical separation and digestion techniques used in this study, several international reference materials were separated and measured as well (BHVO-2, IAEA-B5, BM). The results for BHVO-2 ($^{87}Sr/^{86}Sr$ = 0.70347±2 (2SD, n=2)) are within analytical uncertainty in agreement with literature values ($^{87}Sr/^{86}Sr$ = 0.70348±6 (2SD, n=80).

For Li isotope analysis at least 100 ng Li was loaded onto the column. Li was separated from its sample matrix using a two-step column separation modified after Moriguti and Nakamura (1998). Separated Li fractions were checked for their purity and measured on a ThermoScientific Neptune MC-ICP-MS (Multicollector inductively coupled plasma mass spectrometer). Li isotope ratios were measured using the standard-sample-bracketing method with the international reference material L-SVEC as bracketing standard. Isotope data for Li- is reported in delta notation relative to a standard material and is expressed in per mill (‰).

$$\delta^7 Li\ [‰] = \left[\frac{\left(\frac{^6Li}{^7Li}\right)_{sample}}{\left(\frac{^6Li}{^7Li}\right)_{L-SVEC}} - 1\right] \cdot 1000 \qquad (5)$$

To control the preparation procedure and examine the effects of contamination and parameter change, solutions of continuously measured standard materials were included in each sample batch and handled in the same way as the actual samples. Procedural blanks were lower than 0.01%. Hence, they were not affecting the sample composition. The accuracy and precision of the method was obtained by repeated preparation and analysis of an internal seawater standard (bottom seawater from SuSu Knolls), and the international reference materials L-SVEC and BHVO-2. Long-time reproducibility of L-SVEC was δ⁷Li of 0.0±0.1‰ (2SD, n=17). Li isotope ratios and concentrations of an internal laboratory seawater standard (bottom seawater from SuSu Knolls) (δ^7Li of 31.1±0.2‰ (2SD, n=5)) are in agreement with literature values (+31.1±0.3‰ (2SD), Huang et al., 2010; Wimpenny et al., 2010; Pogge von Strandmann et al., 2010). The basalt reference material BHVO-2 has a δ^7Li value of 4.3±0.3‰ (2SD, n=2), which is within the range of the published isotope values (4.5±0.3‰, 2SD) (Gao et al., 2012; Genske et al., 2014; Magna et al., 2015).

4.4.2 End-member calculation

During sampling of the hydrothermal vent fluids, the samplers were prefilled with small amounts of seawater. In addition, vent fluids can mix during sample collection and prior to venting with seawater, the collected samples represent a two-component mixture between seawater and hydrothermal fluid. To correct for seawater entrainment, a weighted linear regression for the vent fluids from the same orifice to Mg=0 was done (Von Damm et al., 1985) assuming a complete removal of Mg during hydrothermal circulation and conservative behaviour of the elements during the mixing with seawater (Mottl and Holland, 1987; Seyfried and Bischof, 1981; Ogawa et al., 2005). The calculation of end-member Li and Sr isotope ratios was done with the inverse concentration of Li and Sr, respectively.

4.5 Results

4.5.1 Lithium and Strontium concentration and isotope ratios

4.5.1.1 Vent fluids

Li and Sr concentrations and isotope ratios for the vent fluids and end-member compositions are summarized in table 4 and 5. End-member fluids from Nifonea have Li and Sr concentrations which are depleted relative to seawater, with average concentrations between 11.2 and 21.4 µmol/kg and 12 to 54 µmol/kg, respectively. Li concentrations in end-member fluids from Manus Basin are consistently high at Vienna Woods with concentrations ranging 1072 to 1158 µmol/kg. PACMANUS fluids have the highest variation in their Li end-member concentrations ranging

Table 4: Measured Li and Strontium Isotope data in the vent fluids from the EMVZ, MSC and Nifonea together with previously reported data fromthe vent fluids

Vent field	Area: Vent	Sample	Year of sampling	IGT T[a] (°C)	pH[a] 25°C	Mg[a] (mm)	K[a] (mm)	Li[a] (µm)	Sr[a] (µm)	Cl[a] (mm)	δ^7Li ± 2sd (‰)	$^{87}Sr/^{86}Sr$ ± 2se
Eastern Manus Volcanic Zone (EMVZ)												
PACMANUS												
Fenway	F1	J2-210-IGT1	2006	296	2.5	6.0	54	637	95	463		
		J2-210-M4	2006		2.6	5.8	54	654	96	465	5.5 ± 0.2	0.70496 ± 0.00001
	F3	J2-212-M2	2006	330	2.8	8.9	67	793	93	573	6.6 ± 0.2	
		J2-212-IGT2	2006	358	2.7	4.5	74	904	103	586	5.3 ± 0.3	0.70433 ± 0.00000
	F4	J2-216-M2	2006		2.4	10.2	58	688	83	527		
		J2-216-IGT6	2006	284	2.5	8.7	61	685	86	524	5.2 ± 0.1	0.70466 ± 0.00001
	F5	J2-216-M4	2006		5.8	48.8	12	65	97	535		
		J2-216-IGT3	2006	80	4.9	44.0	15	119	104	517	10.6 ± 0.1	0.70845 ± 0.00001
	F7	029-ROV-01	2011	304	2.5	12.4	69	719	94	625	5.6 ± 0.2	0.70500 ± 0.00001
		029-ROV-02	2011	304	2.4	9.4	72	764	95	625	5.1 ± 0.1	0.70755 ± 0.00001
	F8	041-ROV-03	2011	314	2.7	11.8	52	633	78	532	5.5 ± 0.0	0.70525 ± 0.00001
Roger's Ruins	RGR1	J2-213-IGT3	2006	320	2.7	5.1	74	788	111	635	5.5 ± 0.1	0.70470 ± 0.00001
	RGR2	J2-222-IGT3	2006	274	2.6	9.0	69	753	102	631	5.5 ± 0.5	
		J2-222-IGT4	2006	130	3.0	22.3	50	498	92	606	6.0 ± 0.3	
Roman Ruins	RMR1	J2-208-IGT8	2006	312	2.3	7.3	72	986	78	617	4.6 ± 0.1	
	RMR3	J2-213-IGT7	2006	278	3.2	22.7	59	778	85	648	4.9 ± 0.2	
	RMR4	J2-222-IGT1	2006	341	2.7	3.6	77	1059	88	650	4.9 ± 0.2	0.70445 ± 0.00001
	RMR5	039-ROV-02	2011	333	3.3	20.3	59	665	74	656	5.4 ± 0.1	0.70646 ± 0.00000
		039-ROV-03	2011	324	2.6	5.3	81	965	72	716	4.9 ± 0.2	0.70498 ± 0.00001
Snowcap	SC1	J2-210-IGT8	2006	120	4.6	30.8	25	298	44	499	6.5 ± 0.2	0.70713 ± 0.00001
		J2-210-IGT5	2006	152	5.0	48.5	13	89	82	532	12.8 ± 0.1	
	SC2 2006	J2-211-M4	2006		3.4	24.5	34	503	56	530	5.6 ± 0.1	0.70640 ± 0.00001
		J2-211-IGT4	2006	180	3.4	24.2	35	486	56	532	5.9 ± 0.2	0.70646 ± 0.00001
	SC2 2011	027-ROV-02	2011	102	4.8	41.0	19	221	77	557	7.5 ± 0.1	0.70495 ± 0.00001
		027-ROV-03	2011	224	4.0	26.7	28	429	66	562	5.8 ± 0.1	0.70685 ± 0.00001
Solwara 7	SL7	037-ROV-01	2011	348	2.9	3.9	86	681	115	661	5.1 ± 0.3	0.70440 ± 0.00001
Satanic Mills	SM1	J2-209-M4	2006		2.6	8.2	60	646	63	519		
		J2-209-IGT6	2006	295	2.7	9.8	58	641	63	523	5.5 ± 0.2	0.70524 ± 0.00001
	SM2	J2-209-M2	2006		2.4	16.9	39	441	35	455		
		J2-209-IGT4	2006	241	2.7	26.6	31	311	49	478	6.5 ± 0.1	0.70885 0.00001
	SM3	J2-214-IGT8	2006	281	3	10	58	601	70	510		
		J2-214-IGT5	2006	288	2.5	9.8	56	587	70	510	5.3 ± 0.2	0.70520 ± 0.00001
	SM4	031-ROV-12	2011	345	3.0	4.2	44	426	44	371	5.3 ± 0.1	0.70495 ± 0.00001

Table 4 (continued)

Vent field	Area: Vent	Sample	Year of sampling	IGT T[a] (°C)	pH[a] 25°C	Mg[a] (mm)	K[a] (mm)	Li[a] (µm)	Sr[a] (µm)	Cl[a] (mm)	δ^7Li ± 2sd (‰)	$^{87}Sr/^{86}Sr$ ± 2se
Tsukushi	TK1	J2-214-IGT2	2006	55	5.8	45.2	20	209	93	570	7.7 ± 0.2	0.70840 ± 0.00000
Northeast Pual	NP1	J2-218-IGT3	2006	33	6.9	50.6	10	44	99	536	21.5 ± 0.1	0.70871 ± 0.00001
		J2-218-IGT4	2006	35	6.9	49.9	11	46	105	535	18.8 ± 0.1	0.70855 ± 0.00001
SuSu Knolls												
South Su	SS1	J2-224-IGT4	2006	265	2.6	5.3	44	559	369	612	6.0 ± 0.1	0.70470 ± 0.00000
		J2-224-M2	2006		4.5	36.9	21	215	180	564	8.4 ± 0.2	0.70619 ± 0.00000
	SS2	J2-224-IGT2	2006	287	2.7	8.4	42	539	263	598	6.1 ± 0.2	0.70466 ± 0.00001
Suzette	SZ1	J2-217-IGT5	2006	303	3.8	5.4	44	683	251	617	5.9 ± 0.1	0.70446 ± 0.00001
	SZ3	J2-219-IGT6	2006	290	3.5	5.9	45	710	362	672	5.7 ± 0.1	
North Su	NS3	J2-223-IGT7	2006	300	3.5	3.4	62	806	232	665	5.8 ± 0.1	0.70471 ± 0.00001
		J2-223-IGT8	2006	299	4.4	21.3	42	509	164	620	6.1 ± 0.1	
	NS5	J2-227-IGT2	2006	299	3.4	7.4	44	562	215	550	6.0 ± 0.2	0.70475 ± 0.00001
		J2-227-M2	2006		4.8	27.4	28	348	151	544	6.8 ± 0.1	0.70582 ± 0.00001
	NS6	J2-227-IGT3	2006	325	2.8	1.6	63	833	410	nd	5.7 ± 0.2	0.70453 ± 0.00001
		J2-227-M4	2006		2.9	5.1	54	766	367	668	5.9 ± 0.3	0.70466 ± 0.00001
	NS7	019-ROV-01	2011	332	3.2	15.3	48	581	297.1	662.5	5.9 ± 0.2	0.70487 ± 0.00001
	NS8	021-ROV-01	2011	169	2.4	43.5	16	122	95.1	555.1	9.5 ± 0.2	0.70813 ± 0.00000
	NS10	045-ROV-02	2011	312	4.8	18.9	45	500	199	662.3	6.1 ± 0.1	0.70516 ± 0.00001
Manus Spreading Center (MSC)												
Vienna Woods	VW1	J2-207-IGT3	2006	282	4.41	1.5	21	1055	240	683	3.9 ± 0.1	0.70439 ± 0.00001
	VW2	J2-207-IGT4	2006	273	4.22	1.0	21	1137	244	660	4.0 ± 0.1	
	VW3	J2-207-IGT8	2006	285	4.7	1.1	20	1061	224		4.1 ± 0.1	
		J2-207-IGT6	2006	240	5.4	14.9	17	759	183	611.1	4.0 ± 0.2	0.70481 ± 0.00000
New Hebrides Trench												
Nifonea	NIF-1	27 ROV 14 KIPS C	2013	>>250		15.1	4	11	36	193	24.5 ± 0.4	0.70842 ± 0.00001
		66 ROV 1 KIPS B	2013	107	4.4	27.6	6	16	54	311	29.2 ± 0.3	0.70901 ± 0.00001
	NIF-2	60 ROV 1 KIPS B	2013	345	4.7	25.4	6	17	51	296		0.70901 ± 0.00001
		60 ROV 1 KIPS C	2013			42.5	9	23	77	462	28.9 ± 0.2	0.70917 ± 0.00001
	NIF-3	66 ROV 6 KIPS D	2013	165		43.3	9	22	74	458	29.9 ± 0.1	0.70911 ± 0.00001
	NIF-4	77 ROV 6 KIPS A	2013	368	2.9	14.9	6	30	64	340	16.2 ± 0.1	0.70768 ± 0.00001
	NIF-5	77 ROV 10 KIPS B	2013	368	3.4	3.9	1	4	17	63	23.3 ± 0.2	0.70787 ± 0.00001
	NIF-7	66 ROV 3	2013	132		43.2	9	26	80	484	27.5 ± 0.1	
		66 ROV 5 NISKIN	2013			51.7	10	26	86	545	30.6 ± 0.3	0.70913 ± 0.00001
Bottom Seawater						52.4	10	28	91	540	31.0 ± 0.1	0.70916 ± 0.00001

mm = mmol/kg fluid; µm = µmol/kg fluid

[a] Previously reported by: Tivey et al., 2006; Craddock et al., 2010; Reeves et al., 2011 ; Seewald et al (2015) for fluids from Manus Basin collected in 2006; Bach et al., 2011 andunpublished data for fluids from the EMVZ collected in 2011 and Schmidt et al., 2017 for vent fluids from Nifonea volcano

Table 5: Endmember compositions for vent fluids from the the vent fields within the EMVZ, Vienna Woods and Nifonea volcano

		IGT T[a] [°C]	pH_{min}[a] 25°C	Mg_{min}[a] (mm)	K[a] (mm)	Li[a] (µm)	Sr[a] (µm)	Cl[a] (mm)	δ^7Li (‰)	$^{87}Sr/^{86}Sr$
Eastern Manus Volcanic Zone										
PACMANUS										
Fenway	F1	296	2.5	5.8	59	724	97	454	5.4	0.7045
	F3	358	2.7	4.5	79	970	100	586	5.8	0.7040
	F4	284	2.4	8.7	70	832	84	522	5.1	0.7038
	F5	80	4.9	44.0	43	606	196	404	6.0	0.7067
	F7	304	2.4	9.4	86	930	97	647	5.1	0.7057
	F8	314	2.7	11.8	64	809	75	529	5.3	0.7039
Roger's Ruins	RGR1	320	2.7	5.1	81	870	113	645	5.4	0.7043
	RGR2	274	2.6	9.0	81	904	105	650	5.4	
Roman Ruins	RMR1	312	2.3	22.7	82	1140	77	629	4.5	
	RMR3	278	3.2	3.6	96	1353	84	730	4.5	
	RMR4	341	2.7	3.6	82	1136	88	658	4.9	0.7041
	RMR5	333	2.6	5.3	89	1070	69	733	4.9	0.7043
Solwara 7	SL7	348	2.9	3.9	92	734	117	671	5.1	0.7041
Satanic Mills	SM1	295	2.6	8.2	70	772	58	517	5.3	0.7038
	SM2	241	2.4	16.9	52	628	9	414	5.4	0.7057
	SM3	288	2.5	9.8	68	724	66	503	5.1	0.7040
	SM4	345	3.0	4.2	47	461	40	356	5.2	0.7042
Snowcap	SC1	120	4.6	30.8	46	687	-18	440	5.6	0.7213
	SC2 2006		3.4	24.5	56	922	28	521	5.4	0.7060
	SC2 2011	224	4.0	26.7	47	858	43	589	5.1	0.6995
Tsukushi	TK1	55	5.8	45.2	83	1367	131	760	4.9	0.7052
Northeast Pual	NP1	35	6.9	49.9	29	472	446	432	6.4	0.7062
SuSu Knolls										
South Su	SS1	265	2.6	5.3	48	623	401	620	6.0	0.7046
	SS2	287	2.7	8.4	49	637	297	609	5.9	0.7044
Suzette	SZ1	303	3.8	5.4	48	758	270	625	5.8	0.7043
	SZ3	290	3.5	5.9	49	797	396	689	5.6	
North Su	NS3	300	3.5	3.4	65	855	235	674	5.7	0.7046
	NS5	299	3.4	7.4	49	662	233	551	5.8	0.7044
	NS6	325	2.8	1.6	62	852	409	682	5.7	0.7045
	NS7	332	3.2	15.3	64	810	384	713	5.5	0.7045
	NS8	169	2.4	43.5	48	587	134	629	4.9	0.7049
	NS10	312	4.8	18.9	65	768	263	731	5.6	0.7044
Manus Spreading Centre (MSC)										
Vienna Woods	VW1	282	4.4	1.5	21	1086	245	687	3.9	0.7043
	VW2	273	4.2	1.0	21	1159	247	663	3.9	
	VW3	285	4.7	1.1	20	1072	225	639	3.9	0.7041
New Hebrides Trench										
Nifonea	NIF-1		3.3	15.1	1	5	13	53	11.8	0.7064
	NIF-2	345	4.7	25.4	1	8	14	71	21.4	0.7078
	NIF-4	368	2.9	14.9	5	31	54	259	11.2	0.7067
	NIF-5	368	3.4	3.9	0	2	12	24	15.8	0.7070
bottom seawater		3	7.9	52.4	10	28	88	540	31.0	0.7092

mm = mmol/kg fluid; µm = µmol/kg fluid

[a] Previously reported by: Tivey et al., 2006; Craddock et al., 2010; Reeves et al., 2011 ; Seewald et al (2015) for fluids from Manus Basin collected in 2006; Bach et al., 2011 andunpublished data for fluids from the EMVZ collected in 2011 and Schmidt et al., 2017 for vent fluids from Nifonea volcano

from 461 µmol/kg at Satanic Mills to 1353 µmol/kg at Romain Ruins and 1367 µmol/kg at Tsukushi. Vent fluids from SuSu Knolls have Li concentrations between 587 and 855 µmol/kg. End-member Sr in the fluids from Manus Basin is enriched compared to seawater at SuSu Knolls (136 to 409 µmol/kg), whereas vent fluids within PACMANUS have generally lower Sr concentrations between 9 and 446 µmol/kg, respectively.

δ^7Li values in the end-member fluids from Manus Basin are quite homogenous with values of +3.9 ‰ at Vienna Woods, +4.5 to +6.4 ‰ at PACMANUS and +4.9 to +6.0 ‰ at SuSu Knolls. End-member fluids from Nifonea volcano have the highest δ^7Li values, which range from +11.2 to +21.4 ‰.

End-member $^{87}Sr/^{86}Sr$ define relatively small variations in most the vent fluids from Manus Basin with values between 0.7041 and 0.7043 at Vienna Woods, 0.7043 and 0.7046 at SuSu Knolls. At PACMANUS $^{87}Sr/^{86}Sr$ is more variable with values between 0.6995 and 0.7213. End-member Sr isotope ratios in the fluids at Nifonea volcano are significantly higher compared with most of the vent fluids from the Manus Basin, having $^{87}Sr/^{86}Sr$ ratios between 0.7064 and 0.7078.

4.5.1.2 Volcanic samples

Results for Li and Sr concentrations and isotope ratios in the volcanic samples from Nifonea volcano and the EMVZ are summarized in table 6.

Volcanic samples from Nifonea have Li and Sr concentrations ranging from 4.2 to 7.2 µg/g and 162 to 209 µg/g, respectively. Li and Sr isotope ratios define a small range from +2.7 to +5.5 ‰ and 0.70325 to 0.70362, respectively. Volcanic samples from Manus Basin can be divided into two groups: (I) fresh volcanic lava and (II) altered volcanic lava samples. Fresh samples have higher Li concentrations in the range from 1.4 to 10.1 µg/g and δ^7Li values from +4.5 to +7.8 ‰ Sr concentrations vary between 226 to 426 µg/g and $^{87}Sr/^{86}Sr$ from 0.70361 to 0.70470. Altered

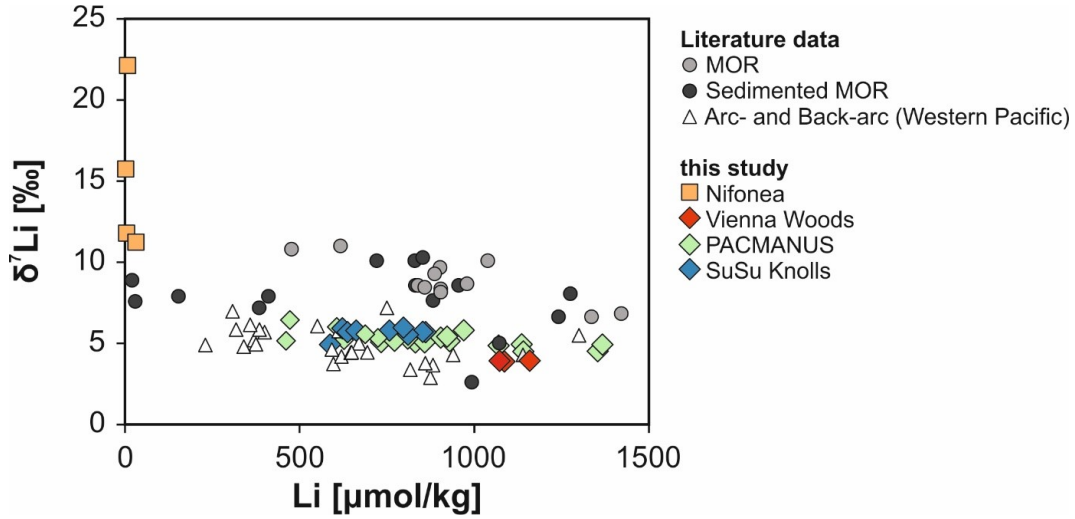

Figure 17: Li concentration versus Li isotope ratios in hydrothermal vent fluids from different tectonic settings. Vent fluids from Nifonea have the highest δ^7Li values measured so far in the different settings. Vent fluids from the Manus Basin are more enriched in Li and match in their concentrations and isotope ratios with other vent fluids sampled in the Western Pacific. On the contrast mid ocean ridge fluids have higher δ^7Li values. Literature values for mid-ocean ridges (MOR) and sedimented MOR are from Chan et al., (1993, 1994) and Foustoukos et al. (2004), for Arc and Back-arc samples from the Western Pacific from Araoka et al. (2016) and Mottl et al. (2011).

Table 6: Li and Sr isotope ratios of fresh and altered rocks from Nifonea volanco and the Eastern Manus Volcanic Zone

Sample	Location	alteration degree	SiO_2[a] [%]	TiO_2[a] [%]	Li[a] [µg/g]	Sr[a] [µg/g]	δ^7Li ± 2sd [‰]	$^{87}Sr/^{86}Sr$ ± 2se[b]
Vate Trough								
62-TVG-03 WR	Nifonea	fresh	50.6	2.1	7.2	209	4.8 ± 0.3	0.70332 ± 3
73-TVG-01 WR	Nifonea	fresh	48.5	1.3	4.2	162	2.7 ± 0.1	
73-TVG-01 A	Nifonea	alteration rind			6.0	172	4.1 ± 0.2	0.70362 ± 1
73-TVG-02 WR	Nifonea	fresh	48.6	1.3	4.2	173	3.0 ± 0.1	0.70325 ± 1
73-TVG-02 A	Nifonea	alteration rind			4.8	167	4.2 ± 0.1	0.70339 ± 1
72-ROV-10 WR	Vate Trough	fresh	50.2	1.1				
Eastern Manus Volcanic Zone								
J2-209-9-R1	Satanic Mills	fresh	66.3	0.7	6.2	293	4.5 ± 0.1	0.70361 ± 1
J2-224-10-R1	South Su	fresh	62.8	0.7	10.1	426	5.1 ± 0.3	0.70366 ± 1
J2-221-16-R2	North Su	fresh	60.1	0.5	2.7	377	4.9 ± 0.2	0.70367 ± 1
J2-220-13 R1	DESMOS	slightly altered	58.0	0.6	8.5	422	4.9 ± 0.1	0.70420 ± 4
J2-221-4-R1	North Su	slightly altered	64.1	0.6	1.4	226	7.8 ± 0.2	0.70470 ± 4
J2-216-11-R2	Fenway	altered	26.2	0.9	0.4		11.3 ± 0.4	0.70713 ± 10
J2-209-8-R1	Satanic Mills	altered	27.9	1.1	5.6	190	-1.0 ± 0.3	0.70520 ± 13
J2-224-2-R1	South Su	altered	79.7	1.1	0.2	616	17.8 ± 0.0	0.70673 ± 7
J2-221-6-R1	North Su	altered	59.2	0.5	0.7	356	3.0 ± 0.1	0.70501 ± 18
J2-220-8-R1	DESMOS	altered	67.4	0.7	3.0	541	4.9 ± 0.2	0.70501 ± 18
J2-220-9-R1 crust	DESMOS	altered	68.2	0.7	1.0	138	9.1 ± 0.3	0.70547 ± 6
J2-220-9-R1 interior	DESMOS	altered	50.2	0.5	0.4	369	12.2 ± 0.3	0.70482 ± 24

[a] Unpublished values and data previously reported by Beier et al. (2015) for volcanic rocks from Manus Basin and Lima et al. (2017) for volcanic rocks samples from Nifonea volcano

[b] errors for the last digit

rock samples have significantly lower Li concentrations ranging from 0.2 to 5.6 µg/g. Sr concentrations both lower and higher compared to their fresh analogues (138 to 616 µg/g). δ^7Li values have a high variability in the altered volcanic rocks and vary between -1.0 and +17.8 ‰. Sr isotope ratios show also a wide variability with ratios from 0.70501 to 0.70713.

4.6 Discussion

4.6.1 Li isotope ratios in vent fluids as indicator for water-rock interaction with fresh oceanic crust

End-member fluids from the different locations within the Manus Basin define a quite small range in their δ^7Li values in comparison with the global variation in submarine hydrothermal fluids from different tectonic settings (+1.6 to 11‰) (Fig. 17), whereas Li concentrations are in the same range. Although its homogeneity, there are small differences in the end-member Li isotope ratios from Vienna Woods, PACMANUS and SuSu Knolls, which might relate to differences in the composition of the oceanic crust.

In contrast to the vent fields within the EMVZ (PACMANUS and SuSu Knolls), Vienna Woods hydrothermal site hosts MOR-like basalts, which have lower Li concentrations than the dacitic to rhyodacitic rocks from the EMVZ. However, Li concentrations in the end-member vent fluids from Vienna Woods are even higher than in most fluids from the EMVZ and vent fluids from MOR settings and sedimented ridges. δ^7Li values in the fluid from Vienna Woods are

significantly lower compared to the fluids from the before mentioned settings. Hence, the difference in the Li concentrations of the host rocks cannot explain the different Li signatures in the vent fluids. Nevertheless, Li isotope ratios of the fresh dacite samples from the PACMANUS and SuSu Knolls are higher in comparison with Li isotope ratios of fresh MORB (0.94 mmol/kg and +3.7‰) (Gale et al., 2013; Tomascak et al., 2008), which could explain the differences in end-member δ^7Li from the EMVZ and Vienna Woods.

To evaluate and understand the Li composition in the vent fluids we used a mass balance model designed by Araoka et al. (2016), which is based on the models by Verney-Carron et al. (2015) and Magenheim et al. (1995). This mass balance model describes the interaction between fluid and the oceanic crust assuming a steady state between Li in the fresh rocks $[Li]_{rock\text{-}I}$ and initial fluid $[Li]_{SW}$, and Li in the hydrothermal fluid $[Li]_{HF}$ and altered rock $[Li]_{rock\text{-}a}$. Further, the model consideres Li isotope fractionation between the fluid and altered mineral phases during water-rock interaction.

$$[Li]_{HF} = \frac{([Li]_{rock-i} + W/R[Li]_{SW})}{(K + W/R)} \quad (6)$$

$$K = \frac{[Li]_{rock-a}}{[Li]_{HF}} \quad (7)$$

$$\left(\frac{^7Li}{^6Li}\right)_{HF} = \frac{\left(\left(\frac{^7Li}{^6Li}\right)_{rock-i}[Li]_{rock-i} + W/R\left(\frac{^7Li}{^6Li}\right)_{SW}[Li]_{SW}\right)}{([Li]_{rock-i} + W/R[Li]_{SW})} \frac{([Li]_{rock-a} + W/R[Li]_{HF})}{(\alpha[Li]_{rock-a} + W/R[Li]_{HF})} \quad (8)$$

K is the bulk distribution coefficient of Li between liquid and solid and $\alpha_{solid\text{-}liquid}$ is the isotope fractionation factor during water-rock interaction. Both parameters are T-dependent. Their estimated and calculated values are 0.35 and 0.994 at 260°C, 0.32 and 0.995 at 300°C and 0.27 and 0.996 at 350°C (Millot et al., 2010). $[Li]_{rock\text{-}i}$ and δ^7Li values for the fresh rocks are taken from this study. For the calculation for fluids from the EMVZ a fresh rock from Satanic Mills (J2-209-9-R1) was used, because this sample was most representative in a study using B isotope ratios (Wilckens et al., in prep). For the fluids from Nifonea volcano, sample 73-TVG-02 was used. Because this study didn't prepare rock samples from the MSC (Vienna Woods), the composition of fresh MORB was taken.

However, Fig. 18 (a-c) shows, that none of the measured fluids matches with the calculated fluid compositions. To understand and explain these isotopic offsets, we will focus on the properties of the individual hydrothermal vent field.

4.6.1.1 Vienna Woods in comparison with MOR settings

In their chemical composition, hydrothermal vent fluids from Vienna Woods are similar to vent fluids from MOR settings (Von Damm, 1995; German and Von Damm, 2003, Reeves et al., 2011). Hence, these vent fluids are characterized by water-rock interaction at low water/rock

(W/R) ratios with a basaltic host rock (Reeves et al., 2011). In addition, Li contents and δ^7Li values of the host rocks are similar to those of MORB as well (Tomascak et al., 2008; Gale et al., 2013, Araoka et al., 2016). However, Li is enriched in vent fluids from Vienna Woods and has significantly lower δ^7Li values compared to most MOR settings, similar to the isotopic composition of vent fluids from the Eastern Lau Spreading Centre (Fig. 17).

Araoka et al. (2016) also analysed vent fluids from Vienna Woods. Their calculated end-member Li concentrations match with the Li concentrations obtained in this study. However, there is a small offset of about 0.5 ‰ in δ^7Li between the results from Araoka et al. (2016) and the data from this study. Because there are also small differences in pH and maximum measured temperatures, this minor offset might reflect natural changes in a hydrothermal system through time. Another explanation can be higher uncertainties in the end-member composition of Araoka et al. (2016), because of higher minimum Mg concentrations. Nonetheless, Sr concentrations and $^{87}Sr/^{86}Sr$ in the end-member fluids from both years match each other. Araoka et al. (2016) explained the Li isotopic composition in the fluids from Vienna Woods with (i) a lack of well-constrained bulk distribution coefficients and (ii) a potential influence of low-temperature diffusive hydrothermal fluids on MOR hydrothermal fluids. To understand it is useful to compare these results with other vent fluids showing similar Li isotope ratios. Vent fluids from South Field in the Guaymas Basin have comparable Li isotope ratios to Vienna Woods (Chan et al., 1994). Chan et al. (1994) suggested, that the low δ^7Li values at South Field are a result of low W/R ratios during water-rock interaction and a high influence of in ^{6}Li enriched marine sediments. However, at Vienna Woods, these hypotheses appear to be invalid. Indeed, calculated water-rock ratios with B concentrations at Vienna Woods are slightly lower in comparison with MOR settings, but this small difference has a negligible effect on the Li isotopic composition in vent fluids. Furthermore, there is no significant sediment cover at the MSC. Hence, interaction with sediments cannot influence hydrothermal fluids from Vienna Woods. Another explanation for the low Li isotope ratios might be influenced by diffusion of Li into the fluids, which could shift δ^7Li values to lower values (Verney-Carron et al., 2011). However, this process also appears to be not reasonable, since at these high temperatures the amount of Li leached from basalts should be significantly higher as Li derived from diffusion. Another explanation would be a different composition of the oceanic crust at the MSC, which is not in accordance with the composition of MOR basalts and hence more enriched in ^{6}Li. Fig. 18d shows, that end-member Li compositions in the fluids from Vienna Woods could be explained by a host rock composition of 6.5 ppm and +2.5‰. Indeed, Tomascak et al., (2008) showed that Li in MORB varies between +1.5 and +5.6‰. Hence, these conclusions might be valid but since there is no data for the isotopic composition of basalts from the MSC, this hypothesis remains speculative, but offers the potential for further research.

4.6.1.2 Li isotope fractionation during water-rock interaction in the EMVZ

Similar to the vent fluids from Vienna Woods, end-member Li compositions in the vent fluids have lower δ^7Li values compared to the calculated composition of the vent fluids (Fig. 18b). This

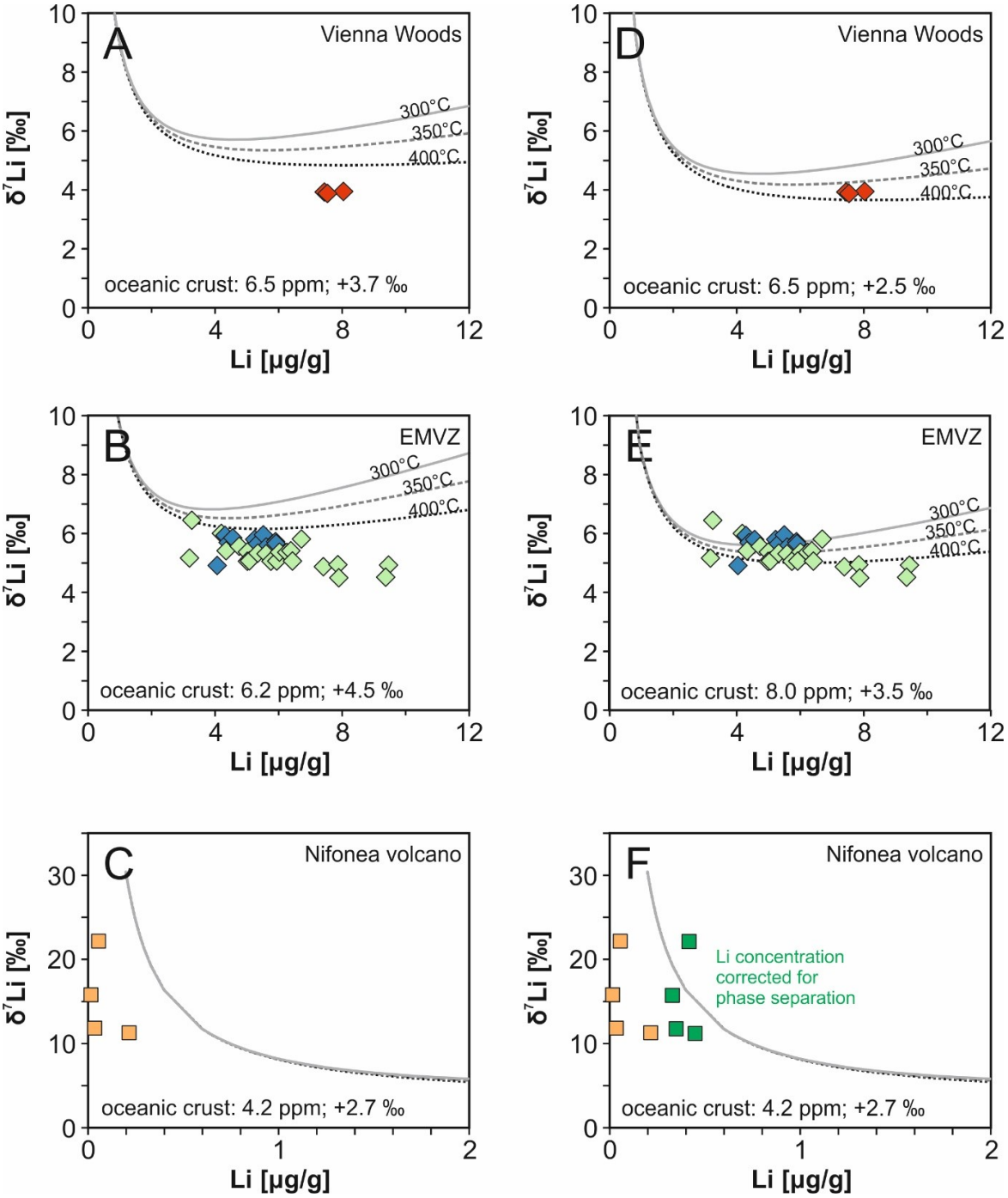

Figure 18: Li concentrations against δ^7Li values in the vent fluids from the different study areas. Solid and dashed lines are calculated fluid compositions at 300°C, 350°C and 400°C based on a steady state assumption. The composition of the oceanic crust is (A) fresh MORB at Vienna Woods, (B) fresh dacite from Satanic Mills in the EMVZ and (C) fresh lava from Nifonea volcao. However, fluid samples do not match with the calculated mixing lines. (D) and (E) show that the fluid match the calculated fluid compositions with adjusted rock compositions. In (F) vent fluids are corrected for the extreme boiling, which affects the fluids from Nifonea volcano.

could imply, that either the fresh rocks from the EMVZ are not representative for the oceanic crust as proposed for the Vienna Woods fluids or that the Li distribution coefficients or isotope fractionation factors are invalid as suggested by Araoka et al. (2016). Fig. 18d shows that an oceanic crust composition of 8.0 ppm and +3.5 ‰ could explain the Li composition in the vent fluids, using the mass balance model by Araoka et al. (2016). However, these results are in conflict with the Li composition of the fresh volcanic rocks, which were also obtained in this study. Hence, we rather propose that the isotopic fractionation of Li, which is associated with the formation of secondary minerals during hydrothermal alteration, is either overprinted by the high leaching rates of Li from the oceanic crust as these tectonic settings or not valid for arc- and back-arc basins. Vent fluids from Romain Ruins support these hypotheses. Fluids there have the highest B concentrations, indicative for extreme low W/R ratios (Yamaoka et al., 2015; Wilckens et al. (submitted). In addition, these have the lowest Li isotope ratios, which match the composition of the fresh oceanic rocks analysed in this study. However, whether this process is related to differences in the mineralogy of the host rocks, fluid pathways during hydrothermal circulation or to the fluid chemistry of arc-/back-arc fluids remains unsolved.

In addition, fluids from the EMVZ are not homogeneous. There are small isotopic differences in the vent fluid compositions from PACMANUS and SuSu Knolls with higher mean Li isotope ratios in the vent fluids from SuSu Knolls. To understand this difference, it is beneficial to compare the Li isotope ratios with the Sr signal in the fluids, because Sr is also a good tracer for water-rock interaction during hydrothermal circulation.

4.6.1.3 The influence of altered oceanic crust and sediments on Li in the vent fluids from PACMANUS and SuSu Knolls

Anhydrite dissolution and precipitation cause a huge variability in the end-member Sr isotope ratios in the fluids from PACMANUS, which results in some cases in too high Sr isotope ratios (F5, F7, SM2, SC1, TK1 and NP1). Nevertheless, Sr isotope ratios in the vent fluids, which are not affected by anhydrite dissolution, are generally lower in end-member fluids from PACMANUS relative to SuSu Knolls, displaying lower W/R ratios during water-rock interaction in the vent fluids from PACMANUS. However, small differences in W/R ratios would affect the Li concentrations but not the Li isotopic composition of the vent fluids. Furthermore, W/R ratios vary also in the individual vents within PACMANUS and SuSu Knolls. If this variation in W/R ratios would affect the isotopic composition of Li in the vent fluids, the individual vents from PACMANUS and SuSu Knolls would have a higher variation in their Li isotope ratios. B isotope ratios in the vent fluids from PACMANUS have also lower values relative to most fluids from SuSu Knolls, which was interpreted to be the result of higher W/R ratios and interaction with a higher proportion of altered oceanic crust at SuSu Knolls (Wilckens et al., accepted). Indeed,

higher Sr isotope ratios in vent fluids could also display this higher proportion of altered oceanic crust.

Altered volcanic rocks from the EMVZ have a broad range in their Li isotopic composition. In general, it is assumed, that Li isotope ratios are influenced by two processes during alteration of the oceanic crust. One process is the dissolution of primary minerals, where Li is released into the solution without isotopic fractionation. In a second step, Li is incorporated into secondary minerals. Depending on the precipitating minerals, Li isotopes fractionate during this process (Magenheim et al., 1995; Verney-Carron et al., 2015; Araoka et al., 2016). The analysed rocks from the Manus Basin show two alteration trends (Fig. 19). However, in a first step, Li is leached from the fresh dacites, which get depleted in Li without a change in their isotopic composition. Generally, alteration products, which formed during the alteration of the oceanic crust, are thought to be enriched in ^{6}Li (Vigier et al. 2008, Verney-Carron et al., 2015). Fig. 19a shows that all altered rocks from the EMVZ are depleted in Li compared with the fresh rocks. Some of the volcanic rocks tend to lower Li isotope ratios, which is in accordance with the preferential incorporation of ^{6}Li during formation of secondary minerals. The other volcanic rocks define a trend to low Li concentrations and high isotope ratios. These rocks may be increasingly affected by seawater (Chan et al., 1992). These two alterations trends (formation of secondary minerals and seawater influence) can be also seen in Sr isotope ratios of the rock samples (Fig. 19b). Coming back to the question, whether a higher proportion of altered rocks in the hydrothermal circulation cell might influence Li signatures in the fluids from North Su, Fig. 19a shows that all rocks are depleted in Li. Thus, a higher percentage of altered oceanic crust reacting with

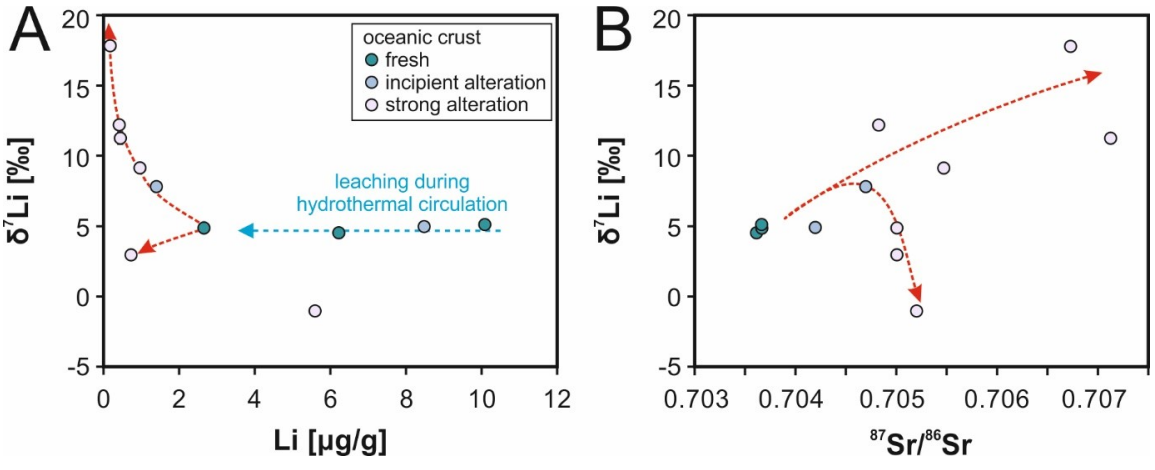

Figure 19: (A) Li concentrations against δ^{7}Li values in rock samples from the Eastern Manus Volcanic Zone show, that Li is depleted during alteration of the oceanic crust. In a first step, Li is leached from the fresh rocks without any significant isotope fractionation (blue dashed line). In a second step Li in still leached, but can be incorporated into alteration minerals leading to lower Li isotope ratios or the composition of the rocks is overprinted by seawater, which leads to higher Li isotope ratios. These two trends to higher an lower Li isotope ratios can be also observed in (B). Sr in the rocks which define a trend to lower Li isotope ratios is less influenced compared to those reacted at higher temperature, where Sr also follows a trend towards seawater composition.

hydrothermal fluids would shift also their Li contents to lower values. However, Li concentrations in the vent fluids from SuSu Knolls and PACMANUS match with each other. Hence, a higher propoertion of altered oceanic crust at SuSu Knolls cannot explain the isotopic difference in the fluids from PACMANUS and SuSu Knolls.

Li can also be added to hydrothermal fluids during interaction with marine sediments (Chan et al., 1993; Araoka et al., 2016). At PACMANUS sediment cover is negligible to minor, whereas at SuSu Knolls sediment cover can be up to several meters (Hrischeva et al., 2007). The mineralogical and geochemical composition of the sediments found at SuSu Knolls have varying inputs of hydrothermal, volcaniclastic, terrigeneous and bionic components (Hrischeva et al., 2007). Unfortunately, no data of Li concentrations and isotope ratios from the sediments from SuSu Knolls are available. However, Li in sediments is gereally enriched relative to Li in fresh basalts and dacites (James et al., 1999; Bouman et al., 2004; Chan et al., 2006) and the isotopic composition of marine sediments varies from -4.3 to +14.5‰ (Chan et al., 2006). Detrital sediments have typically low δ^7Li values, whereas metalliferous clays have higher isotope ratios (Chan et al., 2006). δ^7Li values in hydrothermally altered and volcaniclastic sediments are similar to fresh MORB, but can be also depleted or enriched in ^{7}Li. Although the sediments at SuSu Knolls have a huge compositional variation, they are generally described as metalliferous clays (Hrischeva et al., 2007). Hence, we can assume δ^7Li values, which are similar or higher compared to fresh dacites. In addition, Li in metallifereous sediments is enriched by a factor of 5 compared to fresh dacites from Manus Basin (Chan et al., 2006). Thus, already small amounts can affect the composition of hydrothermal vent fluids and lead potentially to higher δ^7Li values. This implies that the difference Li isotopic composition of the vent fluids from PACMANUS and SuSu Knolls could be explained by the influence of sediments on the vent fluids at SuSu Knolls. However, we cannot exclude an effect of the different W/R ratios on the Li concentrations of the vent fluids.

4.6.2 Li behaviour in vent fluids associated with limited water-rock interaction and extreme boiling

Vent fluids from Nifonea volcano have the highest Li isotope ratios measured so far in hydrothermal vent systems. Chemical composition of the vent fluids reveal in their low Cl and high volatile species extreme “boiling” of the fluids, which is also displayed in the low contents of the elements, which do not partition into the vapour phase. Some of these elements are similar to seawater or in case of Li even lower. Further, Sr isotope ratios have values that are close to seawater. This implies extreme high water-rock ratios with limited water-rock interaction during hydrothermal circulation as proposed by Schmidt et al. (2017). Fig 18c. shows that the calculated Li composition in the vent fluids does not match end-member Li compositions of the vent fluids. However, this can be explained by the preferential partitioning of Li into the brine phase during boiling of the fluids. Li and Cl concentrations in the vent fluids from Nifonea have a positive

correlation, which indeed implies that extreme boiling in the Nifonea fluids subsequent to water-rock interaction depletes Li in the emanating vent fluids. The absence of a correlation between Cl and δ^7Li indicates that this process is not influencing Li isotope ratios. Thus, we can correct the Li concentrations in the vent fluids for phase separation by assuming seawater Cl as initial Cl content prior to boiling. Fig. 18f shows, that vent fluids with corrected Li concentrations plot closer to the calculated composition of the hydrothermal vent fluids.

4.7 Summary and implications

Vent fluids from Manus Basin and Nifonea volcano show that different sources and processes affect the Li signatures in the vent fluids from Nifonea and the Manus Basin. In general, the fluids are mainly controlled by the interaction of the oceanic crust with hydrothermal fluids. However, the calculated fluid compositions do not match with end-member fluid compositions using the available mass balance model by Araoka et al. (2016). We propose, that this is due to a different leaching behaviour of Li from the host rocks, where isotopic effects due to the formation of secondary minerals are either overprinted or incorporation of Li into secondary minerals is negligible during alteration of the oceanic crust in back-arc settings. To investigate these findings, further experimental and detailed studies analysing both hydrothermal fluids as well as samples from the oceanic crust are necessary. Beside this hypothesis, small difference in the Li compositions from PACMANUS and SuSu Knolls can be explained by an influence of metalliferous sediments reacting with hydrothermal fluids at SuSu Knolls. The extreme boiling subsequent to water-rock interaction in vent fluids from Nifonea leads to lower Li concentrations in the emanating fluids without having an influence on Li isotope ratios. In addition, the fluids might also be influenced by low-temperature removal of Li during hydrothermal circulation.

The estimated Li flux from hydrothermal vent fluids has a δ^7Li value of +8.3 ‰ (Misra and Froehlich, 2012). The estimation is based on the composition from hydrothermal vent fluids at MOR settings. However, Li isotope ratios in vent fluids from arc- and back-arc settings in the Western Pacific have generally lower values (+2.9 to +7.2‰), whereas Li concentrations are concordant with each other (Mottl et al., 2011; Araoka et al., 2016). Unfortunately, the percentage of global hydrothermal discharge associated with back-arc basins is unknown, but intraoceanic arcs settings are thought to account for about 10% of the global hydrothermal discharge (Baker et al., 2008). This implies that the hydrothermal Li flux has a lower δ^7Li value than estimated. If we assume an average δ^7Li value +4.6 ‰ for vent fluids from arc and back-arc setting, the isotopic composition of the hydrothermal Li flux will be about 0.4 ‰ lower. However, to constrain the isotopic composition of the hydrothermal Li flux into the ocean, better estimations for the global hydrothermal flux from back-arc basins are necessary and the dataset on Li compositions in vent fluids from arc and back-arc settings has to be extended.

4.8 Acknowledgments

The authors would like to thank the crew of the R/V Melville and R/V Sonne as well as the technical groups of ROV Jason II, ROV-MARUM-QUEST and ROV Kiel 6000. We thank Katja Schmidt and Selma Lima for discussion and data access. This study was part of MARUM project GB4 and was funded by the DFG-Research Centre/Cluster of Excellence "The Ocean in the Earth System" at MARUM – Centre for Environmental Sciences, University of Bremen and was supported from the German Research Foundation (DFG) Major Research Instrumentation Program (INST 144/308-1).

4.9 References

Araoka, D., Nishio, Y., Gamo, T., Yamaoka, K., Kawahata, H. (2016) Lithium isotopic systematics of submarine vent fluids from arc and back-arc hydrothermal systems in the western Pacific. *Geochim. Geophys. Geosys*. **17**, 3835-3853.

Bach W., Dubilier N., Borowski C., Breuer C., Brunner B., Franke P., Herschelmann O., Hourdez S., Jonda L., Jöns N., Klar S., Koloa K., Mai A., Meyerdierks A., Müller I., Petersen S., Pjevac P., Ratmeyer V., Reeves E., Rehage R., Reuter C., Schaen A., Shu L., Thal J., Zarrouk M. (2011) Cruise Report for SONNE cruise SO 216 – BAMBUS, Back-Arc Manus Basin Underwater Solfataras. Universität Bremen (https://elib.suub.uni-bremen.de/edocs/00102250-1.pdf).

Baker E. T., Embley R. W., Walker S. L., Resing J. A., Lupton J. E., Nakamura K., de Ronde C. E. J., Massoth G. J. (2008) Hydrothermal activity and volcano distribution along the Mariana arc. *J. Geophys. Res.: Solid Earth* **113**, B08S09, doi:10.1029/2007JB005423

Beier, C., Bach, W., Turner, S., Niedermeier, D., Woodhead, J., Erzinger, J., Krumm, S. (2015) Origin of Silicic Magmas at Spreading Centres – an Exampe from the South East Rift, Manus Basin. *J Petrol.* **56**, 255-277.

Binns R. A. and Scott S. D. (1993) Actively forming polymetallic sulfide deposits associated with felsic volcanic-rocks in the Eastern Manus Back-Arc Basin, Papua New Guinea. *Econ. Geol.* **88**(8), 2226–2236.

Both, R., Crook, K., Taylor, B., Brogan, S., Chappell, B., Frankel, E., Tiffin, D. (1986). Hydrothermal chimneys and associated fauna in the Manus Back-Arc Basin, Papua New Guinea. *Eos, Transactions American Geophysical Union* **67**(21), 489-490.

Bouman, C., Elliott, T., Vroon, P. Z. (2004). Lithium inputs to subduction zones. *Chem. Geol.* **212**(1), 59-79.

Chan, L.H., Edmond, J.M. (1988) Variation of lithium isotope composition in the marine environment: A preliminary report. *Geochim. Cosmochim. Acta* **52**, 1711-1717.

Chan, L. H., Edmond, J. M., Thompson, G., Gillis, K. (1992). Lithium isotopic composition of submarine basalts: implications for the lithium cycle in the oceans. *Earth Planet. Sci. Lett.* **108**(1-3), 151-160.

Chan, L.H., Edmond, J.M., Thompson, G. (1993) A lithium isotope study of hot springs and metabasalts from mid ocean ridge hydrothermal systems. *J. Geophys. Res.* **98**, 9653–9659.

Chan, L.H., Gieskes, J.M., You, C.F., Edmond, J.M. (1994) Lithium isotope geochemistry of sediments and hydrothermal fluids of the Guaymas Basin, Gulf of California. *Geochim. Cosmochim. Acta* **58**, 4443–4454.

Chan, L. H., Leeman, W. P., Plank, T. (2006). Lithium isotopic composition of marine sediments. *Geochem. Geophys. Geosyst.* **7**(6).

Craddock, P. R., Bach, W., Seewald, J. S., Rouxel, O. J., Reeves ,E. and Tivey, M. K. (2010) Rare earth element abundances in hydrothermal fluids from the Manus Basin, Papua New Guinea: indicators of sub-seafloor hydrothermal processes in back-arc basins. *Geochim. Cosmochim. Acta* **74**, 5494–5513.

Edmond, J.M., Measures, C., McDuff, R.E., Chan, L.H., Grant, C. B. (1979) Ridge crest hydrothermal activity and the balances of the major and minor elements in the ocean: The Galapagos data. *Earth Planet. Sci. Lett*. **46**, 1-18.

Elderfield, H. and Schultz, A. (1996) Mid-Ocean Ridge Hydrothermal Fluxes and the Chemical Composition of the Ocean. *Annual Rev. of Earth and Plan. Sciences* **24**, 191-224.

Elliott, T., Jeffcoate, A., Bouman, C. (2004). The terrestrial Li isotope cycle: light-weight constraints on mantle convection. *Earth and Planet. Sci. Lett.* **220**(3), 231-245.

Elliott, T., Thomas, A., Jeffcoate, A., Niu, Y. (2006) Lithium isotope evidence for subduction-enriched mantle in the source of mid-ocean-ridge basalts. *Nature* **443**, 565-568.

Foustoukos, D.I., James, R.H., Berndt, M.E., Seyfried Jr., W.E. (2004) Lithium isotopic systematic of hydrothermal vent fluids at the Main Endeavour Field, Northern Juan de Fuca Ridge. *Chem. Geol.* **212**, 17–26.

Gale, A., Dalton, C.A., Langmuir, C.H., Su, Y., Schilling, J.G. (2013) The mean composition of ocean ridge basalts. Geochim. Geophys. Geosyst. 14, 489-518.

Gamo T., Okamura K., Charlou J. L., Urabe T., Auzende J. M., Ishibashi J., Shitashima K. and Chiba H. (1997) Acidic and sulfate-rich hydrothermal fluids from the Manus back-arc basin, Papua New Guinea. *Geology* **25**(2), 139–142.

Gao Y, Vils F., Cooper K.M., Banerjee N., Harris M., Hoefs J., Teagle D.A.H., Casey J.F., Elliott T., Altzitzoglou T., Alt J.C., Muehlenbachs K. (2012) Downhole variation of lithium and oxygen isotopic compositions of oceanic crust at East Pacific Rise, ODP Site 1256. *Geochem. Geophys. Geosys*. **13** (10), doi: 10.1029/2012GC004207.

Garbe-Schönberg D., Koschinsky A., Ratmeyer V., Jähmlich H., Westernströer U. (2006) KIPS – A new multiport valve-based all-Teflon fluid sampling system for ROVs. In *Geophys. Res. Abstr.* **8** p. 07032.

Genske F.S., Turner S.P., Beier C., Chu M.-F., Tonarini S., Pearson N.J., Haase K.M. (2014) Lithium and boron isotope systematics in lavas from the Azores islands reveal crustal assimilation. *Chem. Geol*. **373**, 27-36.

German, C. R., Von Damm, K. L. (2003) Hydrothermal Processes. In: *Treatise on Geochemistry* Vol **6** (Eds: H. D. Holland and K. K. Turekian), 182 – 216.

Huang K.-F., You C.-F., Liu Y.-H., Wang R.-M., Lin P.-Y., Chung C.-H. (2010) Low memory, small sample size, accurate and high-precision determinations of lithium isotopic ratios in natural materials by MC-ICP-MS. *J. Anal. At. Spectrom*. **25**, 1019-1024.

Huh, Y., Chan, L.H., Zhang, L., Edmond, J.M. (1998) Lithium and its isotopes in major world rivers: implication for weathering and the oceanic budget. *Geochim. Cosmochim. Acta* **62**, 2039-2051.

Huh, Y., Chan, L. H., Edmond, J. M. (2001). Lithium isotopes as a probe of weathering processes: Orinoco River. *Earth and Planet. Sci. Lett.* **194**(1), 189-199.

Hrischeva, E., Scott, S. D., Weston, R. (2007). Metalliferous sediments associated with presently forming volcanogenic massive sulfides: the SuSu knolls hydrothermal field, eastern manus basin, Papua New Guinea. *Econom. Geol.* **102**(1), 55-73.

Iizasa, K., Kawasaki, K., Maeda, K., Matsumoto, T., Saito, N., Hirai, K. (1998) Hydrothermal sulfide-bearing Fe-Si oxyhydroxide deposits from the Coriolis Troughs, Vanuatu backarc, southwestern Pacific. *Marine Geology* **145**, 1-21

Kamenetsky, V.S., Binns, R.A., Gemmell, J.B., Crawford, A.J., Mernagh, T.P., Maas, R., Steele, D. (2001) Parental basaltic melts and fluids in eastern Manus backarc Basin: implications for hydrothermal mineralisation. *Earth Planet. Sci. Lett.* **184** (3-4), 685-702

Lee, S. M. and Ruellan, E. (2006) Tectonic and magmatic evolution of the Bismarck Sea, Papua New Guinea: review and new synthesis. In: *Back-Arc Spreading Systems: Geological, Biological, Chemical, and Physical Interactions*, vol. **166** (eds. D. M. Christie, C. R. Fisher, S.-M. Lee and S. Givens). AGU Monograph. American Geophysical Union, 263–286.

Lima, S.M., Haase. K.M., Beier, C., Regelous, M., Brandl, P.A., Hauff, F., Krumm, S. (2017) Magmatic evolution and source variation at the Nifonea Ridge (New Hebrides Island Arc). *J. Petrol.,* in press.

Magenheim, A.J., Spivack, A.J., Alt, J.C., Bayhurst, G., Chan, L.H., Zuleger, E., Gieskes, J.M. (1995) Borehole fluid chemistry in hole 504B,leg 137: Formation water or in-situ reaction?, *Proc. Ocean Drill. Program Sci. Results* **137/140**, 141–152.

Magna T., Day J.M.D., Mezger L., Fehr M.A., Dohmen R., Aoudjehane H.C.A., Agee C.B. (2015) Lithium isotope constraints on crust–mantle interactions and surface processes on Mars. *Geochim. Cosmochim. Acta* **162**, 46-65.

Martinez F., Taylor B. (1996) Backarc spreading, rifting, and microplate rotation, between transform faults in the Manus Basin. *Marine Geophysical Researches* **18** , 203–224.

McConachy, T. F., Arculus, R. J., Yeats, C. J., Binns, R. A., Barriga, F.J.A.S., McInnes, B.I.A., Sestak, S., Sharpe, R., Rakau, B., Tevi, T (2005): New hydrothermal activity and alkali volcanism in the backarc Coriolis Troughs, Vanuatu. *Geology* **33**, 61-64.

Millot, R., Guerrot, C., Vigier, N. (2004) Accurate and high-precision measurement of lithium isotopes in two reference materials by MC-ICP-MS. *Geostand. Geoanal. Res*. **28**, 153–159.

Millot, R., Scaillet, B., Sanjuan, B. (2010) Lithium isotopes in island arc geothermal systems: Guadeloupe, Martinique (French West Indies) and experimental approach. *Geochim. Cosmochim. Acta* **74**, 1852–1871.

Misra, S., Froelich, P.N. (2012) Lithium isotope history of Cenozoic seawater: changes in silicate weathering and reverse weathering. *Science* **335**, 818–823.

Monjaret, M.C., Bellon, H., Maillet, P. (1991) Magmatism of the troughs behind the New Hebrides island arc (RV Jean Charcot SEAPSO 2 cruise): K-Ar geochronology and petrology. *J. Volcanol. and Geotherm. Res.* **46**, 265-280.

Moriguti, T., & Nakamura, E. (1998). High-yield lithium separation and the precise isotopic analysis for natural rock and aqueous samples. *Chem. Geology* **145**(1-2), 91-104.

Mottl, M. J. and Holland, H. D. (1978) Chemical exchange during hydrothermal alteration of basalt by seawater: I. Experimental results for major and minor components of seawater. *Geochim.Cosmochim. Acta* **42**(8), 1103–1115.

Mottl, M. J., Seewald, J. S., Wheat, C. G., Tivey, M. K., Michael, P. J., Proskurowski, G., McCollom, T. M., Reeves, E., Sharkey, J., You, C.-F., Chan, L.-H., Pichler, T. (2011) Chemistry of hot springs along the Eastern Lau Spreading Center. *Geochim. Cosmochim. Acta* **75**, 1013–1038.

Neef, G., McCulloch, M.T. (2001) Pliocene-Quaternary history of Futuna Island, south Vanuatu, southwest Pacific. *Australian Journal of Earth Sciences* **48**, 805-814.

Ogawa, Y., Shikazono, N., Ishiyama, D., Sato, H. and Mizuta, T. (2005) An experimental study on felsic rock–artificial seawater interaction: implications for hydrothermal alteration and sulfate formation in the Kuroko mining area of Japan. *Mineral. Deposita* **39**(8), 813–821.

Palmer, M.R., Edmond, J.M. (1989) The strontium isotope budget of the modern ocean. *Earth. Planet. Sci. Lett.* **92**, 11-26.

Palmer, M. R., Edmond, J. M. (1992) Controls over the strontium isotope composition of river water. *Geochim. Cosmochim. Acta* **56**(5), 2099-2111.

Park, S. H., Lee, S.-M., Kamenov, G. D., Kwon, S.-T., Lee, K.-Y. (2010) Tracing the origin of subduction components beneath the South East rift in the Manus Basin, Papua New Guinea. *Chem. Geol.* **269**, 339–349.

Pearce, J. A. and Stern, R. J. (2006) Origin of back-arc basin magmas: trace element and isotope perspectives. In Back-Arc Spreading Systems: Geological, Biological, Chemical, and Physical Interactions, vol. 166 (eds. D. M. Christie, C. R. Fisher, S.-M. Lee and S. Givens). AGU Monograph. American Geophysical Union, 63–86.

Pin, C., Bassin, C. (1992). Evaluation of a strontium-specific extraction chromatographic method for isotopic analysis in geological materials. *Analytica Chimica Acta* **269**(2), 249-255.

Pogge von Strandmann P.A.E., Burton K.W., James R.H., van Calsteren P., Gislason S.R. (2010) Assessing the role of climate on uranium and lithium isotope behaviour in rivers draining a basaltic terrain. *Chem. Geol*. **270** (1-4), 227-239.

Reeves, E. P., Seewald, J. S., Saccocia, P., Bach, W., Craddock, P. R., Shanks, W. C., Sylva, S. P., Walsh, E., Pichler, T. and Rosner, M. (2011) Geochemistry of hydrothermal fluids from the PACMANUS, Northeast Pual and Vienna Woods hydrothermal fields, Manus Basin, Papua New Guinea. *Geochim. Cosmochim. Acta* **75**, 1088–1123.

Reeves E.P., Thal J., Schaen A., Ono S., Seewald J., Bach W. (2015) Temporal evolution of magmatic-hydrothermal systems in the Manus Basin, Papua New Guinea: Insights from vent fluid chemistry and bathymetric observations (Invited). AGU Fall Meeting, abstract OS42A-05, San Francisco

Schellart, W. P., Lister, G. S., Toy, V. G. (2006). A Late Cretaceous and Cenozoic reconstruction of the Southwest Pacific region: tectonics controlled by subduction and slab rollback processes. *Earth-Science Reviews* **76**(3), 191-233.

Schmidt, K., Garbe-Schönberg, D., Hannington. M.D., Aderson, M.O., Bühring, B., Haase, K., Haruel, C., Lupton, J.E., Koschinsky, A. (2017) Boiling vapour-type fluids from the Nifonea vent field (New Hebrides Back-Arc, Vanuatu, SW Pacific): Geochemistry of an early-stage, post-eruptive hydrothermal system. *Geochim. Cosmochim. Acta* **207**, 185-209.

Seewald, J. S., Doherty, K. W., Hammar, T. R., & Liberatore, S. P. (2002). A new gas-tight isobaric sampler for hydrothermal fluids. *Deep Sea Research Part I: Oceanographic Research Papers* **49**(1), 189-196.

Seewald, J. S., Reeves, E. P., Bach, W., Saccocia, P. J., Craddock, P. R., Shanks III, W. C., Sylva, S. P., Pichler, T., Rosner, M., Walsh, E. (2015) Submarine Venting of magmatic volatiles in the Eastern Manus Basin, Papua New Guinea. *Geochim. Cosmochim. Acta* **163**, 179-199.

Seyfried, W. E. and Bischoff, J. L. (1981) Experimental seawater–basalt interaction at 300 C, 500 bars, chemical exchange, secondary mineral formation and implications for the transport of heavy metals. *Geochim. Cosmochim. Acta* **45**(2), 135–147.

Sinton, J. M., Ford, L. L., Chappell, B. and McCulloch, M. T. (2003) Magma genesis and mantle heterogeneity in the Manus back-arc basin, Papua New Guinea. *J. Petrol.* **44**(1), 159–195.

Taylor, B., Crook, K. and Sinton, J. (1994) Extensional transform zones and oblique spreading centers. *J. Geophys. Res.: Solid Earth* **99**(B10), 19707–19718.

Thal, J., Tivey, M. A., Yoerger, D, Jöns, N., Bach, W. (2014) Geologic setting of PACManus hydrothermal vents – High-resolution mapping and in situ observations. *Marine Geol*. **355,** 98-114.

Thal, J., Tivey, M., Yoerger, D. R., Bach, W. (2016) Subaqueous cryptodome eruption, hydrothermal activity and related seafloor morphologies on the andesitic North Su volcano. *J.of Volcanol. Geotherm. Res*. **323**, 80-96.

Tivey M., Bach W., Seewald J., Tivey M. K., Vanko D. A. and the Shipboard Science J. I. A. A. T. T. (2006) Cruise Report for R/V Melville cruise MGLN06MV – Hydrothermal systems in the Eastern Manus Basin: Fluid Chemistry and Magnetic Structure as Guides to Subseafloor Processes. Woods Hole Oceanographic Institution (available upon request to authors).

Tomascak, P.B., Langmuir, C.H., Roux, P.J., Shirey, S.B. (2008) Lithium isotopes in global mid-ocean ridge basalts. *Geochim. Cosmochim. Acta* **72**, 1626-1637.

Verney-Carron, A., N. Vigier, and R. Millot (2011), Experimental determination of the role of diffusion on Li isotope fractionation during basaltic glass weathering, *Geochim. Cosmochim. Acta* **75**, 3452–3468.

Verney-Carron, A., Vigier, N., Millot, R., Hardarson, B.S. (2015) Lithium isotopes in hydrothermally altered basalts from Hengill (SW Iceland). *Earth Planet. Sci. Lett.* **41**, 62-71.

Vigier, N., Decarreau, A., Millot, R., Carignan, J., Petit, S., France-Lanord, C. (2008). Quantifying Li isotope fractionation during smectite formation and implications for the Li cycle. *Geochim. Cosmochim. Acta* **72**(3), 780-792.

Von Damm K. L., Edmond J. M., Measures C. I. and Grant B. (1985) Chemistry of submarine hydrothermal solutions at Guaymas Basin, Gulf of California. *Geochim. Cosmochim. Acta* **49**, 2221-2237.

Von Damm, K.L. (1995) Controls on the chemistry and temporal variability of seafloor hydrothermal fluids, in: Humphris, S.E., Zierenberg, R.A., Mullineaux, L.S., Thomson, R.E. (Eds.), *Seafloor Hydrothermal Systems: Physical, Chemical, Biological, and Geological Interactions*. American Geophysical Union, Washington, D. C., pp. 222–247.

Wilckens, F.K., Reeves, E.P., Bach, W., Meixner, A., Seewald, J.S., Koschinsky, A., Kasemann, S.A. (submitted) The influence of magmatic fluids and phase separation on B systematics

in submarine hydrothermal vent fluids – A case study from the Manus Basin and Nifonea volcano. Submitted to *Geochim. Cosmochim Acta.*

Wilckens, F.K., Bach, W., Meixner, A., Reeves, E.P., Seewald, J.S., Koschinsky, A., Kasemann, S.A. (in preparation) Lithium isotope ratios in submarine hydrothermal vent fluids from Manus Basin and Nifonea volcano reveal evidence for negligible Li isotope fractionation during water-rock interaction.

Wimpenny J., James R.H., Burton K.W., Gannoun A., Mokadem F., Gislason S.R. (2010) Glacial effects on weathering processes: New insights from the elemental and lithium isotopic composition of West Greenland rivers. *Earth Planet. Sci. Lett.* **290**, 427-437.

Yamaoka, K., Hong, E., Ishikawa, T., Gamo, T., Kawahata, H. (2015) Boron isotope geochemistry of vent fluids from arc/back-arc seafloor hydrothermal systems in the western Pacific. *Chem. Geol*. **392**, 9-18.

Chapter 5: Assessing water-rock interaction and basement alteration from B, Mg, Li and Sr isotopes in acid-sulfate fluids

Frederike K.Wilckens[1*], Wolfgang Bach[1], Anette Meixner[1], Jeffrey S. Seewald[2] and Simone A. Kasemann[1]

[1] MARUM – Center for Marine Environmental Sciences and Faculty of Geosciences, University of Bremen, Germany (*corresponding author: fwilckens@marum.de, telephone: +49 (0) 421 218 65941)

[2] Department of Marine Chemistry and Geochemistry, Woods Hole Oceanographic Institution, USA

In preparation for submission to *Journal of Volcanology and Geothermal Research*

5.1 Abstract

Acid-sulfate fluids form through direct injection of magmatic fluids into unmodified seawater and reveal evidence for limited and water-dominated water-rock interaction with a strongly altered oceanic crust. Nevertheless, it has been argued, that their high Mg concentrations are a result of dissolution of Mg-bearing minerals in the subsurface. This study investigates B, Li, Mg and Sr isotope ratios in acid-sulfate fluids from the Eastern Manus Volcanic Zone, Papua New Guinea in order to understand water-rock interaction at acid-sulfate conditions and to understand the fluids chemistry. Mg isotope ratios show, that the high Mg concentrations of acid-sulfate fluids are seawater derived and not associated with dissolution of Mg bearing minerals, whereas B, Li and Sr isotope ratios reflect water-rock interaction with the basement rocks. The results reveal that Sr, Li and B are affected differently by water-rock interaction with acid-sulfate fluids. Further our data implies that it might be possible to trace the alteration of the oceanic crust in those environments, which are associated with acid-sulfate alteration, with a combination of these isotopic systems. This might be beneficial in order to understand advanced argillic alteration of the oceanic crust and to estimate the alteration period, during which the fluids have reacted with the host rocks.

5.2 Introduction

Hydrothermal vent fluids in island arcs and back-arc basins have a broad chemical and physical variability, which is related to their tectonic setting. In recent years, the reasons for this variability was increasingly investigated (Gamo et al., 1997; Gena et al., 2006; Resing et al., 2007; Reeves et al., 2011; Seewald et al., 2015; Yamaoka et al., 2015; Araoka et al., 2016). In subduction-related settings, vent fluids are influenced by a complex interplay between mantle wedge, subducting slab, seafloor morphology and volcanic activity. One of the major factors controlling the composition of the oceanic crust and hence of the hydrothermal fluids is the proximity to the subducting slab (Sinton et al., 2003; Pearce and Stern, 2006; Mottl et al., 2011; Shaw et al., 2012).

The Manus back-arc basin hosts a broad range of hydrothermal vent fluids. Fluids venting at the Manus Spreading centre are in their physical and chemical composition similar to hydrothermal vent fluids at mid-ocean ridge settings (Reeves et al., 2011; Yamaoka et al., 2015). In contrast, vent fluids from the Eastern Manus Volcanic Zone have a broader chemical range. This higher variability is a result of phase separation processes, basaltic andesitic to dacitic composition of the oceanic crust and higher inputs of magmatic fluids (Gamo et al., 1997; Gena et al., 2006; Reeves et al., 2011). An extraordinary vent type venting in this area is characterized by low pH $\leq$2 and high SO_4 contents, which exceed the concentrations of seawater. These acid sulfate fluids are thought to be a submarine analogue to subaerial fumaroles (Seewald et al., 2015). In contrast to black smoker fluids they have a high magmatic contribution, which explains their low pH and

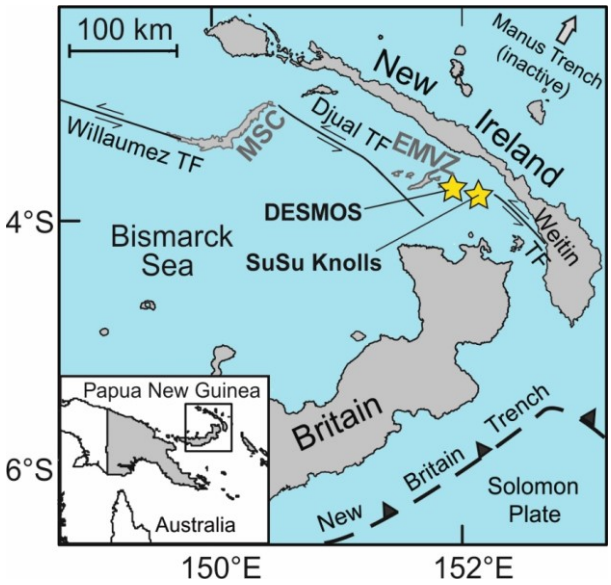

Figure 20: Tectonic setting and of the Manus Basin. Yellow stars indicate the sample locations within the Eastern Manus Volcanic Zone. Major tectonic plates and the plate motions are indicated with black and grey arrows. (map modified after Seewald et al., 2015). MSC = Manus Spreading Centre, EMVZ = Eastern Manus Volcanic Zone, TF = Transform Fault

high sulphate concentrations. Today, several of these acid-sulfate fluids are also known from other arc related settings (Lupton et al., 2006, 2011; Resing et al., 2007; de Ronde et al., 2011; Butterfield et al., 2011). They appear to have a huge influence on global hydrothermal aluminium and carbon dioxide (CO_2) fluxes into the ocean (Butterfield et al., 2011; Lupton et al., 2011). Furthermore, the magmatic fluids are associated with a preferential mobilization of metals either from the magmatic fluids directly or from the oceanic crust (de Ronde et al., 2005; Embley et al., 2006; Resing et al., 2007). However, the interaction of acid-sulfate fluids with the oceanic crust is poorly understood.

Previous studies on acid-sulfate fluids from the Manus Basin discussed a water-dominated water-rock interaction with a highly altered crust during the rise of the hydrothermal fluid in the discharge zone subsequent to the mixing between the magmatic fluid and seawater (Gamo et al., 1997; Gena et al., 2006; Seewald et al., 2015). Temporal differences in the chemical composition of acid-sulfate fluids from DESMOS were explained by a stronger alteration of the oceanic crust and equilibrium in some of the fluid components between oceanic crust and fluid. Hence, finding a proxy for the alteration of the oceanic crust displayed in acid-sulfate fluids might offer the possibility to study the duration of acid-sulfate venting activity at the vent sites.

In order to understand the fluid composition of acid-sulfate fluids as well as the associated alteration of the oceanic crust, we analysed Li, Mg and Sr isotope ratios in acid-sulfate fluids from DESMOS and North Su, both from Manus Basin, Papua New Guinea and compared them to black smoker fluids from the same locations. Furthermore, we compared these results with previously published B isotope ratios from the same fluids (Wilckens et al., submitted). Our results show that Mg in the vent fluids is mainly seawater-derived. Furthermore, Li isotope ratios

in combination with B isotope ratios or SiO_2 concentrations in acid-sulfate fluids appear to be promising proxies to estimate the alteration of the oceanic crust.

5.3. Geologic setting

The Manus Basin is a young, rapidly opening back-arc basin. It is located in the northeastern Bismarck Sea (Fig. 20) and bordered to the South by the Willaumez Rise and New Britain trench and to the northeast by the inactive Manus Trench (Taylor et al., 1994; Lee and Ruellan, 2006) (Fig. 20). The formation of the Manus Basin is related to the northward subduction of the Solomon plate along the New Britain Trench. The area between the Djaul and Weitin transform faults in the easternmost part of the Manus Basin host a chain of neovolcanic ridges and volcanoes that represent initial rifting in a pull-apart basin (Martinez and Taylor, 1996). The composition of the oceanic crust in this area ranges from basaltic andesites to dacites and the volcanic rocks show strong similarities to island arc basalts (Kamenetsky et al., 2001; Sinton et al., 2003; Pearce and Stern, 2006; Park et al., 2010; Beier et al., 2015).

5.3.1 Hydrothermal vent fields

5.3.1.1 North Su

North Su hydrothermal vent field is located within the EMVZ and is part of the SuSu Knolls series. SuSu Knolls describe three individual volcanic edifices, Suzette, North Su and South Su from north to south. These edifices overlie the andesitic Tumai Ridge (Binns et al., 1997; Tivey et al., 2006; Hrischeva et al., 2007). SuSu Knolls volcanic edifices are covered with sediments of variable thickness, which are most likely a mixture of pelagic/hemipelagic and volcanoclastic material (Hrischeva et al., 2007). Hydrothermal vent fluids at North Su have a broad range in their chemical and physical properties due to different fluid pathways in the subsurface and variable magmatic fluid influx. In this study, we will focus on acid-sulphate fluids venting on the flanks of the North Su dome. These fluids are mostly white smoker fluids with variable exit temperatures between 48 and 241°C and pH between 0.9 and 1.9 (Bach et al., 2011; Seewald et al., 2015). Prior to the cruise in 2011, the white smoker site with most vigorous venting in 2006 was buried by the products of volcanic cryptodome eruption (Thal et al., 2016). During the sampling campaign in 2011, the Sulfur Candle field was discovered, which describes an area with meter-thick flows of liquid sulfur as well as hundreds of white smokers and bubbles of liquid CO_2 (Bach et al., 2011).

5.3.1.2 DESMOS caldera

DESMOS caldera is also located in the EMVZ and describes a neovolcanic edifice north of SuSu Knolls, which is rising to about 1810 m depth. DESMOS has a caldera with a depression of 150 to 250 m, a width of about 1.5 to 2 km and negligible sediment cover. DESMOS is less hydrothermally active in comparison with North Su. Hydrothermal vents at DESMOS are only at

a small poorly focussed vent site of 30 m in diameter. The so-called Onsen site, with white smoker fluids venting on a hedge of the northern caldera wall vents acid-sulfate fluids (Seewald et al., 2015). Similar to North Su vent fluids are characterized by low exit temperatures of 69 to 117 °C and low pH from 1.0 to 1.4.

5.4 Methods

The collection of samples was done during the July-August 2006 MAGELLAN-06 expedition aboard the R/V Melville and the follow-up June-July 2011 SO-216 (BAMBUS) expedition aboard the R/V Sonne. During MAGELLAN-06 vent fluid sampling was done with isobaric gas-tight (IGT) fluid samplers (Seewald et al., 2002) and syringe style "major" samplers deployed from the ROV Jason II. Craddock et al. (2010), Reeves et al. (2011), and Seewald et al. (2015) describe sampling methods and locations from the sampling campaign in 2006 in more detail. During SO-216 vent fluid sampling was done with IGT fluid samplers as well as the "KIPS" (Kiel Pumping System) (Garbe-Schönberg et al., 2006) fluid pumping system deployed from ROV MARUM-QUEST (Bach et al., 2011). At every individual orifice, at least one fluid sample was taken with an IGT fluid sampler. During sampling real-time measurements of temperature and shipboard analysis of pH units as well as volatile compounds were determined.

5.4.1 Sample preparation and isotope ratio measurements

Before isotope analysis Li and Sr were separated from their sample matrix using different separation methods. For the preparation of rock samples, the rock chips were pulverized and digested using a mixture of HF, HNO_3 and H_2O_2. To prepare the vent fluids for Sr and Li column separations the fluids were dried.

For Sr isotope analysis about 300 ng Sr was loaded onto the columns. The chromatographic separation of Sr was done with Sr spec resin using a modified method described by Pin and Bassin (1992). The separated Sr fraction was than loaded together with an tantalum emitter onto rhenium filaments and measured with a ThermoFischerScientific TIMS (thermal ionization mass spectrometry). Strontium isotopic ratios are given in $^{87}Sr/^{86}Sr$ notation and were normalizuzed to $^{86}Sr/^{88}Sr$ of 0.1194. The instrumental precision for $^{87}Sr/^{86}Sr$ was obtained by repeated analysis of the international reference NIST 987, which has a value of 0.710248±15 (2SD, n=12). To validate and verify the chemical separation and digestion techniques used in this study, several international reference materials were separated and measured as well (BHVO-2, IAEA-B5, BM). The results for BHVO-2 ($^{87}Sr/^{86}Sr$ = 0.70347±2 (2SD, n=2)) are within analytical uncertainty in agreement with literature values ($^{87}Sr/^{86}Sr$ = 0.70348±6 (2SD, n=80).

For Li isotope analysis at least 100 ng Li was loaded onto the column. Li was separated from its sample matrix using a two-step column separation modified after Moriguti and Nakamura (1998). Separated Li fractions were checked for their purity and measured on a ThermoScientific Neptune

MC-ICP-MS (Multicollector inductively coupled plasma mass spectrometer). Li isotope ratios were measured using the standard-sample-bracketing method with the international reference material L-SVEC as bracketing standard. Isotope data for Li- is reported in delta notation relative to a standard material and is expressed in per mill (‰).

$$\delta^7 Li\ [‰] = \left[\frac{\left(\frac{^6Li}{^7Li}\right)_{sample}}{\left(\frac{^6Li}{^7Li}\right)_{L-SVEC}} - 1 \right] \cdot 1000 \qquad (9)$$

To control the preparation procedure and examine the effects of contamination and parameter change, solutions of continuously measured standard materials were included in each sample batch and handled in the same way as the actual samples. Procedural blanks were lower than 0.01%. Hence, they were not affecting the sample composition. The accuracy and precision of the method was obtained by repeated preparation and analysis of an internal seawater standard (bottom seawater from SuSu Knolls), and the international reference materials L-SVEC and BHVO-2. Long-time reproducibility of L-SVEC was δ^7Li of 0.0±0.1‰ (2SD, n=17). Li isotope ratios and concentrations of an internal laboratory seawater standard (bottom seawater from SuSu Knolls) (δ^7Li of 31.1±0.2‰ (2SD, n=5)) are in agreement with literature values (+31.1±0.3‰ (2SD), Huang et al., 2010; Wimpenny et al., 2010; Pogge von Strandmann et al., 2010). The basalt reference material BHVO-2 has a δ^7Li value of 4.3±0.3‰ (2SD, n=2), which is within the range of the published isotope values (4.5±0.3‰, 2SD) (Gao et al., 2012; Genske et al., 2014; Magna et al., 2015).

Mg was separated from the sample matrix using a 2-step column separation based on published distribution coefficients for the resin AG 50W X8, 200-400 mesh (Strelow, 1960; Strelow et al., 1965). The first separation step was performed with 1 ml of the BIORAD cation exchange resin AG 50W X8 (200-400 mesh) in BIORAD BIO-spin® columns in 1M HCl. For the second separation step, the same columns were used, and the separation was done in 1M HNO_3. The reliability of each chemical session was checked with a procedure blank and at least one column was blocked for an international reference material. To monitor loss of Mg during sample preparation, the head and tail of each Mg fraction was checked for its Mg concentration. Further, the separated Mg fractions were checked for their purity. Mg isotope measurements were performed on a Neptune MC-ICP-MS (ThermoFischer) equipped with a stable introduction system and a high-efficiency x-cone. Pure Mg solutions were adjusted to Mg concentrations of 200 ng/g. Samples were measured using the standard-sample bracketing method with a pure Mg ICP standard (Alfa Aesar Magnesium plasma standard solution, Specpure) as bracketing standard. Each sample was analyzed at least three times. Isotope data is reported in delta notation relative to a standard material and expressed in per mill (‰).

$$\delta^{26}Mg_{MgICP}\,[‰] = \left[\frac{\left(\frac{^{26}Mg}{^{24}Mg}\right)_{sample}}{\left(\frac{^{26}Mg}{^{24}Mg}\right)_{Mg\ ICP}} - 1\right] \cdot 1000 \qquad (10)$$

To evaluate single measurement sequences and to convert Mg isotope ratios into the DSM-3 scale the international reference materials DSM-3 and Cambridge-1 (Cam-I) were analyzed in every sequence. The conversion of Mg isotope ratios into the DSM-3 scale was done using the following expression by Young and Galy (2004):

$$\delta^{26}Mg_{DSM-3}^{sample} = \delta^{26}Mg_{MgICP}^{sample} + \delta^{26}Mg_{DSM-3}^{MgICP} + 0.001\delta^{26}Mg_{MgICP}^{sample}\ \delta^{26}Mg_{DSM-3}^{MgICP} \qquad (11)$$

To validate and verify the chemical separation and digestion techniques used in this study, in each series of samples international reference materials were separated and measured as well. The instrumental precision for δ^{26}Mg is ±0.09‰ (2 SD, n=8), that was obtained by the repeated analysis of the international reference material Cambridge-I (Cam-I). Procedural blanks were lower than 80 pg and thus did not affect isotope ratios of the samples (<0.1% of sample). The external precision is based on a repeatedly prepared and analysed internal seawater standard (bottom water SuSu Knolls) and is better than 0.02‰ (2SD) for δ^{26}Mg. δ^{26}Mg values for seawater (δ^{26}Mg = -0.87±0.02‰, n = 3) and Cam-I (δ^{26}Mg = -2.56±0.09‰, n = 8) are within analytical uncertainty in agreement with literature values (-0.82±0.06, n = 26, Foster et al., 2010 and -2.62±0.04, Tipper et al., 2006, 2010; Pogge von Strandmann et al., 2011).

5.5 Results

5.5.1 Strontium Isotope ratios

Strontium isotope ratios are summarized in table 7. Most of the acid-sulfate fluids at SuSu Knolls have similar or lower Sr concentrations relative to seawater. The only sample enriched in Sr, is sample NS11, which was collected in 2011. $^{87}Sr/^{86}Sr$ in the vent fluids from North Su have lower ratios compared to seawater (0.70916) ranging from 0.70466 at NS11 to 0.70899 at NS1. All samples from DESMOS are depleted in Sr and $^{87}Sr/^{86}Sr$ ratios are lower relative to seawater ranging from 0.70886 to 0.70906.

5.5.2 Lithium Isotope ratios

The data for Li isotope ratios is summarized in table 7. Li in the acid-sulphate fluids from North Su defines a broad variation. Li concentrations in all fluids exceed those of seawater (28 µmol/kg) ranging from 30 to 419 µmol/kg with the lowest concentrations in the fluids from NS1 and NS2 and the highest concentrations in the fluids from NS4. δ^{7}Li values vary between 6.2 and 24.3‰. δ^{7}Li values correlate with the Li concentration, thus vent fluids from NS1 and NS2 have the highest values (from 29.2 to 30.1 ‰) and vent fluids from NS4 the lowest (from 6.2 to 6.5 ‰). At DESMOS the acid-sulfate fluids have much lower Li concentrations which vary from 21 to 31

Table 7: Measured boron, lithium, strontium and magnesium concentrations and isotope data in acid-sulfate fluids from North Su and DESMOS together with previously reported data from the same vent fluids

Edifice	Working ID	Year of sampling	IGT T °C	pH[a] 25°C	Mg[a] (mm)	SiO_2[a] (mm)	B[b] (µm)	Li[a] (µm)	Sr[a] (µm)	$\delta^{11}B$ ± 2sd[b] (‰)	$\delta^{7}Li$ ± 2sd (‰)	$^{87}Sr/^{86}Sr$ ± 2se	$\delta^{26}Mg$ ± 2sd (‰)
acid-sulfate fluids													
North Su													
NS1	J2-221-IGT7	2006	48	1.8	49.6	4	505	35	86	35.0 ± 0.1	23.1 ± 0.1	0.70899 ± 0.00001	-0.82 ± 0.02
NS1	J2-221-IGT8	2006	47	1.9	50.4	3	484	30	85	36.0 ± 0.1	24.3 ± 0.1	0.70903 ± 0.00001	-0.91 ± 0.03
NS1	J2-221-M4	2006	nd	1.9	49.8	3	464	34	87	36.0 ± 0.1	23.8 ± 0.2	0.70902 ± 0.00001	-0.92 ± 0.01
NS2	J2-221-IGT6	2006	206	0.9	39.2	10	797	27	58	23.3 ± 0.1	20.6 ± 0.1	0.70876 ± 0.00001	-0.83 ± 0.04
NS2	J2-221-IGT5	2006	215	0.9	41.1	9	718	34	64	24.8 ± 0.2	22.0 ± 0.0		-0.83 ± 0.03
NS2	J2-221-M2	2006		0.9	41.1	9	704	34	63	24.9 ± 0.1	21.7 ± 0.1	0.70885 ± 0.00001	-0.86 ± 0.04
NS4	J2-223-IGT5	2006	241	1.5	23.5	11	1047	419	73	20.7 ± 0.1	6.2 ± 0.1	0.70740 ± 0.00000	-0.89 ± 0.03
NS4	J2-223-IGT6	2006	203	1.5	24.2	10	1057	380	75	20.7 ± 0.0	6.5 ± 0.2	0.70745 ± 0.00001	-0.87 ± 0.02
NS9	023-ROV-01	2011	95	1.4	44.7	4	465	37	66	33.0 ± 0.2	19.2 ± 0.3	0.70890 ± 0.00001	-0.90 ± 0.02
NS9	023-ROV-02	2011	103	1.2	42.7	6	472	41	59	31.4 ± 0.1	17.2 ± 0.1	0.70876 ± 0.00001	-0.86 ± 0.02
NS11	047-ROV-03	2011	149	2.0	44.2	5	570	130	95	30.2 ± 0.1	9.8 ± 0.1	0.70792 ± 0.00001	-0.90 ± 0.02
NS11	047-ROV-04	2011	129	1.9	40.8	7	662	164	100	28.1 ± 0.1	8.5 ± 0.1	0.70466 ± 0.00001	-0.93 ± 0.01
DESMOS													
D1	J2-220-IGT1	2006	113	1.0	44.9	8	474	24	71	35.3 ± 0.1	29.2 ± 0.1	0.70887 ± 0.00001	
D1	J2-220-IGT2	2006	117	1.0	45.1	8	471	25	72	35.0 ± 0.1	29.3 ± 0.1	0.70896 ± 0.00001	-0.83 ± 0.06
D1	J2-220-M4	2006		1.3	50.0	3	446	29	86	38.6 ± 0.1	29.8 ± 0.1	0.70896 ± 0.00001	-0.90 ± 0.01
D2	J2-220-IGT3	2006	69	1.4	49.2	6	471	21	79	36.0 ± 0.1	29.7 ± 0.1	0.70888 ± 0.00001	-0.86 ± 0.01
D2	J2-220-M2	2006		1.4	49.4	6	473	25	80	35.8 ± 0.1	29.5 ± 0.1	0.70886 ± 0.00001	-0.90 ± 0.03
D2	J2-220-IGT4	2006	70	1.4	49.3	6	487	31	78	35.8 ± 0.1	30.1 ± 0.2	0.70886 ± 0.00001	-0.89 ± 0.02
bottom seawater			3	7.9	52.4	0	419	28	91	39.6 ± 0.0	31.0 ± 0.1	0.70916 ± 0.00001	-0.87 ± 0.03

[a] Previously reported by: Tivey et al., 2006; Craddock et al., 2010; Reeves et al., 2011 ; Seewald et al (2015) for fluids from Manus Basin collected in 2006; Bach et al., 2011 andunpublished data for fluids from the EMVZ collected in 2011

[b] Previously reported by Wilckens et al. (submitted)

µmol/kg. Hence, they are similar to Li in seawater (28 µmol/kg). $\delta^{7}Li$ values are also close to

seawater and vary between 29.2 and 30.6.

5.5.3 Mg Isotope ratios

Results for Mg isotope measurements are summarized in table 7. Mg concentrations in the acid-sulfate fluids from North Su are all depleted relative to seawater (52.4 mmol/kg). Fluids from the orifice NS4 have the lowest Mg concentrations (23.5 mmol/kg), whereas fluids from orifice NS1 have the highest Mg concentrations (50.4 mmol/kg). Mg concentrations in the vent fluids from DESMOS are similar ranging from 39.2 to 50.0 mmol/kg. The isotope ratios of Mg in all acid-sulfate fluids define a small array of 0.11 ‰, ranging from -0.82 to -0.93 ‰. Seawater, which was collected close to the sample sites in the EMVZ has a δ^{26}Mg value of -0.87 ‰.

5.6 Discussion

5.6.1 Smoker versus acid-sulfate fluids

Not all of the fluids from the vent fields at North Su are in a strict sense acid-sulfate fluids. Vent fluids from NS4 and NS11 have both characteristics of acid-sulfate fluids and of "smoker-type" fluids. They are characterized by low pH of $\leq$ 2.0 and NS11 has high Mg and ΣSO_4 contents, which are similar to those in acid-sulfate fluids. However, alkali elements are clearly enriched in these fluids and in case of NS4 Mg contents are also significantly lower compared to the other acid-sulfate fluids. These chemical characteristics could either imply a reaction of the fluids in the discharge zone with fresh or only slightly altered volcanic rocks or these fluids formed due to a three component mixing of magmatic fluid, seawater and hydrothermal fluid.

Vent fluids from NS9 within North Su, which were collected in 2011, have temperatures, pH, Mg concentrations, low concentrations of alkali elements and elevated ΣSO_4, which are similar to the acid-sulfate fluids D1, D2 from DESMOS and NS1 and NS2 from North Su (Gamo et al., 1997; Seewald et al., 2015). However, in contrast to the other acid-sulfate fluids, NS9 fluids have extremely high CO_2 concentrations (up to 1073 mmol/kg). Phases of liquid CO_2 during venting imply that these fluids were supersaturated with respect to CO_2. The CO_2 concentration measured in the fluids from NS9 is the second highest measured so far in hydrothermal fluids. The highest dissolved CO_2 content was detected in a fluid from the summit of NW Eifuku within the Mariana Arc (Lupton et al., 2006; 2011). Lupton et al., (2006) explained this enrichment in CO_2 by a volatile phase, which was degassed from the magma chamber. Afterwards this gaseous phase got stored in the subsurface and hot water, which entrained into this area, became enriched in CO_2.

5.6.2 Source of Mg in acid-sulfate fluids

Seewald et al. (2015) suggested that acid-sulfate fluids form due to direct injection of magmatic volatiles into seawater in the subsurface. However, almost all fluids show evidence for water-rock interaction (e.g in their elevated Al or SiO_2 concentrations). Mg concentrations in acid-sulfate

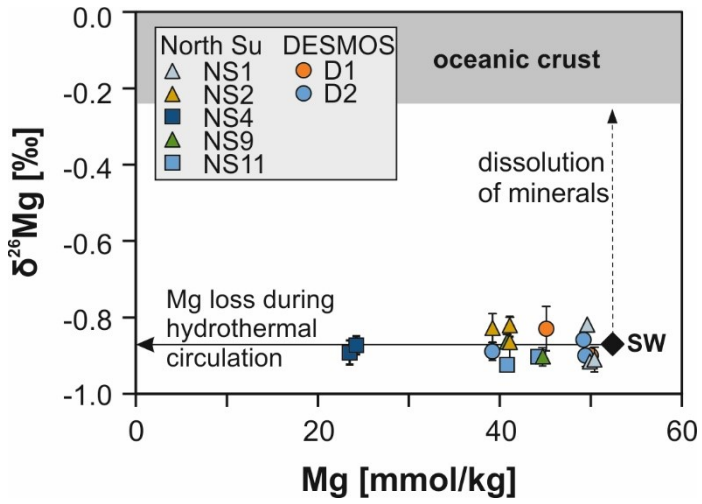

Figure 21: Although their huge variation in Mg concentration, acid-sulfate fluids have homogeneous δ^{26}Mg value similar to seawater. This implies that Mg is removed without significant isotopic fractionation during hydrothermal circulation. Furthermore, Mg in acid-sulfate fluids is not affected by the dissolution of minerals.

fluids from DESMOS and North Su are up to 30 times higher than Mg in the black smoker fluids from the same study area (Reeves et al., 2011; Seewald et al., 2015). Due to the high acidity in acid-sulfate fluids, the high Mg concentrations in acid-sulfate fluids from DESMOS were first explained by dissolution of Mg-bearing silicates in the discharge zone (Gamo et al., 1997). However, Seewald et al. (2015) suggested, that the high Mg concentration are a result of a direct injection of magmatic volatile phases into unmodified seawater and that the seawater-like Na/Mg and K/Mg ratios in the acid-sulfate fluids display interaction with highly altered rocks in the discharge zone. Because those highly altered rocks do not contain Mg-bearing minerals (Gena et al., 2001; Paulick and Bach, 2006; Binns et al., 2007), the high Mg concentrations in the acid-sulfate fluids are thought to be mostly seawater derived. However, Seewald et al. (2015) also discussed, that minor amounts of Mg (<2 mmol/kg for fluid D2) could still be added by leaching from the oceanic crust. To investigate, whether Mg is seawater derived or leached from the oceanic crust, Mg isotope ratios might be a useful tool. Mg has a different isotopic composition in seawater (δ^{26}Mg = -0.82‰, Tipper et al., 2006) and fresh as well as altered MORB (δ^{26}Mg = -0.25±0.11‰, Huang et al., 2015). Mg isotope ratios in island arc lavas are potentially even higher than in MORB with δ^{26}Mg values between -0.25 and -0.10‰ due to fluid-peridotite interactions (Teng et al., 2016). Thus, already small amounts of Mg leached from the oceanic crust should change the isotopic composition of the vent fluid towards higher δ^{26}Mg values. All acid-sulfate fluids, which were measured in this study, have Mg isotope compositions matching seawater (Fig. 21). This supports the hypothesis that Mg is mainly seawater derived. Nevertheless, it does not preclude that minor amounts of Mg can be leached from the oceanic crust, which cannot be resolved due to the analytical limits.

Mg concentrations in the acid-sulfate fluids from NS4 (23.5 to 24.2 mmol/kg) are about half the concentration of the other acid-sulfate fluids. The comparable low Mg concentration implies that Mg is lost in these fluids due to water-rock interaction at lower temperatures. Thus, this sample may not display a direct injection of magmatic volatiles into unmodified seawater, but rather into

a mixture of hydrothermal fluid and seawater. However, Mg isotope ratios in these fluids have the same isotopic composition as seawater. These results indicate that there is also no significant isotopic fractionation of Mg during the incorporation of Mg into the oceanic crust during hydrothermal circulation.

In summary, Mg isotope ratios imply that the variation of the Mg contents in acid-sulfate fluids displays Mg loss from seawater during alteration of the oceanic crust. During this reaction Mg-OH silicates form and Mg gets depleted in the fluid. Nonetheless, Mg concentrations are almost as high as in seawater, implying that this reaction is not complete as during hydrothermal circulation. This implies that indeed water-rock interaction is limited during the formation and rise of acid-sulfate fluids. Furthermore, there is no indication whether the Mg loss takes place prior or subsequent to the mixing with the magmatic phase. However, it appears to be more likely that this reaction takes place prior to venting, because of the high acidity in acid-sulfate fluids and thus the high efficiency in dissolving minerals as well as the lack of Mg in the advanced argillic altered rocks (Gena et al., 2001), which are associated with the interaction of acid-sulfate fluids.

5.6.3 Sr isotope ratios as tracer for water-rock interaction in acid-sulfate fluids

The composition of acid-sulfate fluids from DESMOS varies in its chemical and physical properties as displayed in the studies by Gamo et al. (1997) and Seewald et al. (2015). Fluids sampled in 1993 had slightly elevated K and Na concentrations compared to seawater, whereas the fluids sampled in 2006 have K/Mg and Na/Mg ratios, which are similar to seawater. Seewald et al. (2015) explained these differences with fluid-rock interaction with less altered rocks in the discharge zone during an earlier phase of venting. The acid-sulfate fluids, which were sampled in 2006 and 2011 from DESMOS and North Su show also different enrichments of Na and K relative to seawater values. Fluids from DESMOS have for example slightly lower K/Mg ratios than seawater, whereas fluids from North Su have slightly higher K/Mg ratios. Furthermore, those fluids (NS4 and NS11), which show characteristics of both acid-sulfate type and “smoker-type” fluids have clearly elevated K/Mg ratios. Since the Mg concentrations in all samples except for NS4 are similar, these different enrichments may reflect the different alteration stages of the oceanic crust.

A good tracer for the interaction of water and rock is the Sr isotopic composition of the vent fluids. However, leaching of Sr from the oceanic crust is a temperature dependent process. At temperatures above 250°C, Sr is quantitatively leached from the oceanic crust (Araoka et al., 2016). Thus, Sr concentration and isotope ratios might be affected by the temperature. During advanced argillic alteration, the rocks from the EMVZ appear to have both lower and higher Sr concentrations relative to their fresh counterparts (Wilckens et al., in preparation). This might relate to the incorporation of Sr into secondary minerals. Indeed, Sr concentrations in all acid-

sulfate fluids expect for NS11 are lower than in seawater, whereas the smoker fluids from North Su are enriched in Sr (Wilckens et al.,submitted). Nevertheless, $^{87}Sr/^{86}Sr$ ratios in all acid-sulfate fluids are less radiogenic in comparison with seawater (Fig. 22a). This implies that Sr was leached from the oceanic crust during water-rock interaction in all acid-sulfate fluids from the EMVZ. The low Sr concentrations in the acid-sulfate fluids can be explained by anhydrite precipitation during venting or in the subsurface similar to smoker fluids from PACMANUS (Reeves et al., 2011). Since this process does not fractionate Sr isotopes, Sr isotope ratios in the vent fluids

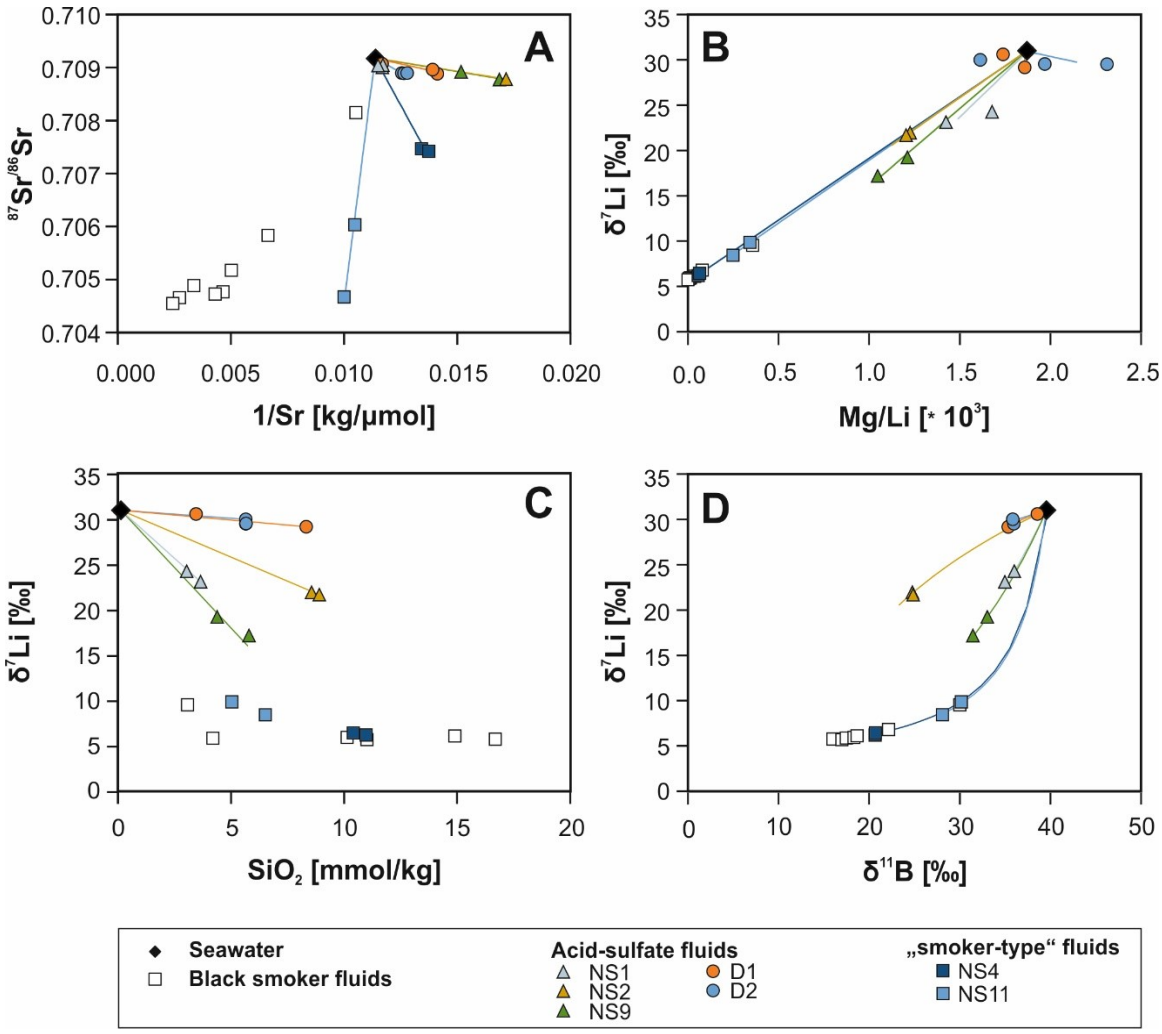

Figure 22: (A) Sr concentrations in almost all acid-sulfate fluids are depleted relative to seawater, whereas black smoker fluids show higher Sr concentrations. (B) Acid-sulfate fluids from DESMOS are depleted in Li relative to seawater, which indicates high water-rock ratios during water-rock interaction with a highly altered basement. Li in some of the acid-sulfate fluids from North Su (NS1, NS2 and NS9) is depleted relative to black smoker fluids but enriched relative to seawater, implying also high water-rock ratios during water-rock interaction with a less altered oceanic crust. NS4 and NS11 and black smoker fluids are highly enriched in Li. (C) SiO_2 is enriched in all acid-sulfate and "smoker-type" fluids relative to seawater implying that water-rock interaction is involved in all fluids. Different slopes between SiO_2 and δ^7Li imply different alteration stages of the oceanic crust. (D) All vent fluids have lower δ^{11} B values in comparison with seawater. The different mixing lines between Li and B isotope ratios (coloured lines) imply also different alteration degrees of the oceanic crust (see text).

represent a mixture between seawater Sr and Sr leached from the oceanic crust. Hence, it is a proxy for water-rock interaction. $^{87}Sr/^{86}Sr$ in acid-sulfate fluids from DESMOS and NS1, NS2 and NS9 are slightly less radiogenic than seawater, implying that either $^{87}Sr/^{86}Sr$ in the oceanic crust has a similar composition as seawater, or the values reflect limited water-rock interaction in the discharge zone. In contrast, the fluids from NS4 and NS11 have obviously less radiogenic isotope ratios than seawater, which is either due to a more intense water-rock interaction or due to the interaction with fresh oceanic crust. However, the isotopic composition of the fluids appears to be not influenced by the temperature differences, because $^{87}Sr/^{86}Sr$ in the fluids from NS2 match those of NS9 although their temperature difference of about 100°C. Thus, the Sr isotopic composition of acid-sulfate fluids reveals evidence for interaction with the oceanic crust in all fluids, but it is not known whether the different Sr isotope signatures reflect changing water-rock ratios during water-rock interaction or rather alteration of the oceanic crust.

5.6.4 Li isotopes in acid-sulfate fluids as proxy for oceanic crust alteration

Li is a fluid mobile element, which is leached in great amounts from the oceanic crust during water-rock interaction at high temperatures (Chan et al., 1992; Seyfried et al., 1984; Verney-Carron et al., 2015). Li is enriched in hydrothermal fluids relative to seawater and gets depleted in the oceanic crust during high temperature alteration (Seyfried et al., 1984; Chan et al., 2002; Verney-Carron et al., 2015). Thus, Li might be a sensitive tracer to investigate the alteration of the oceanic crust in acid-sulfate fluids. Furthermore, Li isotopes are thought to fractionate during water-rock interaction (Vigier et al., 2008, Verney-Carron et al., 2015, Araoka et al., 2016) and therefore the isotopic composition of the fluid might change with advancing alteration of the oceanic crust. However, similar to Sr, leaching of Li and its isotopic fractionation is a temperature dependent process (e.g. Araoka et al., 2016), which makes the interpretation of Li concentrations and isotope ratios in acid-sulfate fluids challenging. Nevertheless, it is uncertain if the high acidity of acid-sulfate affects the leaching behaviour of Li from the oceanic crust. In addition, Li can be also affected by low-temperature interactions with the oceanic crust. During low temperature reaction with the oceanic crust, ^{6}Li is thought to be preferentially incorporated into secondary minerals. Because the Mg concentrations in acid-sulfate fluids imply low-temperature interactions with the oceanic crust prior or subsequent to mixing with the magmatic gas, Li as well as the other alkali elements can be affected.

Similar to K and Na, Li/Mg ratios in acid-sulfate fluids from DESMOS are similar or slightly depleted relative to seawater, whereas the acid-sulfate fluids from North Su are slightly enriched in Li. NS4 and NS11 have clearly higher Li/Mg ratios. Li in the DESMOS fluids, which are depleted in Li relative to seawater, can be explained by an incorporation of Li into the oceanic crust in the recharge zone prior to mixing with the gas phase (Seyfried et al., 1984). However, Li isotope ratios in all acid-sulfate fluids are lower in comparison with seawater implying that Li in

all fluids was leached from the oceanic crust in a high temperature reaction, which is similar to the observations from the Sr isotope ratios. Vent fluids NS2, NS4 and NS11 plot on the same trend between Mg/Li and δ^7Li as black smoker fluids from North Su (Fig. 22b), implying that these fluids reacted with fresh or only slightly altered oceanic crust. In contrast, acid-sulfate fluids from NS1 and NS9 might react with stronger altered rocks. However, the different Mg/Li ratios might be also a result of the different temperatures of these fluids. Since NS2, NS4 and NS11 have temperatures ≥150°C, whereas NS1 and NS9 have temperatures ≤ 100°C, the difference in Li concentrations and isotope ratios might be an artefact of different distribution coefficients and/or isotope fractionation factors, which are related to the temperature (Seyfried et al., 1984; Wunder et al., 2006). Because there is no correlation between Li contents and temperature of the fluids, a temperature-dependent leaching of Li might be not the only factor controlling the Li content in the fluids. Furthermore, temperatures in the fluids from NS1 and NS9 are similar to those from DESMOS and SiO_2 contents of these fluids are in the same range, suggesting that acid-sulfate fluids from DESMOS reacted with highly altered rocks, which are significantly depleted in Li. Because of the high contents of SiO_2 in volcanic rocks showing advanced argillic alteration (Gena et al., 2001), the combination of SiO_2 contents and δ^7Li helps to further understand the influence of oceanic crust alteration on the composition of the acid-sulfate fluids. Acid-sulfate fluids from D1 and D2, NS2, and NS1 and NS9 have linear correlations between SiO_2 and δ^7Li with different slopes (Fig. 22c). Fluids from NS4 and NS11 plot in the field of the smoker fluids and hence display mainly water-rock interaction with fresh volcanic rocks during hydrothermal circulation rather than the limited, water-dominated water-rock interaction in the discharge zone as postulated for acid-sulfate fluids. However, the different slopes for the “pure” acid-sulfate fluids appear to reflect the different alteration stages of the oceanic crust, with the least altered crust at NS1 and NS9 and the strongest altered crust at DESMOS. These results show that Li isotopes appear to be a good tracer for assessing the alteration of the oceanic crust. However, whether temperature in the acidic fluids influences the leaching of Li from the oceanic crust remains unclear.

5.6.5 Influence of B isotope ratios in acid-sulfate fluids

B isotope ratios in the acid-sulfate fluids were interpreted to display the rock signature due to preferential leaching of B from the oceanic crust with a potentially minor influence of B added by magmatic volatiles, except for the fluids from NS9, which might have a strong magmatic signature (Wilckens et al., submitted). End-member B compositions in all other acid-sulfate fluids match the composition of black smoker fluids. Fig. 22d shows the relationship between B and Li isotope ratios. Again, the fluids from orifices NS4 and NS11 plot on the same trend as black smoker fluids. Hence, their signatures can be interpreted as the result of intense water-rock interaction with fresh oceanic crust. Fluids from DESMOS and NS2 as well as those from NS1

and NS9 define two distinct mixing trends, which might reflect the different alteration stages of the oceanic crust. Because of their high temperatures, fluids from NS2 leach B more efficiently from the oceanic crust, which leads to lower B isotope ratios in these fluids. This implies that the depletion of B during advanced argillic alteration is slower as compared to Li and that B isotope ratios in the altered rocks might not change significantly.

5.7 Conclusions

Mg isotope ratios show that the high Mg concentrations in the acid-sulfate fluids cannot be explained by dissolution of Mg-bearing minerals, but rather by an incomplete removal of seawater-derived Mg. In addition, these results imply that Mg is apparently not fractionated during its incorporation into the oceanic crust at low temperatures, which is in accordance with studies showing that the Mg isotopic composition of altered MORB is similar to fresh MORB (Teng et al., 2016). Because of the low temperatures of most acid-sulfate fluids, Sr isotope ratios in acid-sulfate fluids appear to be not a good tracer to trace water-rock interaction and the alteration of the oceanic crust, since Sr is not efficiently extracted from the oceanic crust. In addition, Sr concentrations and isotope ratios might be overprinted due to anhydrite dissolution and precipitation. Nevertheless, all acid sulfate fluids have less radiogenic Sr isotope ratios than seawater, implying interaction with the oceanic crust. The combination of SiO_2 with Li isotope ratios in acid-sulfate fluids appears to be a powerful tracer to trace oceanic crust alteration. During the interaction of acid-sulfate fluids with the oceanic crust, the volcanic rocks get progressively depleted in Li, which is apparent in the fluid signature. Further, the combination of Li and B isotope ratios in acid-sulfate fluids may also help to unravel the processes during alteration of the oceanic crust with acid-sulfate fluids. However, B isotope ratios may be influenced by B derived from magmatic gases, which makes their interpretation challenging. Furthermore, the enrichments of B in acid-sulfate fluids, which are similar to those of black smoker fluids, reveal evidence for a preferential leaching of B from the oceanic crust into low salinity, high vapour fluids. This might be also related to a preferential leaching of metals, which form the massive sulphide deposits, implying that also the metals have their origin in the oceanic crust rather than in the magmatic fluids. However, to further test the eligibility of B and Li isotope ratios to trace the alteration of the oceanic crust in these acidic environments, further studies on acid-sulfate fluids from other settings would be beneficial.

5.8 Acknowledgments

The authors would like to thank the crew of the R/V Melville and R/V Sonne as well as the technical groups of ROV Jason II and ROV-MARUM-QUEST. This study was part of MARUM project GB4 and was funded by the DFG-Research Centre/Cluster of Excellence “The Ocean in the Earth System” at MARUM – Centre for Environmental Sciences, University of Bremen and

was supported from the German Research Foundation (DFG) Major Research Instrumentation Program (INST 144/308-1).

5.9 References

Araoka, D., Nishio, Y., Gamo, T., Yamaoka, K., Kawahata, H. (2016) Lithium isotopic systematics of submarine vent fluids from arc and back-arc hydrothermal systems in the western Pacific. *Geochim. Geophys. Geosys.* **17**, 3835-3853.

Bach W., Dubilier N., Borowski C., Breuer C., Brunner B., Franke P., Herschelmann O., Hourdez S., Jonda L., Jöns N., Klar S., Koloa K., Mai A., Meyerdierks A., Müller I., Petersen S., Pjevac P., Ratmeyer V., Reeves E., Rehage R., Reuter C., Schaen A., Shu L., Thal J., Zarrouk M. (2011) Cruise Report for SONNE cruise SO 216 – BAMBUS, Back-Arc Manus Basin Underwater Solfataras. Universität Bremen (https://elib.suub.uni-bremen.de/edocs/00102250-1.pdf).

Beier C., Bach W., Turner S., Niedermeier D., Woodhead J., Erzinger J., Krumm S. (2015) Origin of Silicic Magmas at Spreading Centres – an Exampe from the South East Rift, Manus Basin. *J Petrol.* **56**, 255-277.

Binns, R.A., Scott, S.D., Gemmell, J.B., and Crook, K.A.W.C., and Shipboard Party, 1997b. The SuSu Knolls hydrothermal field, Eastern Manus Basin, Papua New Guinea. *Eos* **78**,:F772.

Binns, R.A., Barriga, F.J.A.S., Miller, D.J. (2007) Leg 193 synthesis: Anatomy of an active felsic-hosted hydrothermal system, Eastern Manus Basin, Papua New Guinea (2007) *Proceeding of the Ocean Drilling Program, Scientific Results* Volume **193** (Barriga, F.J.A.S., Binns, R.A., Miller, D.J., Herzig, P.M. (Eds.), DOI: 10.2973/odp.proc.sr.193.201.2007, 1-71.

Butterfield, D. A., Nakamura, K. I., Takano, B., Lilley, M. D., Lupton, J. E., Resing, J. A., Roe, K. K. (2011). High SO2 flux, sulfur accumulation, and gas fractionation at an erupting submarine volcano. *Geology* **39**(9), 803-806.

Chan, L. H., Edmond, J. M., Thompson, G., Gillis, K. (1992). Lithium isotopic composition of submarine basalts: implications for the lithium cycle in the oceans. *Earth Planet. Sci. Lett.* **108**(1-3), 151-160.

Chan, L. H., Alt, J. C., Teagle, D. A. (2002). Lithium and lithium isotope profiles through the upper oceanic crust: a study of seawater–basalt exchange at ODP Sites 504B and 896A. *Earth Planet. Sci. Lett.* **201**(1), 187-201.

Craddock, P. R., Bach, W., Seewald, J. S., Rouxel, O. J., Reeves ,E. and Tivey, M. K. (2010) Rare earth element abundances in hydrothermal fluids from the Manus Basin, Papua New Guinea: indicators of sub-seafloor hydrothermal processes in back-arc basins. *Geochim. Cosmochim. Acta* **74**, 5494–5513.

de Ronde, C. E., Hannington, M. D., Stoffers, P., Wright, I. C., Ditchburn, R. G., Reyes, A. G., ... & Greene, R. R. (2005). Evolution of a submarine magmatic-hydrothermal system: Brothers volcano, southern Kermadec arc, New Zealand. *Econom. Geol.* **100**(6), 1097-1133.

Embley, R. W., Chadwick, W. W., Baker, E. T., Butterfield, D. A., Resing, J. A., De Ronde, C. E., et al. (2006). Long-term eruptive activity at a submarine arc volcano. *Nature* **441**(7092), 494-497.

Foster G.L., Pogge von Strandmann P. A. E., Rae J. W. B. (2010) Boron and magnesium isotopic composition of seawater. *Geochem. Geophys. Geosyst.* **11**(8), Q08015, doi:10.1029/2010GC003201.

Gamo, T., Okamura, K., Charlou, J. L., Urabe, T., Auzende, J. M., Ishibashi, J., et al. (1997). Acidic and sulfate-rich hydrothermal fluids from the Manus back-arc basin, Papua New Guinea. *Geology* **25**(2), 139-142.

Garbe-Schönberg D., Koschinsky A., Ratmeyer V., Jähmlich H., Westernströer U. (2006) KIPS – A new multiport valve-based all-Teflon fluid sampling system for ROVs. In *Geophys. Res. Abstr.* **8** p. 07032.

Gao Y, Vils F., Cooper K.M., Banerjee N., Harris M., Hoefs J., Teagle D.A.H., Casey J.F., Elliott T., Altzitzoglou T., Alt J.C., Muehlenbachs K. (2012) Downhole variation of lithium and

oxygen isotopic compositions of oceanic crust at East Pacific Rise, ODP Site 1256. *Geochem. Geophys. Geosys*. **13** (10), doi: 10.1029/2012GC004207.

Gena, K., Mizuta, T., Ishiyama, D., Urabe, T. (2001) Acid-sulphate Type Alteration and Mineralization in the Desmos Caldera, Manus Back-arc Basin, Papua New Guinea. *Resource Geol.* **51**, 31-33.

Gena, K. R., Chiba, H., Mizuta, T., & Matsubaya, O. (2006). Hydrogen, Oxygen and Sulfur Isotope Studies of Seafloor Hydrothermal System at the Desmos Caldera, Manus Back-arc Basin, Papua New Guinea: An Analogue of Terrestrial Acid Hot Crater-lake. *Resource Geology*, *56*(2), 183-190.

Genske F.S., Turner S.P., Beier C., Chu M.-F., Tonarini S., Pearson N.J., Haase K.M. (2014) Lithium and boron isotope systematics in lavas from the Azores islands reveal crustal assimilation. *Chem. Geol*. **373**, 27-36.

Hrischeva, E., Scott, S. D., Weston, R. (2007). Metalliferous sediments associated with presently forming volcanogenic massive sulfides: the SuSu knolls hydrothermal field, eastern manus basin, Papua New Guinea. *Econom. Geol.* **102**(1), 55-73.

Huang K.-F., You C.-F., Liu Y.-H., Wang R.-M., Lin P.-Y., Chung C.-H. (2010) Low memory, small sample size, accurate and high-precision determinations of lithium isotopic ratios in natural materials by MC-ICP-MS. *J. Anal. At. Spectrom*. **25**, 1019-1024.

Lee, S. M. and Ruellan, E. (2006) Tectonic and magmatic evolution of the Bismarck Sea, Papua New Guinea: review and new synthesis. In *Back-Arc Spreading Systems: Geological, Biological, Chemical, and Physical Interactions*, vol. **166** (eds. D. M. Christie, C. R. Fisher, S.-M. Lee and S. Givens). AGU Monograph. American Geophysical Union, 263–286.

Lupton, J., Butterfield, D., Lilley, M., Evans, L., Nakamura, K. I., Chadwick, W. et al. (2006) Submarine venting of liquid carbon dioxide on a Mariana Arc volcano. Geochemistry, Geophysics, Geosystems, 7(8).de Ronde, C. E., Massoth, G. J., Butterfield, D. A., Christenson, B. W., Ishibashi, J., Ditchburn, R. G., et al. (2011) Submarine hydrothermal activity and gold-rich mineralization at Brothers Volcano, Kermadec Arc, New Zealand. *Mineralium Deposita* **46**(5-6), 541-584.

Magna T., Day J.M.D., Mezger L., Fehr M.A., Dohmen R., Aoudjehane H.C.A., Agee C.B. (2015) Lithium isotope constraints on crust–mantle interactions and surface processes on Mars. *Geochim. Cosmochim. Acta* **162**, 46-65.

Martinez F. and Taylor B. (1996) Backarc spreading, rifting, and microplate rotation, between transform faults in the Manus basin. *Mar. Geophys. Res.* **18**(2–4), 203–224.

Moriguti, T., & Nakamura, E. (1998). High-yield lithium separation and the precise isotopic analysis for natural rock and aqueous samples. *Chem. Geol.* **145**(1-2), 91-104.

Park S. H., Lee S.-M., Kamenov G. D., Kwon S.-T. and Lee K.-Y. (2010) Tracing the origin of subduction components beneath the South East rift in the Manus Basin, Papua New Guinea. *Chem. Geol.* **269**, 339–349.

Paulick, H., & Bach, W. (2006). Phyllosilicate alteration mineral assemblages in the active subsea-floor Pacmanus hydrothermal system, Papua New Guinea, ODP Leg 193. *Econ. Geol*. **101**(3), 633-650.

Pearce J. A. and Stern R. J. (2006) Origin of back-arc basin magmas: trace element and isotope perspectives. In *Back-Arc Spreading Systems: Geological, Biological, Chemical, and Physical Interactions*, vol. **166** (eds. D. M. Christie, C. R. Fisher, S.-M. Lee and S. Givens). AGU Monograph. American Geophysical Union, 63–86.

Pin, C., & Bassin, C. (1992). Evaluation of a strontium-specific extraction chromatographic method for isotopic analysis in geological materials. *Analytica Chimica Acta* **269**(2), 249-255.

Pogge von Strandmann P.A.E., Burton K.W., James R.H., van Calsteren P., Gislason S.R. (2010) Assessing the role of climate on uranium and lithium isotope behaviour in rivers draining a basaltic terrain. *Chem. Geol*. **270** (1-4), 227-239.

Pogge von Strandmann, P.A.E.P , Elliott, T., Marschall, H. R., Coath, C., Lai, Y. J., Jeffcoate, A. B., Ionov, D. A. (2011). Variations of Li and Mg isotope ratios in bulk chondrites and mantle xenoliths. *Geochim. Cosmochim. Acta* **75**(18), 5247-5268.

Reeves, E. P., Seewald, J. S., Saccocia, P., Bach, W., Craddock, P. R., Shanks, W. C., Sylva, S. P., Walsh, E., Pichler, T. and Rosner, M. (2011) Geochemistry of hydrothermal fluids from the PACMANUS, Northeast Pual and Vienna Woods hydrothermal fields, Manus Basin, Papua New Guinea. *Geochim. Cosmochim. Acta* **75**, 1088–1123.

Resing, J. A., Lebon, G., Baker, E. T., Lupton, J. E., Embley, R. W., Massoth, G. J., De Ronde, C. E. J. (2007). Venting of acid-sulfate fluids in a high-sulfidation setting at NW Rota-1 submarine volcano on the Mariana Arc. *Econ. Geology*, *102*(6), 1047-1061.

Seewald, J. S., Doherty, K. W., Hammar, T. R., & Liberatore, S. P. (2002). A new gas-tight isobaric sampler for hydrothermal fluids. *Deep Sea Research Part I: Oceanographic Research Papers* **49**(1), 189-196.

Seewald, J. S., Reeves, E. P., Bach, W., Saccocia, P. J., Craddock, P. R., Shanks III, W. C., Sylva, S. P., Pichler, T., Rosner, M., Walsh, E. (2015) Submarine Venting of magmatic volatiles in the Eastern Manus Basin, Papua New Guinea. *Geochim. Cosmochim. Acta* **163**, 179-199.

Seyfried, W.E., Janecky, D.R., Mottl, M.J. (1984) Alteration of the ocean crust: Implications for geochemical cycles of lithium and boron. *Geochim. Coscmochim. Acta* **48**(3), 557-569.

Sinton J. M., Ford L. L., Chappell B. and McCulloch M. T. (2003) Magma genesis and mantle heterogeneity in the Manus back-arc basin, Papua New Guinea. *J. Petrol.* **44**(1), 159–195.

Strelow, F. W. E. (1960). An ion exchange selectivity scale of cations based on equilibrium distribution coefficients. *Anal. Chem.* **32**(9), 1185-1188.

Strelow, F. W., Rethemeyer, R., & Bothma, C. J. C. (1965). Ion Exchange Selectivity Scales for Cations in Nitric Acid and Sulfuric Acid Media with a Sulfonated Polystyrene Resin. *Analytical Chemistry* **37**(1), 106-111.

Taylor, B., Crook, K. and Sinton, J. (1994) Extensional transform zones and oblique spreading centers. *J. Geophys. Res.: Solid Earth* **99**(B10), 19707–19718.

Teng, F.-Z., Hu, Y., Chauvel, C. (2016) Magnesium isotope geochemistry in arc volcanism. *Proc. Natl. Acad. Sci.* **113**(26), 7082-7087.

Tipper, E. T., Galy, A., Gaillardet, J., Bickle, M. J., Elderfield, H., & Carder, E. A. (2006). The magnesium isotope budget of the modern ocean: constraints from riverine magnesium isotope ratios. *Earth Planet. Sci.Lett.* **250**(1), 241-253.

Tipper, E. T., Gaillardet, J., Louvat, P., Capmas, F., & White, A. F. (2010). Mg isotope constraints on soil pore-fluid chemistry: evidence from Santa Cruz, California. *Geochim. Cosmochim. Acta* **74**(14), 3883-3896.

Tivey M., Bach W., Seewald J., Tivey M. K., Vanko D. A. and the Shipboard Science (2006) Cruise Report for R/V Melville cruise MGLN06MV – Hydrothermal systems in the Eastern Manus Basin: Fluid Chemistry and Magnetic Structure as Guides to Subseafloor Processes. Woods Hole Oceanographic Institution (available upon request to authors).

Verney-Carron, A., Vigier, N., Millot, R., Hardarson, B.S. (2015) Lithium isotopes in hydrothermally altered basalts from Hengill (SW Iceland). *Earth Planet. Sci. Lett.* **41**, 62-71.

Vigier, N., Decarreau, A., Millot, R., Carignan, J., Petit, S., France-Lanord, C. (2008). Quantifying Li isotope fractionation during smectite formation and implications for the Li cycle. *Geochim. Cosmochim. Acta* **72**(3), 780-792.

Wimpenny, J., S. R. Gislason, R. H. James, A. Gannoun, P. A. E. Pogge von Strandmann, and K. W. Burton (2010), The behavior of Li and Mg isotopes during primary phase dissolution and secondary mineral formation in basalt, *Geochim. Cosmochim. Acta* **74**, 5259–5279.

Yamaoka, K., Hong, E., Ishikawa, T., Gamo, T., Kawahata, H. (2015) Boron isotope geochemistry of vent fluids from arc/back-arc seafloor hydrothermal systems in the western Pacific. *Chem. Geol.* **392**, 9-18.

Chapter 6: Conclusions and Outlook

Li, B, Mg and Sr concentrations and isotope ratios in vent fluids from Manus Basin and Nifonea volcano show systematic variations that yield valuable insights into the processes, which are related to hydrothermal circulation in back-arc basins. Water-rock interaction appears to be the main control on Li, B and Sr isotope ratios in vent fluids from back-arc settings. However, the lack of correlation between the isotopic systems shows that the elements are controlled by additional and different parameters. Therefore, multi-proxy studies appear to be a great tool helping to understand and unravel the controls of the vent fluid's chemistry.

Our data supports the idea, that B in "smoker-type" vent fluids with moderate to high Cl contents can be best explained by a two-component mixing between B in seawater and B leached from the oceanic crust. Hence, B signatures in the vent fluids are a useful tool to for estimating the B composition of the oceanic crust, which is controlled by the B signature of the mantle and B added by dehydration of the subducting slab (e.g. Shaw et al., 2012). However, the data reveals also evidence that B in the vent fluids might be shifted from this calculated two end-member mixing curves (between seawater and fresh oceanic crust) by interaction with altered volcanic rocks and phase separation. Further, because of contrasting results in the acid-sulfate fluids, it remains unclear, whether B is added directly by magmatic fluids into hydrothermal systems or not. Although characterized by limited water-rock interaction, most of the acid-sulfate fluids have B compositions, which are similar to smoker fluids. Thus, B appears to be preferentially mobilised from the oceanic crust during interaction with these acidic, high-vapour fluids. The results of the vapour-rich fluids from Nifonea volcano may support this idea. Although B in these boiling fluids appears to be enriched due to boiling, phase separation cannot explain the low B isotope ratios. There might be the possibility that these fluids have undergone intense water-rock interaction at low W/R ratios prior to phase separation, which would imply that the apparent high W/R ratios stated by Schmidt et al. (2017) are invalid. Nevertheless, the combination of B isotope ratios with Li and Sr isotopes reveal that this idea is not suitable. Thus, also in these fluids a preferential mobilisation of B from the oceanic crust seems to be the most reasonable interpretation. Some of the vapour-rich fluids from PACMANUS and one of the acid-sulfate fluids from North Su (NS9) define a trend to lower B concentrations and isotope ratios, which are similar to the composition of the oceanic crust. The interpretation of this trend is challenging. Because of the high acidity and high gas-contents, this trend might be related to a different style of basement alteration, where B isotope fractionation factors and bulk distribution coefficients during water-rock interaction might differ from the proposed model. Nevertheless, this trend could also reflect a magmatic B signature or loss of B from the solution during condensation of gaseous components (e.g. condensation together with liquid CO_2). This could be also a result of different fluid residence times in the subsurface. Fluids with a short residence time might be stronger influenced by magmatic fluids, whereas fluids with long residence times in the

subsurface mainly display the composition of the oceanic crust. In summary, our B concentration and isotope ratio data strongly suggests that the behaviour of B during hydrothermal circulation at back-arc basins is much more complex that at MORs. Although some of the data interpretations are still ambiguous, it shows the potential of B isotopes to serve as proxy for manifold processes during hydrothermal circulation. Since B signatures in the vent fluids might be altered by preferential mobilisation of B from the oceanic crust, by phase separation and by magmatic fluids, B should always be evaluated with other proxies to assess W/R ratios and further to unravel and understand the additional processes influencing B, which are discussed in this thesis.

Our investigations on Li isotope ratios in the vent fluids show that the published mass balance models (e.g. Araoka et al., 2016), which should predict the composition of Li in vents fluids during hydrothermal water-rock interaction, are not suitable for the vent fluids from the Manus Basin. This provides evidence that the behaviour of Li during high-temperature water-rock interaction in back-arc basins might differ from MOR settings. We propose, that this is related to a negligible Li loss during formation of secondary minerals, which is generally thought to account for the isotopic offset between vent fluids and oceanic crust. Those fluids from PACMANUS showing the lowest W/R ratios have the same Li isotopic composition as the host rocks. The absence of any isotope effect during water-rock interaction might relate to the different mineralogy of MORB and BABB and hence a different leaching behaviour of Li. Further, the isotopic fractionation factor of Li during its incorporation into alteration minerals depends on the mineral species (e.g. Vigier et al., 2008). The different leaching behaviour of Li at the different tectonic settings is supported by the Li contents of the vent fluids. Although Li concentrations in dacitic rocks are much higher than in MOR-like basalts, Li contents in the vent fluids are similar at comparable W/R ratios during water-rock interactions. The reason for this different behaviour of Li in back-arc and MOR settings remains ambiguous, but might be mineralogically controlled and may also relate to different fluid pathways in the oceanic crust. The boiling fluids at Nifonea volcano support the theory that Li is depleted in the vapour rich phases, whereas the isotope ratios appear to be not affected. Furthermore, the extraordinary high Li and Sr isotope ratios at Nifonea volcano reveal extreme high W/R during water-rock interaction. These findings support the theory of Schmidt et al. (2017) that the fluids are controlled by a fast transit through the oceanic crust with only limited water-rock interaction. In summary, our results clearly show that Li in vent fluids from back-arc basin match the isotopic signature of the oceanic crust and hence is mainly controlled by high-T leaching from the host rocks. Thus, it appears to be a useful tool to investigate water-rock interaction during hydrothermal circulation. Furthermore, the results match with Li isotope data from other vent fluids from arc and back-arc settings, which have generally lower isotope ratios than vent fluids sampled from MORs. This provides evidence that the

estimated Li isotope ratio of the hydrothermal Li flux into the ocean, which is based on the Li composition of MOR fluids, should be adjusted to lower ratios.

The data on Mg isotopes has two major outcomes. First, Mg isotope ratios appear to be not fractionated during incorporation of the oceanic crust, which implies that the isotopic offset between seawater and riverine input (Tipper et al., 2006) can solely be explained by the formation of Mg-carbonates and especially dolostones. Second, Mg isotope ratios in acid-sulfate fluids show that Mg is seawater derived, which contrasts the theory from Gamo et al. (1997) that high Mg concentrations in acid-sulfate fluids might relate to the dissolution of Mg-bearing minerals.

Further, the study on acid-sulfate fluids shows that the combination of Li, B and Sr isotopes in acid-sulfate fluids might be useful to understand alteration processes in the oceanic crust, which related interaction with acid-sulfate fluids. Due to their different mobility at different temperatures as well as their progressive depletion during advancing alteration of the host rocks, the combination of these isotope systems in vent fluids helps to assess the alteration degree of the oceanic crust. This may offer the opportunity to estimate the relative time-span, in which these acid-sulfate fluids reacted with the oceanic crust.

The results obtained in this PhD project clearly show, that the used isotopic offer a wide range of applications in order to understand the processes during hydrothermal circulation. Furthermore, the manifold findings in the vent fluids from the Manus Basin and Nifonea volcano demonstrate that both study areas are particularly suitable to study hydrothermal circulation systems in back-arc settings. Nevertheless, many of the interpretations remain ambiguous and further research would be beneficial.

In the following different options for additional research are provided:

- A detailed investigation of Li and B isotopes in the altered oceanic crust at PACMANUS and SuSu Knolls would be beneficial. In combination with their signatures in the vent fluids this may help to further understand the behaviour of these elements during the alteration of oceanic crust. Especially, isotope analyses in different mineral phases of fresh and altered volcanic rocks will provide insights into their behaviour during hydrothermal alteration and might help to explain the differences in hydrothermal water-rock interaction between MOR and subduction-related settings.
- To further test whether B is added by magmatic fluids to hydrothermal systems and if B indeed is preferentially mobilized from the oceanic crust in vapour-rich fluids, B signatures in acid-sulfate fluids and “smoker-type” with significant magmatic fluid fluxes from other study areas should be analysed.

- A temporal study on Li, B and Sr isotope ratios in acid-sulfate fluids, where the same orifices are sampled several times within a timeframe of several months to years, will help to assess the sequential leaching during progressive alteration of the oceanic crust.
- Experimental setups, which simulate water-rock interaction at high temperatures between basaltic rocks and vapour-rich and/or acidic fluids, can be a tool to investigate, whether B mobility from the rocks depends on gas contents or not.

6.1 References

Araoka, D., Nishio, Y., Gamo, T., Yamaoka, K., Kawahata, H. (2016) Lithium isotopic systematics of submarine vent fluids from arc and back-arc hydrothermal systems in the western Pacific. *Geochim. Geophys. Geosys.* **17**, 3835-3853.

Gamo, T., Okamura, K., Charlou, J. L., Urabe, T., Auzende, J. M., Ishibashi, J., ... & Chiba, H. (1997). Acidic and sulfate-rich hydrothermal fluids from the Manus back-arc basin, Papua New Guinea. *Geology* **25**(2), 139-142.

Schmidt, K., Garbe-Schönberg, D., Hannington. M. D., Aderson, M. O., Bühring, B., Haase, K., Haruel, C., Lupton, J. E., Koschinsky, A. (2017) Boiling vapour-type fluids from the Nifonea vent field (New Hebrides Back-Arc, Vanuatu, SW Pacific): Geochemistry of an early-stage, post-eruptive hydrothermal system. *Geochim. Cosmochim. Acta* **207**, 185-209.

Shaw A. M., Hauri E. H., Behn M. D., Hilton D. R., Macpherson C. G., Sinton J. M. (2012) Long-term preservation of slab signatures in the mantle inferred from hydrogen isotopes. *Nature Geoscience* **5**, 224-228.

Tipper, E. T., Galy, A., Gaillardet, J., Bickle, M. J., Elderfield, H., & Carder, E. A. (2006). The magnesium isotope budget of the modern ocean: constraints from riverine magnesium isotope ratios. *Earth and Planet. Sci. Lett.* **250**(1), 241-253.

Vigier, N., Decarreau, A., Millot, R., Carignan, J., Petit, S., France-Lanord, C. (2008). Quantifying Li isotope fractionation during smectite formation and implications for the Li cycle. *Geochim. Cosmochim. Acta* **72**(3), 780-792.

Acknowledgments

First, I would like thank my supervisor Prof. Dr. Simone Kasemann for giving me the opportunity to conduct this PhD project. I am very grateful for your support and guidance during the last three years, and especially for your calmness, when I was sending abstracts last minute. Thank you for all the discussions about my data and the constructive ideas and thank you especially for your understanding and support in non-scientific topics.

Further, I want to thank Prof. Dr. Wolfgang Bach for sharing his expertise about hydrothermal vent systems with me. All the discussion about the overall picture and individual samples helped me a lot for the interpretation of my data.

I also would like to thank the other member of my thesis committee: Anette Meixner and for her support and help in the lab. Thank you so much for introducing me to the methods I did not know before and for the discussions on analytical problems.

I also would like to thank Prof. Dr. Andrea Koschinsky for discussions and her good mood during my thesis committee meetings and the fast corrections on my first manuscript.

Special thanks also to Katja Schmidt, Selma Lima, Eoghan Reeves and Jeffrey Seewald for providing the sample materials and additional data for the samples and further for their input on my data and manuscripts.

Bastian Bieseler is thanked for helping me with the preparation of the volcanic material.

Further, Friedrich Lucassen is thanked for the nice discussion on analytical, geological and world problems. Special thanks also go to Barbara Muntz for the administrative help and pleasant conversations.

Furthermore, I would like to thank GLOMAR graduate school for financial support and the training.

And now to my ISOTOPE GIRLS: Gustavo, Leri, Natalie and of course Aneka. I want to thank you soooo sooo much for the awesome time we had in the office. Thank you so much for all the laughing (sorry to our neighbour Ulla), for all the gossip, 9gag and yahoo news, for playing lotto, designing of future careers, for all the unicorns, ice-cream and horses, for helping each other in the lab, during measurements, with texts… but most importantly thank you so much for every smile you gave me in the time, when I was not feeling good! I am so happy, that we created such a strong bond and I am happy that I met such awesome friends!

At this point I would also like all the people from Bremen, who made my time here enjoyable. First of all, thanks to Timo for all the nice coffee breaks during work (and the wine afterwards). Thanks also to Ricci, Sally, Matt, Anne, Björn and many more.

And of course I can also not forget my beloved Berlin crew: Manu, Jule, Aline, Alexa, Rene, Marie and Marfi. Thank you for many nice moments and memories.

I also would like my wonderful family, my father and brother, my sisters and my nieces for the assistance during all phases of my life. Special thanks go to my sister Kristina, who motivated me enormously in the last days before submitting.

My deepest thanks go to Jannis. I am so happy to have you in my life. Thank you so much for your support and the love you gave me in the last two years, especially also in the finishing phase of the PhD. Thank you for cooking and filling my fridge and thank you for always calming me down (and right know I am also really grateful for your last-minute thesis help ;-)).

Appendices

rontium Ion exchange chromatography (for solid and liquid samples)

Separation using Sr spec resin
(handmade columns out of pasteur pipettes)

1. **add 500 µl – 1000 µl 2M HNO_3 to the sample**
2. **load Sr-spec ~70 µl with Milli-Q onto the column**
3. **Cleaning + conditiong**
   1. 2 x 500 µl Milli-Q
   2. 2 x 500 µl 2M HNO_3
4. **Add the sample solution**
   in 100 µl step, depending on amount of sample material
5. **Rinse (2. and 3. for Ba-rich samples)**
   1. 12 x 100 µl 2M HNO_3
   2. 2 x 500 µl 7M HNO_3
   3. 3 x 100 µl 2M HNO_3
6. **Elution (use 3 or 7 ml Savillex beaker)**
   5 x 200 µl 0.05M HNO_3
7. **add 40 µl 0.1M H_3PO_4 and dry at 120°C on the hot plate**
8. **add 40 µl conc. HNO_3 and dry at 120°C on the hot plate**
9. **add 40 µl H_2O_2 and dry at 120°C on the hot plate**

1. Lithium step using Biorad Resin AG 50WX8, 200-400 mesh
(PP-BIORAD-columns)

1. **Stir up resin**
2. **Cleaning**
   2 x 6 N HCL (full reservoir)
   1 x H_2O (full reservoir)
3. **Conditioning**
   2 x 1 ml 0.15N HCl
4. **Add the sample solution (sample dissolved in 2 ml 0.15N HCl) (use 7 ml Savillex beaker)**
   8 x 0.25 ml sample solution
5. **Rinse**
   1. 1 x 0.5 ml 0.15N HCl (wash sample beaker)
   2. 1 x 0.5 ml 0.15N HCl
   3. 1 x 1 ml 0.15N HCl
6. **Elution (use 30 ml Savillex beaker)**
   1. 4 x 5 ml 0.15N HCl
   2. 2 x 4 ml 0.15N HCl
7. **Tail (use 7 ml Savillex beaker)**
   2 x 1 ml 0.15N HCl
8. **Cleaning of resin & columns**
   2 x 6 N HCL (full reservoir)
   1 x H_2O (full reservoir)
9. **Evaporation of sample and tail solutions**

2. Lithium step using Biorad Resin AG 50WX8, 200-400 mesh
(PE-BIORAD Bio-spin columns)

1. **Stir up resin**
2. **Cleaning**
   6 x 6 N HCL (full reservoir)
   3 x H_2O (full reservoir)
3. **Conditioning**
   1 x 1 ml 0.15N HCl
4. **Add the sample solution (sample dissolved in 1 ml 0.15N HCl) (use 7 ml Savillex beaker)**
   4 x 0.25 ml sample solution
5. **Rinse**
   1. 1 x 0.5 ml 0.5N HCl in 50% EtOH (wash sample beaker)
   2. 1 x 0.5 ml 0.5N HCl in 50% EtOH
6. **Elution (use 15 ml Savillex beaker)**
   1. 1 x 0.5 ml 0.5N HCl in 50% EtOH
   2. 12 x 1 ml 0.5N HCl in 50% EtOH
7. **Tail (use 7 ml Savillex beaker)**
   2 x 1 ml 0.5N HCl in 50% EtOH
8. **Cleaning of resin & columns**
   3 x H_2O (full reservoir)
   6 x 6 N HCL (full reservoir)
9. **Evaporation of sample and tail solutions**

Ion exchange chromatography (fo

1. step: Boron - anion exchange using Amberlite IRA 743, 20-50 mesh
(PE-BIORAD Biospin-columns)

1. **Conditioning and cleaning of the columns**
   6.6 N HCL (full reservoir)
   2 x H_2O (full reservoir)
   0.5 ml 2N NH_4OH
   3 x 1 ml H_2O
2. **Add sample + resin**
3. **Rinse sample**
   2 x 1 ml H_2O
   2 x 1 ml NH_4OH
   4 x 1 ml H_2O
4. **Elution (use weighed 15 ml Savillex beaker)**
   24 x 0.5 ml 0.5N HCl
5. **Tail (use 7 ml Savillex beaker)**
   2 x 1 ml 0.5N HCl
6. **concentratrion check**
6. **addition of mannitol**
   0.2 % mannitol solution (1:40)
7. **evaporation of samples at T≤ 65°C overnight**
8. **Cleaning of the columns, discard resin**

2. step: Boron - cation exchange using Biorad Resin AG 50WX8, 200-400 mesh
(PE-BIORAD Biospin-columns)

1. **Stir up resin**
2. **Cleaning**
   2 x 6.2N HCl (full reservoir)
3. **Conditioning**
   4 x 1 ml 0.02N HCl
4. **Add the sample solution (sample dissolved in 1ml 0.02N HCl)**
   (use 15 ml Savillex beaker)
   4 x 0.25 ml
5. **Elution**
   1. 2 x 0.25 ml 0.02N HCl (wash the sample beaker with the first 0.5ml 0.02N HCl!)
   2. 7 x 0.5 ml 0.02N HCl
   3. 4 x 1 ml 0.02N HCl
5. **Tail (use 7 ml Savillex beaker)**
   2 x 1 ml 0.02N HCl
6. **Cleaning of resin & columns**
   2 x 6.6 N HCL (full reservoir)
7. **Evaporation of sample and tail solutions (T about 56°C for 14h)**

1. step: Separation using Biorad Resin AG 50WX8, 200-400 mesh
(PE-BIORAD Bio-spin columns)

1. **Stir up resin**
2. **Cleaning**
   6 x 6N HCL (full reservoir)
   3 x H_2O (full reservoir)
3. **Conditioning**
   1 x 1 ml 1N HCl
4. **Add the sample solution (sample dissolved in 0.5 ml 1N HCl) (use 7 ml Savillex beaker)**
   2 x 0.25 ml sample solution
5. **Rinse**
   1. 1 x 0.5 ml 1N HCl (wash sample beaker)
   2. 1 x 0.5 ml 1N HCl
   3. 2 x 1 ml 1N HCl
6. **Elution (use 15 ml Savillex beaker)**
   13 x 1 ml 1N HCl
7. **Tail (use 7 ml Savillex beaker)**
   2 x 1 ml 1N HCl
8. **Cleaning of resin & columns**
   6 x 6N HCL (full reservoir)
   3 x H_2O (full reservoir)
9. **Evaporation of sample and tail solutions at T=90°C**

2. step: Separation using Biorad Resin AG 50WX8, 200-400 mesh
(PE-BIORAD Bio-spin columns)

1. **Stir up resin**
2. **Cleaning**
   6 x 6N HCL (full reservoir)
   3 x H_2O (full reservoir)
3. **Conditioning**
   1 x 1 ml 1N HNO_3
4. **Add the sample solution (sample dissolved in 0.5 ml 1N HNO_3) (use 15 ml Savillex beaker)**
   2 x 0.25 ml sample solution
5. **Rinse**
   1. 1 x 0.5 ml 1N HNO_3 (wash sample beaker)
   2. 1 x 0.5 ml 1N HNO_3
   3. 5 x 1 ml 1N HNO_3
6. **Elution (use 15 ml Savillex beaker)**
   1. 1 x 0.5 ml 1N HNO_3
   2. 12 x 1 ml 1N HNO_3
7. **Tail (use 7 ml Savillex beaker)**
   2 x 1 ml 1N HNO_3
8. **Cleaning of resin & columns**
   6 x 6N HCL (full reservoir)
   3 x H_2O (full reservoir)
9. **Evaporation of sample and tail solutions at T=90°C**

Appendix 5: Sr isotope ratios for the measured reference materials

Sample ID	Date Measurement	$^{87}Sr/^{86}Sr$		2se
NIST 987	31.07.2014	0.710237	±	6
NIST 987	31.07.2014	0.710254	±	7
NIST 987	31.07.2014	0.710260	±	8
NIST 987	31.07.2014	0.710246	±	6
NIST 987	05.12.2016	0.710238	±	6
NIST 987	07.10.2016	0.710244	±	4
NIST 987	11.08.2015	0.710251	±	8
NIST 987	12.06.2015	0.710246	±	5
NIST 987	04.03.2015	0.710254	±	6
NIST 987	09.01.2015	0.710244	±	6
NIST 987	15.09.2014	0.710239	±	8
NIST 987	31.07.2015	0.710264	±	8
	AVERAGE	**0.710248**	**±**	**15**
B5	12.06.2015	0.703593	±	5
BM	12.06.2015	0.711911	±	6
BHVO-2	11.08.2015	0.703479	±	6
BHVO-2	12.06.2015	0.703468	±	6
	AVERAGE	**0.70347**	**±**	2
SW Manus	09.01.2015	0.709162	±	5

Appendix 6: Li isotope ratios for the measured reference materials

Sample ID	Date Measurement	δ^7Li ‰	2SD
B1	06.10.2014	31.0 ±	0.2
BHVO-2	27.07.2015	4.2 ±	0.6
BHVO-2	07.07.2015	4.4 ±	0.2
	AVERAGE	**4.3 ±**	**0.3**
BM	29.07.2015	-4.3 ±	0.1
BM	07.07.2015	-3.3 ±	0.3
	AVERAGE	**-3.8 ±**	**1.4**
LSVEC	08.10.2015	0.0 ±	0.2
LSVEC	29.07.2015	0.0 ±	0.3
LSVEC	10.11.2014	0.0 ±	0.1
LSVEC	10.11.2014	0.0 ±	0.2
LSVEC	14.10.2014	0.0 ±	0.1
LSVEC	11.06.2015	0.1 ±	0.2
LSVEC	27.10.2015	0.2 ±	0.1
LSVEC	02.02.2016	**0.0** ±	0.2
LSVEC	23.03.2016	**0.1** ±	0.2
LSVEC	23.03.2016	0.2 ±	0.2
LSVEC	04.04.2016	0.0 ±	0.3
LSVEC	04.04.2016	**0.1** ±	0.1
LSVEC	11.11.2014	0.0 ±	0.1
LSVEC	13.01.2015	0.1 ±	0.1
LSVEC	28.01.2015	0.0 ±	0.0
LSVEC	07.07.2015	0.0 ±	0.3
LSVEC	01.04.2015	0.0 ±	0.2
	AVERAGE	**0.0 ±**	**0.1**
SW SuSu Knolls	27.07.2015	31.1 ±	0.1
SW SuSu Knolls	01.04.2015	31.1 ±	0.2
SW SuSu Knolls	04.04.2016	31.2 ±	0.1
SW SuSu Knolls	13.01.2015	31.1 ±	0.1
SW SuSu Knolls	28.01.2015	31.0 ±	0.2
	AVERAGE	**31.1 ±**	**0.2**

Appendix 7: B concentrations and isotope ratios for the measured reference materials

Sample ID	Date Measurement	$\delta^{11}B$ ‰	2SD	B ± 2SD ppb
NIST 951	07.08.2014	0.0	± 0.1	
NIST 951	13.08.2014	0.0	± 0.1	
NIST 951	15.10.2014	0.0	± 0.1	
NIST 951	07.12.2016	0.3	± 0.1	
NIST 951	01.12.2014	0.1	± 0.1	
NIST 951	22.10.2014	0.1	± 0.1	
NIST 951	28.10.2014	0.1	± 0.1	
NIST 951	15.01.2015	0.0	± 0.1	
NIST 951	29.10.2015	0.0	± 0.1	
NIST 951	07.12.2016	0.2	± 0.0	
NIST 951	21.04.2015	-0.1	± 0.1	
NIST 951	03.12.2015	-0.2	± 0.0	
	AVERAGE	**0.0**	**± 0.3**	
SW SuSu Knolls	01.12.2014	40.0	± 0.1	4660
SW SuSu Knolls	30.07.2015	39.6	± 0.0	4954
SW SuSu Knolls	29.10.2015	39.8	± 0.1	5007
SW SuSu Knolls	13.08.2014	39.7	± 0.1	4779
SW SuSu Knolls	15.01.2015	39.6	± 0.1	4760
SW SuSu Knolls	07.08.2014	39.9	± 0.1	4705
	AVERAGE	**39.8**	**± 0.3**	**4811 ± 278**
B1	15.10.2014	39.7	± 0.1	5298
B1	28.10.2014	39.7	± 0.1	5158
B1	07.08.2014	40.0	± 0.1	5683
B1	13.08.2014	39.9	± 0.1	5299
	AVERAGE	**39.8**	**± 0.3**	**5359 ± 451**
B5	21.04.2015	-4.3	± 0.1	9284
B5	21.04.2015	-4.3	± 0.1	9596
B5	03.12.2015	-4.1	± 0.1	9009
B5	03.12.2015	-4.3	± 0.0	9291
	AVERAGE	**-4.2**	**± 0.1**	**9295 ± 479**

Appendix 8: Mg isotope ratios for the measured reference materials

Sample ID	Date Measurement	$^{87}Sr/^{86}Sr$		2se
Cam-I	13.10.2016	-2.53	±	0.03
Cam-I	18.10.2016	-2.59	±	0.04
Cam-I	21.10.2016	-2.60	±	0.05
Cam-I	28.10.2016	-2.58	±	0.06
Cam-I	17.01.2017	-2.52	±	0.03
Cam-I	16.01.2017	-2.52	±	0.01
Cam-I	21.11.2016	-2.63	±	0.06
Cam-I	18.01.2017	-2.53	±	0.03
	AVERAGE	**-2.56**	**±**	**0.09**
SW SuSu Knolls	17.01.2017	-0.88	±	0.01
SW SuSu Knolls	17.01.2017	-0.87	±	0.02
SW SuSu Knolls	16.01.2017	-0.86	±	0.04
	AVERAGE	**-0.87**	**±**	**0.02**